Recruitment of Guanylate-Binding Proteins to Francisella novicida in human macrophages

Stanimira Valeva

THESE de DOCTORAT DE
L'UNIVERSITE CLAUDE BERNARD LYON 1

Ecole Doctorale N° 340
BIOLOGIE MOLECULAIRE, INTEGRATIVE ET CELLULAIRE

Discipline : Infectiologie

Soutenue publiquement le 07/10/2022, par :
Stanimira VALEVA

Recrutement des Guanylate-Binding Proteins sur *Francisella novicida* dans les macrophages humains

Devant le jury composé de :

Pr. FAURE Mathias	Professeur des Universités, UCBL	Président du jury
Dr. BOISSET Sandrine	Maître des conférences-PH, UGA	Rapportrice
Dr. CHARBIT Alain	Directeur de recherche INSERM	Rapporteur
Pr. BROZ Petr	Professeur, Université de Lausanne	Examinateur
Dr. SALCEDO Suzana	Chargée de recherche INSERM	Examinatrice
Dr. HENRY Thomas	Directeur de recherche INSERM	Directeur de thèse

Université Claude Bernard – LYON 1

Président	M. Frédéric FLEURY
Président du Conseil Académique	M. Hamda BEN HADID
Vice-Président du Conseil d'Administration	M. Didier REVEL
Vice-Présidente de la Commission de Formation	Mme Céline BROCHIER
Vice-Président de la Commission de Recherche	M. Petru MIRONESCU
Directeur Général des Services	M. Pierre ROLLAND

COMPOSANTES SANTE

Département de Formation et Centre de Recherche en Biologie Humaine	Directrice : Mme Anne-Marie SCHOTT
Faculté d'Odontologie	Doyenne : Mme Dominique SEUX
Faculté de Médecine et Maïeutique Lyon Sud - Charles Mérieux	Doyenne : Mme Carole BURILLON
Faculté de Médecine Lyon-Est	Doyen : M. Gilles RODE
Institut des Sciences et Techniques de la Réadaptation (ISTR)	Directeur : M. Xavier PERROT
Institut des Sciences Pharmaceutiques et Biologiques (ISBP)	Directrice : Mme Christine VINCIGUERRA

COMPOSANTES & DEPARTEMENTS DE SCIENCES & TECHNOLOGIE

Département Génie Electrique et des Procédés (GEP)	Directrice : Mme Rosaria FERRIGNO
Département Informatique	Directeur : M. Behzad SHARIAT
Département Mécanique	Directeur M. Marc BUFFAT
Ecole Supérieure de Chimie, Physique, Electronique (CPE Lyon)	Directeur : Gérard PIGNAULT
Institut de Science Financière et d'Assurances (ISFA)	Directeur : M. Nicolas LEBOISNE
Institut National du Professorat et de l'Education	Directeur : M. Pierre CHAREYRON
Institut Universitaire de Technologie de Lyon 1	Directeur : M. Christophe VITON
Observatoire de Lyon	Directrice : Mme Isabelle DANIEL
Polytechnique Lyon	Directeur : Emmanuel PERRIN
UFR Biosciences	Directrice : Mme Kathrin GIESELER
UFR des Sciences et Techniques des Activités Physiques et Sportives (STAPS)	Directeur : M. Yannick VANPOULLE
UFR Faculté des Sciences	Directeur : M. Bruno ANDRIOLETTI

Remerciements / Aknowledgements

I am immensely grateful to my thesis director, Dr Thomas Henry, for takin me in as a Master's student and helping me mature throughout my thesis. Thank you for your trust, patience and mentorship and thank you for giving me so many opportunities to speak, meet people, learn and grow.

To my team, which is the best: I am so lucky to have spent these four years with you.

Manon, my partner in crime, it was a pleasure to work with you. Thank you for your help and friendship. I wish you the best for your thesis and whatever the future may hold. May the force be with you, young jedi.

Dasha, my work bestie and bench neighbour - I am so happy to have met you and done my thesis side by side with you. Thank you for the lovely conversations which made the day go faster while learning about interesting books, podcasts, anecdotes and life in general. I am looking forward to cheering you on on your defense day.

Amandine, we all know that the lab cannot run without you. But above all, I want to thank you for your help, generosity and kindness.

Flora and Emilie, thank you for your advice and guidance when I was a young student with no idea what I was doing.

Gabrielle, I have learned so much from you and I wish I could have worked with you a little longer.

Thank you to Brice and Fanny, who started this project, and especially Brice who stayed involved and supportive after leaving the lab.

Sarah, Pauline, Mélissa, Elena, Etienne, Jérémy, Maxence - you made this lab a warm and wonderful place to work at. Thank you for the joy and cakes you brought to the lab. (I hope that Isidore the Dinosaur survives all incoming attacks.)

I want to thank the scientists at the Cervi tower, and Benedicte Py and her group for the interesting exchanges. A big thanks to the Cervi secretaries and Elise Roque who make everything go smoothly.

I want to thank the team at the Platim microscopy platform, where I spent so much time. A great thanks to Elodie Chatre who taught me most of what I know about microscopy, for being so kind and helpful and introducing me to people and opportunities.

I also want to aknowledge the contribution of the French Direction Générale de l'Armement (DGA) from the Ministry of Armed Forces who co-financed my thesis with Inserm, and thank you to my DGA tutor Mme Emanuelle Guillot-Combe.

I am grateful to the members of my thesis supervision committee, Dr Marlène Dreux and Dr Stéphane Méresse, for their time and helpful advice.

Thank you to Dr. Sandrine Boisset and Dr. Alain Charbit for accepting to evaluate my thesis manuscript, and thank you to Prof. Petr Broz, Prof. Mathias Faure and Dr. Suzana Salcedo for agreeing to judge my work at the day of my defense. I am honoured to have all of you in my jury.

To my friends and family, I could not have done this without your support.

To the people I met in France, thank you for making me feel at home. The crocodiles/mouflettes, I have so many great memories with you guys and I'm looking forward to celebrating with you. Léa, Isa, Marie, Eleo, thank you for two amazing years of Masters' and even though we can barely manage to coordinate now, I will always be delighted to see you. Margaux, thank you for your warmth, honesty and generosity. You're the best. Tanya, you've been my friend since the beginning of my studies - I can't believe how fast the time passes! - thank you for sharing this experience with me. To all the lovely people who've been a part of my life during my studies but lost touch, I am grateful for the time we spent together.

My friends from Bulgaria, especially Alex, Rafail, Dimitar, Marieta - I will always cherish our adventures and thank you for having been by my side for so long! Alex, prepare; this is the first step to world domination.

A Catherine, Charlotte, Brian, Tim et Monique qui m'ont accepté comme famille - je vous remercie énormément et je vous aime.

Hugo, I could never thank you enough. This work is yours as well.

To my family – Mom, Dad and Maria, (and my grandparents, even though they can't understand this text) – I am forever grateful for your love, support, generosity and encouragement. Обичам ви безкрайно.

Acronyms and abbreviations

Aim2	Absent in Melanoma 2
ASC	Apoptosis-associated Speck-like protein containing a CARD
BMDM	Bone Marrow-Derived Macrophages
CARD	Caspase Activation and Recruitment Domain
cGAMP	Cyclic Gyanosine monophosphate - Adenosine monophosphate
cGas	Cyclic GMP-AMP synthase
DAPI	4',6'-dimanidino-2-phenylidole
DSS	Disuccinimidyl suberate
FACS	Fluorescence-Activated Cell Sorting
FPI	*Francisella* Pathogenicity Island
FRET	Förster/Fluorescence Resonance Energy Transfer
FRT	Flippase Recognition Target
GBP	Guanylate-Binding Protein
GED	GTPase Effector Domain
hMDM	human Monocyte-Derived Macrophages
HPLC	High-Performance Liquid Chromatography
HUVEC	Human Umbilical Vein Endothelial Cells
IFN	Interferon
IL-	Interleukin
IRG	Interferon-Related GTPase
ISG	Interferon-Stimulated Gene
ISRE	Interferon-Stimuated Responsive Element
LDH	lactate deshydrogenase
LPS	Lipopolysaccharide
LRR	Leucine-Rich Repeat
M-CSF	Macrophage Colony-Stimulating Factor
MOI	Multiplicity of Infection
MYD88	Myeloid Differentiation primary response 88
NK	Natural Killer cell
NRLP3	NOD-, LRR- and Pyrin domain Containing Protein 3
NOD	Nucleotide-Oligomerization Domain
NLRC4	NRL Family CARD Domain Containing 4
OMV/T	Outer Membrane Vesicles/Tubes
PI	propidium iodide
PLA	Proximity-Ligation Assay
PMA	phorbol-12-myristate-13-acetate
PV	parasitophosphorous/pathogen-containing vacuole
ROS	Reactive Oxygen Species
SEM	Standard Error of the Mean
SIM	Structured Illumination Microscopy
SMLM	Single-Molecule Localization Microscopy
STAT	Signal Transducer and Activator of Transcritpion
STED	Stimulated Emission Depletion
STING	Stimulator of Interferon Genes
T6SS	type VI secretion system
TEM	transmission electron microscopy
TNF	Tumor Necrosis Factor
TLR	Toll-like receptor

Figures index

Introduction

Results

Discussion

Contents

Introduction

I. *Francisella tularensis*, a stealth pathogen

Francisella tularensis is a Gram-negative non-motile coccobacillus. It is the etiological agent of tularaemia, a rare zoonosis that can be life-threatening.

F. tularensis replicates in the cytosol of host phagocytic cells such as macrophages. Unlike most professional cytosolic bacteria, *F. tularensis* does not utilize actin-based motility to move within cells and for cell-to-cell spread.

F. tularensis has evolved sophisticated and unique adaptations to evade detection from host immunity. Thus, it is an interesting model for the study of cytosolic host-pathogen interactions, particularly for cytosolic innate and cell autonomous immunity.

The following chapters will describe in detail the historical and current knowledge on *F. tularensis* pathogenicity and its adaptations for survival within the host.

Historical overview of tularaemia

Tularaemia, a sneaky plague: Discovery and early research

North America had largely been spared from plague epidemics until the 20th century. When cases of what appeared to be the bubonic plague started to occur throughout Southern and Central California in the early 1900s, the US government promptly sent Dr George W. McCoy to investigate the outbreak. The cases were concomitant with a massive die-out of the ground squirrel populations in the surrounding regions. '[…] an epizootic affected so many of these rodents in Contra Costa County, California, that they were almost exterminated.' wrote McCoy [1]. Victims were often reported to have had contact with squirrels before falling ill. Consequently, it was suspected that the California ground squirrel *Citellus beecheyi* (today *Otosmpermophilus beecheyi*) was the primary vector for this outbreak.

Throughout 1908-1910 McCoy and his team routinely caught, killed and autopsied over 105 000 ground squirrels. Through serological and microbiological examinations McCoy identified the presence of *Bacillus pestis* (today *Yersinia pestis*) in the samples, confirming what it was feared – there was an epidemic of the bubonic plague in California.

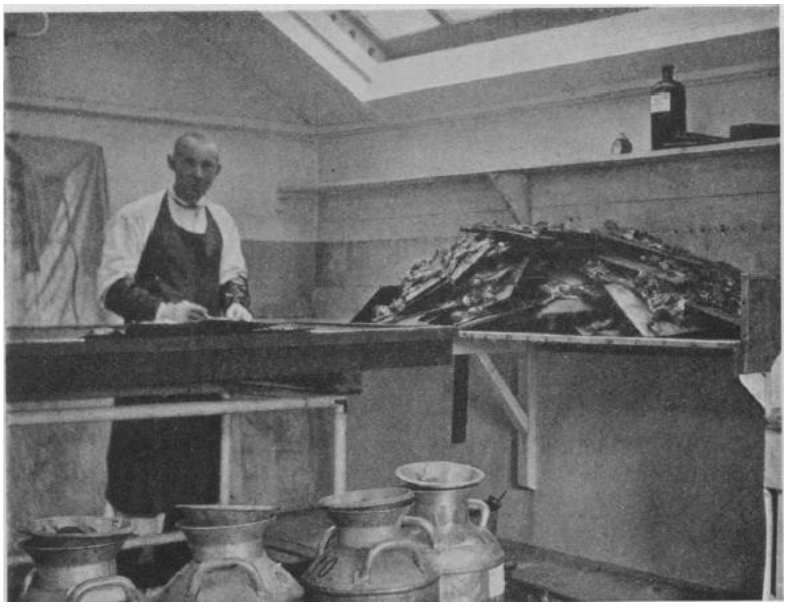

Figure 1. *Photo of a laboratory assistant dissecting squirrels in the Federal Plague Laboratory in San Francisco, published by George W. McCoy in the Journal of Hygiene in 1908.* [1]

As large-scale screen studies tend to do, this one also yielded some unexpected results [2]. The microbiological smears from some of the seemingly plagued squirrels did not grow the characteristic bacilli of *B. pestis*. Upon careful examination, subtle differences were noted in the clinical features of this newly described plague-like disease, i.e., less oedema in the inoculation site, a more pinkish bubo, etc. The etiological agent could not be isolated but the clinical features hinted at a bacterial pathogen with blood dissemination and high infectivity. McCoy and colleagues were unsuccessful in growing the organism on lab culture media and the clinical samples were negative for several microbiological stains (carbol-thionin, Loeffler's methylene blue, Wright's and Giemsa stains). They did note the presence of

'fine, dust-like particles' and 'very small, solid staining bacili' in numerous preparations but were unsure whether these should be assigned any importance.

McCoy further described the pathogenicity of the disease for animal hosts: ground squirrels, guinea pigs, rats, mice, rabbits, monkeys were susceptible; cats and gophers were moderately susceptible while dogs and pigeons seemed immune. The disease could be transmitted to rodents through food, subcutaneous, peritoneal, nasal inoculation and fleas. At the time of this study, clinical manifestations of the disease could only be described in laboratory animals as human cases had not yet been identified. Considering the variety of animal hosts, human susceptibility was highly likely.

The bacterium was finally purified, stained and named *Bacterium tularense*[1] [3]. Cultivation was difficult but Dorset's egg medium seemed to work. When dyed with crystal violet and with carbol fuschin, the very small (0.2-0.7 µm) non-motile oval organisms were surrounded by a clear area (capsule). The organisms were present in very high numbers in spleen samples from diseased animals, often found in leukocytes.

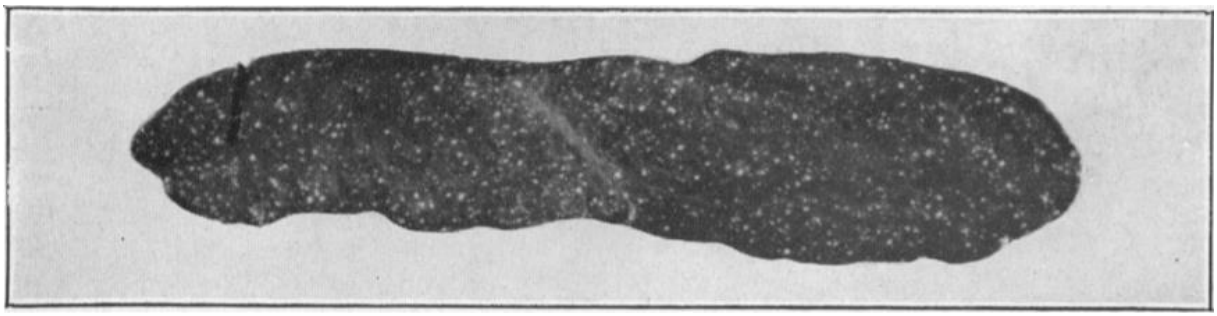

Figure 2. *Spleen of a tularaemia-infected rabbit showing white granules, published in a report by Edward Francis in 1937* [4]. *In his 1911 study, George McCoy remarked the presence of discrete, distinct granules in the spleen specific to animals infected with B. tularense* [2] .

The first human case of tularaemia was confirmed in 1914 [5] using the methods developed by McCoy. The patient came to the hospital with an eye inflammation presenting ulcers and swelling on the lid. Over the course of two weeks, the infection worsened with increasing swelling of the lymph nodes around the area, apparition of abscesses, fever and weakness. The patient was still sick when he left the hospital.

In 1919, Dr Edward Francis was sent to Utah to investigate cases of a mysterious febrile disease, presumed to be transmitted through deer fly bites [6]. The area of the bite and the surrounding lymph nodes would swell. The patients had fever for several weeks and were confined to bed. Francis grew the pathogen in egg yolk medium and identified it as McCoy's *B. tularense*.

Between 1917 and 1919, two dozen cases were reported, one of which was fatal. The main concern with this disease for Francis was the long convalescence period, as he recognized that '[…]a disabling illness which overtakes the farmer in the busy season of midsummer, causing two or three months of sickness in the harvest season, is a serious matter.' [7]

[1] *Bacterium tularense* was named after Tulare County in California, one of the afflicted areas.

In the following years Francis would set out to extensively study the disease he called tularæmia [7] and its agent, *B. tularense*, gathering data from 14 000 cases by 1944 [8] and himself contracting the disease five times. He meticulously described each case, cataloguing vectors, routes of infection, symptoms, outcomes, histology and microbiology of patient samples [4,9,10]. He found that *B. tularensis* was more easily grown by adding cysteine to the medium[2] [11]. He included lice [7] and ticks [12] in the list of tularaemia vectors, and documented cases acquired from rabbits, sheep, tree squirrels, water rats, woodchucks, coyotes, hogs and cats. Based on clinical presentation, Francis categorized four types of tularaemia: ulceroglandular (ulcers with lymph node swelling), oculoglandular (eye inflammation with lymph node swelling), glandular (lymph node swelling) and typhoid (no swelling). Of these, ulceloglandular tularaemia due to insect bite was the most common type and represented 67% of his cases, which is close to the numbers recorded today. He noted around 5% overall fatality [4].

Figure 3. *Photograph of Dr Edward Francis inoculating a rabbit with tularaemia, taken in 1937. National Library of Medicine Digital Collections ID 101679588* [13].

Although the first proven human case of tularaemia was published in 1914, infections had likely been occurring long before the 20th century under different names. Rodent-transmitted zoonotics with similar symptoms that are now believed to be tularaemia have been reported in Norway in 1653 [14], in Siberia and the former USSR throughout the 1800s and in Japan in the early 1800s [15]. Of note, when Francis investigated tularaemia in market workers in 1921, a patient had self-diagnosed with 'rabbit fever', a disease well known among merchants [11].

According to Francis, tularaemia was 'not borne in mind' and was commonly mistaken by clinicians for various infections such as influenza, typhoid, tuberculosis and undulant fever [10]. In 1925 Francis published a curated list of symptoms and criteria for diagnosis: persistent fever, swelling of lymph

[2] Indeed, nowadays, standard *Francisella* culture protocols supplement growth media with 0.1% w/v cysteine.

nodes, lesions around the inoculated area and, importantly, recent contact with rabbits. One could not get infected by a sick person. Diagnosis should additionally be confirmed through serum agglutination tests. As for treatment, he advised bed rest [16].

The first treatment for tularaemia arrived in 1932 when Dr Lee Foshay succeeded in curing patients with goat antiserum of formaldehyde-killed bacteria [17]. Penicillin was purified in 1940, unfortunately *B. tularense* is resistant. Not long after, Selman Waksman's lab isolated streptomycin which became the standard treatment for tularaemia in the years after WWII [18].

The elusive *Bacterium tularense* would be called many names throughout the years. Some of the variations were *Bacillus tularensis*, *Brucella tularensis*, *Pasteurella tularensis*. In 1947, Soviet microbiologist Dorofeev proposed the creation of the genus *Francisella* to contain the agent of tularaemia as it was not sufficiently related to other species in the genus *Pasteurella*. The proposal was subsequently accepted by taxonomists [19]. Francis' favourite organism hence became *Francisella tularensis*.

Questionable ethics: Human experimentation and biowarfare

In January 1924 Japanese doctor Hachiro Ohara received in his clinic a family presenting fever and swelling of the lymph nodes. During his inquiries, the doctor learned that the family had prepared rabbit meat and that a disease of this sort had been a common occurrence in the region for the last 20 years. Before announcing an outbreak of tularaemia and contacting Francis, Ohara diligently confirmed the source of infection by rubbing blood from a dead rabbit on the hand of his wife who had expressed a 'cheerful offer to help'[3] [20].

This example is far from being the only one – the history of tularaemia is an encyclopedia on human experimentation. In early research cases of tularaemia were frequent occurrence among laboratory workers [21–24]. One publication remarks, 'Almost every individual who consistently works with *Pasteurella tularensis* eventually incurs infection' [23]. A highly infectious pathogen provoking a severe, debilitating disease makes for a good candidate for a bioweapon, and several governments took note.

The development of biological weapons was prohibited by the 1925 Geneva Protocol, which was signed by many nations; but loopholes were found and guidelines disregarded.

To Dr. Shiro Ishii, biological warfare had great potential to promote Japan's expansionist ambitions in the first half of the 20th century. He considered that animal experimentation could never be sufficient to do adequate biowarfare research. But he knew that only vaccine research could be done in Japan, and figured offensive research would have to be done abroad [25]. In 1930, he was appointed Major in the Japanese Army and in 1932 sent to the newly acquired Japanese colony in Manchuria where Dr. Ishii could finally begin his work. He is best known for directing the infamous Unit 731 where countless

[3] It should be noted that the only treatment available at the time was bed rest.

atrocities were carried out as part of a biowarfare research program. Tularaemia was among the diseases tested on involuntary subjects [25,26].

In 1943, the US established a bio-defence research laboratory in Fort Detrick, Maryland. Operation Whitecoat, launched in 1954, aimed to evaluate the dangers and develop countermeasures against possible bioterrorism weapons with the help of volunteer subjects. In Fort Detrick a spherical building called Eight ball was constructed, where participants would be exposed to pathogenic aerosols in a controlled environment.

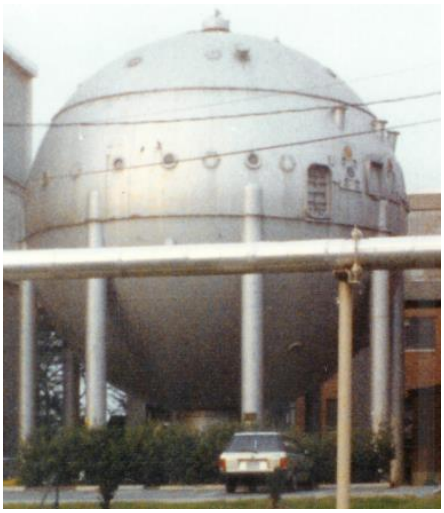

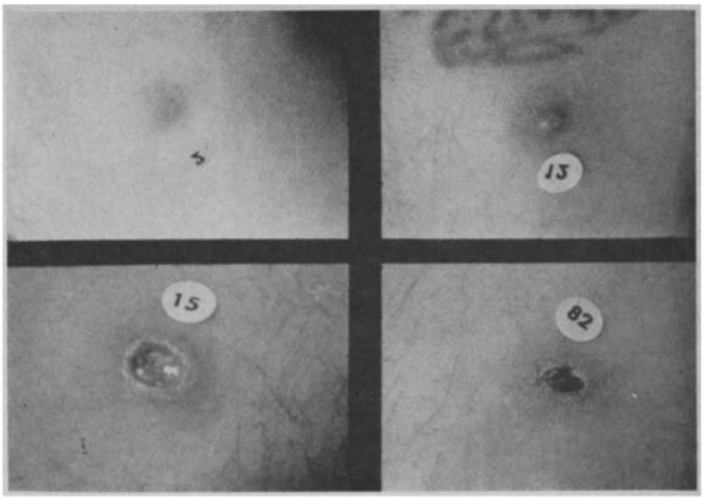

Figure 4. *Eight ball photographed in 1989* [27].

Figure 5. *Lesions following subcutaneous inoculation of F. tularensis to a non-vaccinated volunteer in Saslaw's Tularaemia vaccine study, 1956* [28]*. Photographs show a papule (2), pustule (12), ulcer (15) and eschar (82).*

F. tularensis was one of the pathogens studied in Fort Detrick. In a notable study from 1961, vaccinated and non-vaccinated volunteers were inoculated with tularaemia subcutaneously or through aerosols to test the efficacy of a tularaemia vaccine. The tularaemia respiratory challenge in Eight ball determined that an exposure of less than a minute to 14-15 organisms in 10 litres of air was sufficient to provoke illness in a healthy person [29]. The volunteers were treated with streptomycin once symptoms became too serious. One person agreed to have an inflamed lymph node excised for histological examination [28].

Many of the Whitecoat volunteers were soldiers from the Seventh Day Adventist Church who, for religious reasons, would not fight [30]. Testimonies of participants who were members of the Adventist Church globally demonstrate pride in having served their country in biosecurity research [27,31]. However, US tularaemia research also employed prisoners whose honest consent can be questionable [29]. A study produced by the US Army in 2005 found no statistically significant long-term health effects in Whitecoat participants [32] though this has been disputed by some of the subjects on personal accounts [31].

While researching vaccines in operation Whitecoat, the USA also launched Project 112 aiming to develop biological weapon delivery systems like the M143 bomblet. The M143 was used in the 1966-1967 Red Cloud test to study the biological decay and dissemination capabilities of *F. tularensis* and other pathogens in natural environments [33].

Former soviet scientist Ken Alibek who immigrated to the US in 1992 claims that the USSR, and later Russia, were working on bioweapons well into the 90s [34]. During his role as a First Deputy Director in the USSR Biopreparat facility, he had encountered many instances of research on genetically engineered multidrug resistant and immune subversive *F. tularensis*, among other pathogens. He believed Russia was still developing bioweapons in the mid-90s. In a testimony in front of the US Homeland Security, he recalled having read studies from his former colleagues who wanted to genetically introduce beta-endorphins into vaccine strains of *F. tularensis* and other highly infectious pathogens as vectors for expression in humans. For him, there was no biological or medical justification to do so and the real goal of these works was rather obvious. The publications he speaks of are only available in Russian [35,36].

Today *F. tularensis* is considered in many countries as a possible bioterrorist threat. In France, it is mandatory to declare cases of tularaemia and *F. tularensis* is included in the list of MOT (Microorganismes et Toxines), the use and possession of which is strictly regulated [37]. *F. tularensis* subsp. *tularensis* can only be manipulated in habilitated labs in BSL3 conditions.

Clinical presentation of tularaemia

Occurrence of symptoms

In his classification of tularaemia, Dr. Francis had described four clinical types: ulceroglandular, oculoglandular, glandular and typhoid [10]. Subsequent epidemiological studies identified two more types: pneumonic [38] and orophagyngeal [39]. Table 1 summarizes the specific features associated with different clinical types of tularaemia. These classifications are based on clinical presentation and routes of infection. The six types of tularaemia have different prevalence and outcomes, which are additionally influenced by the strain of *F. tularensis* responsible for disease. *Francisella* species and strains will be detailed in chapter **The *Francisella* genus**. In short, strains unique to North America (type A) are more virulent and infectious than strains present in Eurasia (type B).

Usually the incubation period is 3-5 days but it can vary from 1 to 21 days. All clinical types are accompanied with sustained fever which can reach up to 40°C. Additionally, patients can suffer from weakness, fatigue, chills, malaise, headache, myalgia, loss of appetite, vomiting, diarrhoea and abdominal pain (Fig.6). Bacteria can disseminate to the lungs through the bloodstream and provoke pneumonia. Severe systemic manifestations have also been reported in advanced cases of tularaemia and are more frequently associated with infections with type A strains: septicaemia, meningitis, endocarditis, erythema and liver failure. In type B tularaemia, pneumonia, meningitis, erythema and sepsis can also occur but generally the outcomes are better [40–43].

Table 1. *Clinical types of tularaemia. Data are compiled from reports of the World Health Organization* [40]*, European Center for Disease Control and Prevention* [44]*, US Centers for Disease Control and Prevention* [43,45,46]*, USGS National Wildlife Health Center* [41]*.*

Type	Symptoms	Route of infection	% cases	Outcome
Ulceroglandular	- painful, discolored skin lesion - swelling of regional lymph nodes	Insect bite or skin contact with infected animal or a contaminated surface; bites from infected animals are sometimes reported.	70-85%	May require lymph node removal.
Glandular	- swelling of regional lymph nodes	Insect bite or skin contact with infected animal or a contaminated surface	5-10%	As above.
Oculoglandular	- unilateral eye inflammation - ulceration of the conjunctiva - swelling of regional lymph nodes	Bacteria entry through the eyes e.g., touching one's eyes after handling sick animals, water spray, etc.	<1%	Advanced cases may result in vision loss
Oropharyngeal	- sore throat - mouth ulcers - tonsillitis - swelling of regional lymph nodes	Eating or drinking contaminated food or water.	Common in Turkey (77% of cases)	May require lymph node removal.
Pneumonic	- dry cough - chest pain - difficulty breathing - enlargement of pulmonary lymph nodes may be seen on X-ray	Inhalation of infectious particles; Complication of other tularaemia types through bloodstream spread of bacteria to the lungs (10% of ulceroglandular cases)	rare	30-60% mortality without treatment
Typhoidal	Systemic reactions with no localized symptoms	Can be any of the above.		

Symptom	Patients	
	Number	Percent
Fever	75	85
Chills	46	52
Headache	40	45
Cough	33	38
Myalgia	27	31
Chest pain	18	20
Vomiting	15	17
Arthralgia	13	15
Sore throat	13	15
Abdominal pain	10	11
Diarrhea	9	10
Dysuria	8	9
Back pain	4	5
Stiff neck	3	3

Figure 6. *Symptoms in 88 tularaemia patients in a review by Martin E. Evans et al., 1985* [47]

Diagnosis and treatment

Due to the generality of symptoms, tularaemia can be easily misdiagnosed for other diseases presenting fever and lymph node enlargement or skin lesions (anthrax, brucellosis, plague, various viral infections, etc.) [40]. It is also a rare disease, thus not typically considered when making a diagnosis.

Laboratory confirmation is generally based on serological testing. *F. tularensis* isolation from clinical samples is not easy and the cultures grow slowly. PCR can be used for diagnosis but may require biopsy [48]. Serological assays that are routinely used for detection of tularaemia include microagglutination, immunofluorescence or ELISA tests [49]. Antibodies might cross-react with *Brucella* spp. [50].

Tularaemia is treatable with antibiotics: aminoglycosides (streptomycin or gentamycin), fluoroquinolones or tetracyclines for a minimum of 10 days but can extend up to 3 weeks for doxycycline treatment [43]. *F. tularensis* is not known to acquire drug resistance in clinical settings.

In a report from 1928 [10] before treatment for tularaemia was available, Edward Francis recorded 3.5% overall death rate (24 out of 679 cases): of these deaths 19 had ulceroglandular or glandular tularaemia (4% death rate); 3 had oculoglandular tularaemia (9.4% death rate); one patient had typhoid (3.5% death rate) and another had generalized symptoms with pneumonia, which would have been classified as typhoid tularaemia at the time. Out of the 24 total deaths, 7 had developed pneumonia as a complication or other forms of tularaemia and 1 had probably been infected through inhalation of aerosols. Another review from 1945 declared 57% mortality in patients who had developed pneumonia [51].

No vaccine is currently licensed but an attenuated strain has been used to vaccinate in the former USSR, and the *F. tularensis* subsp. holarctica strain LVS (Live Vaccine Strain) is used in several countries to vaccinate tularaemia researchers.

Epidemiology

Tularaemia is almost exclusively encountered in the Northern hemisphere (Fig. 7). It is a rare disease with occasional outbreaks in endemic regions.

In North America the cases are concentrated in the central US, around the Missouri river and in the states of Oklahoma and Arkansas. In the last 5 years, the US CDC has reported an average of 250 cases per year.

In Eurasia, tularaemia is endemic in Nordic countries and forest regions throughout central Europe, in Turkey, Siberia and Japan. Reporting of tularaemia is mandatory in the European Union. Between 2015 and 2019 the EU recorded a mean number of 900 cases per year. The European average is skewed by large outbreaks in Sweden and Finland that increase the average of 300-400 cases in calm years to >1000 during epidemics [52].

Although so far rare, *Francisella* strains have been isolated on several occasions from patients and wildlife in Australia and Tasmania. A *Francisella*-like organism was also recently isolated from bed bugs in Madagascar [53] suggesting that *Francisella* infections are more ubiquitous than believed.

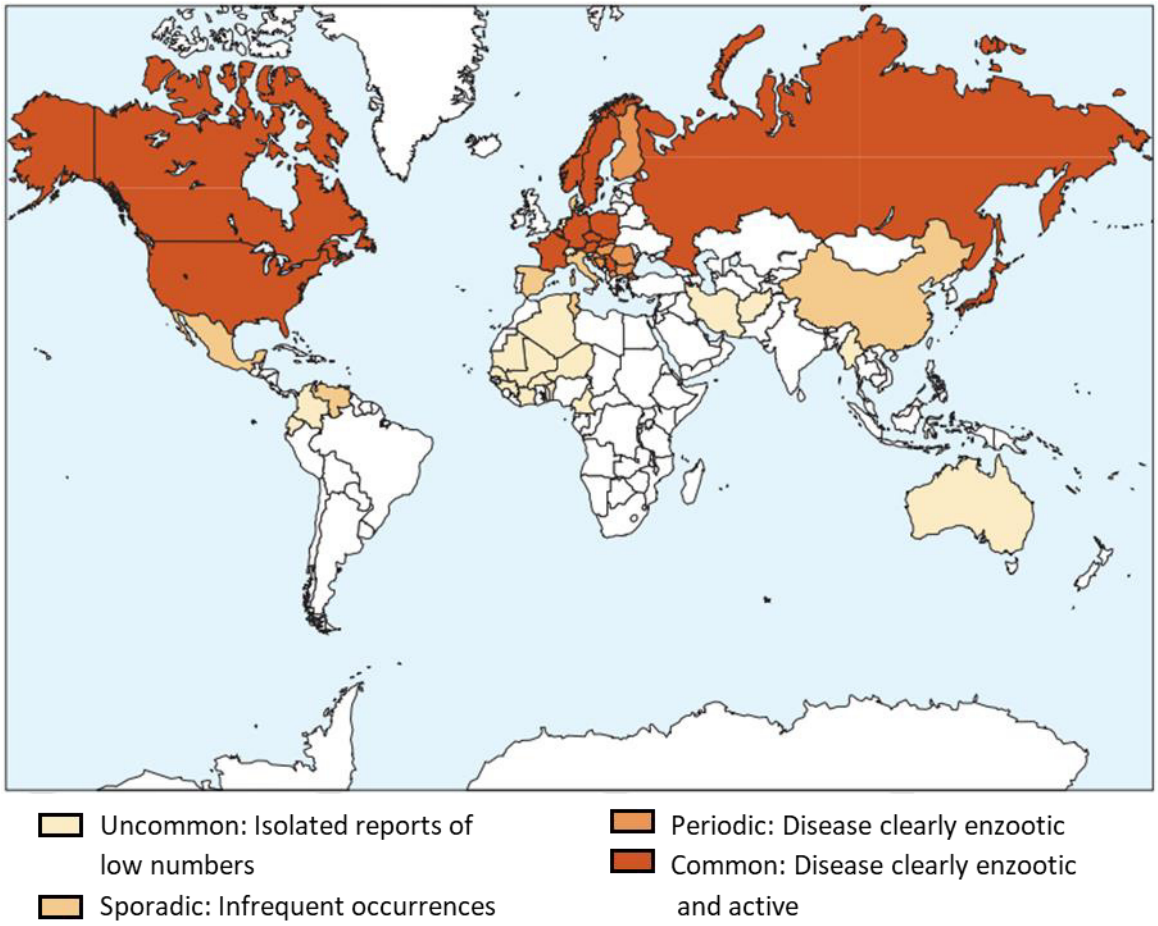

Figure 7. *Geographic distribution of F. tularensis based on reported cases by country. Image taken from a 2006 circular by the US National Wildlife and Health Center* [41].

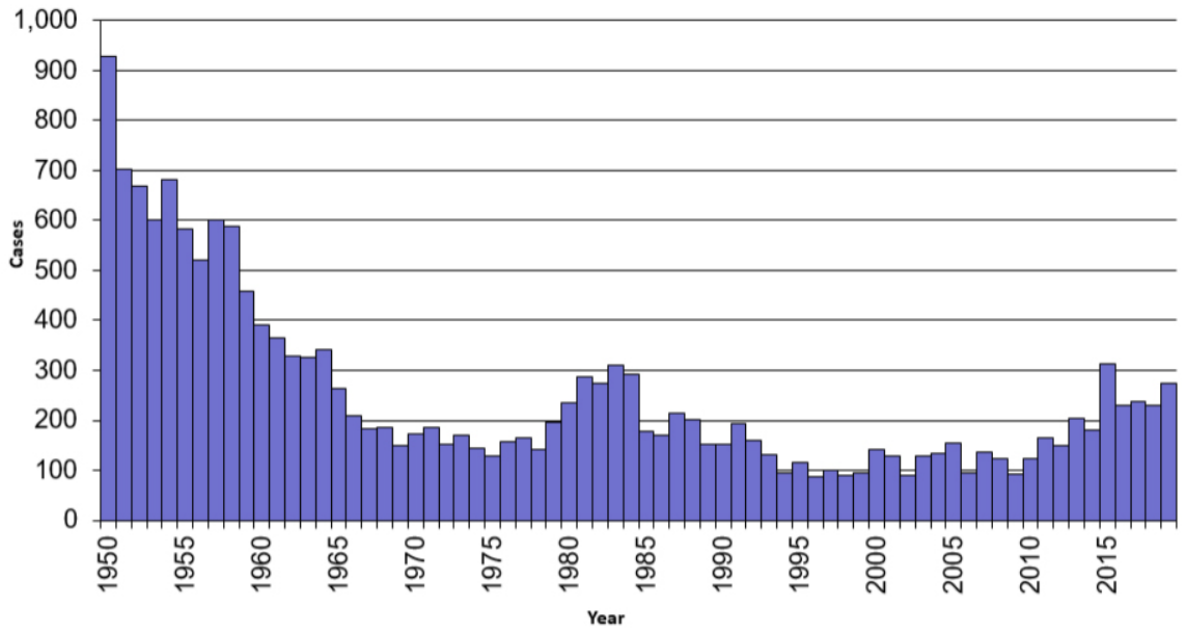

Figure 8. *Yearly number of cases in the US between 1950-2020 reported to the US Centers for Disease Control and Prevention* [43].

Urbanization in the 20th century has significantly decreased the cases of tularaemia reported each year (Fig. 8). Decreased contact with vectors, higher hygiene and sanitation standards contribute to the decline in cases of tularaemia.

In both North America and Europe, tularaemia is most common in the summer months (between May and September) due to increase in tick, fly and mosquito bites and increased participation in outdoor recreational activities (Fig 9). Cases due to hunting occur throughout the year.

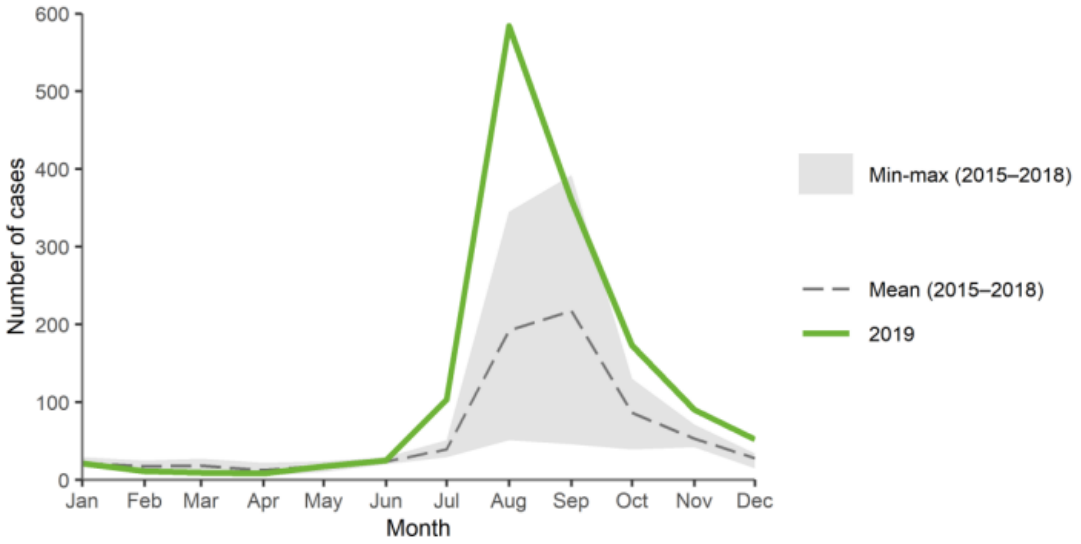

Figure 9. *Monthly distribution of tularaemia cases recorded in the European Union between 2015 and 2019* [52].

The *Francisella* genus

Taxonomy

The *Francisella* genus contains more than 15 species with a continuous addition of newly identified *Francisella*. As of today (31 Jan 2022) the NCBI taxonomy database contains 105 unclassified *Francisella* organisms. Of these, 33 are insect endosymbionts.

The best described species are as follows: *F. tularensis*, *F. noatunensis*, *F. hispaniensis*, and *F. philomiragia*. *F. noatunensis* is a common pathogen in fish such as cod and tilapia, thus it has an economic and ecological importance [54]. *F. hispaniensis* and *F. philomiragia* have been linked to a few cases of tularaemia in immunocompromised persons [55,56]. Almost all cases of tularaemia are caused by *F. tularensis*, the organism identified by George McCoy in California in 1911 [2].

The *F. tularensis* species contains four subspecies: *novicida*, *tularensis*, *holarctica* and *mediasiatica*. *F. tularensis* subsp *tularensis* is unique to North America and associated with type A tularaemia, while *F. tularensis* subsp *holarctica* is endemic to Eurasia and causes type B tularaemia, a less serious form of the disease (refer to chapter **Occurrence of symptoms**). *F. tularensis* subsp. *mediasiatica* is found in Central Asia. No human cases with *mediasiatica* strains have been detected but evidence suggests that this subspecies is at least as pathogenic as *holarctica* for hares and mice [57].

There is disagreement in the scientific community on the categorization of the organism *Francisella novicida* as a separate species or a subspecies of *F. tularensis* [58–60]. On one hand, *novicida* strains share 97% identity and >85% similarity based on DNA-DNA hybridization with *tularensis* strains, considering that 70% is enough to include two organisms in the same species [61,62]. On the other hand, there are significant phenotypic differences between the organisms with regards to metabolism and pathogenicity [62,63]. *F. novicida* has been isolated from tularaemia patients only on few occasions in immunocompromised persons [64–66] or in a near-drowning experience where the patient might have ingested a high bacterial load in the lungs from contaminated water [67].

Microbiologists who support the affiliation of *novicida* to the *F. tularensis* species argue that significant phenotypic differences are often observed within the same species, and that the category of 'subspecies' sufficiently describes the divergence between *novicida* and other *F. tularensis* organisms like *holarctica* and *tularensis* [60].

Currently, genome databases like the NCBI and KEGG classify these bacteria as *F. tularensis* subsp. *novicida*. However, in this dissertation the organism will be referred to as *F. novicida* for simplicity.

Ecology and variety of vectors and hosts

Tularaemia has one of the largest and most diverse spectre of hosts in the animal kingdom among bacterial zoonoses [41,68]. *F. tularensis* has been isolated from mammals [69], birds [70], arthropods [71], fish [72], reptiles, amphibians, crustaceans and molluscs [41].

Historically tularaemia has been associated with rabbits and rodents. Indeed, animals from the orders Rodentia (mice, rats, squirrels, beavers, muskrats, lemmings, voles) and Lagomorpha (rabbits, hares, pikas) are highly susceptible to *F. tularensis* and are the prime source for human infection. Sheep [73] and deer [6] are also naturally infected by *F. tularensis* and common sources for tularaemia in humans. Domestic animals such as swine, horses and dogs [74] are relatively susceptible to tularaemia; cattle, camels and cats [75] have been infected on occasion. [41]

Arthropods are a crucial part of the *Francisella* enzootic cycle as hosts, vectors and reservoirs. The most common forms of human tularaemia in the US are acquired through bites of hard ticks from the genera *Ambylomma* and *Dermacentor*. Ticks also participate in the maintenance of *F. tularensis* in wildlife. Mosquitoes greatly contribute to the occurrence of tularaemia in Northern Europe in wetland regions like Sweden and Finland [76]. Infections in humans have also been associated with horseflies and deerflies in North America and Eurasia [77]. Other arthropods that can carry *F. tularensis* include soft ticks, mites, fleas, lice and bedbugs [41].

Figure 10. *Epidemiologically important tularaemia vectors: A) Ambylomma americanum tick; B) Dermacentor variabilistick; C) Chrysops discalis deerfly; D) Aedes cinereus mosquito*

Although tularaemia is associated with forest regions in terms of hosts and exposure (i.e. hunting and tick bites), aquatic environments comprise a substantial part of the *F. tularensis* infectious cycle. *F. tularensis* subsp. *holarctica* and *novicida* especially are considered to be largely aquatic organisms [48]. *F. novicida* is generally isolated from salty and murky water. Mosquitoes, and aquatic rodents like muskrats and beavers are well-documented sources of infection with *F. tularensis* subsp. *holarctica* in Northern Europe and Russia. Terrestrial and aquatic routes of contamination have been reported in different European countries [48].

A quintessential characteristic of tularaemia is its persistence in environments thanks to survival and propagation of *F. tularensis* in wildlife. It is not clear whether *F. tularensis* survival outside the host, for example in water and soil, significantly contributes to the maintenance of the bacteria in nature [78]. Amoeba may support the persistence of *F. tularensis* in aquatic environments [79].

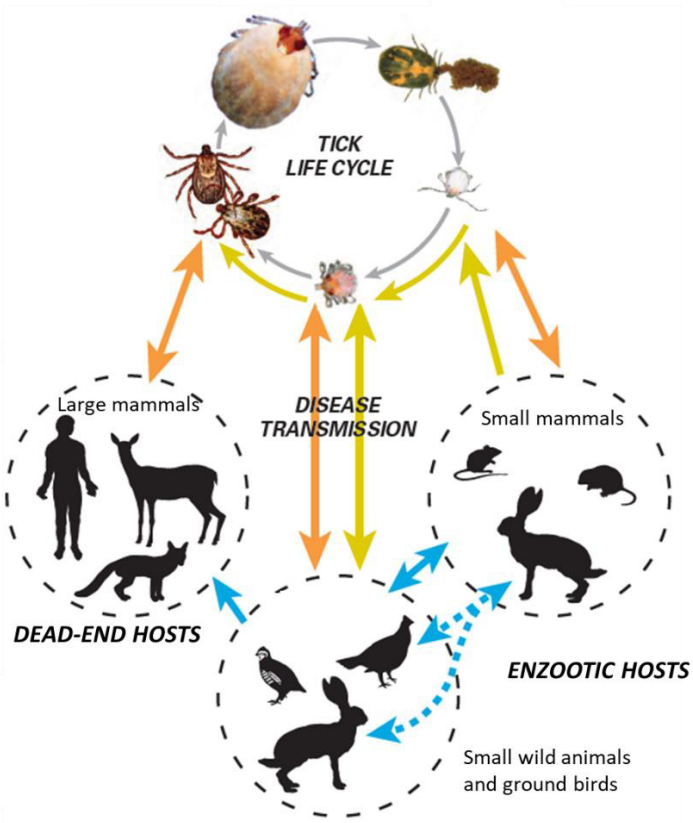

Figure 11. *Example of an enzootic cycle of tularaemia involving transmission through ticks, adapted from the US Wildlife National Health Center report from 2007* [41].

Laboratory models

F. tularensis subsp. *tularensis* is the causative agent of type A tularaemia, the most severe form of tularaemia. Dr. Lee Foshay, a prominent investigator on treatments for tularaemia, isolated a pathogenic strain he named Schu from the ulcer of a patient [80]. A study carried out in Fort Detrick in 1954 further isolated a subtype of Schu, termed Schu S4, based on virulence [81]. Nowadays the strain Schu S4 is the standard laboratory model for virulent tularaemia [82].

Deforestation and increase of rodent populations in town ruins after WWII gave rise to epidemics of tularaemia in the USSR in the years after the war [83]. This led to the development of attenuated strains of *F. tularensis* subsp. *holarctica* to be used for vaccinations. Reportedly, some 60 million people were vaccinated with attenuated strains in the USSR throughout the 1960's. In 1956, a culture was imported into the US but was too heterogeneous; after passage in animals an attenuated strain was purified and designated LVS (live vaccine strain) [84]. This strain was evaluated in an Operation Whitecoat vaccine study [28,29]. LVS conferred immunity in a subcutaneous but not respiratory challenge of *F. tularensis*. Though never licensed for vaccinations, LVS became a commonly used laboratory model for the study of *F. tularensis*. The nature of LVS attenuation is not yet understood.

A *F. tularensis*-like organism was isolated from a lake in Utah in 1950 [85]. This organism was included in the *Pasteurella* genus that contained *Francisella* organisms at the time, and named '*novicida*'. As explained in the chapter **Taxonomy**, this organism has been classified as a subspecies of *F. tularensis* despite controversy in the scientific community. *F. novicida* is not pathogenic to healthy humans, rats or rabbits. It is, however, highly pathogenic for mice and guinea-pigs, in which it causes disease comparably to Schu S4 [63,86]. In a laboratory setting, it readily infects human cells with an intracellular cycle similar to the one of *F. tularensis*. The relative ease of use of *F. novicida* and its close similarity to the genetics and cellular pathogenicity of *F. tularensis*, as well as lower biosafety and regulatory requirements, have contributed to the use of *F. novicida* as a model for the study of tularaemia. *F. novicida* is also easier to manipulate genetically than *F. tularensis* due to its natural competence and to the presence of a single copy of the *Francisella* Pathogenicity Island (in contrast to virulent strains which harbour two almost identical copies) [87]. The strain U112 (Utah 112) originating from the 1950 Utah culture is broadly used in laboratories.

Francisella species represent some of the very few professional-cytosolic pathogenic bacteria. They boast unique pathogenic properties and survival strategies. Thus *F. novicida* is also a great tool to study cytosol-specific host-pathogen interactions.

Francisella pathogenicity

To the lungs and back: Journey through the host

F. tularensis can naturally enter the host through multiple routes: cuts in the skin, injection in the bloodstream by mosquitoes, inhalation of aerosols, ingestion, or through the eyes.

The journey of *Francisella* through the host greatly depends on the route of infection and doubtlessly on the infectious strain as well. Unfortunately, comprehensive studies are lacking. Dissemination kinetics of U112, LVS or Schu S4 are measured with different methods (e.g., quantification of colony-forming units, bioluminescence imaging, positron emission tomography) and produce conflicting timelines.

Generally, regardless of the strain and infection route in mice *Francisella* spread locally during the first day of infection [86,88,89]. In the following days (ranging from day 2-5) the bacteria invade the spleen, liver, lungs, draining lymph nodes and bone marrow [86,89–91]. The mice succumb to the infection in a few days.

Infection in non-human primates follows the same dissemination trend after exposure to aerosolized *F. tularensis* [92,93].

Cell tropism

Francisella strains target mainly phagocytic myeloid cells. Mononuclear phagocytes, notably macrophages, comprise a substantial part of the replicative niche of *F. tularensis* [94,95]. In a comparative study in mice, a day after inhalation of *F. tularensis* bacteria were found primarily in alveolar macrophages and a percentage of dendritic cells but by day 3, more than half of *Francisella*-infected cells in the lungs were neutrophils [86,89]. *F. novicida* had a more neutrophil-targeted tropism early on (Fig. 12) [86,96].

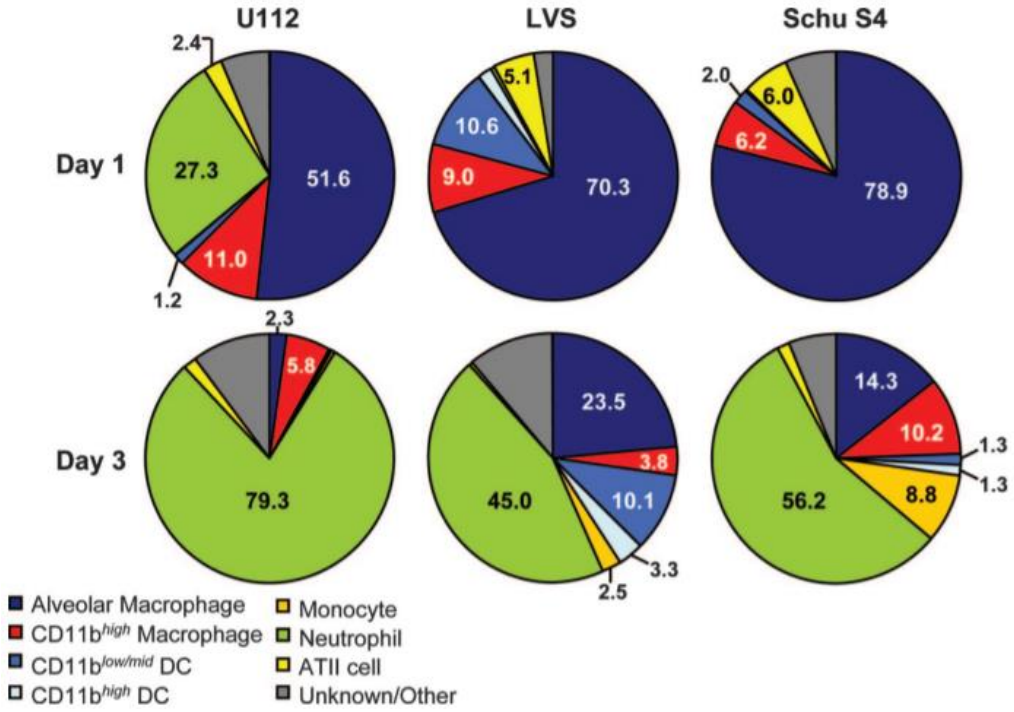

Figure 12. *Cellular tropism of Francisella strains after inhalation in mice, as published by Hall et al., 2008* [86]. *Lung tissue of mice infected with GFP-expressing Francisella analysed by flow cytometry to parse cell populations.*

F. tularensis also infects non-phagocytic cells like epithelial lung cells[4] [97,98] and hepatocytes [99], although the relevance and mechanism of non-phagocyte infection are not clear. *Francisella* invasion and survival in erythrocytes may play an important role in the zoonotic cycle, for example during the transit in arthropods [100,101]. Passage through the respiratory epithelium of mammals could provide access to the bloodstream [97] and allow systemic dissemination of the bacteria, although this process might be less efficient than the colonization of migratory immune cells.

[4] *F. tularensis* Schu S4 replicates abundantly in pneumocytes while LVS replication is severely impacted [97].

The *Francisella* intracellular cycle

Entry into the host cell

F. tularensis manipulates the endocytosis machinery of host cells. Consequently, the mechanism of entry of *F. tularensis* is cell-type dependent. *Francisella* infects non-phagocyting cells like hepatocytes through chlatrin-dependent endocytosis [99] and similarly infects B lymphocyte subsets through a process involving BCR internalization [102]. The invasion of erythrocytes requires spectrin rather than actin rearrangement and the mechanism is unclear [101].

The primary mechanism of *Francisella* host cell entry however is through phagocytosis into myeloid cells. *F. tularensis* induces the formation of a single pseudopod loop that engulfs the bacterium within a spacious vacuole (Fig. 13.A). In contrast, phagocytosis of other intracellular bacteria classically involves two symmetrical pseudopodia. Within several minutes, *F. tularensis* is contained in a closely packed vesicle inside the body of the cell (Fig. 13.B)[103].

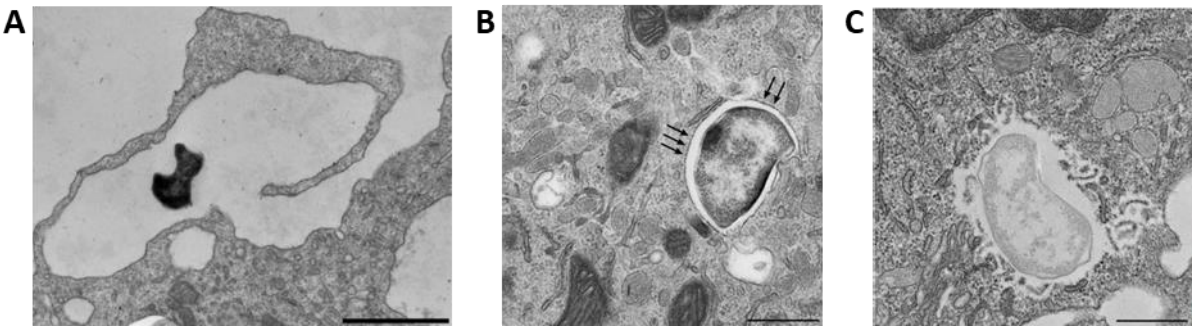

Figure 13. *Electron microscopy images of F. tularensis macrophage invasion. A) Formation of pseudopodia around a F. tularensis bacterium as published in Clemens et al., 2015* [104]*, scale bar 1µm. B) Francisella-containing phagosome imaged 30 min p.i. and C) Disruption of the Francisella-containing phagosome imaged 1h p.i. by Chong and Celli, 2010* [105]*; scale bar 0.5 µm.*

The bacterial effectors involved in the first stages of host cell invasion are obscure. Bacterial outer membrane proteins and type IV pili contribute to adhesion to epithelial cells, and outer membrane vesicles were shown to increase macrophage uptake. Components of the *Francisella* type VI secretion system (T6SS) have also been implicated in host cell entry, although the primary function of the T6SS is phagosome escape (See chapter **Secretion and virulence factors**).

Different macrophage receptors are implicated in the phagocytosis of *F. tularensis*. Uptake of non-opsonized[5] *Francisella* involves the mannose receptor, a pattern recognition receptor that targets bacterial glycoproteins. Complement receptors (notably CR3) and the Fcγ receptor are responsible for phagocytosis of *Francisella* targeted by complement or antibody-mediated opsonization respectively [106–108]. Opsonization greatly enhances *Francisella* entry into macrophages and B cells [102,107]. Opsonization with human serum slows phagosome escape and replication of *F. tularensis* in murine macrophages but not in human cells, in addition to limiting pro-inflammatory responses in the cytosol of human macrophages (see chapter **The complement system**) [109,110].

[5] Opsonization: Pathogens are tagged with opsonins (e.g., antibodies, complement) to facilitate phagocytosis.

Escape from the phagosome

Following phagocytosis, *F. tularensis* resides within a *Francisella*-containing phagosome (FCP). The FCP acquires early and late phagosomal markers such as LAMP-1 and Rab7 but does not fuse with the lysosome [103,111]. Whether the FCP is acidified or not, and whether FCP acidification is a requirement for the escape of *F. tularensis* in the cytosol, is controversial [112–114]. *F. tularensis* does possess enzymes which confer acid resistance but it is unclear whether they play a role while *F. tularensis* is inside the FCP [115].

Similarly, the time required for *F. tularensis* to escape to the cytosol is disputed, ranging from 1h to several hours in various studies[6] [103,105,107]. The conflicting reports might originate in part from the use of different strains and host-cell types, but results are doubtlessly heavily influenced by the detection methods and infection conditions employed (i.e., serum opsonization, as explained above). Commonly used methods for the detection of phagosomal escape are as follows: imaging of FCP with transmission electron microscopy [107,116,117], colocalization with late endosome markers [114], selective permeabilization of the plasma membrane [118], or flow cytometry β-galactosidase activity assay [119]. It seems that different *Francisella* strains begin to disrupt the phagosomal membrane between 1-4h p.i. as observable with TEM (Transmission Electron Microscopy) (Fig. 13.C) and takes between 4 to 12 hours for the phagosome membrane to disappear completely, according to different reports [107,120]. The initial disruption allows access to enzymes and antibodies which might explain earlier escape times reported with other methods.

One unequivocal consensus within the scientific community is the role of the *Francisella* Pathogenicity Island (FPI) and the type VI secretion system (T6SS) encoded within to drive escape into the cytosol [111]. The precise mechanism is not understood, however several T6SS effectors are required for phagosome escape, particularly PdpC and PdpD. These will be detailed in the chapter **Non-canonical type VI secretion system**.

Intracellular life

F. tularensis is non-motile intracellularly. Once the phagosome is permeabilized, the bacteria replicate abundantly. In macrophages and alveolar epithelial cells, *F. tularensis* Schu S4, LVS or *novicida* multiply up to 10^3-fold in 24 hours *in vitro* [97,116,121,122]. *Francisella* T6SS and secreted effectors are not required for intracellular replication specifically [123].

Few bacterial effectors have been identified with precise roles in virulence. Most are involved in nutritional parasitism (transporter channels, enzymes) and targets host metabolic pathways. For example, healthy *Francisella* avoid macroautophagy targeting [124,125] due to the unusual structure of the bacterial envelope (See chapter **Unconventional LPS**) [126]. Rather, *F. tularensis* upregulates and usurps the autophagy machinery of the host cell to supply the bacteria with nutrients. [127,128]

It is generally thought that once the cytosol accumulates sufficiently high bacterial loads, the host cell is lysed and the bacteria are released in the extracellular space where they can re-infect surrounding cells [129]. However experimental evidence to support this idea is lacking. Although macrophages

[6] *Francisella* cytosolic escape has been reported in numerous studies. To avoid encumbrance with citations, only the most pertinent examples are listed in this paragraph. Additional references can be found within the cited articles.

massively undergo cell death upon *F. tularensis* and *F. novicida* infection, this is likely the consequence of immune reactions (i.e., pyroptosis) which will be detailed in subsequent chapters. *F. tularensis* replication in the late stages of infection (between 24h and 48h) is decreased 3-4 log in the presence of gentamycin, a non membrane-permissible antibiotic [130]. This indicates that extracellular bacteria do indeed participate in the infectious cycle at later times. Recent studies have described trogocytosis[7] between macrophages as an efficient mechanism for cell-to-cell spread of *F. tularensis* [131,132]. The *Francisella* containing vacuole resulting from trogocytic infection seems to follow similar maturation and T6SS-mediated lysis as a *de novo Francisella*-containing phagosome [131].

Nutritional virulence

Critical part of *F. tularensis* pathogenicity is the nutritional parasitism. Cysteine is a limiting factor in *Francisella* growth but during infection acquisition of other amino acids by *F. tularensis* (glutamate, arginine, isoleucine) is also essential for survival in the host [130,133,134]. Host glutathione is a source of glutamate and cysteine for *F. tularensis* [135]. Glutamate is cleaved in the bacterial periplasm and transported through the inner membrane by the channel GadC [136]. Glutamate is required during the phagosomal stage of the *F. tularensis* intracellular cycle because it participates in the inactivation of reactive oxygen species through their incorporation in the tricarboxylic acid cycle [137]. Iron acquisition also plays an important role in *Francisella* survival in the host, particularly in response to oxidative stress [138].

To procure essential nutriments and control the fate of the cell, *F. tularensis* alters host metabolism. First, *F. tularensis* exploits autophagy [127] and the unfolded protein response [139]. *F. tularensis* also induces deglycosylation of a number of host proteins through mechanisms that remain to be elucidated but clearly benefit bacterial replication [140]. Further, *F. tularensis* inhibits aerobic glycolysis of macrophages and consequently prevents pro-inflammatory activation [141]. *Francisella* favours gluconeogenesis to glycolysis metabolites. Host fatty acids and amino acids (e.g. glutamate) feed the TCA cycle [137,142]. During infection, the proteome of *F. tularensis* contains increased number of enzymes involved in fatty acid metabolism [143]. *F. tularensis* also uses the pentose phosphate pathway *in vivo* [144].

Secretion and virulence factors

Non-canonical type VI secretion system

Type VI secretion systems (T6SS) are contractile injection systems, similar to bacteriophages. Generally, T6SS serve as killing machines to deliver toxins into other bacteria or host cells. *Francisella* T6SS controls phagosome escape and is indispensable for intracellular replication[8]. Genetically *Francisella* T6SS is an outlier to other characterized T6SS but structurally it is highly similar [111].

T6SS are composed of a membrane complex, a cytosolic sheath and the inner tube (Fig. 14). The membrane complex forms a pore through the inner and outer bacterial membranes and serves as anchor for the secretion system. The cytosolic sheath is a contractible hollow cylinder that forms in

[7] Trogocytosis (or recently renamed merocytophagy) is a process of cytosolic exchange between two cells mediated through cell-to-cell contact.
[8] Another bacterium with a similar T6SS function may be the amoeba pathogen *Amoebophilus asiaticus* [145].

the bacterial cytosol. The inner tube is contained within the cytosolic sheath; it carries a spike at the top and contains the effectors. When the cytosolic sheath contracts, the inner tube passes through the membrane complex and is injected like a needle through the target membrane – in the case of *F. tularensis*, the phagosome membrane [111,146].

F. tularensis T6SS is encoded by the *Francisella* Pathogenicity Island (FPI). *F. tularensis* subsp. *tularensis* and *holarctica* possess two FPI while *F. novicida* carries only one copy, as well as a *Francisella novicida* island (FNI), similar in structure but with unknown implications for *F. novicida* pathogenicity [119].

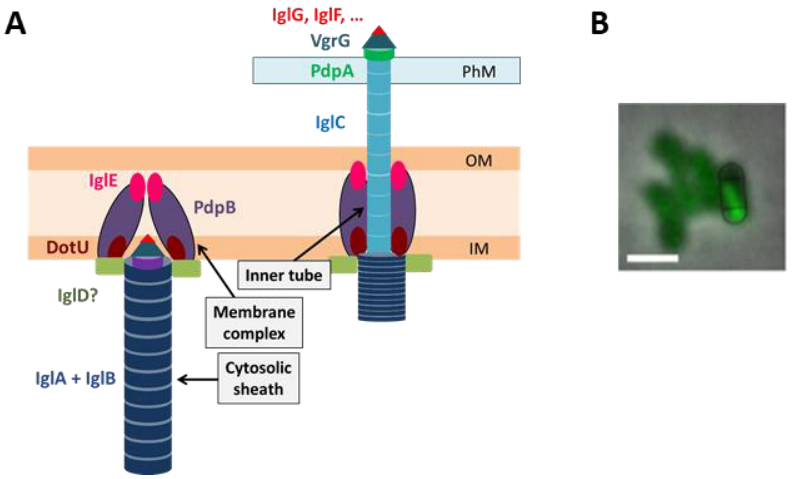

Figure 14. *A) Structure of Francisella T6SS. IM = inner membrane, OM = outer membrane, PhM = phagosomal membrane; B) GFP-tagged IglA illustrating T6SS assembly at the pole of F. novicida* [118]

Francisella T6SS is expressed in conditions mimicking the intracellular environment (iron depletion, oxidative stress etc.) [111]. The transcription factor complex MglA/SspA/PigR and the regulator PmrA control expression of FPI. Their action is dependent on the sensing of environmental cues, for example through the second messenger guanosine tetraphosphate (ppGpp) produced during infection [147,147,148].

Unlike other known T6SS, the *Francisella* T6SS assembles at the bacterial pole [118]. IglA and IglB compose the contractile cytosolic sheath [149]; IglC forms the inner tube and VgrG/PdpA/IglF form the spike [119,150]. The membrane complex consists of DotU, PdpB and IglE [151]. IglF, IgI and IglJ are additionally required for T6SS assembly but their action is unknown [118]. Like other T6SS, *Francisella* T6SS functions in a dynamic manner. Disassembly by the chaperone ClpB are essential for effector delivery and virulence [116,118].

T6SS effectors

Several effectors have been identified thus far but few have a clear role. PdpC and PdpD are critical for phagosomal escape but the mechanism of action is unknown [118]. Deletion of the individual encoding genes has minor effects on survival in macrophages but significantly impacts *Francisella* virulence *in vivo* [152,153]. Interestingly, PdpD is present in *F. novicida* and Schu S4 but absent in LVS [152].

OpiA, OpiB1, OpiB2 and OpiB3 are encoded outside of the FPI. OpiA is a phosphatidylinositol 3-kinase secreted by the T6SS [154]. OpiA delays phagosomal maturation in cells infected with *F. novicida* [155]

but in a study with LVS OpiA did not greatly affect virulence, instead had a role in bacterial fitness [154]. The roles of OpiB1-3 are unknown [156]. Other putative effectors encoded in the FPI are PdpE and AnmK. Mutations of PdpE and AnmK did not detectably effect the infectious cycle in mammal cells [157] but AnmK delayed OpiA-mediated killing of *Galleria mellonella* larvae [158].

Some T6SS proteins have both structural and putative effector roles. IglG/F/I/J, PdpA and VgrG are secreted [118,119]. IglJ may have a function related to the mitochondria, and VgrG might interact with host phagosomal biogenesis systems [159]. IglC, the inner tube component, is also secreted in the host cell. *Francisella* Δ*iglC* mutants are deficient for entry into non-phagocytic cells [102,160].

TolC-like outer membrane proteins

TolC is an outer membrane component of bacterial tripartite efflux systems like multidrug efflux pumps and type I secretion systems. *Francisella* genomes encode for three TolC orthologs: TolC, FltC and SilC. Roles in multidrug resistance have been described for all three *Francisella* proteins. FtlC plays a role in virulence through intradermal route specifically [161]. TolC inhibits pro-inflammatory and apoptotic response in macrophages possibly through effector secretion [161,162]. SilC is involved in resistance to oxidative stress *in vivo* [163].

Type IV pili

Type IV pili are long, thin polymer fibres on the surface of many bacteria and have functions in locomotion, adhesion and virulence. Structures resembling pili have been observed on the surface of Schu S4, LVS and *F. novicida* in different conditions (Fig. 15). Components of the *Francisella* pili (PilE1, PilO, PilA, PilC, PilQ and others) have been attributed roles in virulence [164–166] but their exact functions are unclear.

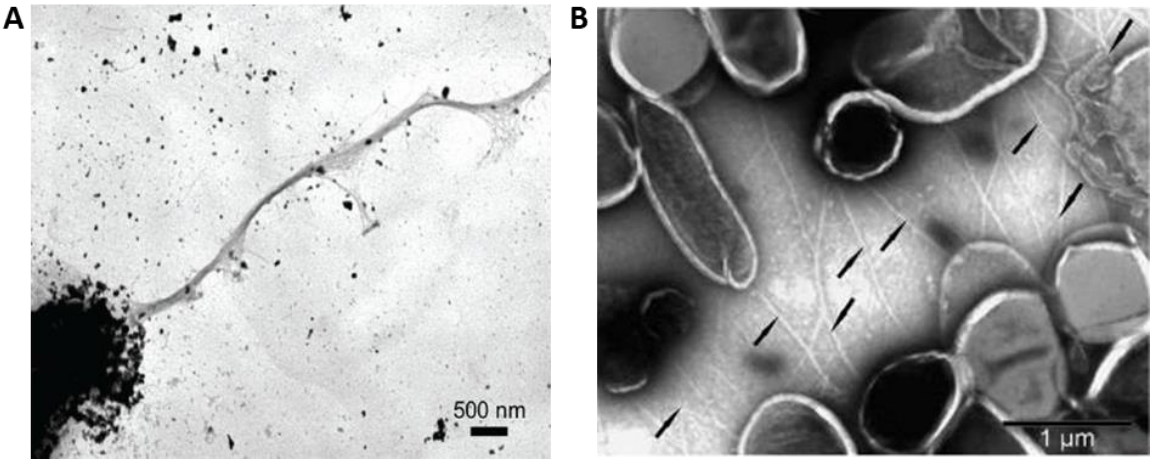

Figure 15. *A) Negative stain TEM of F. tularensis LVS showing a pilus structure, as published in Gil et al., 2004* [167]*;B) TEM of F. novicida pili, as published in Ozanic, Marecic et al., 2022* [165]

Francisella type IV pili might be involved in adhesion to host cells before entry [168,169]. PilE4 is a possible ligand for the surface glycoprotein ICAM-1, expressed in endothelial and lymphoid cells [169].

Certain components of bacterial type IV pili are homologous to proteins involved in type II secretion systems (T2SS). In *F. novicida*, several pilus proteins are considered to be part of a T2SS [170,171]. Effectors include two chitinases (ChiA and ChiB), a metalloprotease (PepO) and a beta-glucosidase (BglX), thus type II secretion in *F. novicida* may be important for virulence in arthropods [170]. Furthermore, expression of PepO and BglX is controlled by MglA – a factor involved in the regulation of *Francisella* pathogenicity genes [170]. The expression and functionality of T2SS is not clear in other *F. tularensis* subspecies.

Outer membrane vesicles or tubes

Outer membrane vesicles, or OMV, are double membrane lipid particles released by Gram-negative bacteria. OMV are composed of the bacterial outer membrane and thus contain LPS, outer membrane proteins, periplasmic proteins and can also harbour bacterial DNA and virulence factors. OMV production is generally induced in stress conditions. OMVs have diverse functions as a communication tool among bacterial communities or in host-pathogen interactions. OMV can act as decoys for bacteriophages, antibacterial peptides or the immune system, e.g., for the complement pathway (See chapter **Immunity to *Francisella***). OMV are internalized in host cells through endocytosis or phagocytosis, thus they can also serve as delivery systems for bacterial virulence factors.

F. novicida and virulent strains of *F. tularensis* produce OMV and OMTs (outer membrane tubes), novel structures with a tubular shape (Fig. 16) [172,173]. Production of OMV/T by *Francisella* is stimulated in contact with host cells or in culture media that mimic the extracellular host environment. Such conditions involve the depravation in amino acids and free iron [174,175], shown to directly induce OMV/T production in *F. tularensis* and *F. novicida* [173,176]. On the other hand, OMV/T production in the cytosol is negligeable [177]. *Francisella* OMV/T might play a role in macrophage adherence and internalisation [177,178].

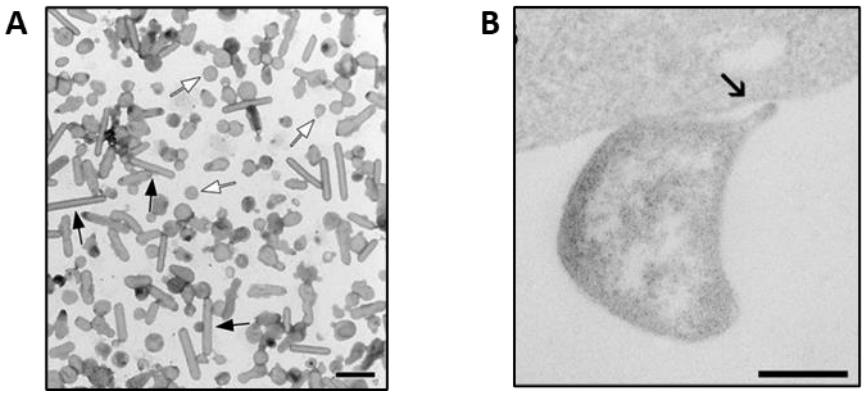

Figure 16. *Francisella strains produce OMV/T. A) TEM images of OMV/OMT (white/black arrows) purified from an early stationary phase culture of F. novicida. Published in McCaig et al., 2013* [172]. *Scale bar, 0.5 µm. B) OMV protrusion of F. tularensis in contact with a macrophage. Published in Pavkova et al., 2021* [177]. *Scale bar, 0.2 µm.*

Other outer membrane and secreted proteins

Many *Francisella* outer membrane proteins are nutrient transporters or metabolism-related enzymes. These are also often characterized as virulence factors because the deletion of the encoding genes affects survival in the host and therefore virulence [179]. Nutritional virulence of *F. tularensis* was described in a previous chapter. Similarly, numerous outer membrane proteins have been identified in virulence screens but for many their precise roles are yet to be elucidated [179,180]. Virulence of an intracellular pathogen is inadvertently dependent on bacterial fitness and survival in the host cell; hence it is complicated to discuss 'true' virulence factors without understanding the exact function of the protein.

F. tularensis produces many anti-oxidant enzymes (SodB, SodC, KatG and others) that might be released through a process involving putative secretion protein EmrA1 or OMVs [181–183].

FsaP is an outer membrane protein involved in adhesion to epithelial cells. Interestingly, *F. novicida* has a mutation in FsaP that interferes with its interaction with epithelium [184].

Surface bacterial lipoproteins such as Lpp3 and LpnA have also been identified in virulence screens somewhat controversially [185,186]. Their function is still unknown; however they are potent activators of the host pattern recognition receptor TLR2 [187]. LpnA is among several lipoproteins, along with outer membrane protein FopA that are putative interactors of plasminogen, a precursor of the proteolytic enzyme plasmin – thus may have a role in *F. tularensis* tissue invasion [188].

The lipoprotein DsbA is an isomerase and disulfide oxoreductase. DsbA is likely not a *bona fide* virulence factor but modifies many putative effectors such as FopA, DipA, MipA [189,190].

Another *F. tularensis* outer membrane protein, FTT0831c, was shown to block NFκB translocation to the nucleus [191]. Yet, a later study suggested that this protein has a structural role and that its deletion impacts bacterial integrity, resulting in an altered immune response [192].

Overall, *F. tularensis* virulence factors are poorly characterized. More in-depth studies should be done on the mechanisms of *F. tularensis* intracellular pathogenicity.

Immunity to *Francisella*

Overview of adaptive and long term anti-*Francisella* immunity

In 1932 before antibiotics were available for the treatment of tularaemia, Dr. Lee Foshay successfully treated nine patients with the serum of goats inoculated with formalin-killed bacteria [17]. A patient 'received in dying condition' did not recover. Years later, Foshay found that serum treatment had certain limitations in comparison to streptomycin, and that to be efficacious, serum had to be prepared with live bacteria and given in the first days of infection [193].

The role of humoral response to *Francisella* has been somewhat disputed. Patients and laboratory animals develop antibodies when infected with tularaemia or inoculated with tularaemia vaccines [194]. However, *F. tularensis* is essentially an intracellular pathogen and as such, cell-mediated

immunity is crucial for the successful control of *F. tularensis* infection [195]. Accordingly, killed bacteria vaccines (like the Foshay vaccine) that induce primarily humoral response, are much less efficient in preventing tularaemia than vaccination with live attenuated strains [196,197].

Immune memory to tularaemia is also not well understood. Most of the work on immune memory and vaccines has been performed in murine models of tularaemia. It should be taken into account that mice have higher susceptibility to attenuated *Francisella* strains than humans or primates [63]. Due to the rare natural occurrence of tularaemia, it is complicated to evaluate vaccine efficacy or the effects of repeated exposure in humans. Reinfections and infections among vaccinated laboratory workers have been documented [23,24,198]. Still, patients who have had previous exposure to tularaemia develop weaker symptoms compared to first-time patients.

Both in humans, and in mice, the vaccination route (intradermal or respiratory) greatly affects the response to challenge with virulent *F. tularensis* [28,29,199]. This implies an important role of resident lymphocyte populations to the establishment of anti-*Francisella* immunity [200]. Despite the high proportion of naturally occurring cutaneous infections, knowledge on skin immunity to *Francisella* is lacking.

Adaptive responses will not be detailed further here as they are not the focus of this dissertation. The current knowledge on adaptive immunity to tularaemia has been well summarized by Roberts *et al*. [201] and Bahuaud et al. [202]; Additionally, Sunagar *et al*. [203], Elkins *et al*. [197], and Conlan and Oyston [204] have written interesting reviews on the challenges of tularaemia vaccine development.

Innate immunity to *Francisella*

The *Francisella* lipopolysaccharide elicits weak immune response

Classical structure of a bacterial lipopolysaccharide

Although a "classical" LPS will have deviations in almost every specie of Gram-negative bacteria, there are certain features that are more predominantly encountered in Gram-negative lab models such as *Enterobacteriaceae* (*Escherichia*, *Shigella*, *Salmonella*, etc.). Fig. 17A and B illustrate the *E. coli* LPS, exemplifying a classical LPS structure.

The LPS is composed of an inner lipid moiety (lipid A) connected through an oligosaccharide core to a glycan polymer (O-antigen) which is exposed on the bacterial surface.

The *E. coli* lipid A is composed of 6 acyl chains, commonly between C12-C14 of length, connected to a glucosamine disaccharide which is phosphorylated at the 1 and 4' position [205]. The core oligosaccharide is composed of two keto-deoxy-octonate (KDO) residues followed by the inner and outer core. The inner and outer core contain respectively heptose and glucose backbones of several residues. Additional sugar residues are attached to the backbone.

The O-antigen is composed of repeating units of several sugars. The composition and number of repeats are highly variable in a species. In fact, the O-antigen variation is what determines serotypes within species and subspecies of bacteria – for instance, the species *S. flexneri* contains 18 different serotypes [206]. Particular serotypes often has clinical and immunological significance.

The atypical *Francisella* envelope

The LPS of *Francisella* species has a relatively conserved and rather particular structure. Fig. 17 shows the composition of Francisella LPS and Fig. 18 illustrates several key enzymes involved in the synthesis and modification of *Francisella* LPS.

First, the lipid A contains only four acyl chains in contrast to the hexa-acylated LPS of E. coli [207]. The acyl chains are also longer: between 16 and 18 carbon residues, although the length is modifiable depending on the temperature: 16C at 25C and 18C at 37C. LpxD1 acyltransferase transfers a C18 acyl group and LpxD2 transfers C16 acyl group. LpxD1 is necessary for host adaptation [208]. LpxD1 is active at 37°C while LpxD2 is active at room temperature (insect or environment adaptation) [209].

A particularity of *Francisella* LPS is the high content of free lipid A (>60%) [210,211], i.e., not linked to a core and O-chain (Fig. 17B). The biological relevance of the high proportion of free lipid A in *Francisella* is yet to be investigated [212]. Free lipid A is similar in lipid composition to the core and O-chain-linked lipid A but they are differently modified in the disaccharide part (Fig. 17B and C). The lipid A disaccharide, which is connected to the core oligosaccharide and the O-chain, is not phosphorylated, unlike the E. coli disaccharide which has two phosphate residues (1'and 4'). *F. novicida* free lipid A can exist in two forms [213]: type I which is phosphorylated on 1', and type II which is phosphorylated on both residues. However, the phosphorylated residues are further modified with an additional galactosamine or mannose/glucose sugar.

LpxE is a phosphatase that removes the phosphate in 1 position [214,215] in O-antigen linked lipid A. LpxF removes the phosphate in 4' position [216] and is required for deacetylase activity to remove the 3' position acyl chain [217]. Free lipid A to LPS ratio is 60/40 [211].

Free lipid A does not carry the 4' phosphate but has the 1 phosphate. The 1 phosphate in free lipid A is modified with galactosamine. Free lipid A can be additionally modified with a mannose in the 4' position [210] or a hexose in the 6' position. This additional modification is stimulated upon acidic pH, thus may be an adaptation related to phagosome survival [218]. FlmX is a flippase associated with transport of galactosamine residue that will be attached to free lipid A [219]. NaxD is a deacetylase participating in the galactosamine synthesis [220]. FlmK transfers the hexose residues [221] and FlmF1 and FlmF2 participate in synthesis [222] of mannose and galactosamine respectively [223].

The core is also unique to *Francisella* species – it is smaller than *E. coli* core as it consists of a single KDO, connected to two mannose residues that form the backbone additionally connected to other sugars [224]. The KDO disaccharide is added to the LPS precursor but the second KDO is later removed in the periplasm by hydrolase KdoH1/KdoH2 [225]. KDO removal was implicated in dampening TLR2 recognition but the mechanism is unknown – might be indirect [226].

The *Francisella* O-antigen is composed of repeated tetrasaccharide units [227].

Francisella species also produce a capsule involved in virulence and survival. Two morphotypes have been described for virulent F. tularensis SchuS4 strains, corresponding to poorly characterized differences in capsule: blue (virulent) and grey (avirulent) phenotypes [179]. *F. novicida* also produces a capsule-like complex which represents an agglomeration of O-antigen units without a particular structure on the surface of the bacterium [228]. The capsule synthesis pathway is genetically inseparable from the LPS-linked O-antigen synthesis with genes participating in both processes, which

hinders the functional characterization of this capsule. The capsule of *F. tulareneis* LVS was described to also contain covalently linked lipid A which is similar in composition to free lipid A [211].

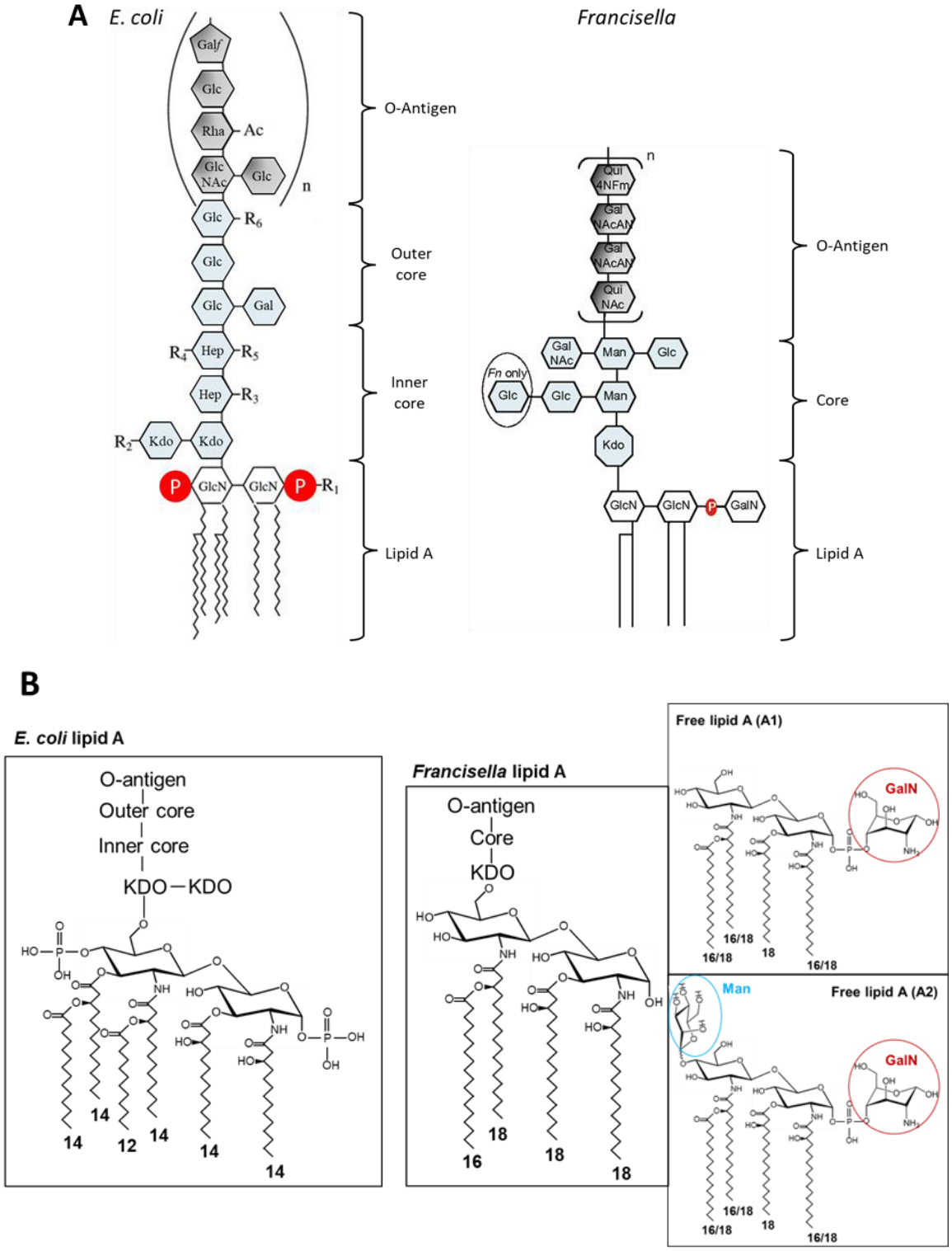

Figure 17. *Atypical* Francisella *LPS compared to* E. coli *LPS. A) Structure of* E. coli *and* Francisella *LPS. Data from Kadrmas and Raetz, 1998* [205] *and Okan and Kasper, 2016* [212]. *B) Structure of* E. coli *and* F. tularensis *lipid A. Free lipid A represents 60% of surface lipid A in F. tularensis.*

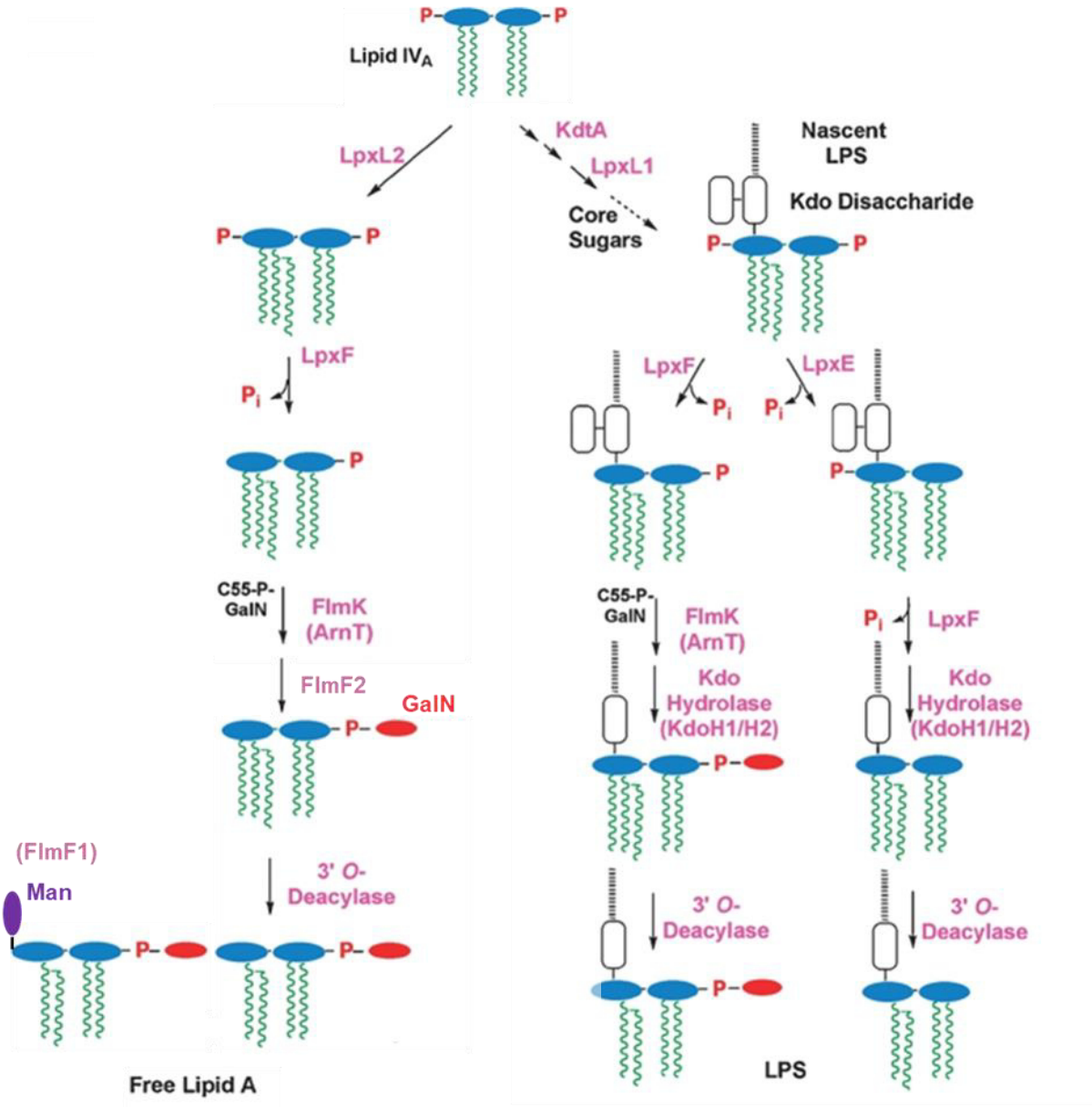

Figure 18. *Modifications of* F. tularensis *LPS, published in Wang et al., in 2009* [229] *and updated with data from Kanistanon et al., 2008* [223].

The *Francisella* LPS as an invisibility cloak

Extracellular LPS is recognized by LPS-binding protein (LBP) in the plasma, then transferred by CD-14 to co-receptor MD-2 which forms a complex with cell membrane-associated TLR-4 (Fig. 19A). TLR-4 activation triggers the NFkB pathway and expression of immune including the ones coding for pro-inflammatory cytokines and interferons [230]. LBP and the MD-2/TLR4 complex bind the lipid A moiety. Lipid A, also called endotoxin, is a PAMP for Gram-negative bacteria and a strong inducer of inflammatory response [231,232]. *E. coli* lipid A is a strong agonist of TLR4 signalling [231]. In contrast, *Francisella* LPS does not elicit TLR4 response due to its hypo-acylated lipid A [233].

Intracellularly, LPS (particularly lipid A) is detected by inflammatory caspase-4 in humans or the orthologue caspase-11 in mice. Similarly, E. coli lipid A elicits strong activation of pro-inflammatory caspases while *Francisella* lipid A is not detected by murine capsase-11 and only weakly activates human caspase-4 [234]. On the other hand, a pentaacylated mutant of *F. novicida* triggers robust caspase-11 activation [217,235] but not TLR4 signalling [216].

Furthermore, the decreased in phosphorylation and the aminosugar conjugation of lipid A contribute to an overall less charged (or more positively charged) LPS which might increase resistance to cationic antimicrobial peptides. Dephosphorylation of *E. coli* LPS by *F. novicida* lipid A phosphatase LpxE increases sensitivity to polymyxin B and decreases TLR4/MD-2 activation [236]. Several other *Francisella* enzymes involved in lipid A dephosphorylation and glycan conjugation have also been linked to virulence and immune system avoidance [220,223].

The presence of a single KDO unit instead of a double KDO also dampens immune recognition. *F. tularensis* mutant with 2 KDO units is less virulent in mice and induces higher inflammatory response than WT *F. tularensis* [226].

Francisella has more free lipid A than other bacteria but removing O-antigen completely in *Francisella* mutants triggers hypercytoxicity [237,238]. This might be due to diminished fitness of the bacteria.

Finally, the O-antigen and the capsule have been linked to autophagy and C3 complement avoidance by *Franicsella* [126,239]. As capsule synthesis is related to the O-antigen machinery, it is tricky to evaluate the contribution of one versus the other [240]. Additionally, deletion of O-antigen also decreases bacterial viability thus may influence autophagy and complement susceptibility [126].

The complement system

The interactions between *Francisella* and the complement system are briefly discussed in the chapters **Entry into the host cell** and **The *Francisella* envelope elicits a weak immune response**. A great summary on the subject can be found in an article by Brock and Parmley [109]. *F. tularensis* is somewhat resistant to human serum and resistant to complement-mediated bacteriolysis [239,241]. *Francisella* strains acquire C3 convertase but divert the complement towards opsonisation, which is beneficial for the bacteria as it facilitates entry into host cells [239,242,243]. Additionally, efficient opsonin-mediated phagocytosis of Schu S4 interferes with TLR2 signalling once inside the host cell [244,245]. The mechanisms of complement resistance are not entirely clear but it might have to do with the *Francisella* capsule and O-antigen structure [239,240].

Toll-like receptors

TLR4 is the classical pattern recognition receptor for Gram-negative bacteria and is activated by the bacterial lipopolysaccharide in conjuncture with LPS-binding protein MD-2 (Fig. 19). TLR4 responds little, if at all, to *Francisella* LPS (see chapter **The *Francisella* lipopolysaccharide**) [246,247]. Instead, *Francisella* lipoproteins induce TLR2 signalling [248]. Only *F. novicida* and *F. tularensis* LVS activate TLR2 but not *F. tularensis* Schu S4 [247,249]. Additionally, in *F. novicida* bacterial lipoproteins are downregulated by CRISPR/CAS9 systems upon infection [250].

Interestingly, TLR2, TLR4 or TLR9 are dispensable for survival of *F. tularensis* LVS infection in mice but MyD88[9] is essential [251,252]. However *in vitro,* in primary human and murine myeloid cells, pro-inflammatory cytokine release is dependent on TLR2 priming [253,254]. Important consequences of TLR2 and MyD88 stimulation are the upregulation of interferons and pro-inflammatory cytokines which participate in anti-*Francisella* response. The reader is referred to chapters **Cytokine production upon infection: major protective role of IFNγ** and **Macrophages and inflammation**.

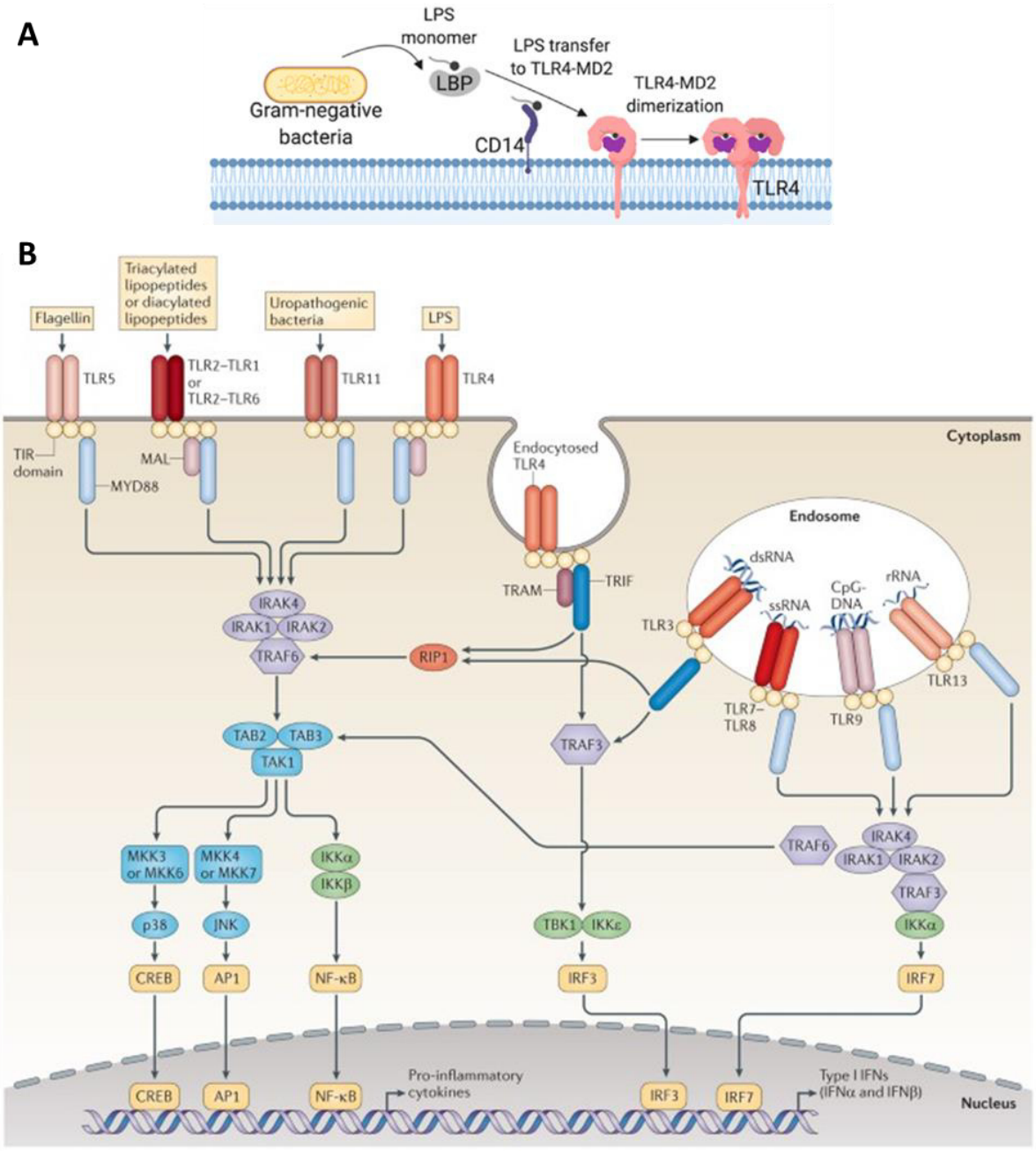

Figure 19. *Toll-like receptors and PAMPS. A) Extracellular LPS recognition and transfer to TLR4, published in Mazgaeen and Gurung, 2020* [255]*. B) Intracellular TLR signalization, published in O'Neill et al., 2013* [256]*.*

[9] MyD88 is a TLR signalling adaptor protein but also acts downstream of other immune receptors like IL-1R or IL-18R.

Cytokine production upon infection: major protective role of IFNγ

Cytokines expressed in early infection of mice are TNF, IL-12, IL-18 and IFNγ [257,258]. IFNγ is crucial for protection against tularaemia. In the first days, TNF and IFNγ are especially important [259–261]. Administration of IFNγ improves resistance of mice to LVS while blocking with IFNγ-specific antibodies increases bacterial loads and increases death rate [259,262].

The major sources of IFNγ upon infection with *Francisella* are first NK cells (which are primed by IL-12 and IL-18 [263]), and later on T lymphocytes [264]. IFNγ induces expression of interferon stimulated genes (ISG) involved in innate and cell autonomous immunity, notably the Immunity Related GTPases (IRG) [265] and Guanylate Binding Proteins (GBP). These will be detailed in subsequent chapters (**Innate immune responses in macrophages** and **Introduction Part II. Guanylate Binding Proteins**).

Type I IFN production also plays a role in controlling *Francisella* infection, particularly in the beginning of the infection by stimulating innate recognition [266]. However high production of type I interferon is deleterious for the host (as is also observed for *Listeria monocytogenes* [267]). The mechanisms are still unclear but may involve a decrease in IL-17 production and neutrophil expansion [268] and an increase in apoptosis [269]. The following article provides a great general review on type I IFN and infections: [267]. Type I IFN can also induce GBPs through STAT and IRF9 signalling (Fig. 20) [270].

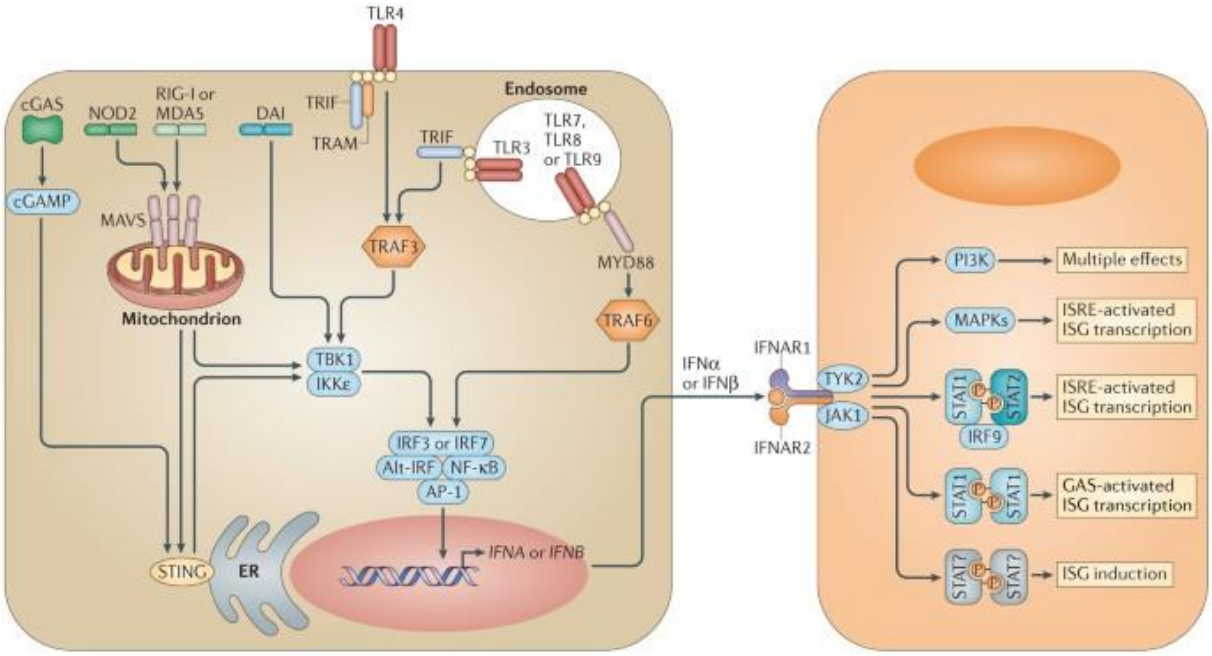

Figure 20. *Type I interferon signalization and induction of interferon-stimulated genes* [271].

Innate immune cells: replicative hosts and sentinels

Neutrophils and oxidative response

Neutrophils are abundant but short-lived leukocytes that succumb to apoptosis 24h-48h after their release into the circulation. Their death is further accelerated upon phagocytosis of pathogens, which is followed by the release of reactive-oxygen species and a type of programmed cell death called phagocytosis-induced cell death (PICD). Additionally, they can release chromatin to trap

microorganisms (NET, or Neutrophil Extracellular Traps), thus undergoing a cell death called NETosis. [272,273]

Neutrophils are recruited to the lungs during *F. tularensis* infection and represent a large percentage of *Francisella*-infected cells (see chapter **Cell tropism**) [274]. Whether neutrophils have a protective role during *Francisella* infection has been somewhat disputed [275,276]. MMP-9 activity (including the induction of neutrophil tissue invasion) is detrimental to infected mice and exacerbates tissue damage. MMP-9-deleted mice survive Schu S4 infection [276]. Additionally, LVS stimulates the release of NETs which contribute to tissue damage but the bacteria survive while entrapped in NETs [277]. While challenge with Schu S4 kills mice regardless of immunocompetency [278], neutrophils protect mice from sublethal infection with LVS [261,279,280]. Importantly, a neutropenic patient succumbed to *F. tularensis* subsp. *tularensis* infection despite intensive antibiotic treatment [281].

Neutrophils readily phagocyte opsonized LVS but do not kill the bacteria efficiently. *F. tularensis* inhibits oxidative burst and NADPH activity through multiple mechanisms which are not perfectly clear [282,283]. Several *Francisella* enzymes have been identified as anti-oxidants and to play a role in resistance to oxidative stress: superoxide dismutases sodC, sodB [183] and the catalase KatG [284,285] which is secreted by membrane fusion protein EmrA1 [182]. T1SS-like SilC pump is also involved in resisting reactive oxygen species [161]. The importance of the *Francisella* acid phosphatase AcpA is controversial [275]. Host amino acids, notably glutamate, are modified by ROS and integrated in the bacterial metabolism [137] (See chapter **Nutritional virulence**).

Additionally, *F. tularensis* SchuS4, LVS and in a lesser degree U112 inhibit neutrophil apoptosis [286–288] and maintain neutrophil mitochondrial integrity [289]. This process is mediated by bacterial outer membrane lipoproteins through pathways involving TLR-2 signalisation [187].

Thus, *Francisella* alter neutrophil function by blocking oxidation and delaying apoptosis. The accumulation of neutrophils might contribute to tissue damage observed in sick animals [290].

Innate immune responses in macrophages

Detection of bacterial DNA in murine macrophages

In murine macrophages cytosolic Gram-negative bacteria typically activate LPS sensor caspase-11 [291] and type III secretion system/flagellin sensor NLRC4 [292]. However caspase-11 does not detect *Francisella* LPS due to modifications in the lipid A moiety [291]. Secondly, *Francisella* do not carry a T3SS/flagellin apparatus. Instead, the primary *Francisella* pathogen-associated molecular pattern (PAMP) in the macrophage cytosol is bacterial DNA[10].

Initially, *Francisella* DNA is detected by the cyclic GMP-AMP synthase (cGas), assisted by gamma-interferon- inducible protein Ifi204 (the murine ortholog of human Ifi16) [295]. Production of secondary messenger cGAMP activates STimulator of Interferon Genes protein (STING) allowing expression of type I interferon (Fig. 21) [296]. Type I IFN signalling is required for subsequent inflammasome activity [269,295,297].

[10] To a lesser degree, this is also the case for Gram positive *Listeria monocytogenes* [293,294].

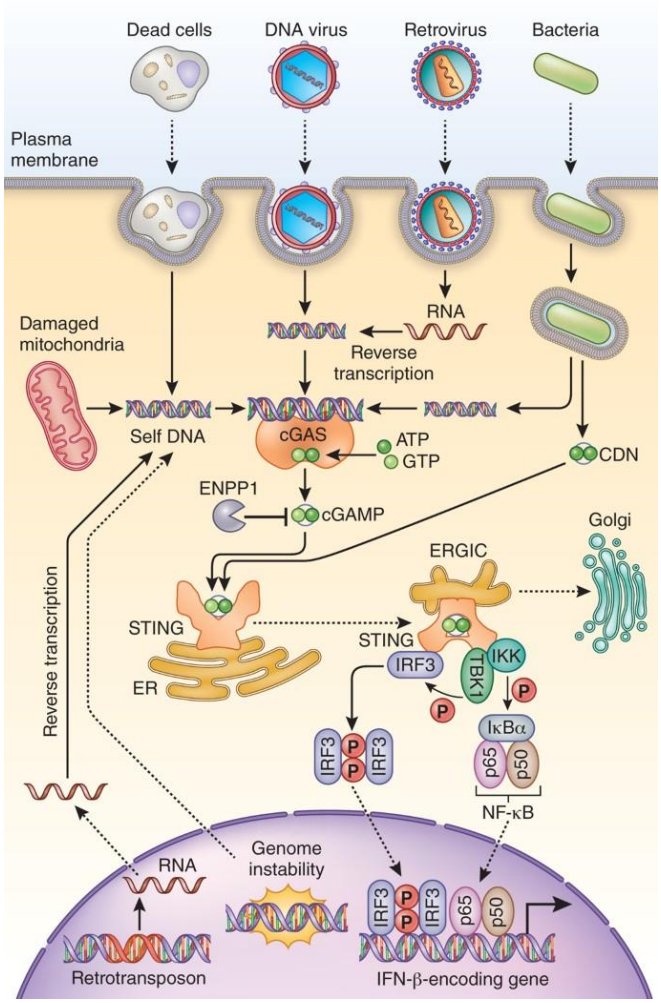

Figure 21. *Schematic representation of cGas-STING pathway, published in Chen et al.,2016* [298].

In a second step, *Francisella* DNA is detected by the Absent in melanoma 2 (Aim2) sensor [296,299]. Aim2 is an inflammasome receptor: Aim2 oligomerizes on cytosolic DNA (which acts as a scaffold) and interacts with adaptor protein ASC to recruit activate pro-inflammatory caspase 1. This multiprotein complex is the Aim2 inflammasome, illustrated in Fig. 22 [300]. Aim2 can cooperate with another inflammatory sensor, pyrin, to boost caspase-1 activation [301], although the role of pyrin in *Francisella* infection is still unclear. Caspase-1 cleaves the pore-forming protein Gasdermin D which inserts itself in the cell membrane [302]. The resulting cellular rupture is accompanied by the release of pro-inflammatory cytokines interleukin 1β and 18, also processed by caspase-1. This inflammatory cell death is referred to as pyroptosis [303]. As a retroactive control, potassium influx through gasdermin D pores inhibits cGas and type I interferon production [304].

Aim2 cofactors: key role of Guanylate Binding Proteins (GBP) and Immunity-Related GTPases (IRG)

Type I interferon, induced by the cGas/STING pathway, activates the expression of interferon-inducible GTPases: Guanylate-Binding Proteins (GBP) and Immunity-Related GTPases (IRG) [305,306]. GBPs, especially mGbp2 and mGbp5, localize to cytosolic *F. novicida* [307] and recruit Irgb10 [306]. GBPs and Irgb10 induce bacteriolysis which has two important consequences: 1. Liberation of bacterial DNA which is detected by Aim2 [305–307], and 2. Restriction of bacterial replication independently of Aim2

activity [307,308]. In fact, Aim2 activation is entirely dependent on GBP and Irgb10 activity. Mice deleted for *GBP*s[11] do not survive sublethal *F. novicida* infections [307,308].

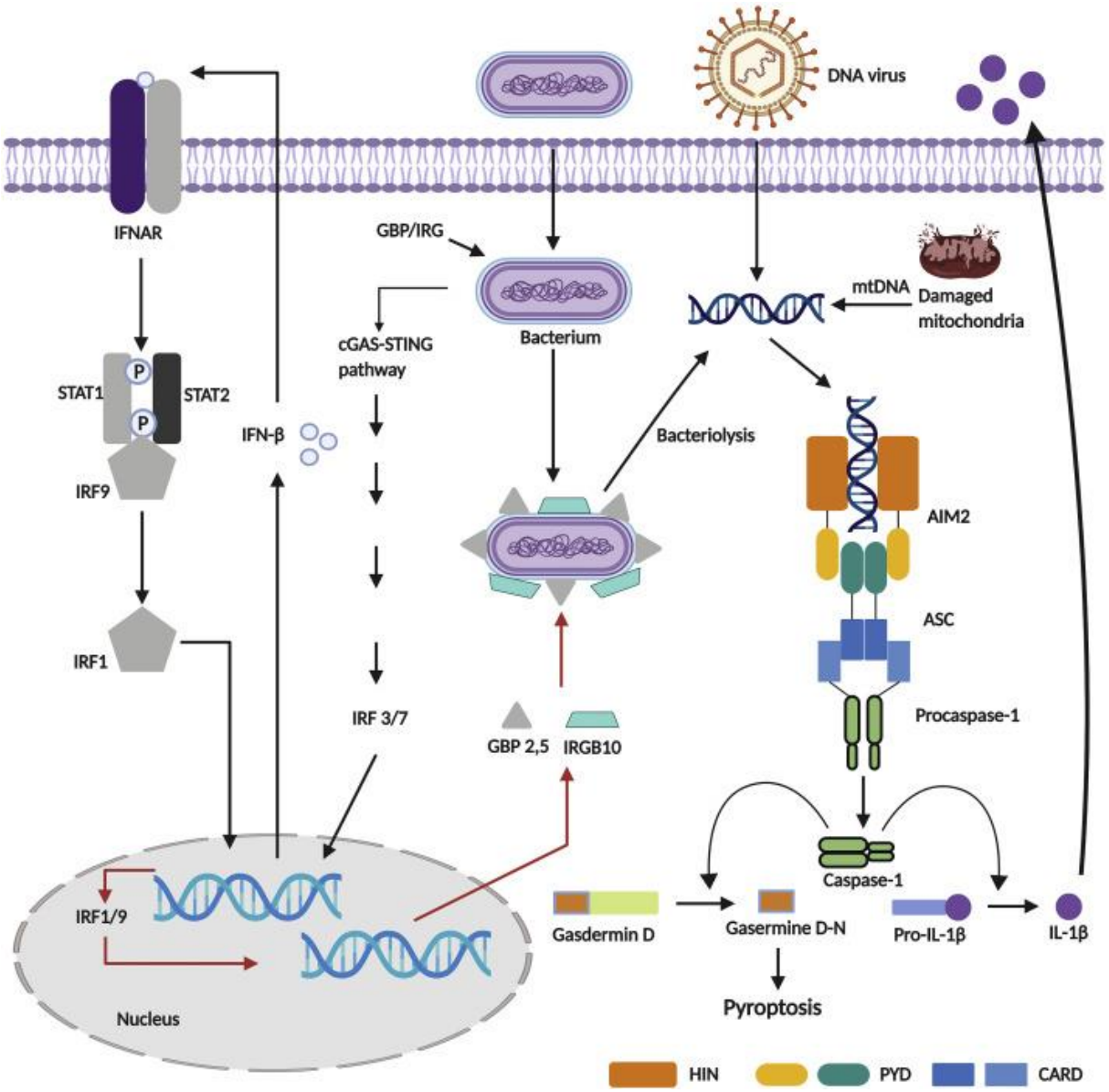

Figure 22. *AIM2 activation in the murine macrophage by diverse stimuli: liberation of bacterial ligands for AIM2 activation depends on GBP and IRG-mediated bacteriolysis (Wang et al., 2020* [300]*).*

It is particularly curious how cGas but not Aim2 is initially activated by cytosolic bacterial DNA before GBP and Irgb10 expression, and why cGas-detected DNA does not activate Aim2 even though Aim2 is basally expressed and can be activated by simple transfection of poly(dA:dT) [299].

A recent study showed that cGas/STING signalization promoted packing of bacterial DNA into vesicles, that were secreted and activated cGas in bystander cells [309]. Still, initial cGas activation is not explained.

[11] Specifically, murine GBPs encoded in chromosome 3 (Gbp2, Gbp3, Gbp5, Gbp7) – see Figure 26.

F. novicida detection in human macrophages

Francisella infection is predominantly studied in primary murine-derived macrophages. However, there are several important differences in the innate immunity defences to *Francisella* in the human and murine macrophages.

Although in murine macrophages Aim2 plays a crucial role in limiting *F. novicida* infections, inflammasome activation in the human macrophage by *F. novicida* is Aim2 and pyrin-independent [234,310]. While murine LPS sensor caspase-11 does not detect *Francisella* LPS, the human orthologue caspase-4 is activated by *F. novicida* [234]. Pro-inflammatory caspase-4 oligomerizes and auto-activates upon detection of cytosolic LPS. Caspase-4 cleaves gasdermin D but not pro-IL-1β and pro-IL-18. Instead, gasdermin D pore formation results in potassium efflux which triggers secondary activation of the NRLP3 inflammasome – or, the non-canonical inflammasome activation (Fig. 23). Cytokine release is triggered as consequence.

Our group previously demonstrated that caspase-4 and NLRP3 activation by *F. novicida* also depend on GBPs in human macrophages [234]. However, in human cells GBPs do not seem to lyse bacteria and this might be explained by the fact that *IRGB10* is not encoded in human genomes [311]. Additionally, murine GBPs are not direct orthologues of human GBPs [312]. Knowledge is lacking on specific GBP roles and activity in human cells.

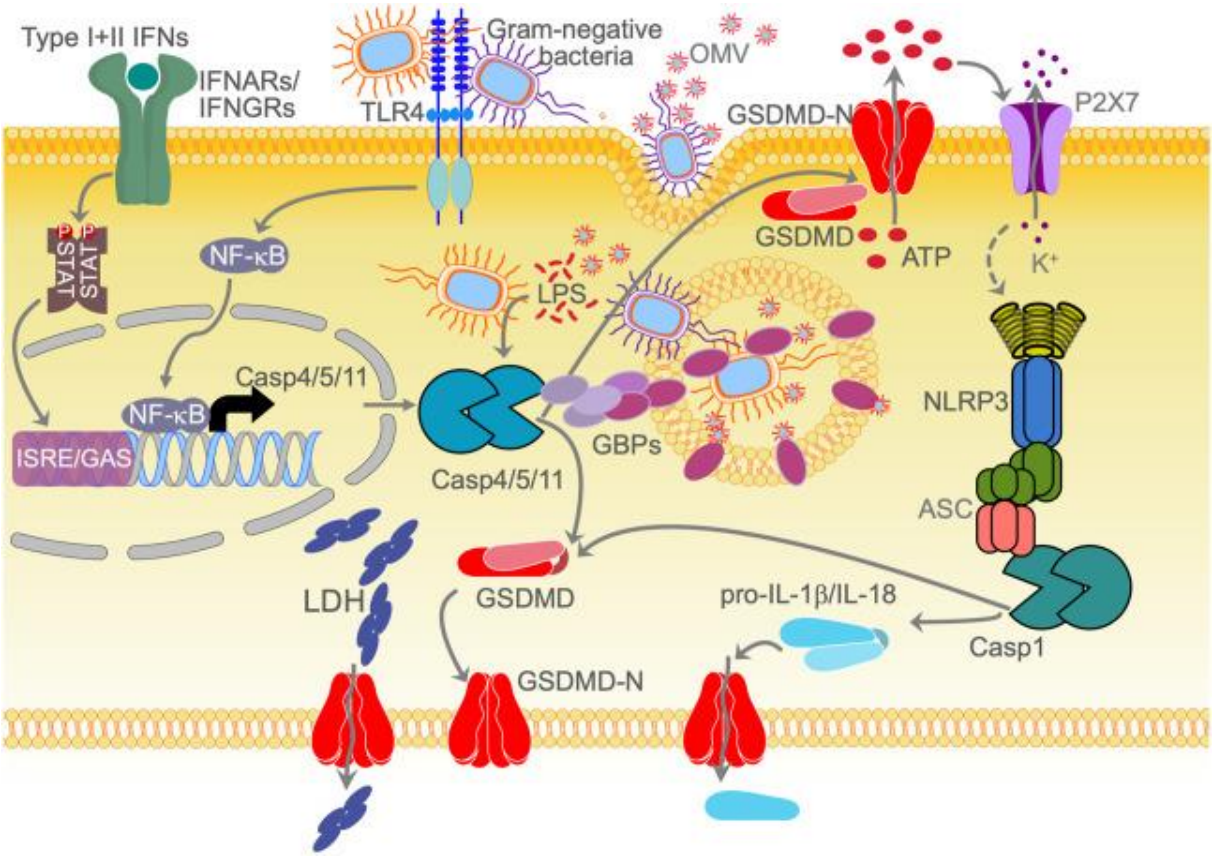

Figure 23. *Non-canonical activation of NLRP3 through caspase-4 and GBP activity, published in a review by Downs et al., 2020* [313].

Virulent *F. tularensis* escapes the inflammasome

Aim2 activation in the murine macrophage is essential in clearing sublethal *F. novicida* infections. Pyroptotic cell death removes the replicative niche of the bacteria while stimulating IFNγ production and cell-mediated immunity through IL-1β and IL-18 release [263,299,314]. On the other hand, *F. tularensis* LVS only weakly stimulate Aim2 and Schu S4 largely evades Aim2 activation [315–317]. It was hypothesized that LVS failure to induce the inflammasome is in part due to weak stimulation of TLR2 resulting in low expression of pro-interleukin 1β [317]. Is has also been proposed that Schu S4 is resistant to mitochondrial ROS in contrast to *F. novicida* and that may contribute to decreased detection of Schu S4 by Aim2 [316]. Furthermore, GBPs mediate IFNγ-dependent growth restriction of *F. novicida* and to a lesser extent of *F. tularensis* LVS but have no significant effect on *F. tularensis* SchuS4 growth [315].

The general evasion of Schu S4 of innate immunity is a key factor in its high virulence. It is therefore essential to understand the inflammatory responses to less virulent strains as a stepping stone to elucidating the mechanisms of immune evasion by virulent *F. tularensis* and targeting them appropriately.

II. Guanylate Binding Proteins (GBPs)

Guanylate-Binding proteins are interferon-inducible GTPases belonging to the dynamin superfamily of mechano-chemical enzymes. There are 7 GBPs in humans (GBP1-7).

GBPs are important actors of innate and cell autonomous immunity against a large spectre of cytosolic pathogens, including numerous viruses, bacteria and protozoa. Although GBPs have been at the centre of attention in the last years, the precise mechanisms of anti-microbial actions are still unclear.

The following chapters will detail the current knowledge on GBP genetics, biochemistry and roles in immunity.

The GBP family

GBPs are part of the dynamin superfamily

The dynamin superfamily is comprised of large (>70 kDa) modular GTPases which function as mechano-chemical enzymes, i.e., they use energy from enzymatic reactions (GTP hydrolysis) to perform mechanical work [318,319].

Many of the members of this family are associated with membrane modulating functions [320]. Well-known examples of dynamin-like proteins (DLP) include:

- The membrane fission protein dynamin which controls cellular endocytosis. Dynamin was the first DLP to be characterized, hence the name of the superfamily [321].
- Membrane fusion proteins like atlastins, involved in functions of the endoplasmic reticulum; or mitofusins which control mitochondrial fusion [322]
- Interferon-inducible GTPases including GBPs and myxovirus resistance proteins (Mx).

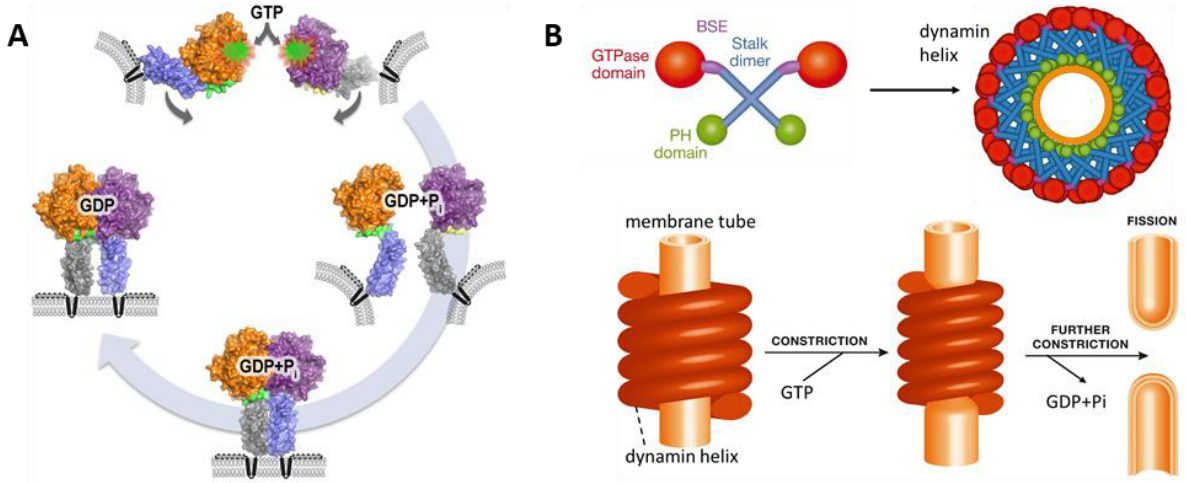

Figure 24. *Membrane-related functions of dynamin-like GTPases. A) Membrane fusion, mediated by atlastin-1 dimerization upon GTP hydrolysis* [323]. *B) Membrane fission, mediated by dynamin polymer movement upon GTP hydrolysis. Adapted from Antonny et al., 2016* [324].

Dynamin-like proteins contain a globular GTPase domain at the N-terminus, and an elongated α-helical bundle at the C-terminus. Additional domains at the C-terminus are related to the specific function of the protein, such as proline-rich domains or transmembrane domains [318].

Dynamin-like GTPases have low affinity for nucleotides but relatively high basal GTP hydrolysis rates [318,325]. Contrary to the Rab/Ras GTPase family, dynamin-like proteins do not require guanine exchange factors or activating proteins to support GTP-GDP turnover. Rather, they contain internal domains or motives that stabilize interaction with nucleotides and catalyse GTP hydrolysis [319,326]. The residues involved in nucleotide binding and GTP hydrolysis are conserved among dynamin-like proteins. They are reviewed in a publication by Jimah and Hindshaw [319].

GTPase domains of dynamin-like proteins allow dimerization in the presence of nucleotides [325]. The dimers are stabilized in the transition state and disassemble upon hydrolysis. The C-terminus stalk mediates dimerization or polymerization of the protein upon GTP hydrolysis. GTP turnover additionally induces rearrangement of the dimers or polymers, producing movement and/or force[325,327].

Interferon-inducible GTPases

As their name suggests, these GTPases are expressed in response to interferon stimulation. They participate in various mechanisms of cell-autonomous and innate immunity. IFN-inducible GTPases can be divided into four families: Myxovirus resistance proteins (Mx), Immunity-Related GTPases (IRG), Guanylate-Binding Proteins (GBP) and Very Large Inducible GTPases (VLIG). Only GBPs and Mx proteins belong to the dynamin-like superfamily. IFN-inducible GTPases have emerged in chordates but different families are more or less conserved [328].

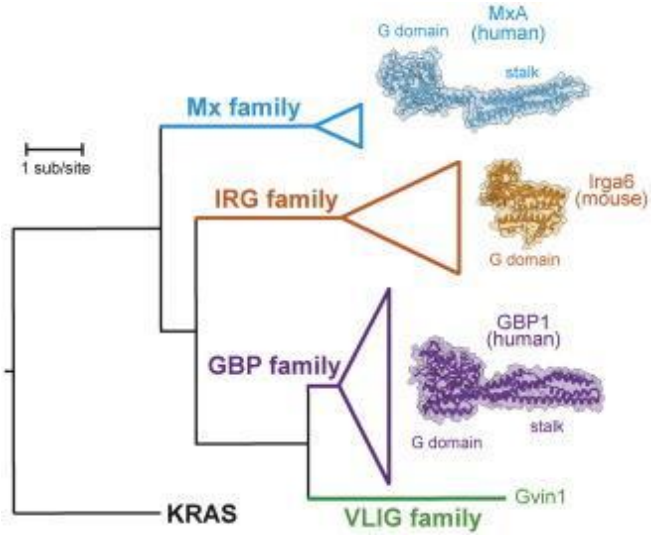

Figure 25. *Maximum likelihood phylogeny of interferon-inducible GTPases, published by Pilla-Moffett et al., 2016* [329].

Mx proteins have inhibitory functions against DNA and RNA viruses, such as the influenza virus, HIV-1, measles virus, herpesvirus and many others [330]. The mechanism of action is not completely clear. They might interact with viral particles but may also exhibit membrane-related functions. Following a dimer or tetramer nucleation event, Mx proteins form ring-like structures necessary for antiviral activity [331].

IRGs are small GTPases (30-47 kDa). They have undergone substantial evolutionary modifications. Whereas mice possess more than 20 identified IRGs, human genomes only carry two [332,333]. Murine IRGs have prominent immune roles against intracellular microbes, notably related to lysis of pathogens or pathogen-containing vacuoles and often in cooperation with GBPs or the autophagy system [329,334] (see chapter **GBPs in cell autonomous immunity**). Human IRGC is constitutively expressed in the testes without a known function [332], while Irgm1 (which is also constitutively expressed) is involved in control of mitochondrial function and autophagy [335].

The VLIG family is still obscure. The murine VLIG-1 produces a giant 280 kDa protein and is strongly induced upon infection with *Listeria monocytogenes* [336]. The only human VLIG gene, GVIN1, is still considered a pseudogene, although there is some transcriptional evidence that it might be expressed [337]. To my knowledge, no functional studies have been conducted so far.

Evolution of the GBP family

GBP-encoding genes have been identified in groups throughout the Chordata phylum, predating the establishment of Vertebrates [328]. *GBP* genes have sustained multiple events of duplication and deletion throughout their evolution. There are substantial genetic and functional differences in *GBP* genes even among closely related species, for instance within order Primates between humans and Old World Monkeys [338–340], or within the order Rodentia between mice (*Mus musculus*) and rats (*Rattus rattus*) [341]. Thus, murine GBPs are not homologous to human GBPs genetically or functionally (Fig. 26) [312]. This adds an element of complexity to the deciphering GBP function as many GBP-related studies, especially earlier ones, were done in murine macrophages.

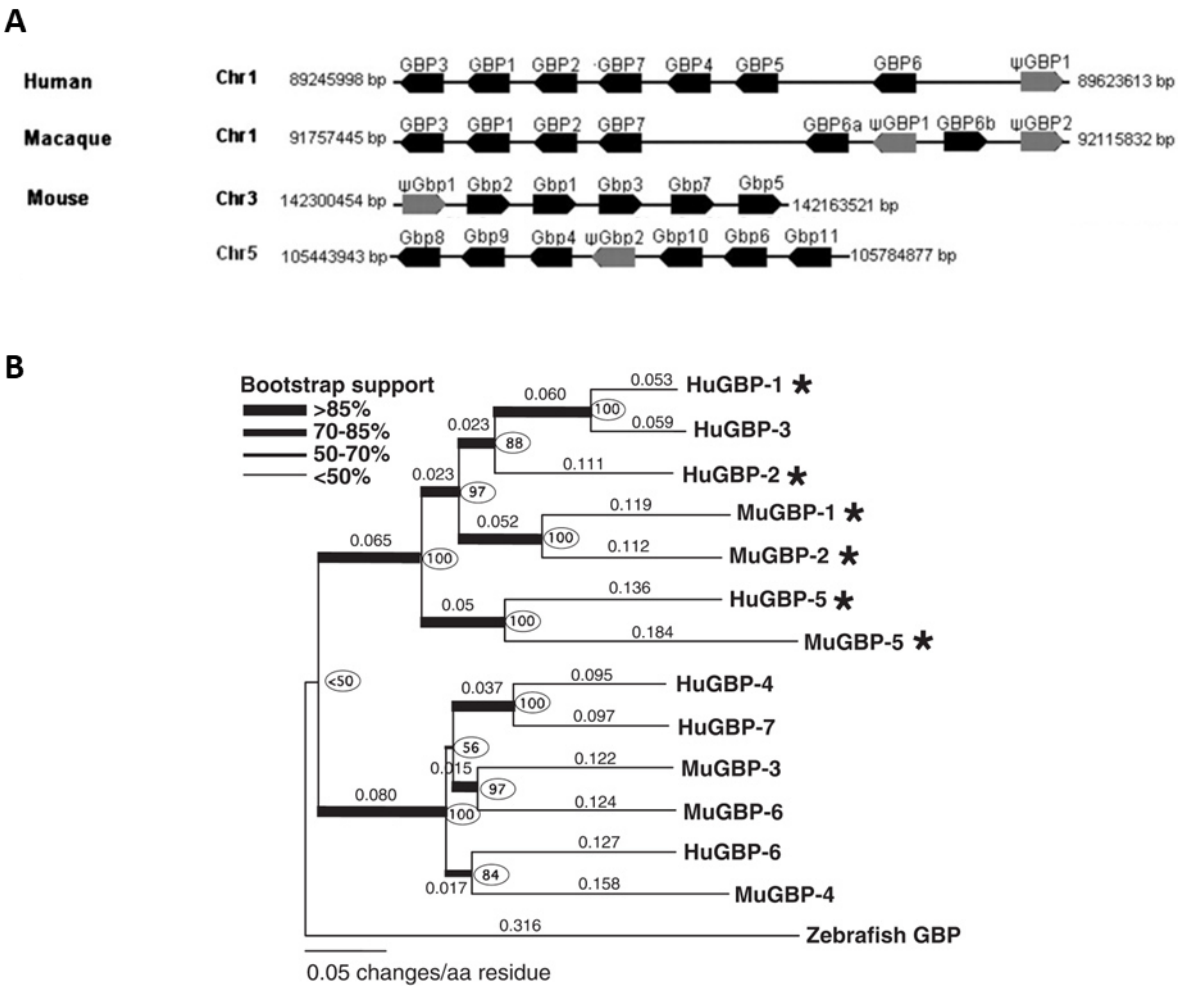

Figure 26. *Phylogeny of GBPs. A) Chromosomal disposition of human, macaque and murine GBP genes as published by Li et al., 2009* [328]*. B) Phylogenetic tree of human and mouse GBPs, published in Olszewski et al., 2006* [312].

```
GBP1_P32455      --------------MASEIHMTGPMCLIENTNGRLMANPEALKILSAITQPMVVVAIVG  45
GBP3_Q9H0R5      --------------MAPEIHMTGPMCLIENTNGELVANPEALKILSAITQPVVVVAIVG  45
GBP2_P32456      --------------MAPEINLPGPMSLIDNTKGQLVVNPEALKILSAITQPVVVVAIVG  45
GBP5_Q96PP8      --------------MALEIHMSDPMCLIENFNEQLKVNQEALEILSAITQPVVVVAIVG  45
GBP4_Q96PP9      MGERTLHAAVPTPGYPESESIMMAPICLVENQEEQLTVNSKALEILDKISQPVVVVAIVG  60
GBP7_Q8N8V2      --------------MASEIHMPGPVCLTENTKGHLVVNSEALEILSAITQPVVVVAIVG  45
GBP6_Q6ZN66      --------------MESGPKMLAPVCLVENNNEQLLVNQQAIQILEKISQPVVVVAIVG  45
                                     :  *:.* :* : .* .* :*::**. *:**:*******

GBP1_P32455      LYRTGKSYLMNKLAGKKKGFSLGSTVQSHTKGIWMWCVPHPKKPGHILVLLDTEGLGDVE  105
GBP3_Q9H0R5      LYRTGKSYLMNKLAGKNKGFSLGSTVKSHTKGIWMWCVPHPKKPEHTLVLLDTEGLGDVK  105
GBP2_P32456      LYRTGKSYLMNKLAGKKNGFSLGSTVKSHTKGIWMWCVPHPKKPEHTLVLLDTEGLGDIE  105
GBP5_Q96PP8      LYRTGKSYLMNKLAGKNKGFSVASTVQSHTKGIWIWCVPHPNWPNHTLVLLDTEGLGDVE  105
GBP4_Q96PP9      LYRTGKSYLMNRLAGKRNGFPLGSTVQSETKGIWMWCVPHLSKPNHTLVLLDTEGLGDVE  120
GBP7_Q8N8V2      LYRTGKSYLMNKLAGKNKGFPLGCTVKSETKGIWMWCVPHPSKPNHTLILLDTEGLGDME  105
GBP6_Q6ZN66      LYRTGKSYLMNHLAGQNHGFPLGSTVQSETKGIWMWCVPHPSKPNHTLVLLDTEGLGDVE  105
                 ***********:***:.:**.:..**:*.*****:***** . * * *:*********::

GBP1_P32455      KGDNQNDSWIFALAVLLSSTFVYNSIGTINQQAMDQLYYVTELTHRIRSKSSPDENENEV  165
GBP3_Q9H0R5      KGDNQNDSWIFTLAVLLSSTLVYNSMGTINQQAMDQLYYVTELTHRIRSKSSPDENEN--  163
GBP2_P32456      KGDNENDSWIFALAILLSSTFVYNSMGTINQQAMDQLHYVTELTDRIKANSSP--GNNSV  163
GBP5_Q96PP8      KADNKNDIQIFALALLLSSTFVYNTVNKIDQGAIDLLHNVTELTDLLKARNSP--DLDRV  163
GBP4_Q96PP9      KSNPKNDSWIFALAVLLSSSFVYNSVSTINHQALEQLHYVTELAELIRAKSCP--RPDEA  178
GBP7_Q8N8V2      KSDPKSDSWIFALAVLLSSSFVYNSMGTINHQALEQLHYVTELTELIRAKSCP--RPDEV  163
GBP6_Q6ZN66      KGDPKNDSWIFALAVLLCSTFVYNSMSTINHQALEQLHYVTELTELIKAKSSP--RPDGV  163
                 *.: :.*  **:**:**.*::***::..*:: *:: *: ****:. ::::...*    :

GBP1_P32455      EDSADFVSFFPDFVWTLRDFSLDLEADGQPLTPDEYLTYSLKLKKGTSQKDETFNLPRLC  225
GBP3_Q9H0R5      EDSADFVSFFPDFVWTLRDFSLDLEADGQPLTPDEYLEYSLKLTQGTSQKDKNFNLPRLC  223
GBP2_P32456      DDSADFVSFFPAFVWTLRDFTLELEVDGEPITADDYLELSLKLRKGTDKKSKSFNDPRLC  223
GBP5_Q96PP8      EDPADSASFFPDLVWTLRDFCLGLEIDGQLVTPDEYLENSLRPKQGSDQRVQNFNLPRLC  223
GBP4_Q96PP9      EDSSEFASFFPDFIWTVRDFTLELKLDGNPITEDEYLENALKLIPGKNPKIQNSNMPREC  238
GBP7_Q8N8V2      EDSSEFVSFFPDFIWTVRDFTLELKLDGHPITEDEYLENALKLISGKNPQIQNSNKPREW  223
GBP6_Q6ZN66      EDSTEFVSFFPDFLWTVRDFTLELKLNGHPITEDEYLENALKLIQGNNPRVQTSNFPREC  223
                 :*.:: .**** ::**:*** * *: :*. :* *:**  :*:   *.. : :. * **

GBP1_P32455      IRKFFPKKKCFVFDRPVHRR-KLAQLEKLQDEELDPEFVQQVADFCSYIFSNSKTKTLSG  284
GBP3_Q9H0R5      IRKFFPKKKCFVFDLPIHRR-KLAQLEKLQDEELDPEFVQQVADFCSYIFSNSKTKTLSG  282
GBP2_P32456      IRKFFPKRKCFVFDWPAPKK-YLAHLEQLKEEELNPDFIEQVAEFCSYILSHSNVKTLSG  282
GBP5_Q96PP8      IQKFFPKKKCFIFDLPAHQK-KLAQLETLPDDELEPEFVQQVTEFCSYIFSHSMTKTLPG  283
GBP4_Q96PP9      IRHFFRKRKCFVFDRPTNDKQYLNHMDEVPEENLERHFLMQSDNFCSYIFTHAKTKTLRE  298
GBP7_Q8N8V2      IRHFFPKQKCFVFDRPINDKKLLLHVEEVREDQLDSNFQMQSENFCSYIFTHAKTKTLRE  283
GBP6_Q6ZN66      IRRFFPKRKCFVFDRPTNDKDLLANIEKVSEKQLDPKFQEQTNIFCSYIFTHARTKTLRE  283
                 *:** *:***:** *   :  * ::: : :.:*: .*  *   *****:::: .***

GBP1_P32455      GIQVNGPRLESLVLTYVNAISSGDLPCMENAVLALAQIENSAAVQKAIAHYEQQMGQKVQ  344
GBP3_Q9H0R5      GIKVNGPRLESLVLTYINAISRGDLPCMENAVLALAQIENSAAVQKAIAHYDQQMGQKVQ  342
GBP2_P32456      GIPVNGPRLESLVLTYVNAISSGDLPCMENAVLALAQIENSAAVEKAIAHYEQQMGQKVQ  342
GBP5_Q96PP8      GIMVNGSRLKNLVLTYVNAISSGDLPCIENAVLALAQRENSAAVQKAIAHYDQQMGQKVQ  342
GBP4_Q96PP9      GIIVTGKRLGTLVVTYVDAINSGAVPCLENAVTALAQLENPAAVQRAADHYSQQMAQQLR  358
GBP7_Q8N8V2      GILVTGNRLGMLVETYLDAINSGATPCLENAMAVLAQCENSAAVQRAANHYSQQMAQQVR  343
GBP6_Q6ZN66      GITVTGNRLGTLAVTYVEAINSGAVPCLENAVITLAQRENSAAVQRAADYYSQQMAQRVK  343
                 ** *.* **  *. **::**. *  **:***: .*** **.***::*  :*.***.*:::
```

```
GBP1_P32455     LPTETLQELLDLHRDSEREAIEVFIRSSFKDVDHLFQKELAAQLEKKRDDFCKQNQEASS 404
GBP3_Q9H0R5     LPAETLQELLDLHRVSEREATEVYMKNSFKDVDHLFQKKLAAQLDKKRDDFCKQNQEASS 402
GBP2_P32456     LPTETLQELLDLHRDSEREAIEVFMKNSFKDVDQMFQRKLGAQLEARRDDFCKQNSKASS 402
GBP5_Q96PP8     LPMETLQELLDLHRTSEREAIEVFMKNSFKDVDQSFQKELETLLDAKQNDICKRNLEASS 402
GBP4_Q96PP9     LPTDTLQELLDVHAACEREAIAVFMEHSFKDENHEFQKKLVDTIEKKKGDFVLQNEEASA 418
GBP7_Q8N8V2     FPTDTLQELLDVHAVCEREAIAVFMEYSFKDKSQEFQKKLVDTMEKKKEDFVLQNEEASA 403
GBP6_Q6ZN66     LPTDTLQELLDMHAACEREAIAIFMEHSFKDENQEFQKKFMETTMNKKGDFLLQNEESSV 403
                :* :*******:*  .****  :::. **** .: **:::      :: *:  :* ::*

GBP1_P32455     DRCSALLQVIFSPLEEEVKAGIYSKPGGYRLFVQKLQDLKKKYYEEPRKGIQAEEILQTY 464
GBP3_Q9H0R5     DRCSALLQVIFSPLEEEVKAGIYSKPGGYCLFIQKLQDLEKKYYEEPRKGIQAEEILQTY 462
GBP2_P32456     DCCMALLQDIFGPLEEDVKQGTFSKPGGYRLFTQKLQELKNKYYQVPRKGIQAKEVLKKY 462
GBP5_Q96PP8     DYCSALLKDIFGPLEEAVKQGIYSKPGGHNLFIQKTEELKAKYYREPRKGIQAEEVLQKY 462
GBP4_Q96PP9     KYCQAELKRLSEHLTESILRGIFSVPGGHNLYLEEKKQVEWDYKLVPRKGVKANEVLQNF 478
GBP7_Q8N8V2     KYCQAELKRLSELLTESISRGTFFVPGGHNIYLEAKKKIEQDYTLVPRKGVKADEVLQSF 463
GBP6_Q6ZN66     QYCQAKLNELSKGLMESISAGSFSVPGGHKLYMETKERIEQDYWQVPRKGVKAKEVFQRF 463
                . * * *: :   * * :  * :  ***: :: :  : :: .*   ****::*.*::: :

GBP1_P32455     LKSKESMTDAILQTDQTLTEKEKEIEVERVKAESAQASAKMLQEMQRKNEQMMEQKERSY 524
GBP3_Q9H0R5     LKSKESVTDAILQTDQILTEKEKEIEVECVKAESAQASAKMVEEMQIKYQQMMEEKEKSY 522
GBP2_P32456     LESKEDVADALLQTDQSLSEKEKAIEVERIKAESAEAAKKMLEEIQKKNEEMMEQKEKSY 522
GBP5_Q96PP8     LKSKESVSHAILQTDQALTETEKKKKEAQVKAEAEKAEAQRLAAIQRQNEQMMQERERLH 522
GBP4_Q96PP9     LQSQVVVEESILQSDKALTAGEKAIAAERAMKEAAEKEQELLREKQKEQQQMMEAQERSF 538
GBP7_Q8N8V2     LQSQVVIEESILQSDKALTAGEKAIAAKQAKKEAAEKEQELLRQKQKEQQQMMEAQERSF 523
GBP6_Q6ZN66     LESQMVIEESILQSDKALTDREKAVAVDRAKKEAAEKEQELLKQKLQEQQQQMEAQDKSR 523
                *:*:  : .::**:*: *:  **         *: :   : :     : :: *: :::

GBP1_P32455     QEHLKQLTEKMENDRVQLLKEQERTLALKLQEQEQLLKEGFQKESRIMKNEIQDLQTKMR 584
GBP3_Q9H0R5     QEHVKQLTEKMERERAQLLEEQEKTLTSKLQEQARVLKERCQGESTQLQNEIQKLQKTLK 582
GBP2_P32456     QEHVKQLTEKMERDRAQLMAEQEKTLALKLQEQERLLKEGFENESKRLQKDIWDIQMRSK 582
GBP5_Q96PP8     QEQVRQMEIAKQN----WLAEQQKMQEQQMQEQAAQLSTTFQAQNRSLLSELQHAQRTVN 582
GBP4_Q96PP9     QEYMAQMEKKLEEERENLLREHERLLKHKLKVQEEMLKEEFQKKSEQLNKEINQLKEKIE 598
GBP7_Q8N8V2     QENIAQLKKKMERERENYMRELRKMLSHKMKVLEELLTEGFKEIFESLNEEINRLKEQIE 583
GBP6_Q6ZN66     KENIAQLKEKLQMEREHLLREQIMMLEHTQKVQNDWLHEGFKKKYEEMNAEISQFKRMID 583
                :* : *:    :      : *         :     *    :     :  ::   :

GBP1_P32455     RRKACTIS------------------------------------------------ 592
GBP3_Q9H0R5     KKTKRYMSHKLKI------------------------------------------- 595
GBP2_P32456     SLEPICNIL----------------------------------------------- 591
GBP5_Q96PP8     NDDPCVLL------------------------------------------------ 586
GBP4_Q96PP9     STKNEQ-LRLLKILDMASNIMIVTLPGASKLLGVGTKYLGSRI------------ 640
GBP7_Q8N8V2     AAENEEPSVFSQILDVAGSIFIAALPGAAKLVDLGMKILSSLCNRLRNPGKKIIS 638
GBP6_Q6ZN66     TTKNDDTPWIARTLDNLADELTAILSAPAKLIGHGVKGVSSLFKKHKLPF----- 633
```

Figure 27. *Alignment of human GBPs done with ClustalW software. In green, GTPase domain. Gap Open penalty: 10; Gap extention penalty: 0.05; Weight mactix: BLOSUM. Uniprot accession numbers are indicated in the name of the sequence.*

Human genomes encode 7 functional GBPs (GBP1-7) and one pseudogene situated in chromosome 1, while murine GBPs are encoded by 11 genes and 2 pseudogenes split between chromosomes 3 and 5. Despite significant functional differences, human GBPs share high homology and between 52-88% sequence identity (Fig. 27 and Table II), especially in the GTPase domain. Subtle differences concentrated in the helical C-terminus may be responsible for divergent functions among GBPs [339].

Interestingly, some GBP proteins in zebrafish carry FIIND and CARD domains in the C-terminus [342]. These domains are classically found on components of the inflammasome complex which, from an evolutionary standpoint, reinforces the association of GBPs with inflammatory functions.

The rapid evolution of GBPs attests to their important role at the intersection of host-pathogen interactions. For example, positive selection of GBP5 among certain primate species [338] may be related to its anti-HIV activity [343] although this is yet to be studied. Further, accelerated evolution of a polybasic motive within certain *GBP1* and *GBP2* genes may be related to host interactions with cytosolic Gram-negative bacteria such as *Shigella flexneri* [339]. Conversely, *S. flexneri* secretes an E3-like ubiquitin ligase to specifically inhibit certain GBPs [344], suggesting host-pathogen co-evolution.

Table II. *Identity between human GBPs with data from Olszewski et al., 2006* [312].

	GBP1	**GBP2**	**GBP3**	**GBP4**	**GBP5**	**GBP6**	**GBP7**
GBP1	100%	77%	88%	56%	68%	54%	56%
GBP2		100%	76%	55%	65%	54%	57%
GBP3			100%	55%	68%	53%	56%
GBP4				100%	52%	74%	81%
GBP5					100%	52%	53%
GBP6						100%	74%
GBP7							100%

GBP expression in human cells and tissues

Different *GBPs* are expressed variably in tissues. *GBP*s *1-5* are expressed in most human tissues in a low basal state and are strongly induced by interferon-γ [312,345,346] (Fig. 28). *GBPs 1-5* also respond, in a lesser manner, to NFκB activation and type I interferons [270,345]. Accordingly, most *GBP* promoter contain a γ-interferon activation site, c-Rel binding site, and an interferon-stimulated response element [312,347].

GBP6 and *GBP7* are not expressed in myeloid cells. Instead, *GBP6* transcripts have been found in the gastrointestinal and vaginal mucosa [346,348]. *GBP7* is constitutively expressed in the liver [349]. Consequently, the roles of GBP6 and GBP7 are not given as much interest as GBPs 1-5. It is not known if and how GBP6 and GBP7 participate in host-pathogen interactions.

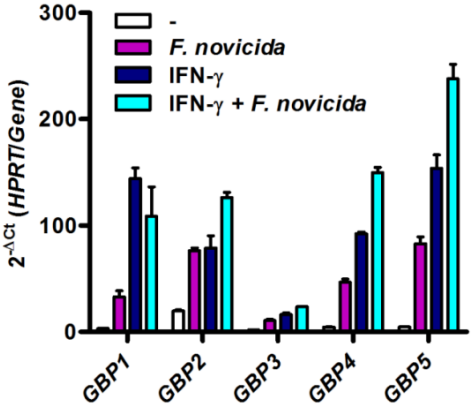

Figure 28. *Endogenous GBP transcripts in primary human monocyte-derived macrophages (hMDM) in response to different stimuli, published in Lagrange et al., 2018* [234].

Subcellular location

In the cell, GBPs 1-5 are present in the cytosol. Ectopically-expressed GFP-GBP2 and GFP-GBP4 have been shown to migrate to the nucleus in HUVEC (human umbilical cord endothelial cells) [350], although this has not been confirmed in other studies. GBP5 locates to the Golgi apparatus in a prenylation-dependent manner [343,351]. Ectopically expressed GBP1 and GBP2 can also locate to the Golgi apparatus through prenylation-mediated interaction with GBP5 [350,351]. Ectopically-expressed GBP2 has also been found in the nucleus [350,351].

GBP1 can be cleaved by caspase-1 and caspase-5 at the 189-LEAD/G-193 motif to form a 47 kDa protein lacking the GTPase domain [352,353]. This cleavage is thought to serve as inhibition of GBP function [353]. Cleaved GBP1 is secreted in the cerebrospinal fluid of meningitis patients [352].

GBP structure and biochemical properties

Overall structure

GBP1 was the first GBP to be characterized in the 90s and early 2000s and it is still the most well understood GBP with regards to biochemistry and host-pathogen interactions [354]. GBP2 and GBP5 have only recently been crystallized [355]. As predicted through homology, their structure is similar to the one of GBP1. An illustration of GBP2 structure can be seen on p. 97 of this manuscript.

The protein sequences of human GBPs are aligned in Fig. 27. GBPs are between 586 and 600 amino acid long, and between 67 and 70 kDa. GBP4 is the longest and carries 15 additional residues in the N-terminus; it is not known if the elongated N-terminus participates in a GBP4-specific function. Otherwise, crystallized GBP1, 2, and 5, and predicted GBP3, 4, 6, and 7 structures are highly similar. As seen in Fig. 29, GBPs contain a 278 AA globular GTPase domain in the N-terminus. The rest of the protein is composed of an α-helical stalk that coils around itself. Since the first published structure of GBP1 [356], helixes α12 and α13 have been referred to as GTPase effector domain (GED) in reference to other dynamin-like proteins [318]. Indeed, it was later described that the GBP C-terminus undergoes conformational changes where the GED is separated from the rest of the protein similar to the opening of a hinge (see **chapter Dimerization and polymerization**) [355].

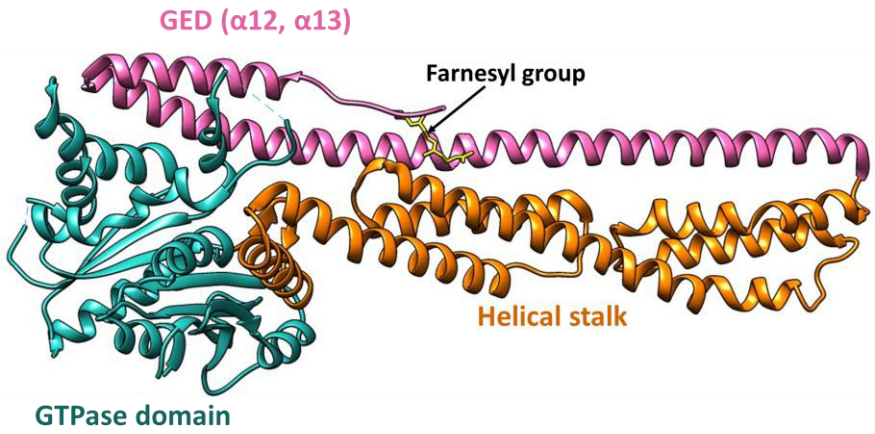

Figure 29. *GBP1 structure and domains. The structure of farnesylated GBP1 was published by Ji et al., 2019* [344]*; PDB accession: 6K1Z. The illustration was prepared with Chimera software.*

GBP1, GBP2 and GBP5 additionally carry a lipid moiety – a post-translational modification called prenylation which is signalled by a CaaX motif in the C-terminus [351]. A CaaX motif is composed of cysteine, followed by two aliphatic amino acids and then either of the following:

- An alanine, methionine, or serine means the protein is modified with a farnesyl moiety of 15 carbon residues; This is the case of GBP1 (CNIS) [357].
- If the CaaX ends in a leucine, the protein will carry a 20 carbon-long geranyl-geranyl moiety; This is the case of GBP2 and GBP5 [351].

GBP1 farnesyl moiety is held in a hydrophobic pocket created by α9 from the helical domain and α12 from the GED. GTP binding and hydrolysis releases the farnesyl tail and allows interaction with membranes [327,358]. Prenylation is critical for dimerization and polymerization of GBP1, GBP2 and GBP5 and controls their interactions with host and pathogen membranes, as will be detailed the following chapters.

GTP hydrolysis and polymerization

Given its key role in initiating immune response and it being the first GBP to be crystalized, it is of no surprise that GBP1 biochemistry is exceptionally well characterized. There is some data on GBP2 and GBP5 as they are prenylated like GBP1; none on GBP4, 6 or 7. GBP3 was recently investigated in a PhD work not yet published in a research article[12].

As members of the dynamin superfamily, GBPs have relatively low affinity for nucleotides but relatively high basal rates of GTP hydrolysis [325]. GTP hydrolysis mechanism is conserved in the dynamin superfamily and it involves several nucleotide binding motifs: P-loop (G1), switch 1 which includes the S73 phosphate cap (G2), switch 2 (G3), and a RD motif (G4) in GBPs instead of the classic NKxD motif in other GTPases [356,359,360] (Fig. 30).

A phosphate cap and guanine cap stabilize the interaction with nucleotide and upon interaction with GTP the caps take a structured conformation (Fig. 29). In the ordered state, the guanine cap facilitates

[12] The dissertation in question being in German which I don't speak, all citations regarding GBP3 in this part are from a great review written by German-speaking authors who are specialists in the domain.

interaction between two GTPase domains which in turn induces conformational change in the pocket and stimulates GTP hydrolysis to GDP [326,361] (Fig. 31 A). Therefore, GTP activity is boosted upon dimerization [326,362]. An excellent detailed explanation on the in-pocket conformational change can be found in the review by Kutsch and Coers [363].

Cleavage of the gamma-phosphate during the processing of GTP to GDP leads to adjustments in the GTP-binding pocket of the globular domain which leads to the disruption of salt bridges between the globular domain and the GED (Fig. 31 B). The GBP1 molecules in the dimer are rendered in an open state [355,362,364] (Fig. 31A). It seems that GBP5 is constitutively in the open monomer state and dimerizes upon activation [365,366] while GBP2, as GBP1, is likely a closed monomer in basal state [363]. In the open conformation, GDP can be released or further processed into GMP. This property is unique to GBP1 (and the closely related GBP3) among other GBPs and dynamin related GTPases [325,363]. Coiled coil interactions between GED helical domains stabilize the open dimer and promote GDP hydrolysis. In fact, a truncated GBP1 comprised only of the globular domain produces more GMP than a whole-molecule GBP1 (i.e., linked to a helical domain) suggesting that the helical domain acts as an internal inhibitor of GDP hydrolysis [367]. An open state however is not sufficient for GDP hydrolysis. The ordered conformation of the guanine cap stabilizes the GDP-bound dimer and is required for efficient GDP hydrolysis [326,368]. Accordingly, the guanine caps of GBP1 and GBP2 are significantly different with regards to secondary structure and this might explain the impossibility of GBP2 to catalyse GDP hydrolysis [368] (Fig. 31 C).

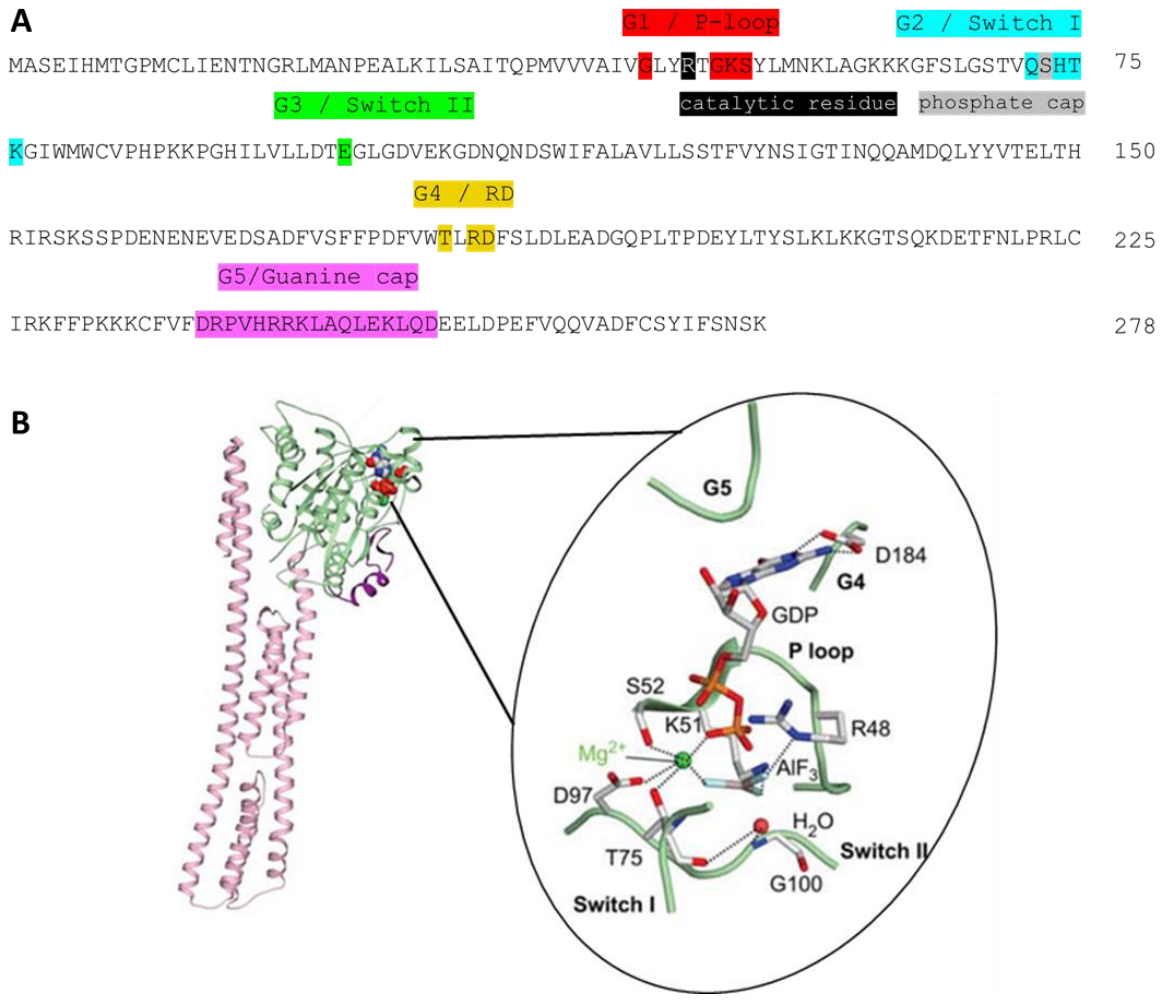

Figure 30. *GBP1 residues involved in GTP and GDP hydrolysis* [360,363]*. The illustration of the GTPase pocket in the lower panel was taken from a review by Daumke and Praefcke, 2016* [325]*. The G5 is*

In an open conformation, the farnesyl tails of GBP1 dimers can bind to lipid vesicles (Fig. 31 A) or form tubular polymers (Fig. 31 B) [327,358,369]. The membrane binding is dynamic and promoted by GTP binding but upon hydrolysis GBP1 dissociate from membranes [358]. On the other hand, polymer formation requires GTP hydrolysis and in fact polymer formation increases GTP turnover rates [327]. Association with the polymer is also dynamic and might represent a GBP1 "depot" ready to be mobilized upon encountering a pathogen [370]. Cytosolic GBP1 puncta have been observed in overexpressing cells by several groups, including ours, and could very well be such mobilizable GBP1 polymers (Fig. 32).

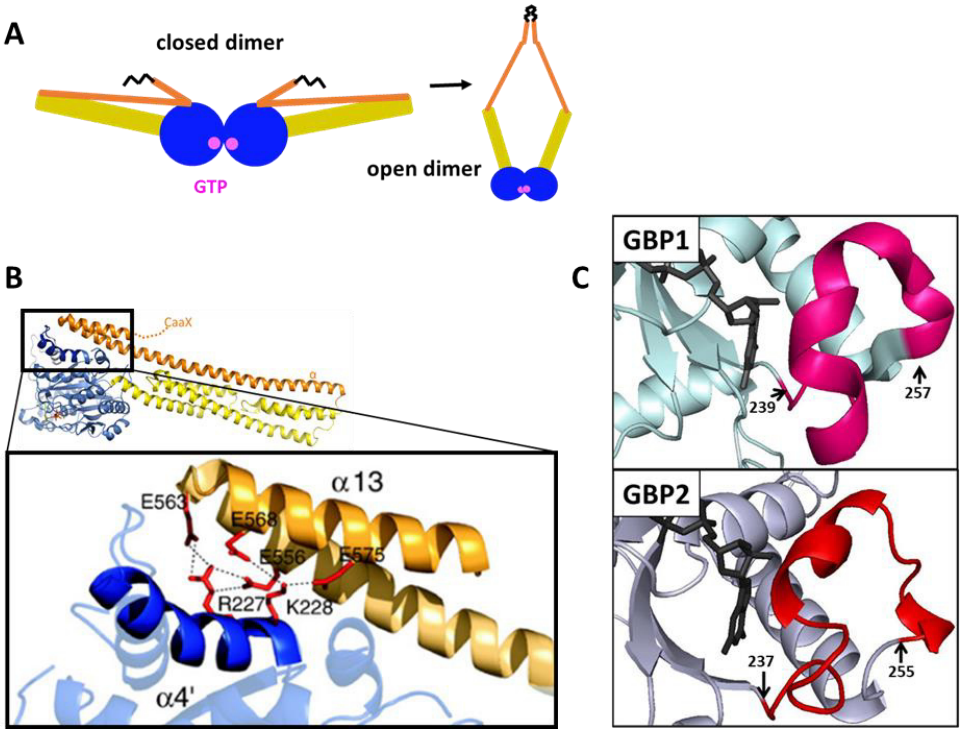

Figure 31. *Structural biochemistry of GBP1. A) Dimerization of GBP1 upon GTP binding; B) Guanine cap structure of GBP1 and GBP2 bound to GppNHp (non-hydrolysable GTP analogue)* [368]*. C) Interactions between the GTPase domain and the GED* [362]*;*

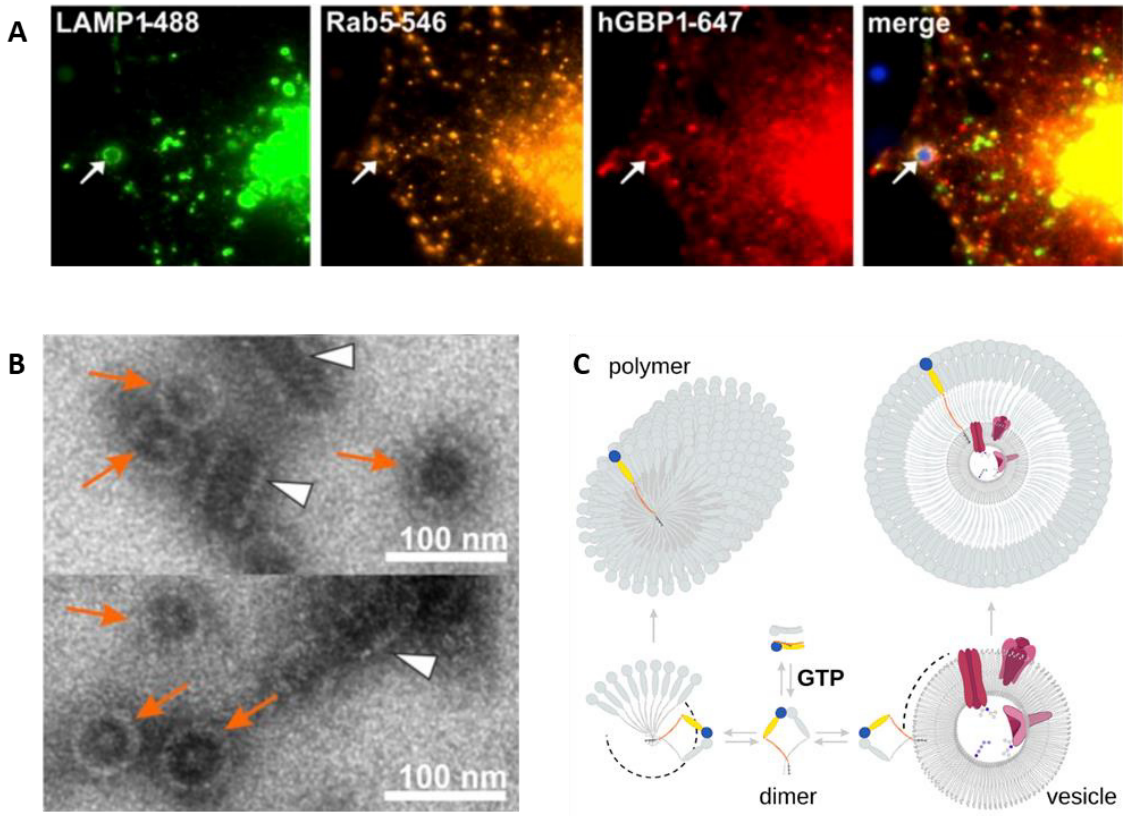

Figure 32. *GBP1 polymerization upon interaction with GTP. A) GBP1 association with phagocyted 2um latex beads* [358]*. B) GBP1 tubular polymers observed in cryo-electron microscopy* [358]*. C) Model for GBP polymerization and membrane interaction* [363].

Interaction with lipid vesicles requires open dimers; upon insertion in the vesicle, the GTPase domains are pointed outwards like “pins in a pincushion”. GTPase domains can interact and tether vesicles to one-another [369]. GBP1 can also act as detergent upon dissociation from the membrane [369] (Fig. 33). Polymerization and membrane binding are crucial in host-pathogen interactions, particularly with parasites and intracellular bacteria, as will be shown further.

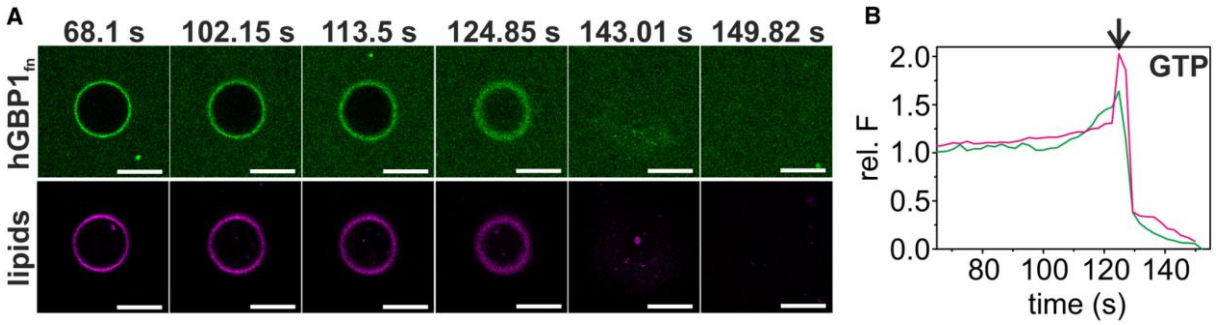

Figure 33. *Detergent activity of GBP1 and dissociation from membranes in temporal relation to GTP hydrolysis* [369].

Roles of GBPs in cell life

Besides confirmed roles in immunity, the roles of GBPs have also been investigated in the life of the cell, specifically in processes involved in cancer progression – cell proliferation, differentiation,

migration. Additionally, GBPs have been examined as possible markers of many different cancers. Annex I summarizes research data on GBPs in cell physiopathology. GBPs have been involved in interactions with actine growth factor receptors signalization and proliferation pathways such as Akt/Erk kinase pathway (see Annex I for a detailed description). Research articles are highly contradictory and point towards the involvement of GBPs in various pathways to both promote and inhibit cancer growth or resistance to treatments. Most studies are lacking in-depth mechanisms explaining the observed phenotypes. Furthermore, there is a plethora of epidemiological studies examining GBPs as prognostic markers but there are no clear correlations between GBP expression and patient outcomes. Results vary between cancer types and there is even contradictory data on the same cancer (ex. lung adenocarcinoma, ovarian cancer, triple negative breast cancer) or pathway (ex. GBP2 and the Wnt/β-catenin pathway).

My opinion is that GBPs are markers of IFN-related response, which may be beneficial or deleterous depending on the cancer and the involved pathways. There is little evidence to suggest that GBPs broadly and directly influence cancer progression more than other IFN-induced responses.

Roles in immunity

Antiviral activity

GBPs were first identified as antiviral proteins when in 1999 it was shown that GBP1 decreased virion production for vesicular stomatitis virus and encephalomyocarditis virus [371]. The same was later shown for mGbp2 [372]. Interestingly, GTP hydrolysis by mGbp2 was required for inhibition of encephalomyocarditis virus but not for inhibition of vesicular stomatitis virus [372].

In fact, antiviral properties of GBPs have been described against a myriad of viruses and, curiously, associated with a variety of pathogen-dependent mechanisms.

Globally, hGBP1, hGBP3, and mGbp2 inhibit RNA virus replication through interaction with nonstructural viral proteins and viral replication complexes, as summarized in Table 3. These interactions are often mediated by the GTPase domain. Some viral nonstructural proteins specifically antagonize the action of GBPs. Similar antiviral activities have been described for porcine GBP1/5/6 against porcine respiratory and reproductive syndrome [373,374] and *Tupaia* GBP1 against vesicular stomatitis virus [375].

Another mechanism of action recently described for human GBP1 and murine Gbp2 is associated with polymerization and the autophagosomal pathway [376,377].

An outlier is the inhibitory action of human GBP1 to Kaposi's Sarcoma-associated herpesvirus which is dependent on actin depolymerization through GBP1 activity [378].

GBP5 is also a potent antiviral factor but it acts on the processing of viral glycoproteins, instead of viral replication. This action depends on the localization in the Golgi apparatus, resulting in blocking of viral packaging [379,380]. A study described a similar action of GBP2 but further research is necessary to confirm and explain this activity [379].

Table 3. *Antiviral properties of human and murine GBPs.*

GBP	Virus	Mechanism
hGBP1	Vesicular stomatitis virus Encephalomyocarditis virus	Unknown [371]
	hepatitis C Virus	Inhibition of viral replication though direct interaction with viral RNA polymerase which requires GBP1 GTPase domain, GTP hydrolysis [381,382] and specifically GMP formation [383].
	influenza A virus	GBP1 GTPase-dependent anti-viral properties [384] are antagonized by viral non-structural protein 1. Direct interaction between GBP1 GTPase domain and NS-1 are dependent on GTP binding residues of GBP1 [385].
	dengue virus	GBP1 decreases dengue virus production and promotes NFκB signaling [386].
	Kaposi's sarcoma-associated herpesvirus (KSHV)	GBP1 inhibits KSHV access to the nucleus by disrupting actin polymerization. Antiviral activity depends on GBP1 GTPase hydrolysis and dimerization. Viral ubiquitin-ligase targets GBP1 to the proteasome [378].
	hepatitis E virus	GBP1 targets viral proteins to the lysosome. Antiviral activity is dependent on GBP polymerization but not GTP hydrolyzation [377].
hGBP2	Enveloped viruses – see GBP5	Actions similar to GBP5 below [379].
hGBP3	Influenza A virus	The GTPase domain of GBP3 blocks viral transcription. A GBP3 splice variant with cleaved C-terminus is more efficient than whole GBP3 or GBP1 [384].
hGBP4	none described	N/A
hGBP5	Influenza A virus	GBP5 interacts with the NEMO complex in the NFκB pathway and boosts inflammatory response to influenza A virus through interferon expression and signalling [15].
	Enveloped viruses: HIV, Zika, measles, influenza A virus, Marburg virus, murine leukaemia virus	GBP5 interferes with the processing of viral glycoproteins by the convertase furin in the Golgi apparatus, inhibiting viral packaging and virion production [379,380,388].
	Respiratory syncytial virus	GBP5 decreases the cellular levels of a viral small hydrophobic protein and induces its release in the cell culture medium. Antiviral activity is dependent on Golgi localization but not GTPase activity [389]. Might be similar to the mechanism described above.
mGbp2	Vesicular stomatitis virus	GTP hydrolysis is required for viral inhibition [372].
	Encelphalomyocarditis virus	GTP hydrolysis is not required for viral inhibition [372].
	Murine norovirus	Inhibition of viral replication is mediated through GBP recruitment to murine norovirus replication complexes in association with the autophagy machinery and IRGs [390]. Antiviral activity is dependent on GTP hydrolysis and is blocked by non-structural protein 7 [376].

Immunity against protozoa (*Toxoplasma gondii* and *Leishmania donovanii*)

Toxoplasma gondii is an eucaryotic intracellular parasite. In the cell, it replicates in parasitophosphorus vacuoles, composed of parts of the cell membrane but devoid of any host proteins and instead decorated with parasitic molecules.

Human GBP1 and murine Gbp1,2,3,5,6,7 localize to and polymerize at the parasitophosphorous vacuole (PV) of *T. gondii* in a prenylation-dependent manner [353,391]. GBP recruitment lyses the vacuole and further might lyse the pathogen itself [353,391,392] (Fig. 34).

In human macrophage THP-1 cell lines, GBP1-induced liberation of *T. gondii* in the cytosol and its subsequent lysis liberate parasitic DNA which is sensed by the AIM2 inflammasome [353,393]. The activation of AIM2 induces recruitment of the adaptor protein ASC to recruit and activate pro-apoptotic caspase-8 thus leading to apoptosis. Usually, the AIM2 inflammasome complex activates pro-inflammatory caspase-1 (Figure 21) but *T. gondii* inhibits inflammatory cell death pyroptosis in favour of apoptosis [353].

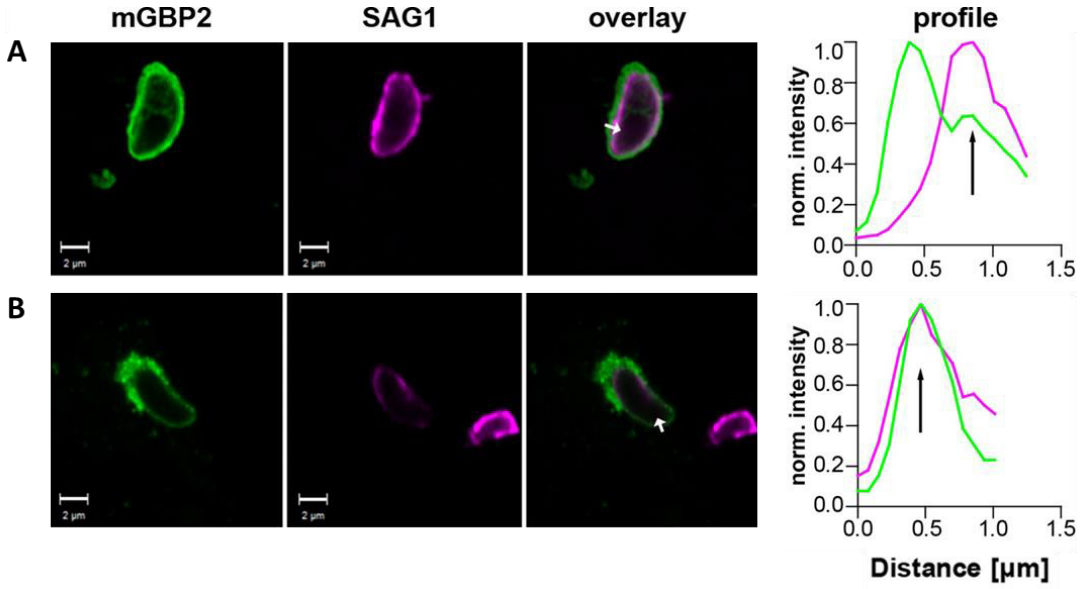

Figure 34. *mGbp2 recruitment to the T. gondii parasitophosporous membrane (A) or the plasma membrane (B) in 37.1% (A) or 61.1% (B) of parasites* [391].

In murine cells, mGbp targeting to the PV is dependent on the autophagy machinery and IRG proteins [370,394,395]. The absence of host protein Irgm from the PV is detected as 'missing self' by other host Irg and the PV is ubiquitinated; this ubiquitination and the subsequent recruitment of autophagy effectors p62 and LC3 induce mGbp recruitment. It was suggested that mGbp2 co-localizes with p62 when not associated with PV, meaning that p62 would be involved in mGbp2 intracellular trafficking [370].

Certain exceptions have been reported. For one, in human epithelial cells no GBP1 recruitment to the PV was detected, but it was nevertheless shown that GBP1 restricts *T. gondii* replication [396]. In

human mesenchymal stromal cells, *GBP1* but not *GBP2* or *GBP5* knock-down increased *T. gondii* burden [397]. In a very recent publication from 2022 it was shown that GBP1, GBP2 and GBP5 restricted *T. gondii* growth but only GBP1 localized to the pathogen in THP-1 cells [398]. Similarly, in murine fibroblasts mGbp2 controls growth of the parasite *Leishmania donovanii* without localizing to the PV; the same was shown for human GBP1 during *L. donovanii* infection of A549 cells [399]. GBP targeting to the PV of *L. donovanii* promoted recruitment of autophagosomal markers LAMP1 and LC3 [399].

As of today and to my knowledge, no mechanisms have been proposed yet to explain the antimicrobial activity of GBPs at a distance from a pathogen or a pathogen-containing vacuole.

Anti-bacterial immunity

The case of *Chlamydia* spp

Chlamydia spp. are intracellular Gram-negative bacteria that replicate in vacuoles called inclusions. In murine cells, human pathogen *C. trachomatis* inclusion membrane is ubiquitinated through the action of IRGs and Atg proteins, similarly to protozoan *T. gondii* [394,395]. Murine Gbps translocate to ubiquitinated inclusions, escorted by p62 [370,394,395]. Recruitment of mGbp1, 2, 4, 6, 7, 9 and 10 can be observed [400]. Two studies by the same group showed that murine Gbps targeted human-adapted *C. trachomatis* but not rodent-adapted *C. muridarum* [401] and vice-versa, human GBPs were recruited to *C. muridarum* but not *C. trachomatis* [402]. Although the authors did not observe murine Gbp recruitment to *C. muridarum*, inflammasome activation was Gbp-dependent [401]. Their findings are in discordance with earlier studies where human GBP1 and GBP2 were shown to target *C. trachomatis* inclusions in HeLa [403] and THP-1 cells [404], and promoted growth restriction [403,404] and autophagy elimination of the pathogen [404]. Further, GTP (but not GDP) hydrolysis by GBP1 controlled growth restriction of *C. trachomatis* in THP-1 cells; On the other hand, GBP1-catalyzed GMP formation activated the NLRP3 inflammasome thanks to catabolism of GMP to uric acid (an danger signal detected by NLRP3) [405].

GBPs and galectins: The chicken or the egg?

One of the earliest studies on GBP antibacterial immunity showed that mGbp1, 7 and 10 are recruited to *Listeria monocytogenes* (30 min) or *Mycobacterium bovis* (2h) containing vacuoles. Gbps recruited elements of the oxidative response and the autophagy machinery (p64, Atg4) by fusing Gbp-carrying vesicles with pathogen vacuoles. [406].

In another study, murine Gbps are recruited to pathogen-containing vacuoles (*Legionella pneumophila*, *Salmonella enterica* serovar Typhimurium, *Yersinia pestis*) by galectin-3 independently of IRGs or the autophagy machinery (unlike Gbp recruitment observed for *C. trachomatis* above) [407]. Galectin-3 detects damaged phagosome membranes, ruptured by type 3 secretion systems of the pathogens cited in this paragraph[13]. Transfected *Y. pestis* T3SS components also colocalized with galectin-3 and induced non-canonical inflammasome activation which required murine Gbp Chr3 [409].

[13] *Chlamydia* also have a T3SS but it is unlike a typical T3SS [408].

Several studies suggest that murine Gbps do not induce vacuolar lysis in the response to *L. pneumophila* [410,411]. Rather, they mediate caspase-11 activation in response to cytosolic bacteria when the pathogen-containing vacuole has been damaged. However in murine macrophages infected with *Brucella abortis*, deletion of GBP^{Chr3} decreased two-fold the disruption of *Brucella*-containing vacuoles [412]. In another study, murine Gbps promoted recruitment of galectin-8 to *Salmonella typhimurium* thus indicating rather that Gbps are responsible for lysis of the pathogen vacuole [413]. In yet another publication, human GBPs did not affect galectin-8 recruitment to *S. typhimurium* nor the percentage of cytosolic bacteria as it did for *T. gondii* [353].

What is clear without a doubt is that GBPs potentiate inflammasome activation, be it caspase-11 and NLRP3 or Aim2 depending on the pathogen [307,414,415]. A commonly advanced theory is that GBPs liberate bacterial ligands for inflammasome sensing – either through releasing the pathogen in the cytosol, or through lysing the pathogen itself [307,308]. Paradoxally, several studies suggest that murine Gbps mediate caspase-11 activation in response not only to live bacteria but also to cytosolic LPS [411,414,416]. Further, murine Gbps control caspase-11 activation in response to bacterial OMVs but do not seem to extract LPS from OMVs [417]. Other studies do not see GBP-dependent activation of caspase-11 in response to cytosolic LPS [413].

Brief note: GBPs and Gram-positive bacteria

GBP1 does not localize to cytosolic *Listeria* [418] which is in agreement with the working model for LPS-mediated recruitment of GBPs [417,419–421] although a pioneer publication showed a GBP-dependent control of *L. monocytogenes* involving inflammasome activation [406]. The discordance of recruitment and inflammasome activation is also seen with *C. trachomatis* and *T. gondii* (see above).

Human GBPs, cytosolic LPS and caspase-4

Although *S.* Typhimurium mainly replicates in a pathogen-containing vacuole, a proportion of bacteria is released into the cytosol [422]. S. Typhimurium and professional cytosolic pathogen *Shigella flexneri* are well established as models for cytosolic interactions with GBPs.

GBP1 is recruited to cytosolic Gram-negative bacteria: *S. Typhimurium* [353,393,419], *S. flexneri* [311,418,420,421,423] and *Burkholderia thailandensis* [424]. Recruitment of GBP1 to these bacteria allows recruitment of GBP2, GBP3 and GBP4. Together, GBPs induce caspase-4 activation in response to LPS [353,419,420,424].

GBP1 interacts with bacterial LPS [419,421] thanks to a polybasic motif located near the farnesyl moiety at the Cter [311,339,418,419]. It was proposed that the polybasic motif interacts with the negatively charged O-antigen [418,421]. GBP1 polymerization and insertion in the LPS would fragilize the bacterial membrane [421] (Fig. 35).

Data from several groups suggests that, in human cells, GBPs do not induce bacteriolysis [311,418,423,426] unlike murine Gbps (who likely cooperate with murine IRGs to do so) [306,426].

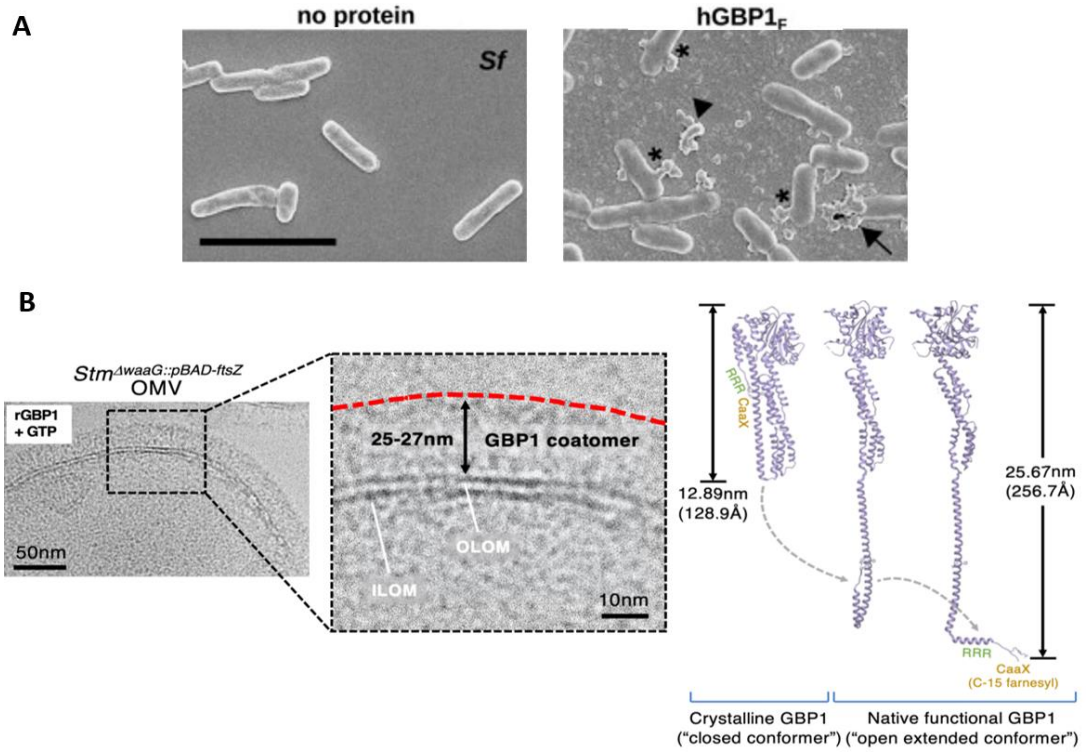

Figure 35. *GBP interaction with bacterial membranes. A) In vitro recruitment of farnesylated GBP1 to* S. flexneri *in the presence of GTP. Arrowheads: unattached GBP1 polymers; arrows: GBP1 polymers attached to bacteria; Asterisks: polymeric structures that appear to fuse with bacterial surfaces. Scanning electron micrographs, scale bar 5 µm. Published in Kutsch et al., 2020* [421]. *B) GBP1 coatomer on* S. *Typhimurium OMVs without O-antigen or core. OLOM, outer leaflet of outer membrane. ILOM, inner leaflet of outer membrane. Preprint by Zhu et al., 2021* [425].

Instead, the current model presents GBPs as caspase-4-activating platforms on the surface of bacteria or in response to cytosolic LPS [419,420]. In GBP-transfected or siRNA-treated HeLa cells, GBP4 was required for caspase-4 recruitment and GBP3 was necessary for caspase-4 activation while GBP2 was dispensable [419,420]. The data is conflicting on GBP2: one study showed GBP2 was involved in caspase-4 recruitment (siRNA) [420] while in another GBP2 was dispensable (transfection) [419]. Still, it is unclear through what mechanism GBPs promote caspase-4 activation.

In addition to inflammasome activation, GBP recruitment interferes with the intracellular actin-based motility of *S. flexneri* [311,418] and the formation of giant multinucleated cells by *B. thailandensis* [424]. These effects could be non-specific and instead consequences of GBP-induced steric hindrance and LPS fragilization [423].

<u>GBPs and *F. tularensis*</u>

In murine macrophages infected with *F. novicida*, GBPs mediate the release of bacterial DNA to activate the Aim2 inflammasome. This was demonstrated specifically for GBP^{Chr3} (mGbp1, 2, 3, 5, 7), and mGbp2 and mGbp5 were recruited to *F. novicida*.

In human macrophages, Aim2 does not participate in anti-*Francisella* response. GBPs were shown to mediate caspase-4 activation in primary human macrophages in response to intracellular *F. novicida* and *Francisella* LPS [234]. Knowledge is lacking on the targeting and specific roles of GBPs against *F. novicida* in human cells.

State of the art in 2019 and scientific questions of this thesis

In 2017, two publications demonstrated recruitment of GBP1 to *S. flexneri* and the subsequent recruitment of GBP2-4 [311,418].

In 2018 our group demonstrated that in human primary macrophages caspase-4 was activated by *F. novicida*, unlike the murine caspase-11 [234]. Furthermore, this was the first evidence of the role of GBPs in inflammatory responses against *F. novicida* in human cells.

The specific roles of GBPs in human cells against intracellular bacteria were yet to be elucidated. Indeed, GBP1 was put forward as 'Captain GBP1' [427] initiating GBP2-4 recruitment and inflammatory response to *S. flexneri* and *S.* Typhimurium. We wondered what were the contributions of other GBPs. In hMDMs, a knock-down of GBP2 had a particularly pronounced effect on inflammasome activation [234]. Prior to the work included in this dissertation, our group had done substantial research on the specific roles of GBPs in inflammasome activation in U937 cells infected with *F. novicida*. The results were complex and difficult to integrate within existing literature. They are yet unpublished and will be mentioned in the discussion.

We were particularly interested as *F. novicida* as a model for intracellular host-pathogen interactions. GBPs had been associated with localization to cytosolic Gram-negative bacteria in human cells [418]. Given that *F. novicida* has an atypical LPS but nevertheless activated caspase-4 in a GBP-dependent manner, we wanted to understand the recruitment of GBPs to *F. novicida* in the human macrophage.

Results

I. *Francisella* escapes GBP targeting

The following chapter is a research article manuscript that was submitted to PLoS Pathogens in December 2021. The manuscript has been rejected following commentary from reviewers.

The manuscript is currently being revisited and the work being consolidated before resubmission to a different journal.

LpxF-mediated LPS modification contributes to *Francisella novicida* escape from targeting by specific GBPs

Stanimira V. Valeva[1], Manon Degabriel[1,*], Fanny Michal[1,*], Gabrielle Gay[1], John R. Rohde[2], Felix Randow[3,4], Robert K. Ernst[5,6], Brice Lagrange[1,7], Thomas Henry[1,@]

1 CIRI, Centre International de Recherche en Infectiologie, Univ Lyon, Inserm U1111, Université Claude Bernard Lyon 1, CNRS, UMR5308, ENS de Lyon, Univ Lyon, F-69007, Lyon, France

2 Department of Microbiology and Immunology, Dalhousie University, Halifax, NS, Canada.

3 Division of Protein and Nucleic Acid Chemistry, MRC Laboratory of Molecular Biology, Cambridge, UK.

4 Department of Medicine, University of Cambridge, Addenbrooke's Hospital, Cambridge, UK.

5 Department of Microbiology and Immunology and Lineberger Comprehensive Cancer Center, University of North Carolina at Chapel Hill, Chapel Hill, NC 27599, USA.

6 Department of Microbial Pathogenesis, University of Maryland Baltimore, Baltimore, MD 21201, USA

7 Present address: Unité de Recherche Confluence, Sciences et Humanités, Université Catholique de Lyon, Lyon, France.

* These authors contributed equally to this work

@ Corresponding author: Thomas.henry@inserm.fr

Running title: *Francisella* escapes GBP targeting

Abstract

Guanylate-Binding Proteins (GBPs) are interferon-inducible GTPases that play a key role in cell autonomous responses against intracellular pathogens. Seven GBPs are present in humans. Despite sharing high sequence similarity, subtle differences among GBPs translate into functional divergences that are still largely not understood. A key step for the antimicrobial activity of GBPs towards cytosolic bacteria is the formation of supramolecular GBP complexes on the bacterial surface. Such complexes are observed when GBP1 binds lipopolysaccharide (LPS) from *Shigella* and *Salmonella* and further recruits GBP2, 3, and 4.

Here, we performed a comparative study on two professional cytosol-dwelling pathogens, *Francisella novicida* and *S. flexneri* to investigate GBPs recruitment. *F. novicida* was coated by GBP1 and GBP2 in human macrophages but contrary to *S. flexneri, F. novicida* escaped targeting by GBP3 and GBP4. Furthermore, coinfection experiments demonstrated that GBP1 targets preferentially *S. flexneri* compared to *F. novicida*. Multiple GBP1 features were identified as required to promote targeting to *F. novicida.* In contrast, GBP1 targeting to *S. flexneri* was much more permissive to *GBP1* mutagenesis suggesting that GBP1 has evolved multiple domains that cooperate to recognize *F. novicida* atypical LPS. Finally, LpxF, a lipid A-modifying enzyme was identified as promoting *F. novicida* escape from GBP3. Altogether our results indicate that GBPs have different affinity for different bacteria and that the repertoire of GBPs recruited onto cytosolic bacteria is dictated both by GBP-specific features and by specific bacterial factors, including the structure of the lipid A.

Author Summary

Few bacteria have adapted to thrive in the hostile environment of the cell cytosol. As a professional cytosol-dwelling pathogen, *S. flexneri* secretes several effectors to block cytosolic immune effectors, including GBPs. This study illustrates a different approach of adapting to the host cytosol: the stealth strategy developed by *F. novicida*. *F. novicida* bears an atypical hypoacylated LPS, which does not elicit neither TLR4 nor caspase-11 activation. Here, this atypical LPS and one key enzyme responsible for Lipid A modification, LpxF, are shown to promote escape from GBP3 targeting. Furthermore, the characterization of GBP1 targeting to *F. novicida* identified the different GBP1 features that cooperate to promote GBP1 recruitment to the bacterial surface. This study illustrates the importance of investigating different bacterial models to broaden our understanding of the intricacies of host-pathogen interactions.

INTRODUCTION

Guanylate-Binding Proteins (GBPs) are interferon-inducible, dynamin-like GTPases, that play an essential role in host defenses against a large variety of pathogens including viruses, intracellular protozoa and bacteria. *GBPs* are present as a multigene family in vertebrates. The *GBP* family exhibits signs of strong evolutionary pressure with gene loss, gene duplication and neofunctionalisation [338,339,341] indicative of a selective adaptation to pathogens. Eleven GBPs are encoded in mice while seven GBPs are present in humans [312]. Human GBPs share a high degree of sequence homology and carry a conserved N-terminal globular GTPase domain followed by a C-terminal helical domain. GTPase activity is required for the antimicrobial activity of GBPs [355,376,393] and allows GBP dimerization and polymerization [327,351,358]. GTP hydrolysis activity is conserved between GBPs. GBP1 is further able to hydrolyze GDP to GMP [368] (Table 1). Additionally, three of the seven GBPs (GBP1, 2 and 5) present a C-terminal CAAX motif and undergo prenylation – i.e. a post-translational addition of a farnesyl or geranylgeranyl lipid group (Table 1). The prenylation allows GBP1, 2, and 5 to be targeted to membranes where they can recruit non-prenylated GBP3/4 [351]. Pioneer GBPs recruit downstream GBPs through heterotypic interactions resulting in the formation of supramolecular complexes containing numerous GBP proteins [391].

The antibacterial and anti-parasitic actions of GBPs are well established and most of them are associated with a striking recruitment of GBPs at the pathogen-containing vacuoles (PCV) or directly onto the pathogen if present in the cytosol. IFN-γ treatment of *Toxoplasma gondii*-infected cells leads to the recruitment of several thousand of mGBP1/2/3/6 proteins and the formation of a densely packed mGBP coat onto the PCV[391]. This recruitment is followed by disruption of the PCV and the ensuing GBP-targeting and lysis of the parasite in the host cytosol. Similarly, GBPs can display antibacterial responses through the targeting of cytosolic bacteria [305,307,308,311,344]. These GBP-mediated responses have been particularly well studied with two enterobacteria, *Shigella flexneri* and *Salmonella enterica* serovar Typhimurium *(S.* Typhimurium) and have demonstrated a hierarchy in GBP recruitment. Indeed, GBP1 directly binds lipopolysaccharide (LPS) and recruits GBP2, GBP3 and GBP4 to the bacterial surface [311,419,421]. GBP1 is thus considered as the master GBP orchestrating downstream GBP recruitment.

Assembly of the GBP multimer onto cytosolic bacteria has several consequences. First, as shown for *S. flexneri* and *B. thailandensis*, it can inhibit the formation of actin tails, bacterial motility and cell to cell spread [311,418,428]. Second, GBPs at the bacterial surface act as a signaling platform to recruit and activate caspase-4, leading to the activation of the non-canonical inflammasome, thus triggering pyroptosis and releasing the pro-inflammatory cytokine interleukin 18 [311,419]. Interestingly, the monitoring of caspase-4 recruitment and activation allowed to ascribe specific functions to the different GBPs. GBP1 acts as the initiator GBP: it is recruited first, exposes bacterial lipid A (the LPS moiety recognized by caspase-4) and elicits both caspase-4 [421] and GBP2/3/4 recruitment. GBP2, 3 and 4 also display redundant or specific roles in caspase-4 recruitment and activation, that are still not fully understood [419,420]. Altogether, these studies suggest that the recruitment of multiple GBPs at the bacterial surface can promote different antibacterial functions. Although highly homologous, growing evidence indicates that subtle differences in GBP sequence and structure may account for functionally relevant divergence. GBP1 was the first GBP to be

crystalized and has been extensively characterized [326,356,367,369,429]. In contrast, the specific structure-function relationship for other GBPs remains largely unknown.

Although IFN and IFN-inducible proteins, including GBPs, are potent antimicrobial agents against intracellular bacteria, professional cytosol-dwelling bacteria can replicate to very high number in the host cytosol suggesting that they have developed strategies to hide from or actively inhibit GBPs action. Accordingly, *S. flexneri* expresses a Type III secreted effector, IpaH9.8, displaying E3 ubiquitin ligase functions. IpaH9.8-mediated GBP ubiquitination addresses GBPs to the proteasome for proteolytic degradation. Consequently, *S. flexneri* escapes from GBPs-mediated growth restriction [311,344,418]. *Francisella tularensis,* the agent of tularemia, is another professional cytosolic Gram-negative pathogen that escapes GBP-mediated growth restriction although to different extents depending on the subspecies considered [308,430]. *F. tularensis* can infect a large number of host cells but has a particular tropism for phagocytic cells, including macrophages [86]. Following phagocytosis, *F. tularensis* rapidly escapes into the host cytosol using an atypical type IV secretion system (encoded in the *Francisella* Pathogenicity Island-FPI) [114]. *F. tularensis* subsp. *novicida* (hereafter referred to as *F. novicida*) is avirulent in immuno-competent individuals but can infect human cells with a similar life cycle as the highly virulent *F. tularensis* subspecies *tularensis* strains. *F. novicida* has emerged as a model pathogen to study cytosolic immune responses [234,306,307,309]. *F. novicida* carries an atypical LPS with tetra-acylated lipid A, which enables escape from the host LPS receptors TLR-4 and the murine caspase-11 [216,234]. *F. novicida* LPS can be recognized by caspase-4, in human cells, although its LPS requires one order of magnitude higher concentration than LPS from enterobacteria to elicit similar responses [234]. In the host cytosol, *F. novicida* is recognized by the AIM2 inflammasome in mice, or the caspase-4 in primary human macrophages [234]. Inflammasome activation in mice and in human macrophages (hMDMs) is mediated by GBPs [307,308]. Particularly in hMDMs, GBP2 is recruited to *F. novicida* [234]. Still, a comprehensive view of the specific recruitment of GBPs on this cytosolic stealth pathogen is lacking.

In this study, we demonstrate that, in contrast to enterobacteria, *F. novicida* specifically escapes GBP3 and GBP4 targeting. Escape from GBP3 was dependent on LpxF, a enzyme key in the biosynthesis of *F. novicida* tetra-acylated Lipid A. Furthermore, through coinfection experiments we revealed that GBP1 targets preferentially *S. flexneri* compared to *F. novicida* suggesting that GBP1 has higher affinity for enterobacteria LPS than for *F. novicida* LPS. Accordingly, our study uncovered multiple GBP1 features required to target to *F. novicida* but largely redundant for recruitment to *S. flexneri.* Our results suggest that GBP1 has evolved distinct domains to target a large diversity of LPS although with different efficacy. Yet, *F. novicida* evades targeting by GBP3 and 4, in part through the modification of its LPS, indicating that, in contrast to the prevailing model, GBP recruitment downstream of GBP1 is not only driven by heterotypic GBP interactions but is largely dependent on microbial envelope structures.

RESULTS

F. novicida specifically escapes GBP3-4 targeting

To study the specific recruitment of individual human GBP to *F. novicida*, we generated stable human monocyte/macrophage U937 cell lines constitutively expressing HA-tagged GBP 1-5 (Fig S1A). GBP6 and 7 were not studied since they are not expressed at substantial level in monocyte-derived macrophages [234]. As observed in primary human macrophages, endogenous GBP1-5 were highly induced in U937 macrophages upon IFNγ treatment (Fig S1B). IFNγ-primed, PMA-differentiated U937 macrophages were infected with *F. novicida* for 7 h to assess specific GBP recruitment. GBP1 and GBP2 were targeted to a subset of bacteria (Fig 1A and 1C) and intimately colocalized with *F. novicida* in ≈25% of infected cells. Surprisingly, targeting of GBP3 or GBP4 to *F. novicida* could not be observed. The absence of GBP3/4 recruitment onto *F. novicida* contrasted with previous studies using other Gram-negative pathogens. Indeed, GBP1, 2, 3 and 4 are recruited to *S. flexneri, S.* Typhimurium and *Burkholderia thailandensis* in HeLa cells [311,419,420,424]. Importantly, GBP3 and GBP4 (and GBP1/2) were recruited to *S. flexneri* ΔipaH9.8 (hereafter referred to as *S. flexneri*) as early as 3 h p.i. in infected U937 macrophages (Fig 1B and 1D), demonstrating the functionality of these GBPs in our experimental system. As expected, GBP5, which is recruited to neither *S.* Typhimurium nor *S. flexneri,* was not recruited to *F. novicida* either.

These findings show that the repertoire of GBPs recruited to *F. novicida* and to *S. flexneri* differs, suggesting that *F. novicida* specifically escapes targeting by GBP3 and 4.

GBP1 is preferentially recruited onto *S. flexneri* than onto *F. novicida in co-infected cells*

Escape from GBP3/4 recruitment might be due to either an active process (e.g. implicating a T6SS-secreted effector) or a lack of recognition (*F. novicida* is described as a stealth pathogen [431]). The role of the T6SS could not be directly tested since a ΔFPI mutant (lacking the T6SS) does not escape into the cytosol and thus fails to recruit GBPs [234]. Treatment of *F. novicida*-infected macrophages with chloramphenicol, an antibiotic blocking protein neosynthesis, did not promote GBP3 recruitment to *F. novicida* (Fig S2A) suggesting that the absence of GBP3 recruitment onto *F. novicida* is not due to active inhibition.

To further evaluate whether *F. novicida* could actively block GBP3/4 recruitment via secreted proteins, U937 macrophages were co-infected with *F. novicida* and *S. flexneri*. The cells were first infected with *F. novicida* and 4 h later with *S. flexneri* until 7 h total to ensure optimal GBP recruitment rates for both species. In co-infected cells, GBP3/4 were robustly recruited to *S. flexneri* (Fig 2A). Similar results were obtained when cells when inoculated with *F. novicida* and *S. flexneri* at the same time (Fig S2B). Therefore, the mechanism allowing *F. novicida* to escape GBP3/4 targeting does not act in trans on *S. flexneri* but is restricted to the bacterium strongly suggesting that this escape is not mediated by a *F. novicida* secreted effector.

Interestingly, while GBP1 and GBP2 recruitment could easily be observed in *F. novicida*-infected cells, we could not detect a single GBP1 or GBP2 recruitment event to *F. novicida* in cells co-infected with *S. flexneri* (Fig 2A). This observation was true for all coinfection experiments, regardless of the time of infection (Fig S2B) and was further validated in primary human macrophages co-infected with *S. flexneri* (Fig 2B). The lack of GBP1/2 recruitment onto *F. novicida* was restricted to cells co-infected with *S. flexneri* since GBP1/2 recruitment on *F.*

novicida was detected in bystander cells infected only with *F. novicida* (Fig S2C). These results indicate that in co-infected cells, GBP1 and GBP2 target preferentially *S. flexneri* than *F. novicida* suggesting a lower affinity of GBP1/2 for *F. novicida* envelope than for the one of *S. flexneri.* Importantly, this is also reflected in the lower frequency and the delayed recruitment of GBP1 on *F. novicida* compared to *S. flexneri* (Compare Fig 1C and 1D) despite the two bacteria having similar kinetics of escape into the host cytosol [432,433].

Recruitment of GBP2 to *F. novicida* depends on GBP1

GBP1 initiates recruitment of GBP2, 3 and 4 to *S. flexneri* and *S.* Typhimurium [311,419,420]. As the above results demonstrated differences in GBP targeting between *F. novicida* and the previously studied enterobacteria, we examined the hierarchy of GBP1 and GBP2 targeting to *F. novicida*.

HA:GBP1 and HA:GBP2 were expressed in *GBP*^{KO} U937 cells (Fig S3A and S3B) and their recruitment to *F. novicida* was scored at 7 h post-infection. Individual *GBP2-5* knock-out did not affect the frequency of HA:GBP1 recruitment to *F. novicida* suggesting that GBP1 is recruited independently of other GBPs (Fig 3A and 3B). Accordingly, in the absence of IFNγ (and hence of endogenous GBPs), ectopically expressed HA:GBP1 was recruited to *F. novicida* (Fig S3C and S3D). In contrast, HA:GBP2 was not recruited to *F. novicida* in IFNγ-treated *GBP1*^{KO} cells (Fig 3A and 3C), nor in WT cells in the absence of IFNγ (Fig S3C and S3D). Recruitment of HA:GBP2 was not affected by invalidation of *GBP3, 4* or *5*. Thus, as previously reported for *S. flexneri* [311,419,420] and *S.* Typhimurium [419], GBP1 is recruited to *F. novicida* independently of other GBPs and of other IFNγ-induced factors whereas GBP2 recruitment requires GBP1.

Using validated antibodies (Fig S3E), we investigated the co-recruitment of GBP1 and GBP2 to *F. novicida*. Whenever one GBP (GBP1 or GBP2) was targeted to a bacterium, the other GBP was detected on the same bacterium in more than 85% of the cases (Fig 3D). Super resolution microscopy demonstrated intimate colocalization between endogenous GBP1, GBP2, and the bacterial LPS in U937 macrophages, and in primary human macrophages (Fig 3E and 3F). Therefore, once recruited, GBP1 consistently recruits GBP2 onto *F. novicida* where both proteins tightly colocalize with LPS on the bacterial surface.

GBP1 CAAX box is suboptimal for *F. novicida* targeting

GBP1 and GBP2 undergo a post-translational addition of a lipid prenyl group [351]. This prenylation is guided by a C terminal CAAX motif, which dictates the nature of the prenyl group (Table 1). Prenylation is required for GBP1 to target *S. flexneri* [418,419,421] and *S.* Typhimurium [393,419]. Deletion of the GBP1 CAAX box (Fig S4A) also abolished GBP1 recruitment to *F. novicida* (Fig 4A). Similarly, deletion of GBP2 CAAX box abrogated its recruitment to *F. novicida* (Fig 4B and 4D), and to *S. flexneri* (Fig 4C and 4D). GBP prenylation is thus necessary for GBP1 and GBP2 targeting to *F. novicida*.

Table 1. Properties of macrophage-expressed GBPs

	CAAX box	Prenylation	GDP hydrolysis	Closest homologue (s)
GBP1	CTIS	F (15C)	85% [368]	GBP3
GBP2	CNIL	GG (20C)	5.6% [368]	GBP1
GBP3	none	none	N/A	GBP1
GBP4	none	none	N/A	GBP7
GBP5	CVLL	GG (20C)	0% [434]	GBP1, 3

*GMP formation calculated from [368] at GMP:GDP ratio for GBP1 = 5.7 and GBP2 = 0.06
F = farnesyl; GG = geranylgeranyl

The lipid moiety of GBP2 is a geranylgeranyl lipid that consists of a 20-carbon chain whereas GBP1 lipid moiety is a farnesyl, which is a shorter 15 carbon chain (Table 1). Since this farnesyl moiety likely anchors GBP1 into the lipid A leaflet (with 12-14 and 16-18 carbon-long acyl chains in *S. flexneri* and *F. novicida*, respectively) [421,425] we assessed whether the difference in prenylation played a role in the efficacy of GBP targeting. GBP1 and GBP2 CAAX motives were swapped to generate cell lines expressing HA:GBP1-CNIL or GBP2-CTIS (Fig S4A). In the absence of IFNγ, both GBP1 and GBP1-CNIL were recruited to *F. novicida* while GBP2 and GBP2-CTIS were not (Fig 4E). Therefore, GBP farnesylation is not sufficient to initiate GBP recruitment. Remarkably, HA:GBP1-CNIL was consistently recruited at higher rates than HA:GBP1 to *F. novicida*. The increased recruitment of GBP1-CNIL was even more striking upon IFNγ treatment. Conversely, GBP2-CTIS recruitment was significantly lower than that of HA:GBP2 (Fig 4F, S4B) to *F. novicida*. No significant differences were observed upon *S. flexneri* infection (Fig. 4G). Additionally, GBP1-CNIL-expressing cells responded to *F. novicida* infection with faster and higher cell death rates than the other cell lines (Fig S4C), suggesting that the increased recruitment has functional consequences on inflammasome-mediated cell death.

Altogether, these results reveal that GBP prenylation is required to target *F. novicida.* While the specificity of GBP prenyl chain does not drive GBP recruitment hierarchy, GBP prenylation type controls GBP recruitment efficiency, possibly in relation to the lipid A acyl chain length.

Multiple GBP1 domains are specifically required for the GBP1 pioneer recruitment onto *F. novicida*

As described above (Fig 3), GBP2 recruitment to *F. novicida* is governed by the initial GBP1 recruitment, while GBP1 is targeted to bacteria independently of IFNγ-induced factors. To identify the GBP1-specific domains driving the initial recruitment to *F. novicida,* GBP1-GBP2 and GBP2-GBP1 chimeras were generated (Fig 5A and S5A). A polybasic patch ($RRR_{584\text{-}586}$) in the GBP1 C-terminus controls GBP1 recruitment to *S. flexneri* and *S.* Typhimurium [339,418]. This CAAX-neighboring sequence is absent in GBP2 and in other human GBPs. The chimera lacking the triple R patch but otherwise displaying most of GBP1 sequence (N1-580-C2) was not recruited to *S. flexneri* nor to *F. novicida* (Fig 5B and 5C) in the absence of IFNγ priming indicating that the triple arginine patch also controls GBP1 targeting to *F. novicida*.

The presence of the 14 last amino-acid residues of GBP1 (including the triple R patch) was sufficient to drive the recruitment of the corresponding GBP2 chimera (N2-577-C1) to *S. flexneri* in the absence of IFNγ (Fig 5C). Surprisingly, the N2-577-C1 chimera was not recruited to *F. novicida* in the absence of IFNγ (Fig 5B and 5C). Further addition of GBP1 central domain and α12-13 region residues did not induce IFNγ-independent recruitment of the corresponding chimeras (N2-554-C1 or N2-315-C1) either. The pioneer recruitment (IFNγ-independent) was restored in chimera N2-26-C1 which additionally bears the globular GBP1 GTPase domain (Q26-L316). Importantly, in the presence of IFNγ, all the above chimeras were recruited to *F. novicida* thus confirming their functionality in terms of recruitment (Fig S5C and S5D). These results demonstrate that different domains (including the GTPase domain) within GBP1 specifically control recruitment to *F. novicida* while, as previously described [418], the polybasic patch seems to be the only factor discriminating GBP1 from GBP2 for its pioneer recruitment onto *S. flexneri*.

The GTPase domains of GBP1 and GBP2 present 90% similarity (Fig 5D) suggesting that discrete differences are responsible for their ability to specifically initiate recruitment to *F. novicida*. Several positively charged patches on the surface of GBP1, of which KKK_{61-63}, present in the GTPase domain, are required for GBP1 recruitment to *S.* Typhimurium [419]. GBP2 carries only two lysine residues (KKN_{61-63}) at the corresponding location. The K63N mutation dramatically reduced GBP1 targeting to *F. novicida* in the absence of IFNγ (Fig 5E). GBP1-63N was recruited onto *F. novicida* in the presence of IFNγ (S5G) and onto *S. flexneri* even in the absence of IFNγ (Fig 5F) indicating that this second patch of three basic residues (KKK_{61-63}) specifically contributes to initiating GBP1 recruitment to *F. novicida.* Furthermore, this result illustrates how subtle differences between GBP proteins deeply affect their hierarchy and their ability to target *F. novicida*.

In addition, GBP1 efficiently hydrolyzes GDP to GMP while GBP2 does not (Table 1, [368]). GMP formation by GBP1 is due to a "guanine cap" loop, situated between R239 and D255, which stabilizes GDP in the GBP1 catalytic pocket. The guanine cap present in GBP2 differs in its tertiary structure and does not promotes GMP formation [368]. To assess whether GBP1 GDPase activity may promote its pioneer recruitment to *F. novicida,* we first mutated GBP1 (p.G68A mutation) to block GDP hydrolysis while leaving GTP hydrolysis intact [405]. This mutation fully abolished GBP1 recruitment to *F. novicida* in the absence of IFNγ (Fig 5E and S5F). GBP1-G68A mutation did not significantly decrease its recruitment to *S. flexneri* in the absence of IFNγ (Fig 5F) nor its recruitment to *F. novicida* in the presence of IFNγ (Fig S5G). To confirm the role of GBP1 GDPase activity in specifically initiating recruitment to *F. novicida*, we generated a GBP1 variant carrying GBP2 guanine cap (GBP1-GC2) (Fig S5E). As observed for the GBP1-G68A mutant, the GBP1-GC2 chimera failed to target *F. novicida* in the absence of IFNγ (Fig 5E). Although a significant decrease in terms of recruitment to *S. flexneri* was also observed (Fig 5F), GBP1-GC2 chimera was robustly targeted to *S. flexneri* in 15% of infected cells (Fig S5F) and to *F. novicida* in the presence of IFNγ. Altogether, these findings strongly suggest that GBP1 requires its GDPase activity in order to initiate recruitment to *F. novicida*. Furthermore, they indicate that not only *S. flexneri* and *F. novicida* differ in the repertoire of GBPs recruited to their surface (Fig 1) but also in the requirement of GBP1 motifs/activity to target the bacterial surface. While the C-terminal triple R patch accounts for the main difference in GBP1/2 recruitment hierarchy onto *S. flexneri*, multiples domains in the globular GTPase domain and the C-terminus are required to initiate GBP1 recruitment onto *F. novicida* likely owing to the atypical nature of its LPS.

LpxF promotes escape from GBP3 targeting

F. novicida LPS includes a tetra-acylated lipid A, which has been associated with immune evasion [234,291,435]. To explore whether lipid A tetra-acylation plays a role in the escape of *F. novicida* from GBP3/4 recruitment, we infected U937 macrophages with a *F. novicida* Δ*lpxF* mutant. LpxF removes the phosphate in position 4' of the lipid A. Its absence results in a penta-acylated lipid A (Fig 6A) due to steric hindrance that blocks the 3' deacylase, LpxR [216]. The Δ*lpxF* mutant had a lower ability than the WT strain to rupture its phagosome (Fig. S6A), which was reflected in the lower rates of GBP1 recruitment (Fig S6B). Complementation of Δ*lpxF* mutant either by correcting the chromosomal locus (*lpxF-CAT*) or by expressing *lpxF* in trans from a complementing plasmid (p-*lpxF*) restored GBP1 recruitment to WT level (Fig S6B). We thus used endogenous GBP1 (Fig S6C) as a marker of cytosolic bacteria and analyzed GBP3 and GBP4 recruitment. We consistently noticed a discrete recruitment of HA-GBP3 on GBP1$^+$ Δ*lpxF* mutant strain that was absent in GBP1$^+$ WT or *lpxF*-complemented *F. novicida* strains (Fig 6B and 6C). The enrichment of GBP3 at the surface of GBP1$^+$ bacteria was quantified using semi-automated analyses on confocal images (Fig S6D). GBP3 was significantly more enriched on the Δ*lpxF* mutant than on the WT and complemented strains (Fig 6B, $p < 0.001$). These results indicate that the LpxF enzyme and the consequent *F. novicida* Lipid A modification contributes to the ability of *F. novicida* to escape to GBP3 targeting. The recruitment of GBP3 onto the Δ*lpxF* mutant was not as extensive as onto *S. flexneri* (Fig 1B) suggesting that other *F. novicida*-specific virulence factors contribute to escape from GBP3 recruitment. Furthermore, we did not observe any GBP4 recruitment or enrichment (Fig S6E and 6F) onto GBP1$^+$ Δ*lpxF* mutants indicating that LpxF-mediated LPS modification controls GBP3 but does not account for GBP4 targeting escape mechanism.

Altogether, these results underline the stealth nature of *F. novicida* which escapes GBP3 recognition owing to its atypical tetra-acylated LPS. Additional prokaryotic factors likely constrain recruitment of GBP3 and, to an even greater extent of GBP4 to *F. novicida*.

DISCUSSION

Professional cytosol-dwelling bacteria either hide from or actively inhibit cell autonomous responses to thrive in the host cytosol. Here, we observed that *F. novicida* escapes from being targeted with specific human GBPs. Furthermore, the kinetics and the frequency of GBP1/2 recruitment onto *F. novicida* suggests that *F. novicida* dampens the whole GBP recruitment process. While GBP1 recruitment requirements have been studied with *S. flexneri and S.* Typhimurium, GBP1 recruitment to *F. novicida* appears to be less resilient to *GBP1* mutations, allowing us to highlight multiple independent features required for GBP1 targeting.

Four features in GBP1 drive recruitment to *F. novicida*. Two of them, the GBP1 CAAX box and the C-terminal triple arginine patch also promote recruitment to *S. flexneri* and *S.* Typhimurium [311,393,421]. Interestingly, the two others were required for GBP1 targeting to *F. novicida* but were fully facultative for *S. flexneri: a* lysine residue (K_{63}) present in a patch of three consecutive positively charged residues (KKK_{61-63}) in the N-terminal region of GBP1 and the GDPase activity (invalidated by the p.G68A mutation) [405]. GMP production by GBP1 and its ensuing catabolism in uric acid contributes to NLRP3 inflammasome activation during *Chlamydia trachomatis* infection [405]. Depending on the infecting pathogen, the GDPase activation may thus have two synergistic functions to promote inflammasome activation, the first one at the bacterial surface to assemble the caspase-4-activating platform [419–421] and

the second one to activate the NLRP3 inflammasome. The role of GBP1 GDPase activity to target *F. novicida* was confirmed by replacing the guanine cap of GBP1 (which plays a specific role in GMP formation [368]) with the one of GBP2. Contrary to the p.G68A mutation, the guanine cap exchange decreased targeting to *S. flexneri*. The guanine cap of GBP1 contains a third positive patch ($RRK_{243-245}$) that is mirrored by a $KKY_{243-245}$ in GBP2. Although, the $RRK_{243-245}$ was not required for GBP1 binding to *E. coli* LPS in an in vitro assay [419], we cannot exclude that this patch may play a role in *S. flexneri* targeting possibly in synergy with the GDPase activity. Altogether, our study extends the findings from previous publications demonstrating that several independent GBP1 features contribute to targeting to Gram-negative bacteria. Furthermore, studying *F. novicida* targeting in comparison with *S. flexneri* identified specific GBP1 features that are required for *F. novicida* but facultative for *S. flexneri* targeting suggesting that GBP1 has evolved these different domains to recognize a diversity of pathogens.

In addition to GBP1 prenylation, we observed that GBP2 recruitment to *F. novicida* and *S. flexneri* was dependent on the CAAX box. This result indicates that further GBP specificities exist to control GBP recruitment downstream of GBP1. Indeed, GBP3 and GBP4, which are recruited to *S. flexneri* are devoid of a CAAX box while the prenylated GBP5 is not recruited. More surprisingly, the presence of the GBP2 CAAX box on either GBP1 or GBP2 was associated with a significantly higher recruitment to *F. novicida* than GBP1 or GBP2 with GBP1 CAAX box. GBP1 and GBP2 CAAX boxes drive farnesylation or geranylgeranylation, respectively (Table 1). The longer size of the GBP2 lipid anchor (20 carbons) might increase the stability of GBP recruitment in the membrane of *F. novicida*, which displays long lipid A acyl chains with 16 to 18 carbons (Fig 6A).

In addition to the above discussed host features, our work further revealed that bacterial factors control GBP recruitment. Indeed, *F. novicida* escapes targeting by the non-prenylated GBP3 and GBP4. GBP2-4 recruitment to *S. flexneri* or *S.* Typhimurium depends solely on GBP1 and on no other GBP [419,420] suggesting that no further recruitment hierarchy exists downstream of GBP1. However, facing two different pathogens in the same experimental system, GBP2, GBP3 and GBP4 were differentially recruited. Therefore, additional mechanisms control the selective GBP recruitment downstream of GBP1, and those mechanisms are dependent on bacterial factors. GBP3/4 might require the presence of a specific bacterial molecule that would act, together with GBP1, as a co-receptor to allow GBP3/4 recruitment, and that would be absent from *F. novicida* envelope. Alternatively, GBP1/2 polymer conformation at the surface of *F. novicida* may not be favorable to promote GBP3 or GBP4 binding. While the O-chain moiety of LPS drives GBP1 encapsulation of bacteria [421], several evidence suggest that other LPS domains contribute to GBP recruitment/function. First, GBPs are recruited at the surface of *S. flexneri* rough mutants (without O-chain) although at lower levels than to WT strain [418]. Second, in vitro, GBP1 still binds *S. flexneri* Δ*rfaL* rough mutant although it does not promote GBP1 encapsulation [421]. Third, mGBPs are required for full inflammasome activation in response to smooth LPS, rough LPS or even synthetic lipid A [417]. Importantly, our work suggests that one of the bacterial factor that controls GBP recruitment is the number of lipid A acyl chains. Indeed, GBP3 was recruited on *F. novicida ΔlpxF* mutant, which bears a penta-acylated lipid A. Interestingly, LPS from *ΔlpxF F. novicida* mutant is also recognized by caspase-11 [291] suggesting a convergent evolution of cytosolic LPS sensors. Of note *lpxF* deletion also results in the presence of an additional phosphate group in the disaccharide anchor of lipid A, which is absent in wild-type *F. novicida* but is otherwise present in

enterobacteria LPS (Fig 6A). This phosphate addition increases the negative charge of the LPS and may thus account for or contribute to the recruitment of GBP3.

Interestingly, the GBP3 recruitment observed on *ΔlpxF* mutant strain was not comparable to the GBP1/2 recruitment observed on WT *F. novicida* or to the GBP3 recruitment observed on *S. flexneri*, suggesting that besides lipid A tetra-acylation, *F. novicida* has evolved other strategies to hide from GBP3 (and GBP4) recruitment. In addition to the tetra-acylation of its LPS, *F. novicida* has numerous other unique envelope characteristics, including a high proportion of free lipid A, and the presence of additional sugars in the lipid A anchor. Multiple properties of its bacterial envelope may thus cooperate to enable escape from GBP targeting. Finally, the highly virulent *F. tularensis* subspecies tularensis evades mGBP-mediated growth restriction more efficiently than *F. novicida* [308]. Future studies should examine the role of the *F. tularensis* envelope "invisibility cloak" in the escape of GBP-mediated immune responses.

MATERIALS AND METHODS

Ethics statement

Blood from healthy donors was obtained from the Etablissement Français du Sang Auvergne-Rhône Alpes, France under the convention EFS 16-2066. Informed consent was obtained from all subjects in accordance with the declaration of Helsinki. Ethical approval was obtained from Comité de Protection des Personnes SUD-EST IV (L16-189).

Bacterial strains

Francisella novicida strain Utah (U112) and related mutants were grown in Tryptic Soy agar and broth (Pronadisa) supplemented with 0.1% w/v L-cysteine. *F. novicida* ΔFPI and Δ*lpxF* mutants were previously described [217,436]. Lipid A composition of the Δ*lpxF* mutant was validated by mass spectrometry. Complemented Δ*lpxF* mutants were generated and cultivated as described below. *Shigella flexneri* str. M90T ΔipaH9.8 [437] was grown in Tryptic Soy agar and broth. *Escherichia coli* DH5α were grown in Lysogeny broth and agar (Pronadisa) supplemented with ampicillin (100 µg/ml), kanamycin (30 µg/ml), tetracycline (50 µg/ml) or chloramphenicol (20 µg/ml) when necessary.

Cell cultures

U937 cells were maintained in RPMI Medium 1640 - GlutaMAX™-I (ThermoFisher Scientific) supplemented with 10% v/v fetal calf serum. HEK293T cells were maintained in Dulbecco's Modified Eagle Medium with GlutaMAX™-I (ThermoFisher Scientific) with 10% v/v fetal calf serum and geneticin (200 µg/ml). Primary human $CD14^+$ monocytes were isolated from blood and differentiated into macrophages for a week as previously described [234].

Bacterial complementation

F. novicida genome sequence was retrieved from GenBank (accession number GCF_000014645.1 and entry number FTN_0295 for the *lpxF* gene). For chromosomic complementation of *lpxF*, the coding sequence was amplified from wild-type *F. novicida* DNA using a Phusion® High-Fidelity DNA polymerase (New England BioLabs) starting from 600 bp

upstream of the gene to the stop (PCR A) or from the stop codon to 600 bp downstream of *lpxF* (PCR C). Chloramphenicol resistance cassette (*CAT* gene) under the control of *F. novicida groES/EL* promoter was amplified from a chloramphenicol-resistant *F. novicida* strain using primers containing FRT sequences (PCR B). The FRT-flanked *CAT* sequence was integrated between PCR A and PCR C using joint PCRs. The PCR product was introduced in *F. novicida* Δ*lpxF* strain by chemical transformation. *F. novicida* culture of OD_{600nm} = 0.9 was concentrated 10 times in a chemical transformation buffer (270 mM NaCl, 24 nM $MgSO_4$, 20 mM $CaCl_2$, 35 mM $MnCl_2$, 50 mM Tris, 2mM L-Arg, 1 mM L-His, 2 mM L-Met, 3 mM L-Asp, 0.2 mM Spermine, pH = 6.8) and incubated for 20 min at 37°C, 100 rpm with 1 µg DNA per 500 µl of bacterial suspension. The bacteria were then incubated for 2 h in TSB + 0.1% cysteine and 0.4% glucose, then spread onto selective TSA cysteine medium containing 4 µg/µl chloramphenicol. Selected clones were validated by sequencing.

For trans-complementation, *lpxF* was amplified using primers containing PstI and EcoRI restriction sites. The digested PCR product was ligated into pKK214 [438] using T4 DNA ligase (New England BioLabs) and transformed into DH5α. Plasmids extracted from tetracycline-resistant clones were validated by sequencing. pKK214-*lpxF* construct was introduced in *F. novicida* Δ*lpxF* through chemical transformation as described above. Clones were selected using tetracycline 3 µg/µl on TSA cysteine plates or routinely grown in TSB with tetracycline at 0.75 µg/µl.

Primers are available in Table S1.

Plasmid constructions

GBP fragments were amplified from pAIP plasmids containing *GBP1, GBP2, GBP5* cDNA in frame with a N-terminal HA tag-coding sequence using primers listed in Table S1. Chimeric *GBP* sequences were produced by joint PCR using a Phusion® High-Fidelity DNA polymerase. Point mutations were introduced into *GBP* sequences cloned in a pUC57 plasmid, using PFU Ultra II DNA polymerase. The methylated template was digested with DpnI and the mutated plasmid was transformed in *E. coli* DH5α cells. The chimeric or mutated *GBP* sequences were then transferred into pAIP using NotI and BamHI and the T4 DNA ligase and transformed into *E. coli* DH5α. All final constructs were verified by sequencing.

Lentiviral production and generation of stable U937 cell lines

HEK293T cells were seeded in complete DMEM medium at 2.10^6 cells per 25 cm^2 cell culture flask and transfected 24h later with 4.3 µg pPAX2 (gag-pol expression), 1.43 µg pMDG (VSV-G expression) and 5.6 µg pAIP construct. Transfection was carried out in 1.4 ml OptiMEM™ reduced serum medium (ThermoFisher Scientific) supplemented with 20 µM polyethylenimine (Sigma-Aldrich #408727). Complete DMEM was added 4 h later. On the following day, the medium was changed for 1.4 ml DMEM. Lentiviruses were collected 48 h after transfection. U937 cells were seeded at $2.5x10^5$ per well in a P24 plate and transduced by adding 500µl lentiviral particles to the culture medium. Starting from 72 h post-transduction, transduced cells were selected by treating with puromycin (2 µg/ml) for 14 days. Protein expression was controlled by Western Blot. All produced cell lines are described in Table S2. Control, *GBP1*^{KO}, *GBP2*^{KO}, *GBP3*^{KO} cells were previously described [420]. *GBP4*^{KO} and *GBP5*^{KO} U937 cell lines were generated similarly using the following sgRNA: GBP4: GTAACCCTAAGAATGACTCG (guide 1), TGTGCGGTATAGCCCTACAA (guide 2); GBP5: AAACTCACCCGACCTTGACA

(guide 1), GTTCACAGTATTGTACACAA (guide 2). Wild-type U937 and HEK-293T cells tested negative for *Mycoplasma*.

Infections

To obtain macrophages, U937 monocytes were seeded 36h prior to infection in complete RPMI supplemented with 100 ng/ml phorbol myristate acetate (PMA, Sigma-Aldrich). Primary human monocytes were treated with 50 ng/ml M-CSF (Sigma-Aldrich) in complete RPMI for a week before infection. Treatment with 10^3 U/ml hIFN-γ (Sigma-Aldrich) was done 18 h prior to infection unless otherwise specified. Bacteria were grown in overnight culture in 2 ml TSB + 0,1% cysteine (*F. novicida*) or TSB (*S. flexneri*). Infection with *F. novicida* was done using overnight culture. For infection with *S. flexneri*, the overnight culture was diluted at 1/100 and the subculture was grown until it reached an OD_{600nm} 1. The bacteria were suspended in RPMI at the desired MOI and added onto the cells followed by a spinoculation at 1000 g for 15 min (32°C). After 1 h of incubation at 37°C, the cells were washed and the medium was replaced in RPMI with gentamycin (5µg/ml for *F. novicida* or 100 µg/ml for *S. flexneri*) until the desired time post-inoculation. When applicable, chloramphenicol (4 µg/mL) was used to inhibit protein neosynthesis at 5 h p.i.

Immunofluorescence

U937 macrophages and hMDMs were differentiated as described above and seeded at 5.10^5 cells/ml in P12 plates (U937) or onto sterile glass coverslips (hMDMs). Infection was carried out as described above. At the indicated time of infection, the cells were washed and fixed with 2% formaldehyde (Sigma-Aldrich) in PBS for 10 min at RT. U937 cells were mounted on poly-L-lysine slides (Sigma-Aldrich) using Shandon Cytospin 3 cytocentrifuge for 10^5 cells per slide. hMDMs were stained directly on the glass coverslips. Permeabilization was done with in PBS-Triton 0.1% for 10 min at RT. The samples were submerged in blocking buffer (5% BSA, 0.1% Triton, 0.02% NaN_3 in PBS) for 1 h at RT or 4°C O/N then stained with the appropriate antibodies, listed in Table S3. DAPI (4′,6-diamidino-2-phenylindole at 100 ng/ml, ThermoFischer Scientific) was used for DNA staining. Coverslips were mounted using Fluoromount G™ (Invitrogen) mounting medium. Images for statistical analysis were taken on a Nikon Eclipse Ts2R-FL inverted microscope. For representative images, the samples were imaged on a Zeiss LSM 800 confocal microscope or Zeiss Elyra 7 SIM/STORM microscope. ImageJ software was used for analysis.

Phagosomal rupture assay

Quantification of vacuolar *F. novicida* escape was done using the β-lactamase/CCF4 assay (Life Technologies) [439]. Briefly, U937 monocytes were seeded in P48 plates at $1.25x10^5$ cells/well in PMA-supplemented RPMI. The cells were treated with 10^3 U/lm IFNγ and infected as described above., the cells were washed at 3 h post-infection and incubated with CCF4 for 1 h at RT in the presence of 2.5 mM probenecid (Sigma-Aldrich). Live cells (propidium-iodide negative, CCF4 positive) were tested for *F. novicida*-mediated phagosomal rupture by flow cytometry using excitation at 405 nm and detection at 450 nm (cleaved CCF4) or 510 nm (intact CCF4).

Cell death assay

U937 cells were differentiated for 10^5 cells/well in 96 well plates, treated with 100 U/ml IFNγ and infected with *F. novicida* at MOI 100 as described above. The cells were washed with PBS at 1 h p. i. and the medium was replaced with CO2-independent medium supplemented with 10% FCS, 5 µg/ml gentamycin and 5 µg/ml propidium iodide (PI, ThermoFischer Scientific). PI fluorescence was measured every 15 min during 24 h on a Tecan microplate fluorimeter. Data were normalized using uninfected cells and cells treated with 1% Triton X100 (100% cell death).

Real time PCR

PMA-differentiated U937 were treated or not with IFNγ and infected or not as described above. Total RNA was extracted using chloroform and TRI Reagent ® (Sigma-Aldrich #93289) and reverse transcribed with random primer combined with Im-Prom Reverse Transcription System (Promega #A3800). Quantitative real-time PCR was performed using FastStart Universal SYBR Green Master Mix (Roche #04913850001) and an Applied StepOnePlus™ Real-Time PCR System (ThermoFisher Scientific). Gene-specific transcript levels were normalized to the amount of human *HPRT* transcripts. Primer sequences are available in [234].

Western blotting

U937 cells were washed in PBS and lysed for 30 min on ice using Radioimmunoprecipitation buffer supplemented with EDTA-free protease inhibitor cocktail cOmplete™ (Roche). Cleared lysate was obtained by centrifugation at 11,000 g for 10 min at 4°C. Total protein concentration of the lysates was determined using a Micro BCA™ Protein Assay Kit (ThermoFisher Scientific) according to the manufacturer's protocol. Laemmli Sample Buffer (Bio-Rad) with 10% v/v β-mercaptoethanol (Sigma-Aldrich) was added to the protein samples before boiling them for 10 minutes at 95°C. Protein extracts were deposited onto a 4-15% Mini-PROTEAN® TGX™ gel (Bio-Rad) for migration. Following migration, the samples were transferred onto a membrane using Trans-Blot® Turbo™ RTA transfer system (Bio-Rad). The membranes were saturated with 5% skimmed milk, then stained with the appropriate primary and secondary antibodies (Table S3) and revealed with an ECL detection reagent (Dd Biolab).

Statistical analysis

Statistical analysis was performed with GraphPad Prism 9 software. Normality was assessed for data sets with n > 20 entries using D'Agostino & Peerson omnibus normality test. Multiple comparison was done with analysis of variance tests with post-hoc corrections (Dunnett's or Sidak's depending on the selected comparisons). In the case of single comparisons, two tailed t tests were performed.

Data availability

All relevant data are available in the paper or the supplementary material. Plasmid constructs have been deposited in Addgene (public access pending). Additional data is available upon request.

ACKNOWLEDGMENTS

We thank D. Monack (Stanford University) and A. Cimarelli (CIRI) for reagents. We acknowledge the contribution of SFR Biosciences (UAR3444/CNRS, US8/Inserm, ENS de Lyon, UCBL) flow cytometry and imaging facilities (especially Elodie Chatre). This project is supported by an ANR grant to TH (Tulamibe, ANR-17-ASTR-0024-02). SVV is supported by a scholarship from AID (AID 2019013) & Inserm. GG is supported by a FRM grant (SPF201809006927).

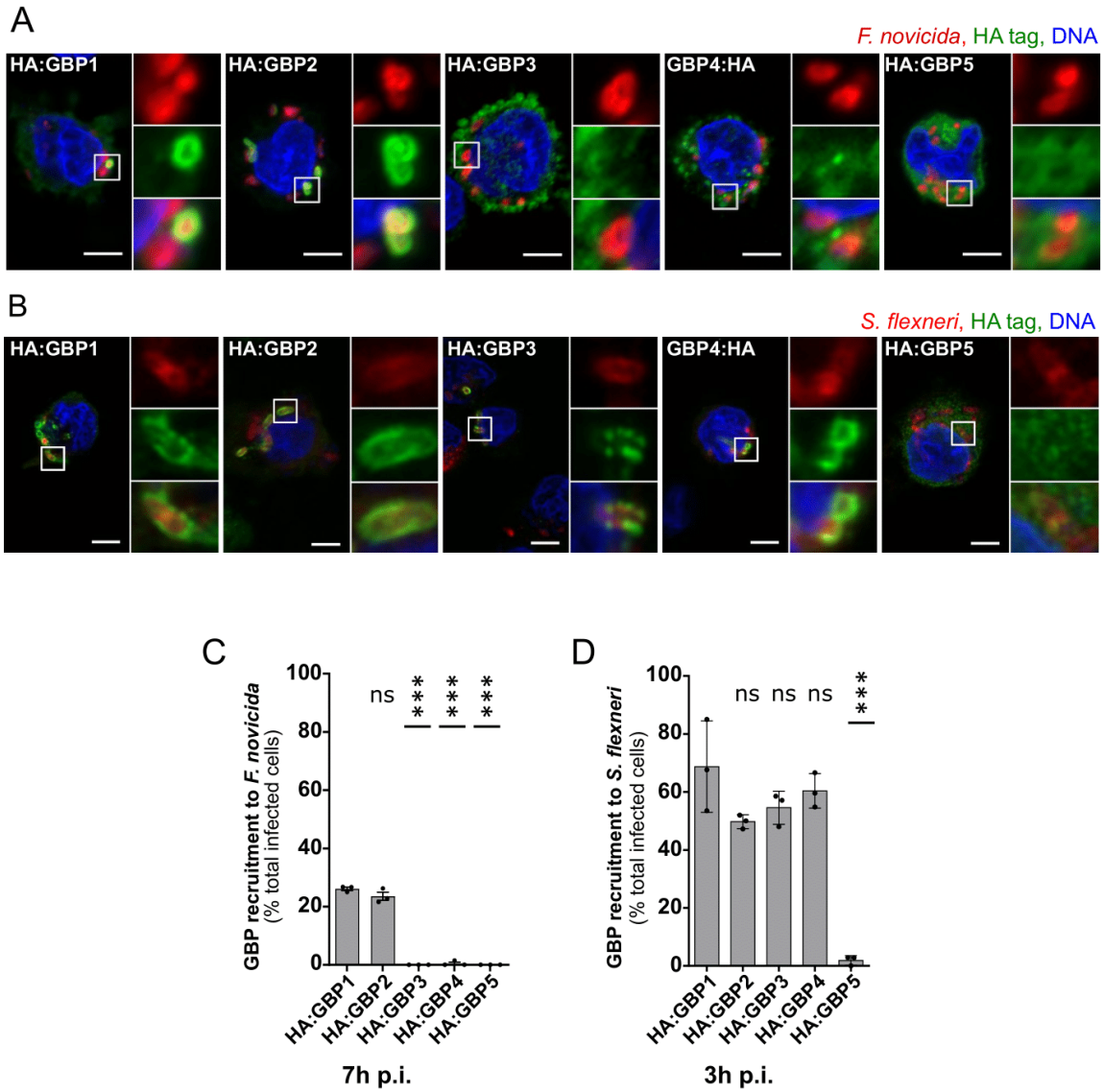

Fig 1. *F. novicida* and *S. flexneri* are targeted by a different repertoire of GBPs.

IFNγ-treated, HA:GBP-expressing, U937 macrophages were infected with *F. novicida* (A, C) or *S. flexneri* ΔipaH9.8 (B, D) at the indicated time post-infection (p.i.). (A) and (B) show representative images, scale bar 5 μm and 3X zoom on the right panels. (C) and (D) GBP recruitment was quantified as the percent of infected cells in which GBPs are targeted to bacteria. Each point represents the value from one experiment with 50-100 infected cells counted per experiment. The bar represents the mean +/- SEM of three independent experiments. ANOVA with Dunnett's analysis was performed in comparison to GBP1 recruitment frequency: ***, $p < 0.001$; ns, not significant.

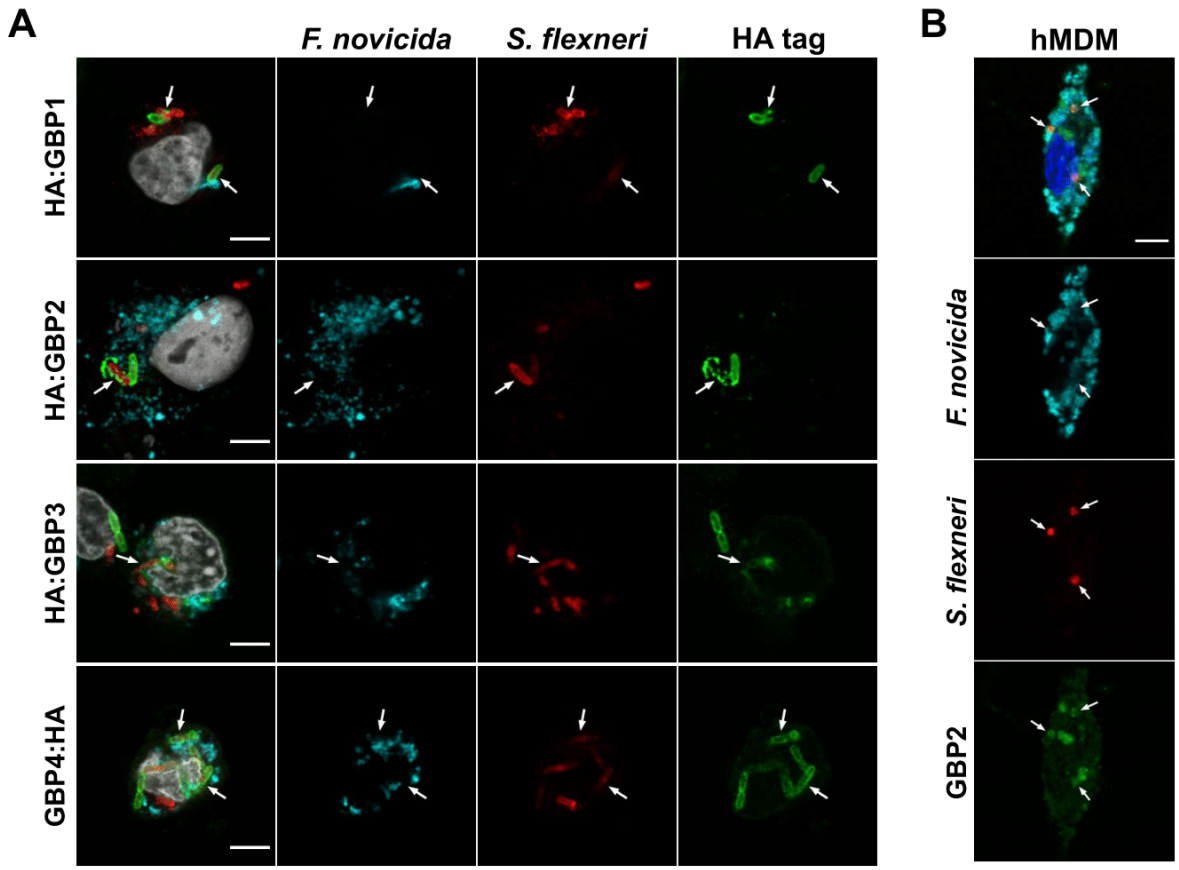

Fig 2. GBPs are selectively recruited to *S. flexneri* in *F. novicida*-co-infected cells.

IFNγ-primed U937 macrophages (A) or human monocyte-derived macrophages (hMDMs, B) were infected with *F. novicida* at MOI 50 and then 4 h later with *S. flexneri* ΔipaH9.8 at MOI 50 for 3 h (A) to 4 h (B). Representative images are shown. The arrows indicate GBP recruitment to *S. flexneri*. Scale bar, 5 μm.

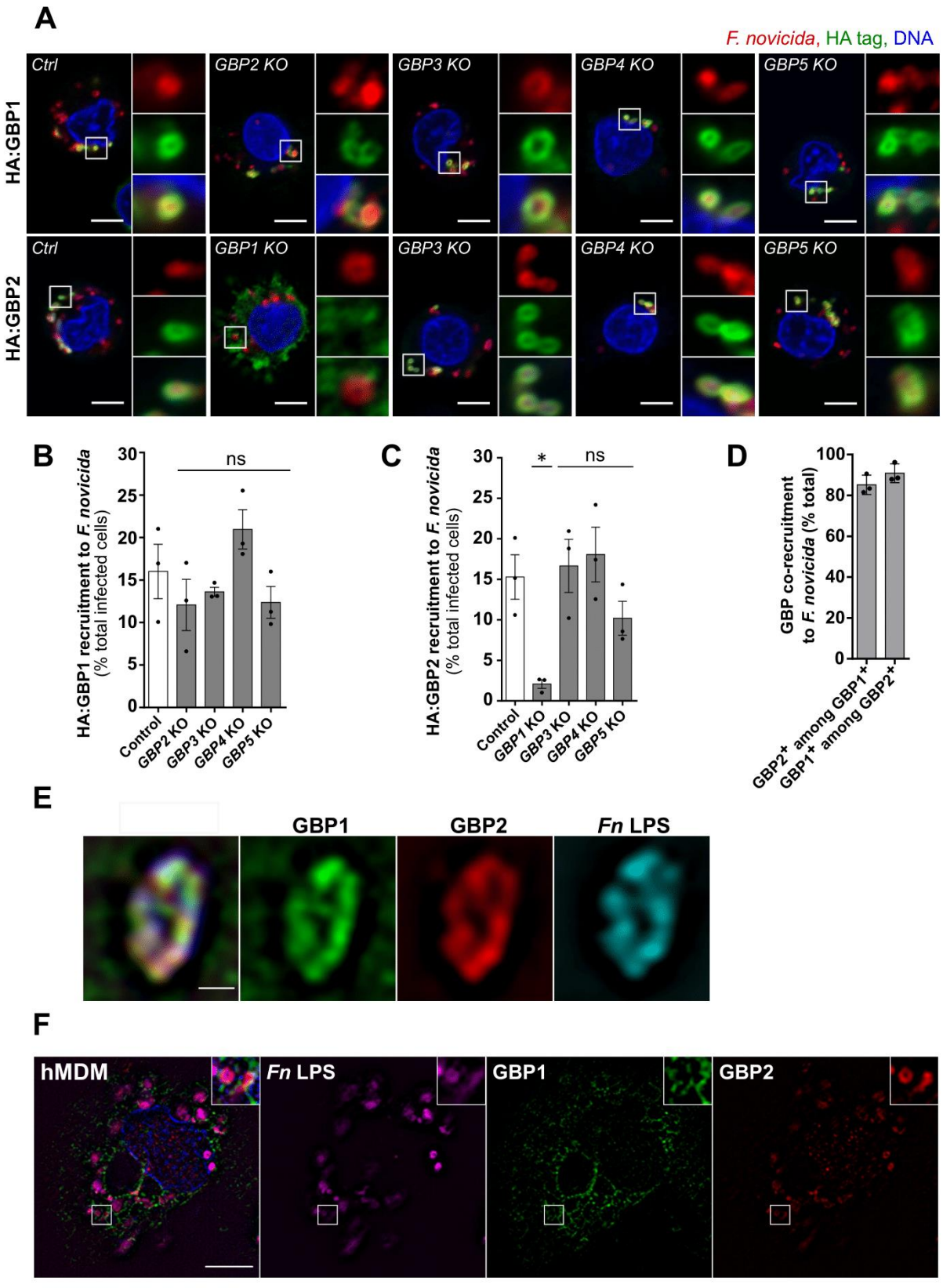
A
F. novicida, HA tag, DNA
HA:GBP1
HA:GBP2
Ctrl
GBP2 KO
GBP3 KO
GBP4 KO
GBP5 KO
Ctrl
GBP1 KO
GBP3 KO
GBP4 KO
GBP5 KO
B
HA:GBP1 recruitment to F. novicida (% total infected cells)
ns
Control
GBP2 KO
GBP3 KO
GBP4 KO
GBP5 KO
C
HA:GBP2 recruitment to F. novicida (% total infected cells)
*
ns
Control
GBP1 KO
GBP3 KO
GBP4 KO
GBP5 KO
D
GBP co-recruitment to F. novicida (% total)
GBP2+ among GBP1+
GBP1+ among GBP2+
E
GBP1
GBP2
Fn LPS
F
hMDM
Fn LPS
GBP1
GBP2

Fig 3. GBP2 is recruited in a GBP1-dependent manner to *F. novicida*.

IFNγ-treated U937 (A-E) or monocyte-derived macrophages (F) were infected with *F. novicida* for 7 h (A-E) or 10 h (F). (A) Representative images of GBP^{KO} or control U937 cells stably expressing HA:GBP1 (top panels) or HA-GBP2 (lower panels) are shown with scale bar 5µm and 3X zoom. (B, C) HA:GBP recruitment was expressed as the percentage of infected cells presenting GBP-bacteria colocalization. (D) Endogenous GBP co-recruitment to *F. novicida* measured as the percent of GBP2-positive bacteria among the GBP1-positive and vice-versa. (E, F) Structured illumination microscopy of endogenous GBP localization to *F. novicida* in U937 cells (E) or human monocyte-derived macrophages (hMDMs) (F), scale bar 0.5µm in (E) and 5 µm in (F).

Data information (B-D): Each point indicates the value of one experiment with 50-100 infected cells analyzed. The bar represents the mean +/-SEM of 3 independent experiments. ANOVA with Dunnett's analysis was performed in comparison to recruitment frequency in control cells: *, $p < 0.05$; ns, not significant.

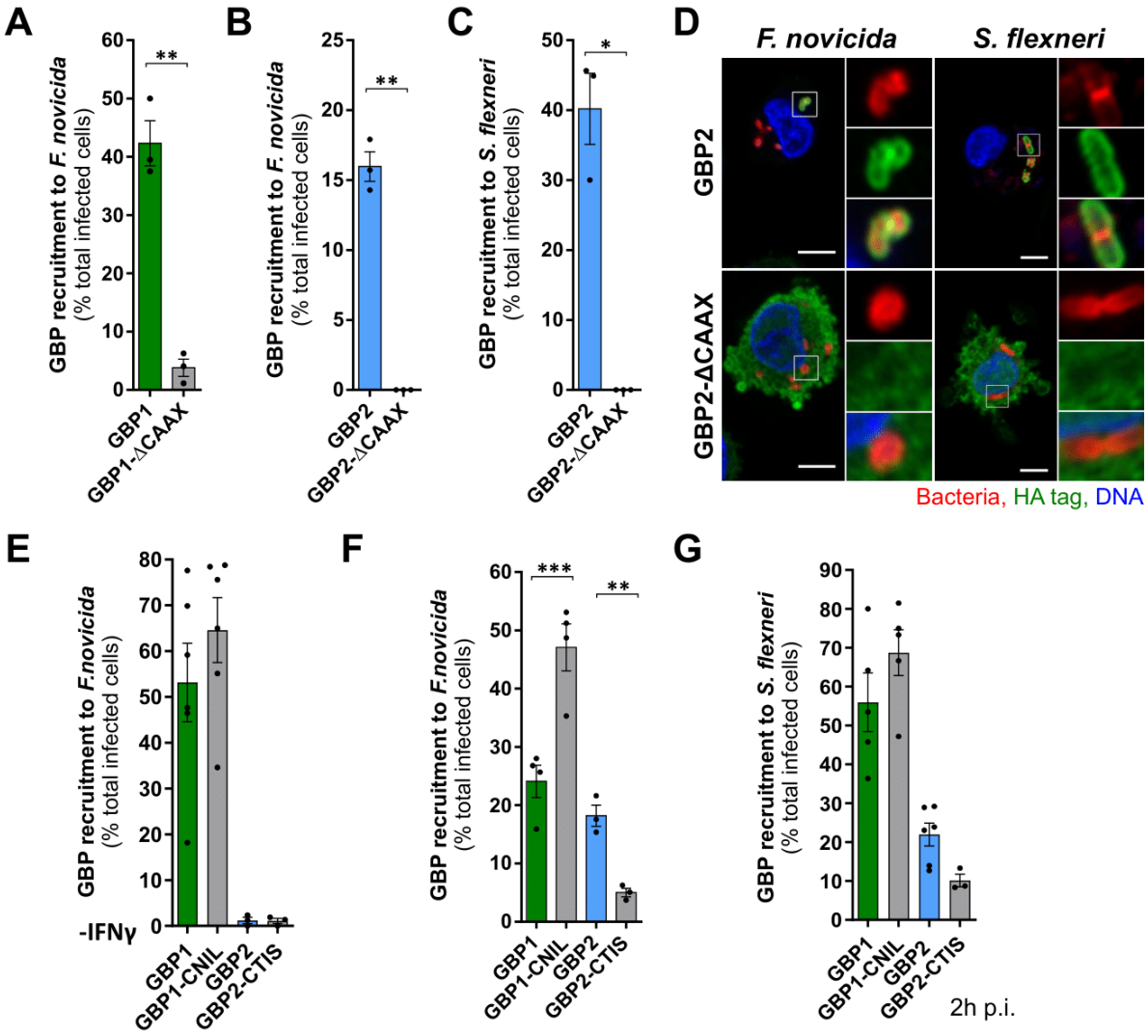

Fig 4. GBP1 CAAX box is suboptimal to target *F. novicida*.

U937 macrophages treated (A-D, F, G) or not (E) with IFNγ, were infected with *F. novicida* for 7 h (A, B, D-F) or *S. flexneri* ΔipaH9.8 for 2 (G) to 3 h (C-D). (D) Representative images with scale bar 5µm and 3X (*F. novicida*) or 2X (*S. flexneri*) zoom on the right panels are shown. (A-C, E-G) GBP recruitment was scored as the percentage of infected cells with GBP-bacteria colocalization. Each point corresponds to the value from one experiment with 50-100 infected cells analyzed. The bar represents the mean +/- SEM of three independent experiments. Two-tailed t test with Welch's correction (A-C) or ANOVA with Sidak's (E-G) analysis was performed: *, $p < 0.05$; **, $p < 0.01$; ***, $p < 0.001$.

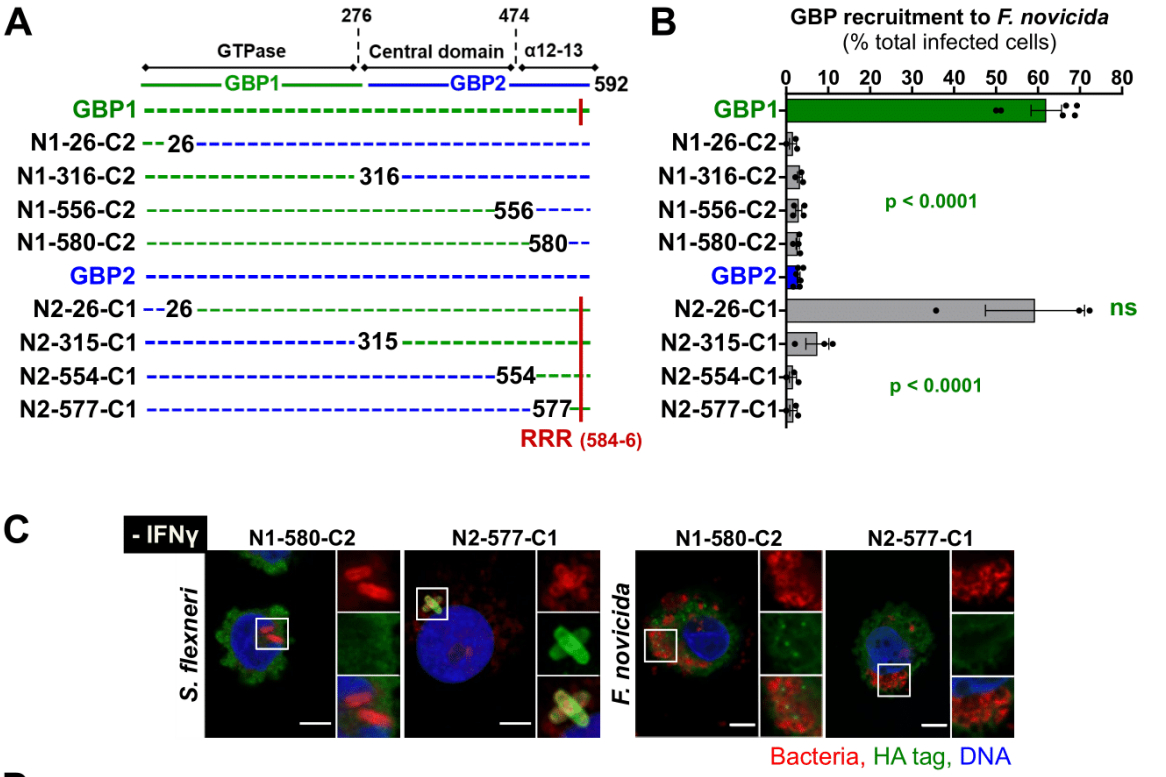
A
276
474
GTPase
Central domain
α12-13
GBP1
GBP2
592
GBP1
N1-26-C2
26
N1-316-C2
316
N1-556-C2
556
N1-580-C2
580
GBP2
N2-26-C1
26
N2-315-C1
315
N2-554-C1
554
N2-577-C1
577
RRR (584-6)
B
GBP recruitment to F. novicida
(% total infected cells)
0 10 20 30 40 50 60 70 80
GBP1
N1-26-C2
N1-316-C2
N1-556-C2
p < 0.0001
N1-580-C2
GBP2
N2-26-C1
ns
N2-315-C1
N2-554-C1
p < 0.0001
N2-577-C1

C
- IFNγ
N1-580-C2
N2-577-C1
N1-580-C2
N2-577-C1
S. flexneri
F. novicida
Bacteria, HA tag, DNA


D
Lysine patch
61 63
68
GDPase
GBP1 ALKILSAITQPMVVVAIVGLYRTGKSYLMNKLAGKKKGFSLGSTVQSHTKGIWMWCVPHPKKPGHILVLLDTEGLGDVEKGDNQNDSWIFALAVLLS
GBP2 ALKILSAITQPVVVVAIVGLYRTGKSYLMNKLAGKKNGFSLGSTVKSHTKGIWMWCVPHPKKPEHTLVLLDTEGLGDIEKGDNENDSWIFALAILLS
26 133
GBP1 STFVYNSIGTINQQAMDQLYYVTELTHRIRSKSSPDENENEVEDSADFVSFFPDFVWTLRDFSLDLEADGQPLTPDEYLTYSLKLKKGTSQKDETFN
GBP2 STFVYNSMGTINQQAMDQLHYVTELTDRIKANSSP--GNNSVDDSADFVSFFPAFVWTLRDFTLELEVDGEPITADDYLELSLKLRKGTDKKSKSFN
134 219
239
255
GBP1 LPRLCIRKFFPKKKCFVFDRPVHRRKLAQLEKLQDEELDPEFVQQVADFCSYIFSNSKTKTLSGGIQVNGPRLESLVLTYVNAISSGDLPCMENAVL
GBP2 DPRLCIRKFFPKRKCFVFDWPAPKKYLAHLEQLKEEELNPDFIEQVAEFCSYILSHSNVKTLSGGIAVNGPRLESLVLTYVNAIGSGDLPCMENAVL
220 317
Guanine cap

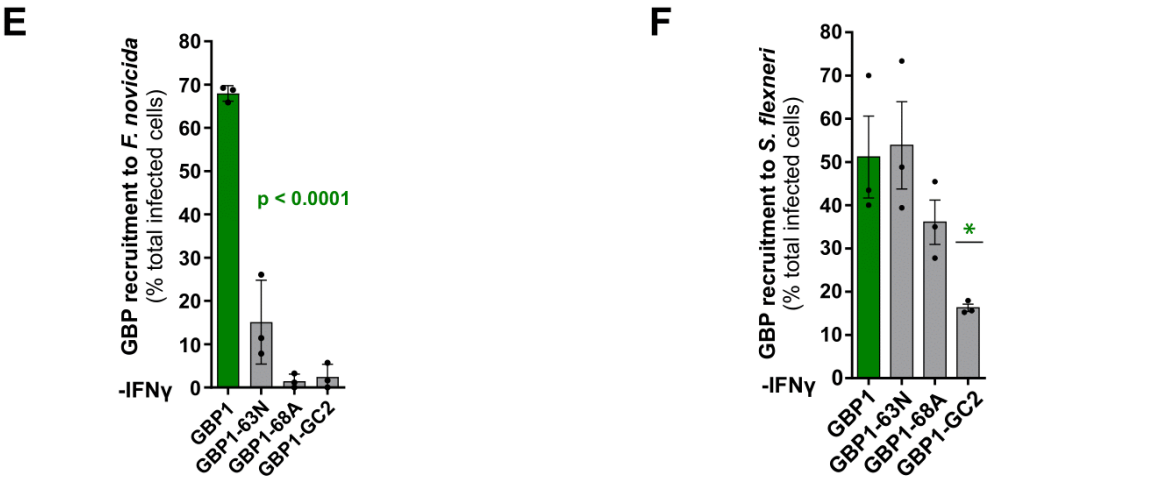
E
GBP recruitment to F. novicida
(% total infected cells)
80
70
60
50
40
30
20
10
0
p < 0.0001
-IFNγ
GBP1
GBP1-63N
GBP1-68A
GBP1-GC2
F
GBP recruitment to S. flexneri
(% total infected cells)
80
70
60
50
40
30
20
10
0
*
-IFNγ
GBP1
GBP1-63N
GBP1-68A
GBP1-GC2

Fig 5. Multiple GBP1 features are required for the pionneer GBP1 recruitment to *F. novicida.*

(A) GBP1-2 or GBP2-1 chimera are schematically shown. (B, C, E, F) U937 macrophages were infected with *F. novicida* for 7 h (B, C, E) or *S. flexneri* ΔipaH9.8 for 2 h (C, F). Recruitment was calculated as the percentage of infected cells with HA-GBP-bacteria colocalization. (D) Clustal alignment of GBP1 and GBP2 GTPase domains with a highlight on the studied domain/residues. (B, E, F) Each point corresponds to the value from one experiment with 50-100 infected cells analyzed. The bar represents the mean +/- SEM of three to six independent experiments. ANOVA with Sidak's (B) or Dunnett's (D, E) analysis was performed in comparison with GBP1 recruitment: *, $p < 0.05$; ns, not significant.

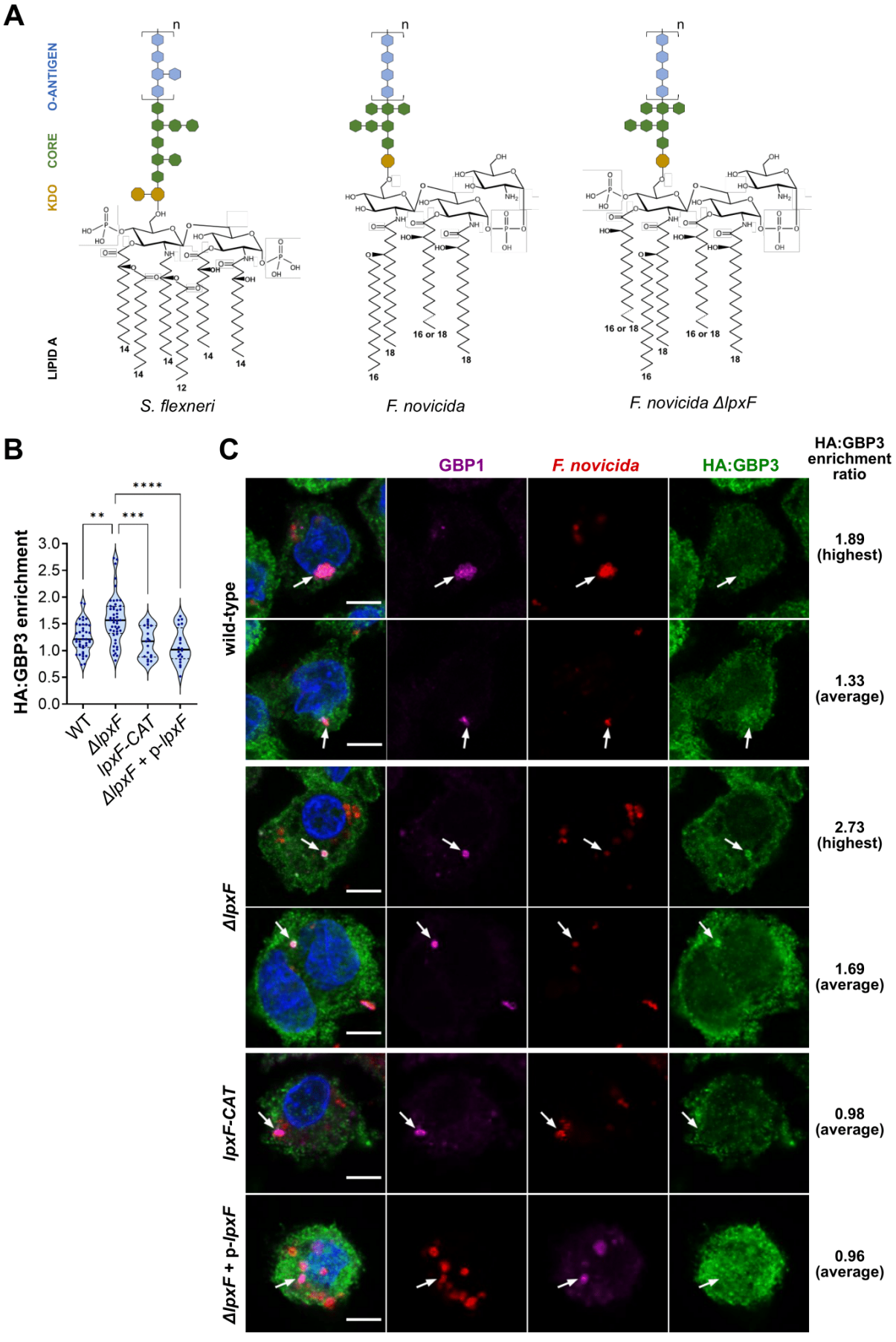
A
O-ANTIGEN
CORE
KDO
LIPID A
S. flexneri
F. novicida
F. novicida ΔlpxF
B
HA:GBP3 enrichment
WT
ΔlpxF
lpxF-CAT
ΔlpxF + p-lpxF
C
GBP1
F. novicida
HA:GBP3
HA:GBP3 enrichment ratio
wild-type
1.89 (highest)
1.33 (average)
ΔlpxF
2.73 (highest)
1.69 (average)
lpxF-CAT
0.98 (average)
ΔlpxF + p-lpxF
0.96 (average)

Fig 6. LpxF and lipid A modifications promote *F. novicida* escape from GBP3 targeting.

(A) Structure of hexa-acylated *S. flexneri*, tetra-acylated *F. novicida* and penta-acylated *F. novicida* Δ*lpxF* LPS. (B, C) IFNγ-treated, U937 HA:GBP3-expressing macrophages were infected with *F. novicida* for 7 h. HA:GBP3 enrichment was calculated as explained in Fig. S6B. (B) Each point represents the value of HA:GBP3 enrichment on one individual GBP1-*F. novicida* colocalization area. The bar represents the mean +/- SEM of 20 to 49 events originating from 4 independent experiments. Kruskal-Wallis multiple analysis with Dunn's correction was performed: **, $p < 0.01$; ***, $p < 0.001$; $p < 0.0001$. (C) Images with the highest or average GBP3 enrichment values are shown as indicated. Scale bar, 5µm.

Supplemental data

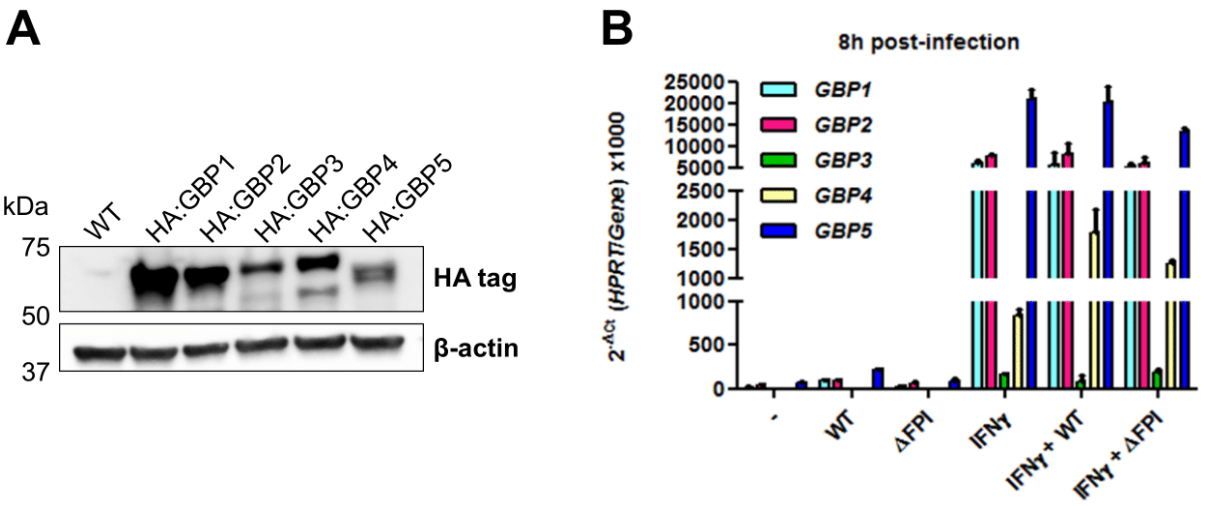

S1 Fig. GBP1-5 expression in U937 cell lines.

(A) Stable expression of HA-tagged GBPs was assessed by Western blot in U937 cell lines. (B) Endogenous levels of *GBP* transcripts were quantified by qRT-PCR and normalized to *HPRT* transcript levels after treatment with IFNγ or infection with WT or ΔFPI *F. novicida* strains.

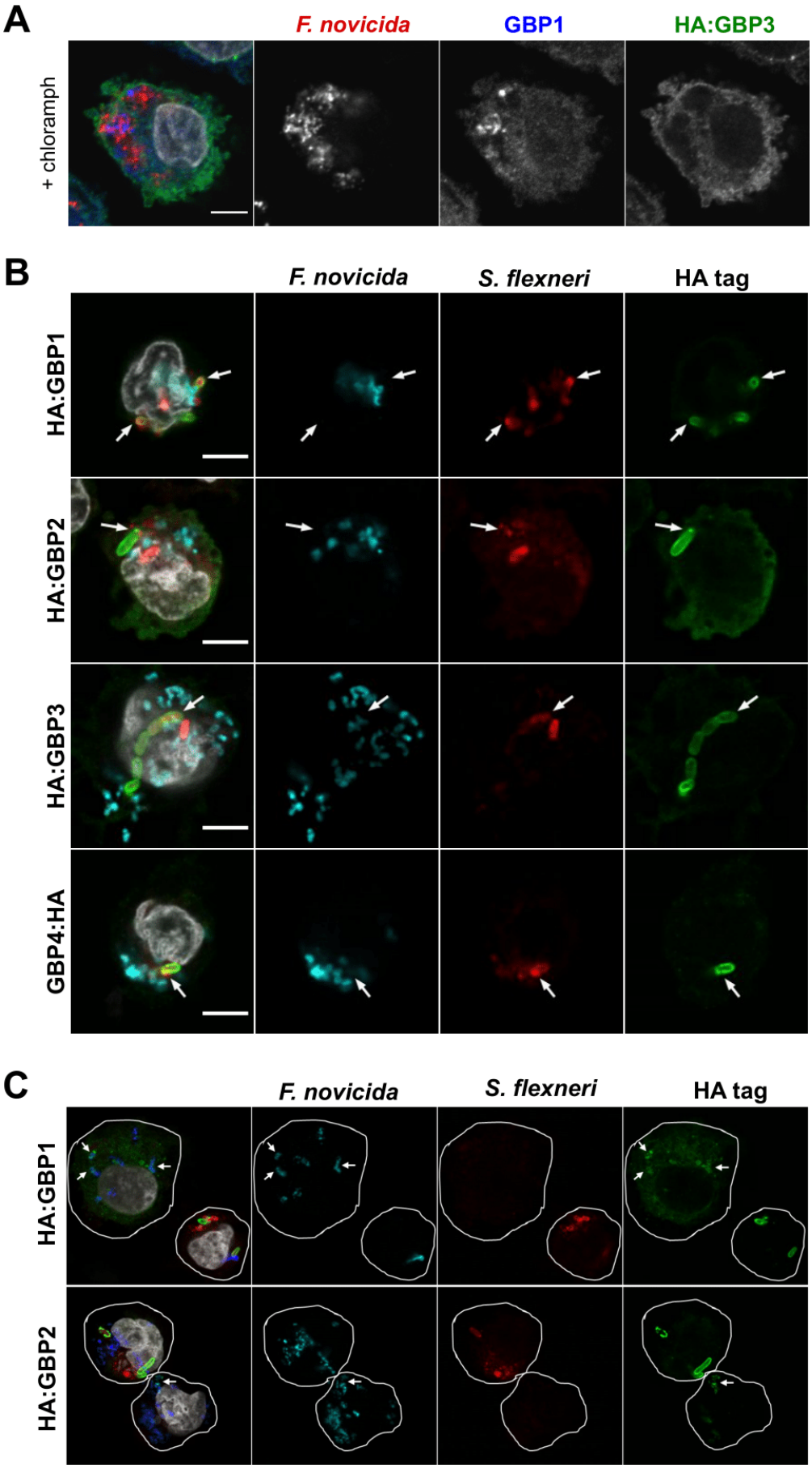
A
F. novicida
GBP1
HA:GBP3
+ chloramph
B
F. novicida
S. flexneri
HA tag
HA:GBP1
HA:GBP2
HA:GBP3
GBP4:HA
C
F. novicida
S. flexneri
HA tag
HA:GBP1
HA:GBP2

S2 Fig. Inhibition of GBP recruitment by *F. novicida* is bacterium-intrinsic.

(A) *F. novicida*-infected U937 macrophages were treated with chloramphenicol for 2 h at 5 h p.i.. Representative images are shown. Scale bar, 5μm. (B) IFNγ-primed U937 macrophages were co-infected with *F. novicida* and *S. flexneri* ΔipaH9.8 for 4 h. Representative images are shown. The arrows show GBP recruitment to *S. flexneri*. (C) GBP1 and GBP2 are recruited to *F. novicida* (arrows) in cells neighboring co-infected cells. The arrows show HA-GBP recruitment to *F. novicida*. Cell perimeter is depicted in white.

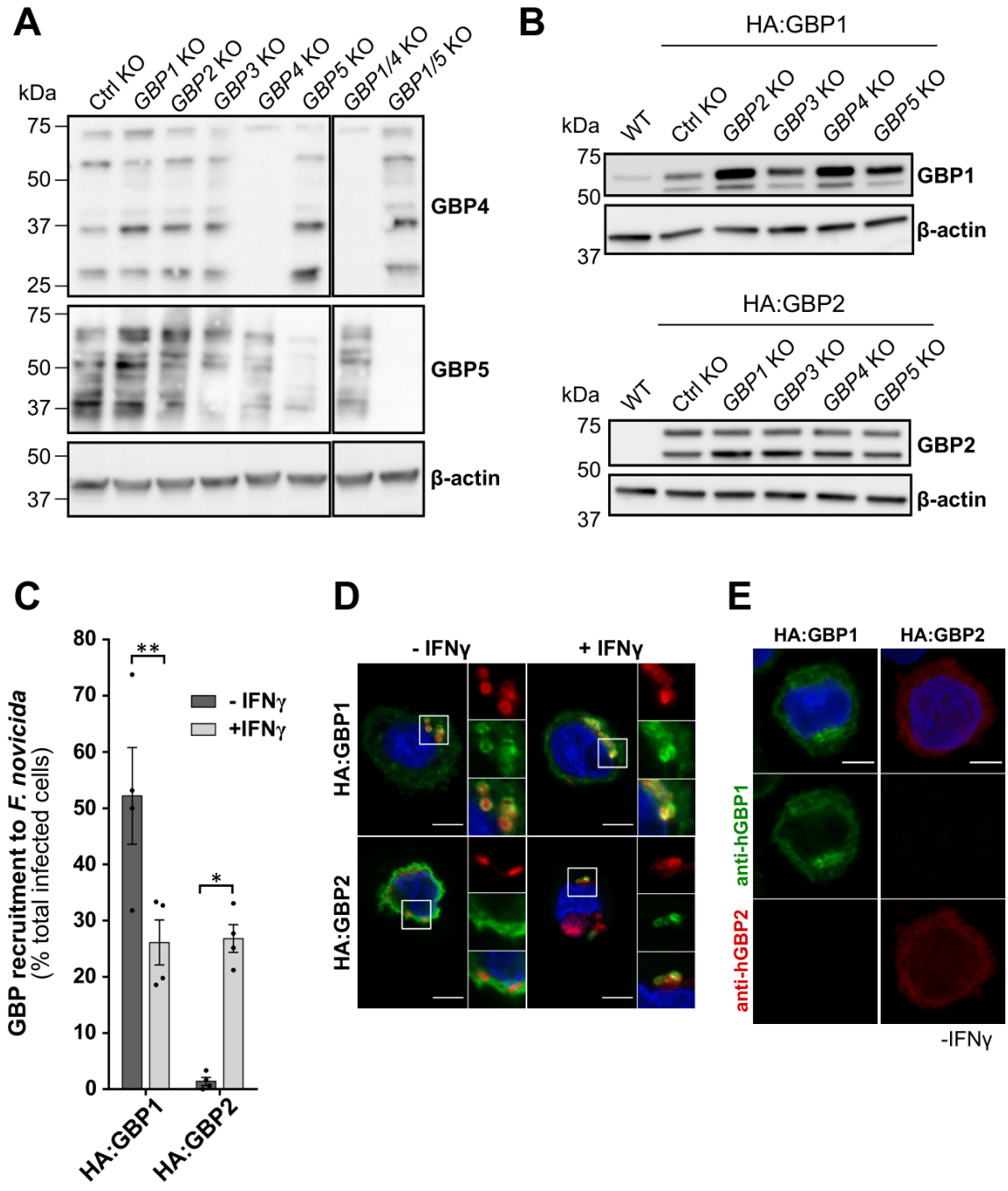

S3 Fig. Expression of HA:GBPs in *GBP* KO cell lines.

(A) *GBP* or control KO U937 cells were assessed for GBP4 or GBP5 expression by Western blot. The residual GBP5 signal in $GBP5^{KO}$ is due to cross-reactivity of the antibody with GBP1 as demonstrated using $GBP1/5^{DKO}$. (B) Stable expression of HA:GBP1 or HA-GBP2 were analyzed by Western blot in the indicated U937 cell lines. (C) GBP recruitment was scored as the percentage of infected cells with GBP-bacteria colocalization in U937 macrophages in the presence or absence of IFNγ. ANOVA with Sidak's multiple analysis test was used: **, $p < 0.01$. (D) Representative images with scale bar 5 μm and 3X zoom are shown. (E) Specificity of anti-hGBP1 and anti-hGBP2 antibodies was illustrated with confocal images acquired with identical imaging settings for both samples. The images are shown without brightness and contrast adjustments. Scale bar, 5 μm.

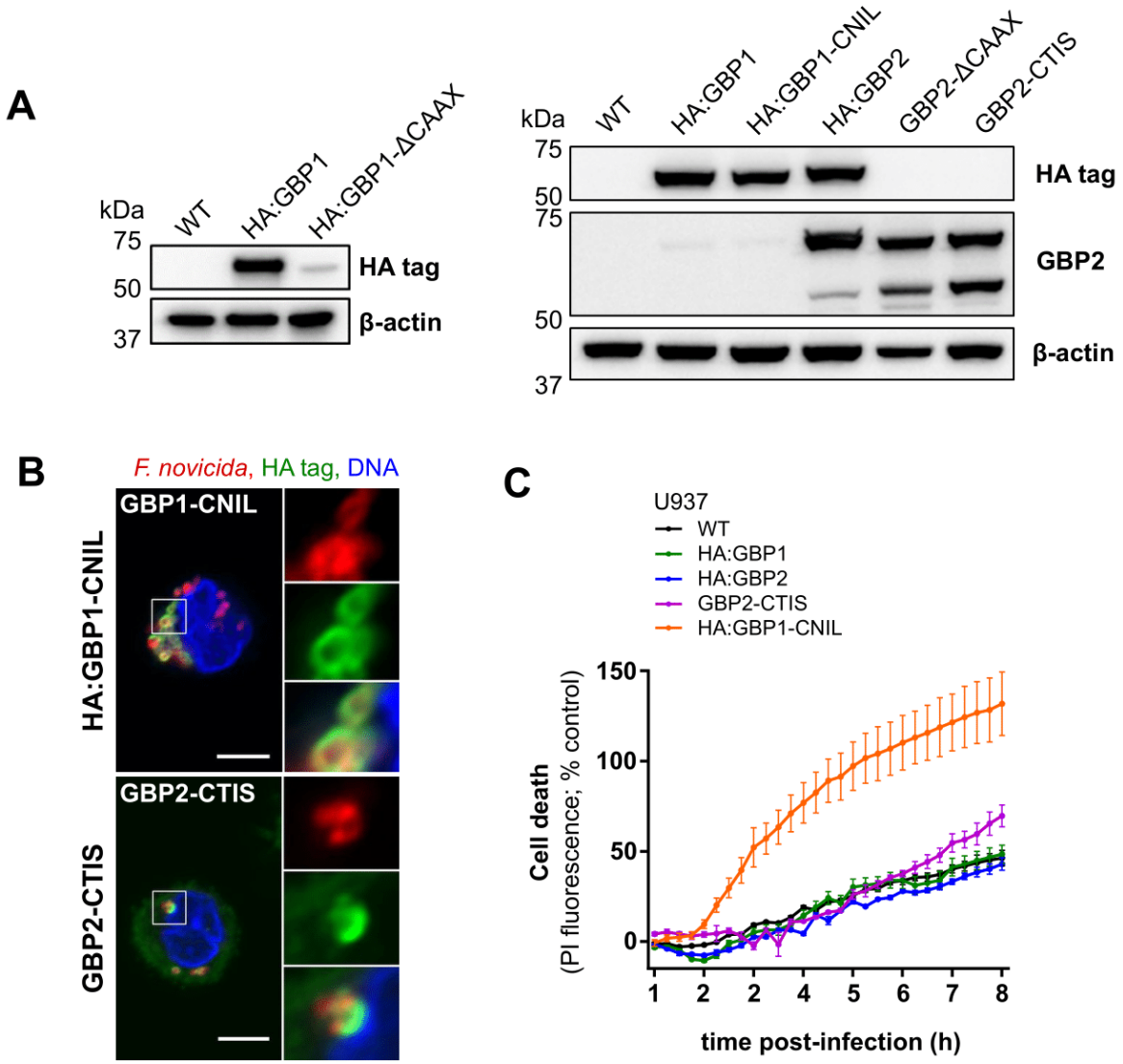

S4 Fig. GBP2 CAAX box promotes recruitment to *F. novicida*.

(A) Stable expression of the indicated GBP constructs was analyzed by Western blot in U937 cell lines. (B) Representative images of IFNγ-treated U937 macrophages, infected with *F. novicida* for 7 h are shown. Scale bar, 5 μm with 2X zoom on the right panels. (C) Propidium iodide (PI) incorporation/fluorescence was monitored every 15 min in IFNγ-primed macrophages, infected with *F. novicida* at MOI 100 and normalized to untreated cells and to Triton X100-treated cells. Each point corresponds to the mean +/- SEM of a biological triplicate from one experiment representative of 3 independent experiments.

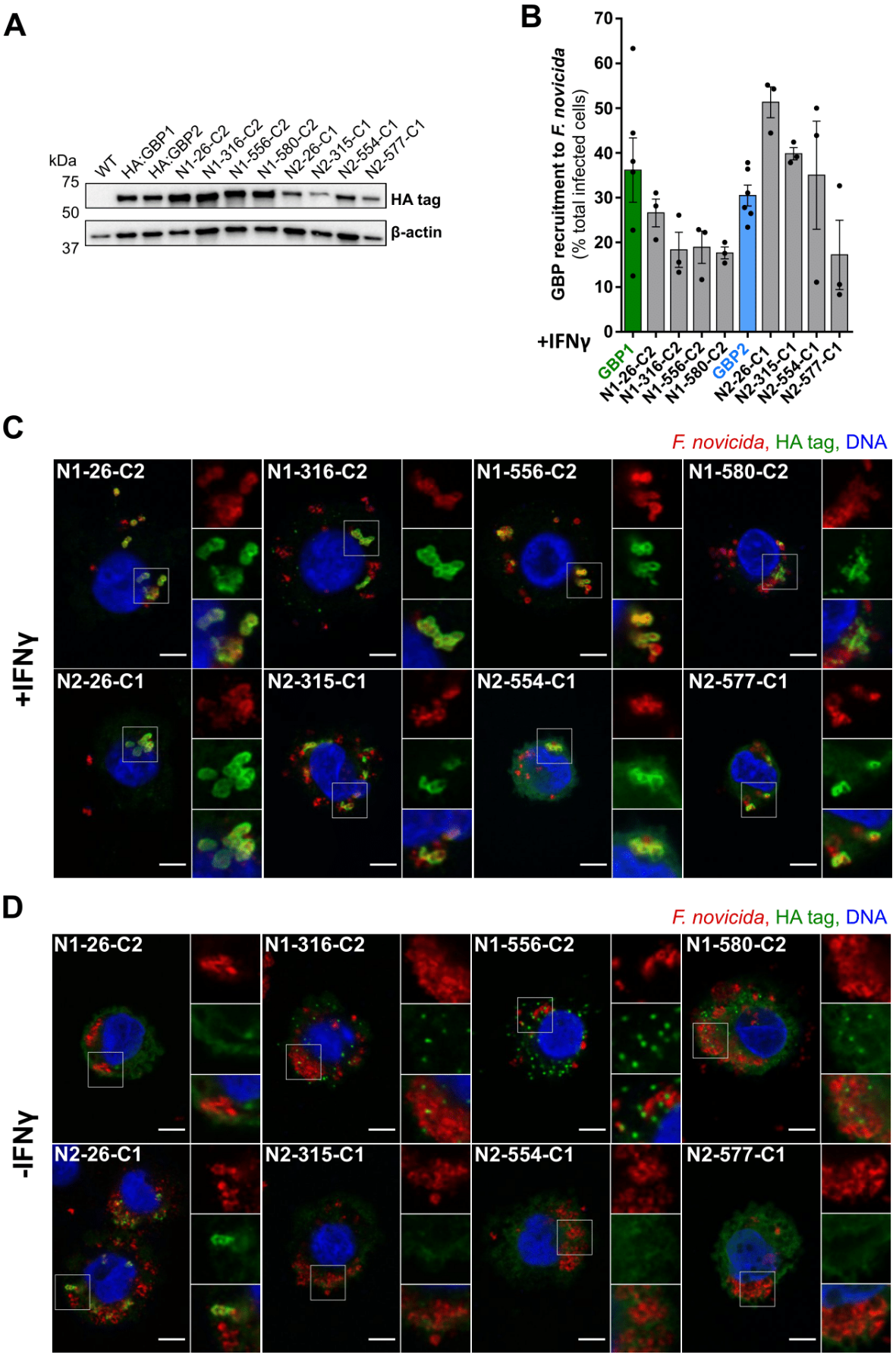
A
kDa
WT
HA:GBP1
HA:GBP2
N1-26-C2
N1-316-C2
N1-556-C2
N1-580-C2
N2-26-C1
N2-315-C1
N2-554-C1
N2-577-C1
75
50
37
HA tag
β-actin
B
GBP recruitment to F. novicida
(% total infected cells)
70
60
50
40
30
20
10
0
+IFNγ
GBP1
N1-26-C2
N1-316-C2
N1-556-C2
N1-580-C2
GBP2
N2-26-C1
N2-315-C1
N2-554-C1
N2-577-C1
C
F. novicida, HA tag, DNA
+IFNγ
N1-26-C2
N1-316-C2
N1-556-C2
N1-580-C2
N2-26-C1
N2-315-C1
N2-554-C1
N2-577-C1
D
F. novicida, HA tag, DNA
-IFNγ
N1-26-C2
N1-316-C2
N1-556-C2
N1-580-C2
N2-26-C1
N2-315-C1
N2-554-C1
N2-577-C1

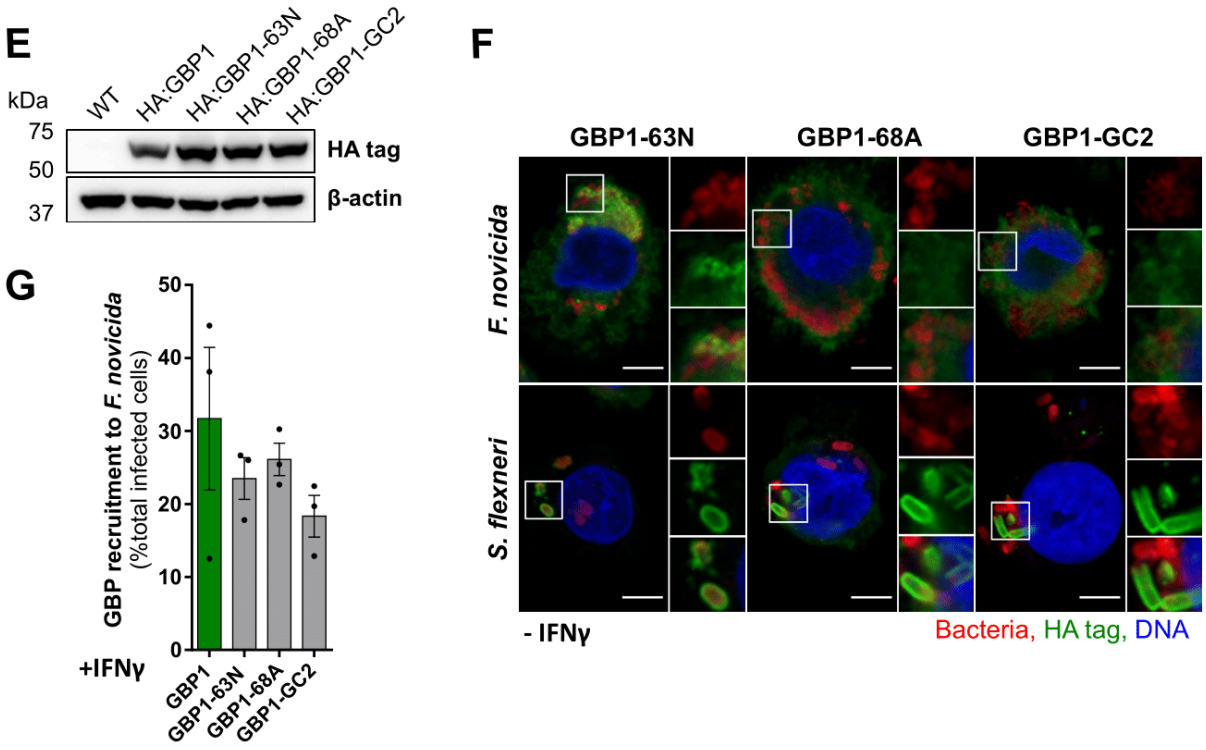

S5 Fig. GBP1 recruitment to *F. novicida* requires multiple GBP1 features.

(A, E) Stable HA-tagged GBP expression in U937 cells was analyzed by Western blot. IFNγ-primed (B-C, G) or untreated (D, F) U937 macrophages were infected with *F. novicida* for 7 h (B-D, F-G) or *S. flexneri* ΔipaH9.8 for 90 min (F). (C-D, F) Representative images are shown with a scale bar of 5 μm and a 2X zoom. (B, G) GBP recruitment was quantified as the percentage of infected cells with HA-GBP-bacteria colocalization. Each point corresponds to the value from one experiment with 50-100 infected cells analyzed. The bar represents the mean +/- SEM of three to six independent experiments. ANOVA with Sidak's analysis did not demonstrate statistical differences in recruitment between GBP chimeric/mutated and control cell lines.

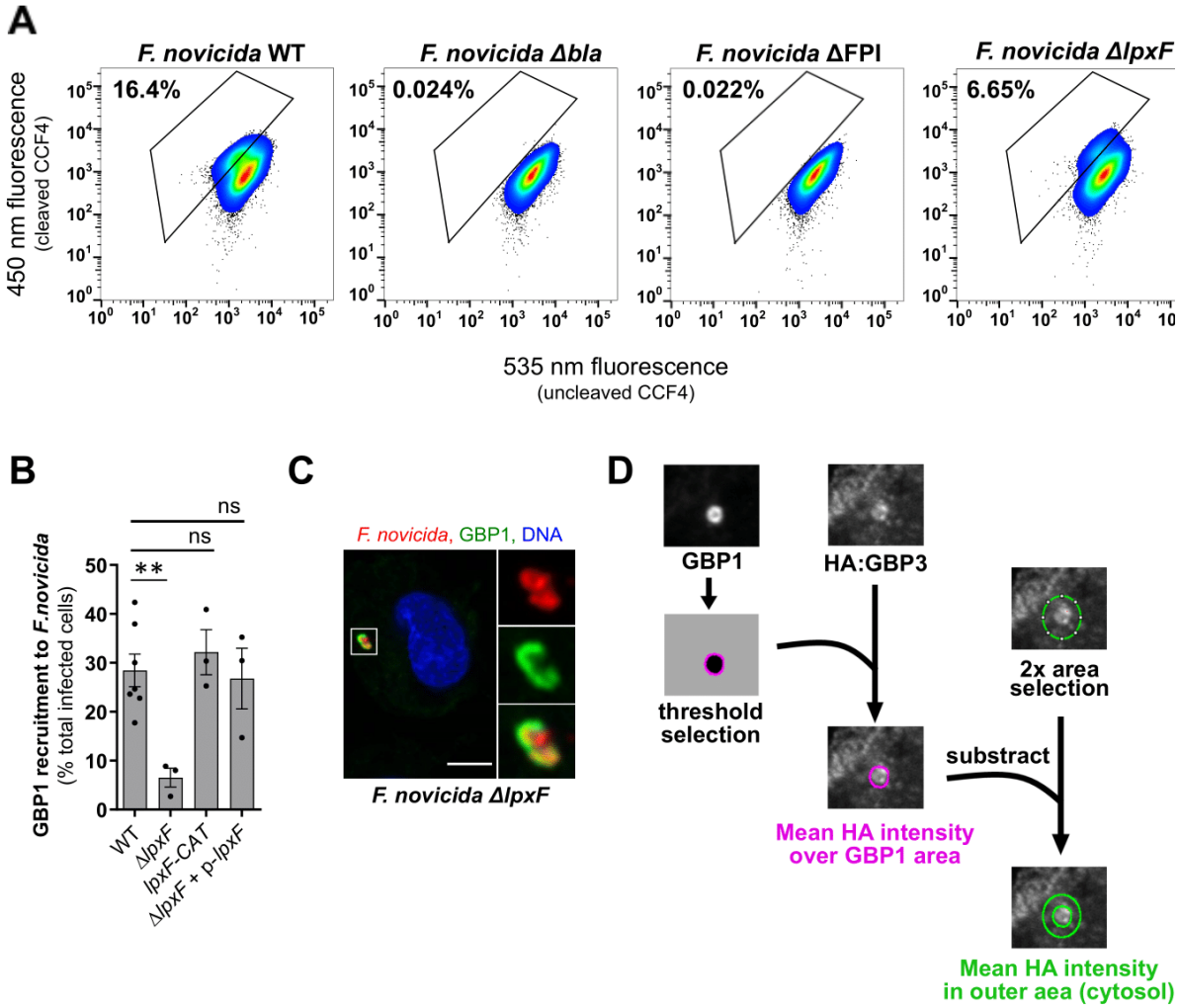
A
F. novicida WT
F. novicida Δbla
F. novicida ΔFPI
F. novicida ΔlpxF
16.4%
0.024%
0.022%
6.65%
450 nm fluorescence
(cleaved CCF4)
535 nm fluorescence
(uncleaved CCF4)
B
GBP1 recruitment to F.novicida
(% total infected cells)
ns
ns
**
WT
ΔlpxF
lpxF-CAT
ΔlpxF + p-lpxF
C
F. novicida, GBP1, DNA
F. novicida ΔlpxF
D
GBP1
HA:GBP3
threshold selection
2x area selection
substract
Mean HA intensity over GBP1 area
Mean HA intensity in outer aea (cytosol)
E
HA:GBP4 enrichment
GBP1-LPS vs. cytosol
ns
WT
ΔlpxF
F
GBP1
F. novicida
HA:GBP4
wild-type
ΔlpxF

S6 Fig. Analysis of *F. novicida* Δ*lpxF* cytosolic escape and GBP recruitment.

IFNγ-treated U937 macrophages were infected with *F. novicida* for 7 h. (A) Phagosomal rupture in *F. novicida*-infected macrophages, was evaluated by CCF4/β-lactamase flow cytometry assay. The cytosolic β-lactam FRET probe CCF4 emits at 535 nm when intact, and 450 nm when cleaved by *F. novicida* β-lactamase. Mutants in the β-lactamase gene (*Δbla*) or in the *Francisella* Pathogenicity Island (ΔFPI) are presented as controls. (B) HA:GBP recruitment was calculated as the percentage of infected cells with HA-GBP-*F. novicida* colocalization. Two-tailed t test with Welch's correction: *, $p < 0.05$. (C) Representative image of endogenous GBP1 recruitment to *F. novicida* Δ*lpxF* strain is shown. Scale bar 5 μm with 3X zoom. (D) Pipeline for scoring HA:GBP3 (or HA:GBP4) enrichment on one bacterium (or a cluster of bacteria) targeted by endogenous GBP1. (E) Each point represents the HA:GBP4 enrichment value of a single GBP1 recruitment area. Two-tailed Mann-Whitney analysis did not reveal any statistical difference in HA-GBP4 recruitment between WT and Δ*lpxF* strains. (F) Representative images are shown, scale bar 5 μm.

Supporting Table 1. Primers

Primer	Sequence	Template	Construct
AIP-Fwd	AATCAGCCTGCTTCTCGCTT	pAIP	All + sequencing
AIP-Rev	GCGGAATTCTGGCCAGTTAAC	pAIP	All + sequencing
GBP1-ΔCAAX	AATCGAATTCTTATGCCTTTCGTCGTCTCATTTTCG	pUC57-HA:GBP1	HA:GBP1-ΔCAAX
GBP2- ΔCAAX-rev	ATTGTTAACTTATATTGGCTCCAATGATTTGCTTC	pAIP-HA:GBP2	HA:GBP2-ΔCAAX
GBP1-CNIL-rev	ATTGCGGCCGCTTAGAGTATGTTACATGCCTTTCGTCGTCTCAT	pAIP-HA:GBP1	GBP1-CNIL
GBP2-CTIS-rev	ATTGTTAACTTAGCTTATGGTACATATTGGCTCCAATGATTTGC	pAIP-HA:GBP2	GBP2-CTIS
GBP2-CVLL-rev	ATTGTTAACTTAGAGTAAAACACATATTGGCTCCAATGATTTGCTTCTC	pAIP-HA:GBP2	GBP2-CVLL
GBP5-CNIL-rev	ATTGCGGCCGCTTAGAGTATGTTACATGGATCATCGTTATTAACAGTCCTC	pAIP-HA-GBP5	GBP5-CNIL
GBP2-R48A-fwd	GGGCCTCTATGCCACAGGCAAATCC	pUC57-HA:GBP2	HA:GBP2-R48A
GBP2-R48A-rev	ACAATCGCCACCACCACC	pUC57-HA:GBP2	HA:GBP2-R48A
GBP1-68A-fwd	AGGGCTTCTCTCTGGCCTCAACAGTCCAAAG	pUC57-HA:GBP1	HA:GBP1-68A
GBP1-68A-rev	CTTTGGACTGTTGAGGCCAGAGAGAAGCCCT	pUC57-HA:GBP1	HA:GBP1-68A
GBP1-63N-fwd	AACAAGCTGGCTGGAAAGAAAAACGGCTTCTCTCTG	pUC57-HA:GBP1	HA:GBP1-63N
GBP1-63N-rev	CAGAGAGAAGCCGTTTTTCTTTCCAGCCAGCTTGTT	pAIP-HA:GBP1	HA:GBP1-63N
GBP1-GC2-fwd	TGGCCCGCTCCTAAGAAGTACCTTGCACATCTGGAACAATTGAAAGAGGAAGAGCTGGACCCCGAATTTG	pAIP-HA:GBP1	HA:GBP1-GC2
GBP1-GC2-rev	CTCTTTCAATTGTTCCAGATGTGCAAGGTACTTCTTAGGAGCGGGCCAATCAAAGACAAAGCATTTTTTCTTTGGGAAG	pAIP-HA:GBP1	HA:GBP1-GC2
GBP1-Nt-rev-A	TGCAGATAGGATCTTCAGAGCTTCTGGATTCGCCATCAG	pUC57-HA:GBP1	HA:GBP1(26)-GBP2(591)
GBP2-Ct-fwd-A	CTGATGGCGAATCCAGAAGCTCTGAAGATCCTATCTGCA	pUC57-HA:GBP2	HA:GBP1(26)-GBP2(591)
GBP2-Nt-rev-A	GCAGAAAGGATCTTCAGAGCTTCTGGATTCACCACCAGC	pUC57-HA:GBP2	HA:GBP2(26)-GBP1(592)
GBP1-Ct-fwd-A	GCTGGTGGTGAATCCAGAAGCTCTGAAGATCCTTTCTGC	pUC57-HA:GBP1	HA:GBP2(26)-GBP1(592)
GBP1-Nt-rev-B	TTCTCTATCTGGGCCAAGGCCAGGACTGCGTTCTCCAT	pUC57-HA:GBP1	HA:GBP1(316)-GBP2(592)
GBP2-Ct-fwd-B	ATGGAGAACGCAGTCCTGGCCTTGGCCCAGATAGAGAA	pUC57-HA:GBP2	HA:GBP1(316)-GBP2(592)
GBP2-Nt-rev-B	TTCTCTATCTGGGCCAAGGCCAGGACTGCGTTCTCCAT	pUC57-HA:GBP2	HA:GBP2(315)-GBP1(591)
GBP1-Ct-fwd-B	ATGGAGAACGCAGTCCTGGCCTTGGCCCAGATAGAGAA	pUC57-HA:GBP1	HA:GBP2(315)-GBP1(591)
GBP1-Nt-rev-C	CTTGAGAAGGCGTTCCTGTTCCTGAAGTTTAAGAGCGAGG	pUC57-HA:GBP1	HA:GBP1(556)-GBP2(592)
GBP2-Ct-fwd-C	CCTCGCTCTTAAACTTCAGGAACAGGAACGCCTTCTCAAG	pUC57-HA:GBP2	HA:GBP1(556)-GBP2(592)
GBP2-Nt-rev-C	TCCCTCTTTTAGTAGTTGCTCCTGCCTCGCTCTTAAACTTCAGGAA	pUC57-HA:GBP2	HA:GBP2(554)-GBP1(591)
GBP1-Ct-fwd-C	TTCCTGAAGTTTAAGAGCGAGGCAGGAGCAACTACTAAAAGAGGGA	pUC57-HA:GBP1	HA:GBP2(554)-GBP1(591)
GBP1-Nt-rev-D	GCTCCAATGATTTGCTTCTCATCTGGAGATCCTGTATCTCATTT	pUC57-HA:GBP1	HA:GBP1(580)-GBP2(592)
GBP2-Ct-fwd-D	AAATGAGATACAGGATCTCCAGATGAGAAGCAAATCATTGGAGC	pUC57-HA:GBP2	HA:GBP1(580)-GBP2(592)
GBP2-Nt-rev-D	CGTCGTCTCATTTTCGTCTGGATATCCCATATGTCTTTTTGAAGTC	pUC57-HA:GBP2	HA:GBP2(577)-GBP1(591)
GBP1-Ct-fwd-D	GATATCCCATATGTCTTTTTGAAGTCCAGACGAAAATGAGACGACG	pUC57-HA:GBP1	HA:GBP2(577)-GBP1(591)

FnLpxF-Fwd (A1)	CAAAGCTACCACCTACTGAGC	*F. novicida* DNA	*lpxF-CAT* complementation
FnLpxF-UpC-Rev (A2)	**gcttatcgataccgtcgacctc**TCAATATTCTTTTTTACGATACATTAGTGCATAAACCACC	*F. novicida* DNA	*lpxF-CAT* complementation
CAT-FRT-Fwd (B1)	gaggtcgacggtatcgataagcGGTTGTCACTCATCGTATTTGG	*F. novicida* DNA	*lpxF-CAT* complementation
CAT-FRT-Rev (B2)	gcatagctgcaggatcgatatcGGAACTTCGGAATAGGAACTTCTTACG	*F. novicida* DNA	*lpxF-CAT* complementation
FnLF-DwC-Rev (C1)	**gatatcgatcctgcagctatgc**TTTATTTTTGATAAAAATAGATAATAAAAATTGAATATATTAAAAGAGGTACGATGATGGATTTGG	*F. novicida* DNA	*lpxF-CAT* complementation
FnLpxF-Rev (C2)	CTCCACAACAGAATTGAACTACCTGG	*F. novicida* DNA	*lpxF-CAT* complementation
LpxF-PstI-F	aattCTGCAGatttaagaaggagatatacatatgGCAAGATTTCATATCATATTAGGTTTAGTTGTTTGTTTTTTTGC	*F. novicida* DNA	pKK214-*lpxF* (=p-*lpxF*)
LpxF-EcoRI-R	aattGAATTCTCAATATTCTTTTTTACGATACATTAGTGCATAAACCACC	*F. novicida* DNA	pKK214-*lpxF* (=p-*lpxF*)

Supporting table 2. Cell lines

Note: All U937 GBP cell lines are transduced for a stable expression of a HA-tagged construct unless otherwise specified.

Cell line	Background	Description	Reference
HA:GBP1	U937 WT	Stable expression; *	Santos *et al.*, 2018 [417]
HA:GBP2	U937 WT	Stable expression; *	Santos *et al.*, 2018 [417]
HA:GBP3	U937 WT	Stable expression; *	This study
HA:GBP4	U937 WT	Stable expression; *	This study
HA:GBP5	U937 WT	Stable expression; *	Santos *et al.*, 2018 [417]
OR5B17 KO	U937 WT	Crispr/Cas9 KO (control)	Wandel *et al.*, 2020 [420]
GBP1 KO	U937 WT	Crispr/Cas9 KO	Wandel *et al.*, 2020 [420]
GBP2 KO	U937 WT	Crispr/Cas9 KO	Wandel *et al.*, 2020 [420]
GBP3 KO	U937 WT	Crispr/Cas9 KO	Wandel *et al.*, 2020 [420]
GBP4 KO	U937 WT	Crispr/Cas9 KO	This study
GBP5 KO	U937 WT	Crispr/Cas9 KO	This study
GBP1/4 KO	U937 *GBP1* KO	Crispr/Cas9 KO	This study
GBP1/5 KO	U937 *GBP1* KO	Crispr/Cas9 KO	This study
OR5B17 KO HA:GBP1	U937 *OR5B17* KO	Stable expression	This study
GBP2 KO HA:GBP1	U937 *GBP2* KO	Stable expression	This study
GBP3 KO HA:GBP1	U937 *GBP3* KO	Stable expression	This study
GBP4 KO HA:GBP1	U937 *GBP4* KO	Stable expression	This study
GBP5 KO HA:GBP1	U937 *GBP5* KO	Stable expression	This study
OR5B17 KO HA:GBP2	U937 OR5B17 KO	Stable expression	This study
GBP1 KO HA:GBP2	U937 *GBP1* KO	Stable expression	This study
GBP3 KO HA:GBP2	U937 *GBP3* KO	Stable expression	This study
GBP4 KO HA:GBP2	U937 *GBP4* KO	Stable expression	This study
GBP5 KO HA:GBP2	U937 *GBP5* KO	Stable expression	This study
HA:GBP1-ΔCAAX	U937 WT	CAAX box deletion by simple PCR	This study
GBP2-ΔCAAX	U937 *GBP2* KO	CAAX box deletion by simple PCR; no tag; *	This study
GBP2	U937 *GBP2* KO	KO complementation (Fig. 3)	This study
HA:GBP2-R48A	U937 WT	GTPase inactive, point mutation PCR	This study
HA:GBP1-CNIL	U937 WT	GBP2 CAAX box, simple PCR; *	This study
GBP2-CTIS	U937 *GBP2* KO	GBP1 CAAX box, simple PCR; no tag; *	This study
GBP2-CVLL	U937 *GBP2* KO	GBP5 CAAX box, simple PCR; no tag; *	This study
HA:GBP5-CNIL	U937 WT	GBP2 CAAX box, simple PCR; *	This study
HA:N1-26-C2	U937 WT	GBP1 Nter – GBP2 Cter chimera, joint PCR	This study
HA:N1-316-C2	U937 WT	GBP1 Nter – GBP2 Cter chimera, joint PCR	This study
HA:N1-554-C2	U937 WT	GBP1 Nter – GBP2 Cter chimera, joint PCR	This study
HA:N1-580-C2	U937 WT	GBP1 Nter – GBP2 Cter chimera, joint PCR; *	This study
HA:N2-26-C1	U937 WT	GBP2 Nter – GBP1 Cter chimera, joint PCR	This study
HA:N2-315-C1	U937 WT	GBP2 Nter – GBP1 Cter chimera, joint PCR	This study
HA:N2-556-C1	U937 WT	GBP2 Nter – GBP1 Cter chimera, joint PCR	This study
HA:N2-577-C1	U937 WT	GBP2 Nter – GBP1 Cter chimera, joint PCR; *	This study
HA:GBP1-63N	U937 WT	63K to 63N, K patch; point mutation PCR; *	This study
HA:GBP1-68A	U937 WT	68G to 68A, GDP hydrolase null; point mutation PCR; *	This study
HA:GBP1-GC2	U937 WT	Guanine cap of GBP2, joint PCR; *	This study

* Negative *Mycoplasma* test (28.04.2021)

Supporting Table 3. Antibodies

Primary

Antigen	Made in	Reference	Experiment (Fig.)	Dilution
HA tag	mouse	Sigma-Aldrich #H3663	**IF** (all except otherwise indicated)	1:3000
HA tag	rabbit	Cell Signaling #3724S	**WB** (all except S3.A, B)	1:1000
hGBP1	rabbit	Abcam #ab131255	**IF** (S2.A; 3.D, E, F; 6.B, C; S3. E; S6. C, E, F)	1:150
hGBP2	mouse	Novus #NBP1-47768	**IF** (2.B; 3.D, E, F; S3.E); non-tagged GBP2 mutants ; **WB** (S3.B)	1:2000
hGBP1	rabbit	ThermoFisher #15303-1-AP	**WB** (S3.B)	1:1000
hGBP4	rabbit	ThermoFisher #17746-1-AP	**WB** (S3.A)	1:1000
hGBP5	rabbit	ThermoFisher #13220-1-AP	**WB** (S3.A)	1:1000
F. tularensis LPS	chicken	Denise Monack lab	**IF** (where indicated)	1:1000
Shigella group LPS	rabbit	Novus #NB100-65058	**IF** (where indicated)	1:1000
actin	mouse	Sigma-Aldrich #A3853	**WB** (all)	1:5000

Secondary

Anti-IgG	Conjugate	Reference	Experiment (Fig.)
chicken	Alexa Fluor 594	Life #A21207	**IF** (all except otherwise indicated)
chicken	Alexa Fluor 647	Sigma-Aldrich #A21449	**IF** (2.A, B; 3.D, E, F; 6.B, C; S2; S6.C, D)
mouse	Alexa Fluor 488	Sigma-Aldrich #A10667	**IF** (all where otherwise indicated)
mouse	Alexa Fluor 594	Sigma-Aldrich #A11032	**IF** (Fig. 3D, E, F; S3. E)
rabbit	Alexa Fluor 488	Life #A21206	**IF** (Fig. 3D, E, F; S3. E)
rabbit	Alexa Fluor 594	Invitrogen #A11012	**IF** (all *S. flexneri* staining; 6.B, C; 6.C,D; S2.A; S6.C, E, F)
mouse	HRP	Promega #W402b	**WB** (all)
rabbit	HRP	Sigma-Aldrich #A0545	**WB** (all)

II. Additional results

The results featured in this chapter were included in an earlier draft of the previous manuscript and are published in BioRXiv as a part of a pre-print.

In this section, we identified hGBP2 domains allowing recruitment to *F. novicida* in IFN-γ-treated macrophages (i.e. downstream of GBP1).

This part of the manuscript was removed from the submission for PLoS Pathogens because the biological question explored did not align with the focus of the manuscript, therefore we believed it would distract from the key message.

The central region of GBP2 controls its recruitment to *F. novicida*

Besides GBP1 and GBP2, GBP5 is the only other GBP presenting a CAAX box. Yet, GBP5 is not recruited to bacteria [311,419,420]. GBP5 is modified by geranylgeranylation similarly to GBP2 [351]. As expected, replacing the CAAX box of GBP2 with that of GBP5 (GBP2-CVLL, Fig. S7.A) did not significantly alter recruitment. Likewise, GBP5 carrying the CAAX box of GBP2 (GBP5-CNIL) did not colocalize with *F. novicida* (Fig. 7A). Thus, although necessary for GBP1/2 targeting to *F. novicida*, GBP prenylation by itself is not sufficient for a GBP to be targeted to bacteria indicating that additional domains govern the selective recruitment of GBP2 to *F. novicida*.

The GTPase activity of GBP2 was also required to target *F. novicida*. Indeed, a GTPase null mutant GBP2-R48A failed to localize to the bacteria (Fig. 7B, S7B-C). However, GBP5 is also capable of GTP hydrolysis [434] and the catalytic residues, highly conserved in the dynamin superfamily [325], are identical in GBP2 and GBP5 (Fig. S7K).

The crystal structures of GBP2 and GBP5 were solved recently [355]. GBP2 and GBP5, similarly to GBP1, contain a globular GTPase domain at the N-terminus, followed by an elongated helical region, which ends on a hairpin-like C-terminus with the CAAX motif at the very end (Fig. 7C). GBP2 and GBP5 also share a high similarity, with the most divergence localized in the C-terminal α12 and α13 helices (Fig. S7K). Owing to the similarity between both proteins, multiple GBP2-GBP5 and GBP5-GBP2 chimeras were generated and stably expressed in U937 cells (Fig. 7D, Fig. S7D). The chimeras were evaluated for gain or loss of targeting to *F. novicida* to pinpoint the specific GBP2 domain driving recruitment. Chimera N2-535-C5, consisting of GBP2 up to residue R535, followed by the GBP5 C-terminus, was recruited to *F. novicida* similarly to GBP2 (Fig. 7E). Thus, contrary to our expectations, the targeting specificity of GBP2 is not driven by the most C-terminal part of GBP2 (535-end containing α13 and 1/3 of α12). Chimera N2-506-C5 presented a 2-fold decrease in recruitment to *F. novicida* compared to GBP2 while chimera N2-475-C5 was not recruited at all. These observations indicate that recruitment to *F. novicida* gradually decreases as GBP2 C-terminus is replaced by GBP5 between residues Q475 and R535, establishing that this region is required for GBP2 recruitment. However, the presence of this GBP2 Q475-R535 was not sufficient to induce the recruitment of the corresponding GBP5-GBP2 chimera (termed N5-474-C2) (Fig. 7F). Further addition of GBP2 residues K340-L474 generated a chimera (termed N5-340-C2) gaining the full ability to be recruited to *F. novicida*.

These experiments revealed two neighboring regions (K340-L474 and Q475-R535) in the central part of GBP2 which are necessary for bacteria targeting in the context of GBP5-GBP2 and GBP2-GBP5 chimeras, respectively. To assess whether the GBP2 K340-R535 region would be sufficient to drive the recruitment of a prenylated GBP to *F. novicida*, we generated cells stably expressing a chimera with the central domain of GBP2 (340-535) in a GBP5 background (chimera N5M2C5, Fig. 7G). This three-part chimera, although only faintly expressed (Fig. S7E), was indeed recruited to *F. novicida* (Fig. 4H, I) thus identifying the central domain of GBP2 (340-535) as necessary and sufficient in the context of GBP5 to drive recruitment to *F. novicida*.

A unique feature of GBP5 is its localization in the Golgi apparatus [343,350]. We thus wondered whether the Golgi apparatus localization of GBP5 could be responsible for the lack of recruitment to cytosolic *F. novicida*. We first calculated Golgi enrichment ratios for all

GBP2/5 chimeras (Fig. S7F-I). Increasing the proportion of GBP5 sequence in the C-terminus gradually increased Golgi apparatus localization in GBP2-GBP5 chimeras. Conversely, an increase in the C-terminal GBP2 proportion paralleled a decrease in Golgi apparatus localization. These results indicate that the central helical domain and the α12-α13 region contribute to GBP5 localization at the Golgi apparatus. Yet, in contrast to recruitment to *F. novicida*, we could not delineate a specific Golgi-targeting domain. We thus analysed all the GBP2/5 chimeras to assess whether the Golgi apparatus localization was inversely correlated with recruitment to *F. novicida*. No correlation could be observed (Fig. S7J) suggesting that Golgi apparatus localization and recruitment to bacteria are independent GBP features.

Altogether, the chimera recruitment assays uncovered an essential role of the central region of GBP2 (340-535) in *F. novicida* targeting. These results also indicate that the corresponding region in GBP5 diverges from GBP2 to a degree that impedes recruitment of GBP5 to *F. novicida,* independently of GBP5 Golgi localization.

Discussion

The factors controlling recruitment of GBPs downstream of GBP1 are still elusive. The current model states that pioneer prenylated GBPs recruit other GBPs through heterotypic interactions [339,391]. Both GBP2 and GBP5 interact with GBP1 in overexpression systems [351,365] while GBP5 is not recruited on cytosolic bacteria indicating that GBP1 interactions are not the only drivers of GBP recruitment. Our chimera experiments (Fig. 7) mapped the GBP2 region directing recruitment to the central helical domain (K340-R535, spanning the second half of the α9 helix to the first half of the α12 helix). The knowledge on the function of this central GBP domain is still sparse [327,355,369]. According to the current model, GBP1 polymerization requires the opening of a α9-α12 structural hairpin [327]. The central helical domain of GBP2 identified may thus allow structural rearrangement to accommodate polymerization with GBP1, whereas this conformational change might not be possible in GBP5, at least on the bacterial surface. The structural requirements for GBP1 homopolymerization are now well known [357]. Yet, GBP heteropolymer formation awaits to benefit from similar exquisite biochemical studies to provide an understanding of how the central helical domain identified here drives the specific recruitment of GBP2 to *F. novicida*.

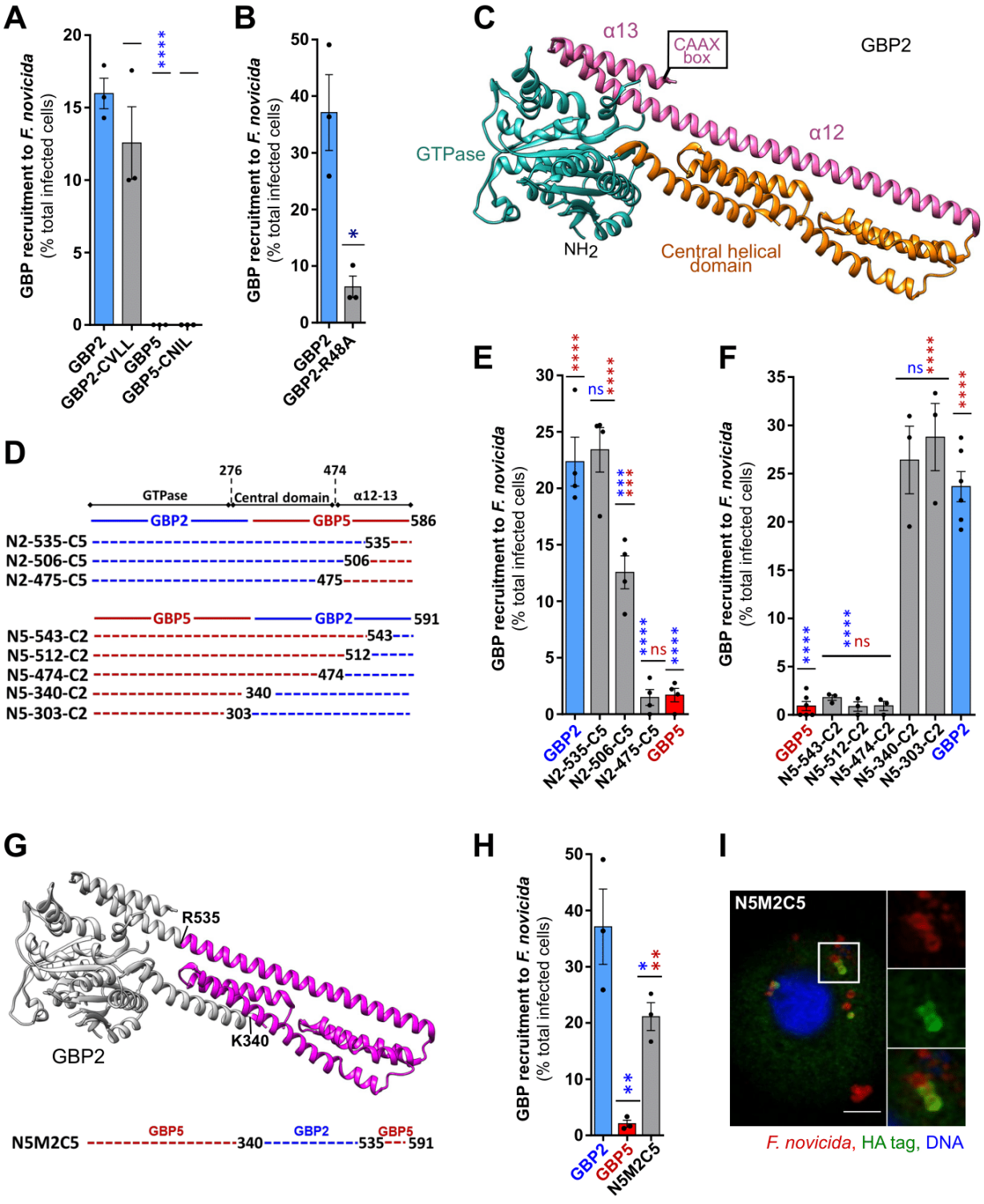
A
GBP recruitment to F. novicida
(% total infected cells)
GBP2
GBP2-CVLL
GBP5
GBP5-CNIL
B
GBP recruitment to F. novicida
(% total infected cells)
GBP2
GBP2-R48A
C
α13
CAAX box
GBP2
α12
GTPase
NH2
Central helical domain
D
276
474
GTPase
Central domain
α12-13
GBP2
GBP5
586
N2-535-C5
N2-506-C5
N2-475-C5
GBP5
GBP2
591
N5-543-C2
N5-512-C2
N5-474-C2
N5-340-C2
N5-303-C2
E
GBP recruitment to F. novicida
(% total infected cells)
ns
GBP2
N2-535-C5
N2-506-C5
N2-475-C5
GBP5
F
GBP recruitment to F. novicida
(% total infected cells)
ns
GBP5
N5-543-C2
N5-512-C2
N5-474-C2
N5-340-C2
N5-303-C2
GBP2
G
R535
K340
GBP2
N5M2C5
GBP5
340
GBP2
535
GBP5
591
H
GBP recruitment to F. novicida
(% total infected cells)
GBP2
GBP5
N5M2C5
I
N5M2C5
F. novicida, HA tag, DNA

Fig. 7. The central domain of GBP2 controls GBP2 recruitment to *F. novicida*.

(A, B, E, G, H) IFNγ-treated, U937 macrophages were infected with *F. novicida*. GBP recruitment was quantified as the percentage of infected cells with *F. novicida*-HA-GBP colocalization. (C) GBP2 structure is presented with coloring corresponding to the studied chimera. (D) GBP2-5 or GBP5-2 chimera stably expressed in U937 cells are schematically shown. (F) The GBP2 region identified as necessary and sufficient to promote GBP2 recruitment is presented with the corresponding schematic GBP5-GBP2-GBP5 chimera, underneath. (H) Representative image is shown with scale bar 5 μm and 2X zoom on the right panels.

Two-tailed t test with Welch's correction (B) or ANOVA with Dunnett's (A, E, G) analyses were performed: *, $p < 0.05$; **, $p < 0.01$; ***, $p < 0.001$; ****, $p < 0.0001$; ns, not significant. Blue and red star/writing indicates the result of the statistical comparison with GBP2 or GBP5, respectively.

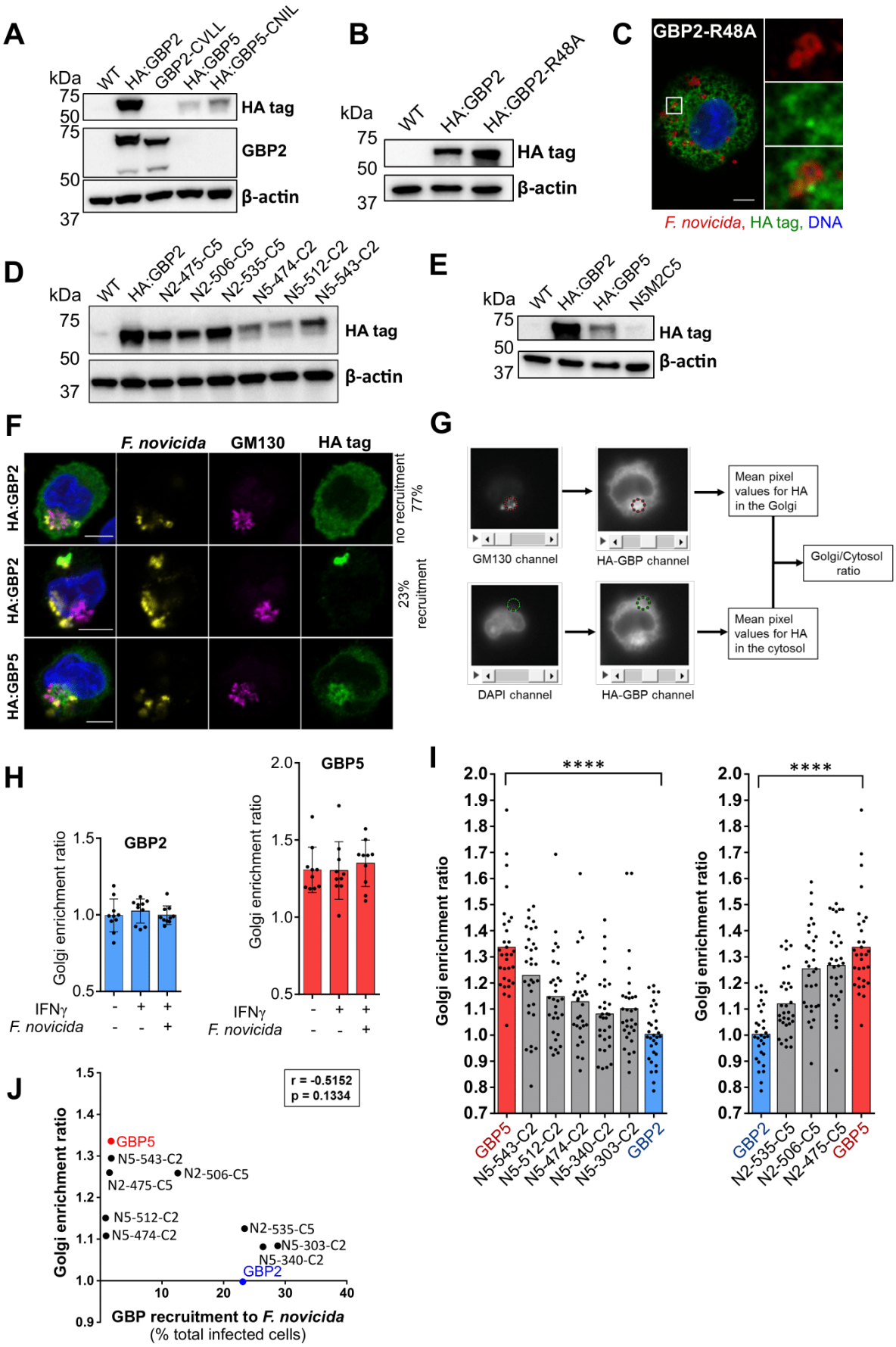
A
kDa
WT
HA:GBP2
GBP2-CVLL
HA:GBP5
HA:GBP5-CNIL
75
50
75
50
37
HA tag
GBP2
β-actin
B
kDa
WT
HA:GBP2
HA:GBP2-R48A
75
50
37
HA tag
β-actin
C
GBP2-R48A
F. novicida, HA tag, DNA
D
kDa
WT
HA:GBP2
N2-475-C5
N2-506-C5
N2-535-C5
N5-474-C2
N5-512-C2
N5-543-C2
75
50
37
HA tag
β-actin
E
kDa
WT
HA:GBP2
HA:GBP5
N5M2C5
75
50
37
HA tag
β-actin
F
F. novicida
GM130
HA tag
HA:GBP2
HA:GBP2
HA:GBP5
no recruitment 77%
23% recruitment
G
GM130 channel
HA-GBP channel
DAPI channel
HA-GBP channel
Mean pixel values for HA in the Golgi
Golgi/Cytosol ratio
Mean pixel values for HA in the cytosol
H
GBP2
GBP5
Golgi enrichment ratio
IFNγ
F. novicida
I
****
****
Golgi enrichment ratio
GBP5
N5-543-C2
N5-512-C2
N5-474-C2
N5-340-C2
N5-303-C2
GBP2
GBP2
N2-535-C5
N2-506-C5
N2-475-C5
GBP5
J
r = -0.5152
p = 0.1334
Golgi enrichment ratio
GBP5
N5-543-C2
N2-506-C5
N2-475-C5
N5-512-C2
N5-474-C2
N2-535-C5
N5-303-C2
N5-340-C2
GBP2
GBP recruitment to F. novicida
(% total infected cells)

K

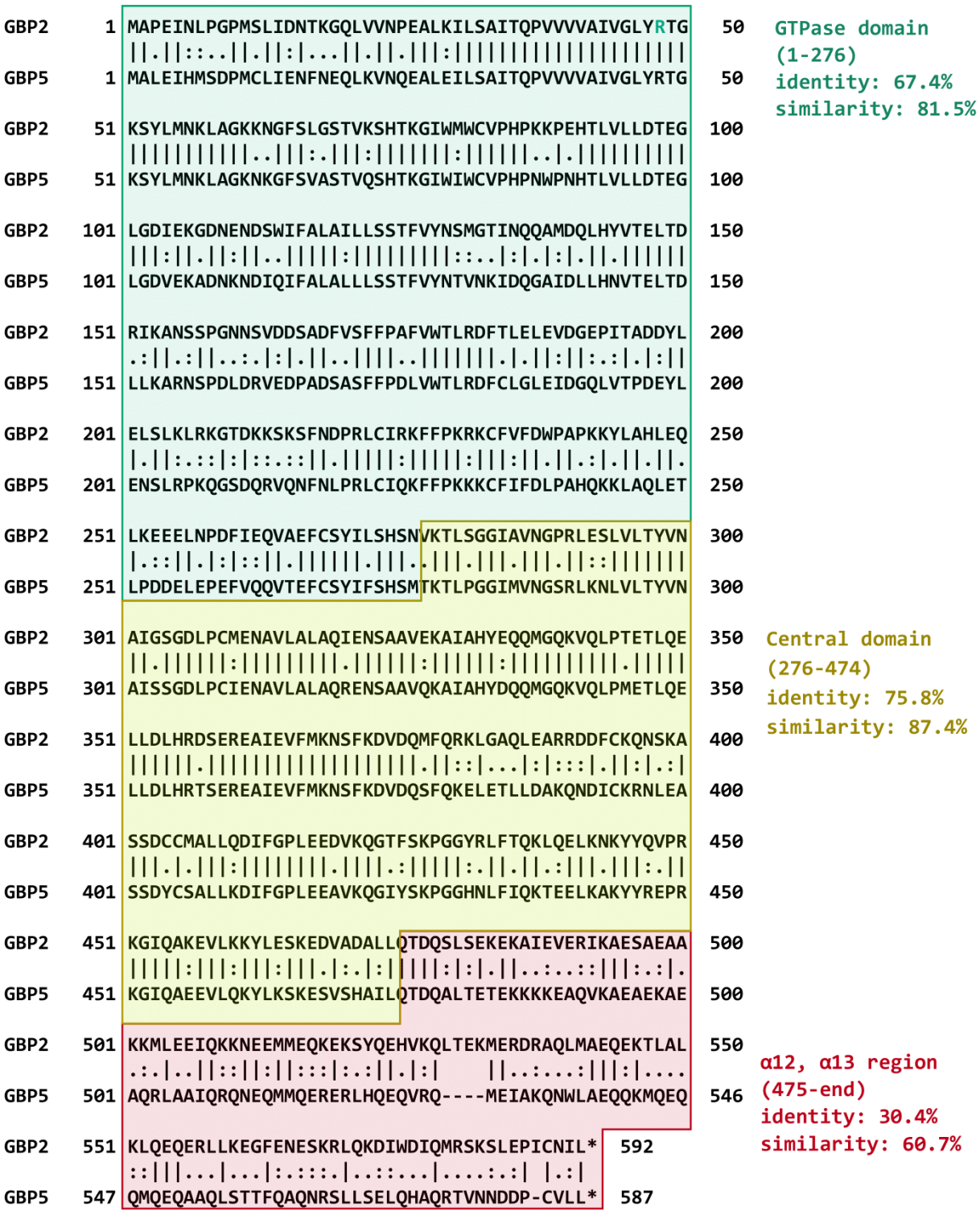
GBP2 1 MAPEINLPGPMSLIDNTKGQLVVNPEALKILSAITQPVVVVAIVGLYRTG 50
GBP5 1 MALEIHMSDPMCLIENFNEQLKVNQEALEILSAITQPVVVVAIVGLYRTG 50
GBP2 51 KSYLMNKLAGKKNGFSLGSTVKSHTKGIWMWCVPHPKKPEHTLVLLDTEG 100
GBP5 51 KSYLMNKLAGKNKGFSVASTVQSHTKGIWIWCVPHPNWPNHTLVLLDTEG 100
GBP2 101 LGDIEKGDNENDSWIFALAILLSSTFVYNSMGTINQQAMDQLHYVTELTD 150
GBP5 101 LGDVEKADNKNDIQIFALALLLSSTFVYNTVNKIDQGAIDLLHNVTELTD 150
GBP2 151 RIKANSSPGNNSVDDSADFVSFFPAFVWTLRDFTLELEVDGEPITADDYL 200
GBP5 151 LLKARNSPDLDRVEDPADSASFFPDLVWTLRDFCLGLEIDGQLVTPDEYL 200
GBP2 201 ELSLKLRKGTDKKSKSFNDPRLCIRKFFPKRKCFVFDWPAPKKYLAHLEQ 250
GBP5 201 ENSLRPKQGSDQRVQNFNLPRLCIQKFFPKKKCFIFDLPAHQKKLAQLET 250
GBP2 251 LKEEELNPDFIEQVAEFCSYILSHSNVKTLSGGIAVNGPRLESLVLTYVN 300
GBP5 251 LPDDELEPEFVQQVTEFCSYIFSHSMTKTLPGGIMVNGSRLKNLVLTYVN 300
GBP2 301 AIGSGDLPCMENAVLALAQIENSAAVEKAIAHYEQQMGQKVQLPTETLQE 350
GBP5 301 AISSGDLPCIENAVLALAQRENSAAVQKAIAHYDQQMGQKVQLPMETLQE 350
GBP2 351 LLDLHRDSEREAIEVFMKNSFKDVDQMFQRKLGAQLEARRDDFCKQNSKA 400
GBP5 351 LLDLHRTSEREAIEVFMKNSFKDVDQSFQKELETLLDAKQNDICKRNLEA 400
GBP2 401 SSDCCMALLQDIFGPLEEDVKQGTFSKPGGYRLFTQKLQELKNKYYQVPR 450
GBP5 401 SSDYCSALLKDIFGPLEEAVKQGIYSKPGGHNLFIQKTEELKAKYYREPR 450
GBP2 451 KGIQAKEVLKKYLESKEDVADALLQTDQSLSEKEKAIEVERIKAESAEAA 500
GBP5 451 KGIQAEEVLQKYLKSKESVSHAILQTDQALTETEKKKKEAQVKAEAEKAE 500
GBP2 501 KKMLEEIQKKNEEMMEQKEKSYQEHVKQLTEKMERDRAQLMAEQEKTLAL 550
GBP5 501 AQRLAAIQRQNEQMMQERERLHQEQVRQ----MEIAKQNWLAEQQKMQEQ 546
GBP2 551 KLQEQERLLKEGFENESKRLQKDIWDIQMRSKSLEPICNIL* 592
GBP5 547 QMQEQAAQLSTTFQAQNRSLLSELQHAQRTVNNDDP-CVLL* 587
GTPase domain
(1-276)
identity: 67.4%
similarity: 81.5%
Central domain
(276-474)
identity: 75.8%
similarity: 87.4%
α12, α13 region
(475-end)
identity: 30.4%
similarity: 60.7%

S Fig. 7. Golgi localization does not explain absence of *F. novicida* targeting in GBP2/5 chimeras.

(A, B, D, E) Stable expression of HA-tagged GBP constructs was analyzed by Western blot in U937 cells. (C, F, H) Representative images of IFN-γ-treated, U937 macrophages infected with *F. novicida* are presented with a 5 μm scale bar. (G) Golgi enrichment was scored using GM130 staining to delineate the Golgi region and extract the corresponding pixel intensity values for the HA-GBP image channel. A similar area outside of the nucleus served to obtain a cytosol baseline value. (H, I) Golgi enrichment ratios of infected (H) or untreated (H, I) U937 cells. Each point represents the Golgi enrichment ratio calculated for a single cell. The bar represents the mean of three independent experiments with the Golgi enrichment ratio calculated in 10 or more cells per experiment. Statistical differences between GBP2 and GBP5 (****, $p < 0.0001$) were evaluated through two tailed Mann-Whitney analysis. (J) The mean Golgi enrichment of each construct is plotted in function of the mean GBP recruitment. Spearman's correlation results are presented. (K) GBP2 and GBP5 protein sequences were aligned with Emboss-Needle Pairwise Sequence Alignment using the BLOSUM 62 matrix. Local identity and similarity were evaluated by separate alignments with the same matrix.

Supplemental materials

Primers

Primer	Sequence	Template	Construct
AIP-Fwd	AATCAGCCTGCTTCTCGCTT	pAIP	All + sequencing
AIP-Rev	GCGGAATTCTGGCCAGTTAAC	pAIP	All + sequencing
GBP5(0-303)-Rev	TGCAGGGTAGATCCCCACTGCTGATGGCATTGACATAGGTCA	pAIP-HA:GBP5	HA:GBP5(0-303)-GBP2(303-591)
GBP2(303-591)-Fwd	TGACCTATGTCAATGCCATCAGCAGTGGGGATCTACCCTGCA	pAIP-HA:GBP2	HA:GBP5(0-303)-GBP2(303-591)
GBP5(0-340)-Rev	TTTCCGTGGGCAGCTGCACTTTCTGGCCCATTTGCTGGT	pAIP-HA:GBP5	HA:GBP2(0-340)-GBP5(340-586)
GBP2(340-591)-Fwd	ACCAGCAAATGGGCCAGAAAGTGCAGCTGCCCACGGAAA	pAIP-HA:GBP2	HA:GBP2(0-340)-GBP5(340-586)
GBP2(0-475)-Rev	CTGTGAGAGCCTGGTCAGTCTGTAGAAGTGCATCAGCCAC	pAIP-HA:GBP2	HA:GBP2(0-475)-GBP5(475-586)
GBP5(475-586)-Fwd	GTGGCTGATGCACTTCTACAGACTGACCAGGCTCTCACAG	pAIP-HA:GBP5	HA:GBP2(0-475)-GBP5(475-586)
GBP5(0-474)-Rev	CTGAGAGTGACTGATCAGTCTGTAATATTGCATGACTCACAGACTCCT	pAIP-HA:GBP5	HA:GBP5(0-474)-GBP2(474-591)
GBP2(474-591)-Fwd	AGGAGTCTGTGAGTCATGCAATATTACAGACTGATCAGTCACTCTCAG	pAIP-HA:GBP2	HA:GBP5(0-474)-GBP2(474-591)
GBP2(0-506)-Rev	CATTTGCTCGTTCTGCCTTTGAATTTCCTCCAACATTTTCTTTGCAGC	pAIP-HA:GBP2	HA:GBP2(0-506)-GBP5(506-586)
GBP5(506-586)-Fwd	GCTGCAAAGAAAATGTTGGAGGAAATTCAAAGGCAGAACGAGCAAATG	pAIP-HA:GBP5	HA:GBP2(0-506)-GBP5(506-586)
GBP5(0-512)-Rev	CTCTTCTCTTTCTGTTCCATCATCTCCTCGTTCTGCCTTTGAATCGC	pAIP-HA:GBP5	HA:GBP5(0-512)-GBP2(512-591)
GBP2(512-591)-Fwd	GCGATTCAAAGGCAGAACGAGCAGATGATGGAACAGAAAGAGAAGAG	pAIP-HA:GBP2	HA:GBP5(0-512)-GBP2(512-591)
GBP2(0-535)-Rev	TTTCTGTTGCTCTGCCAGCCACCTCTCCATCTTCTCAGTCAATTGT	pAIP-HA:GBP2	HA:GBP2(0-535)-GBP5(535-586)
GBP5(535-586)-Fwd	ACAATTGACTGAGAAGATGGAGAGGTGGCTGGCAGAGCAACAGAAA	pAIP-HA:GBP5	HA:GBP2(0-535)-GBP5(535-586)
GBP5(0-543)-Rev	TAAGAGCGAGGGTCTTCTCTTGCTCTTTCTGTTGCTCTGCCAGCCA	pAIP-HA:GBP5	HA:GBP5(0-543)-GBP2(543-591)
GBP2(543-591)-Fwd	TGGCTGGCAGAGCAACAGAAAGAGCAAGAGAAGACCCTCGCTCTTA	pAIP-HA:GBP2	HA:GBP5(0-543)-GBP2(543-591)
GBP2-S	TTTCACCCTGGAACTGGAAG	pAIP-HA:GBP2	Sequencing

Cell lines

Cell line	Background	Description	Reference
HA:N2-475-C5	U937 WT	GBP2 Nter – GBP5 Cter chimera, joint PCR	This study
HA:N2-506-C5	U937 WT	GBP2 Nter – GBP5 Cter chimera, joint PCR	This study
HA:N2-535-C5	U937 WT	GBP2 Nter – GBP5 Cter chimera, joint PCR	This study
HA:N5-303-C2	U937 WT	GBP2 Nter – GBP5 Cter chimera, joint PCR	This study
HA:N5-340-C2	U937 WT	GBP5 Nter – GBP2 Cter chimera	This study
HA:N5-474-C2	U937 WT	GBP5 Nter – GBP2 Cter chimera	This study
HA:N5-512-C2	U937 WT	GBP5 Nter – GBP2 Cter chimera	This study
HA:N5-543-C2	U937 WT	GBP5 Nter – GBP2 Cter chimera	This study
HA:N5M2C5	U937 WT	GBP2 (340-535) in GBP5 background	This study

Antibodies: Primary

Antigen	Made in	Reference	Experiment	Dilution
HA tag	mouse	Sigma-Aldrich #H3663	IF	1:3000
HA tag	rabbit	Cell Signaling #3724S	WB	1:1000
F. tularensis LPS	chicken	Denise Monack lab	IF	1:1000
GM130	rabbit	Cell Signaling #12480	IF	1:1000
actin	mouse	Sigma-Aldrich #A3853	WB	1:5000

Antibodies: Secondary

Anti-IgG	Conjugate	Reference	Experiment (Fig.)
chicken	Alexa Fluor 568	Invitrogen #A11041	**IF** (Fig. S7 F-J)
chicken	Alexa Fluor 594	Life #A21207	**IF** (all except otherwise indicated)
mouse	Alexa Fluor 488	Sigma-Aldrich #A10667	**IF** (all where otherwise indicated)
rabbit	Alexa Fluor 647	ThermoFisher #A21246	**IF** (Fig. S7 F-J)
mouse	HRP	Promega #W402b	**WB** (all)
rabbit	HRP	Sigma-Aldrich #A0545	**WB** (all)

Discussion

Limits of the model

U937 macrophages

Unlike primary macrophages and epithelial cells, U937 cells are small and round, and the nucleus represents more than 50% of the volume of the cell. Microscopic quantifications involving the cell cytosol are difficult to set up and somewhat limited – often requiring high resolution microscopy and confocal microscopy to separate events in the 2D and 3D space which would be less of an issue in an adherent cell like a HeLa cell.

Ultimately, we chose to work in a monocyte/macrophage cell line to faithfully represent the replicative niche of *F. novicida*. The focus of our study being specificity and functionality of human GBPs, we could not use a murine model. Additionally, a small number of experiments could be reproduced in hMDMs but given the limited tools available to investigate specifically the role and the recruitment of endogenous GBPs (GBP1/2 antibodies, siRNA) and the high homology between GBPs, we considered a genetically-based approach to be the most appropriate method for our objective. Thus, using point-mutagenesis and creating chimeric proteins, we have succeeded in unravelling important factors in the specific recruitment of GBPs to *F. novicida*.

However, I believe that the continuation of this work will greatly benefit from more in-depth biochemical experiments and the use of better optimized high-resolution microscopy techniques.

F. novicida

Francisella are small (0.2 µM in diameter, 0.2 to 0.7 µM in length) organisms that replicate abundantly in macrophages. As seen in Fig. 1 and 2 below, individual bacteria are not easily distinguished, particularly because of abundant replication in clusters, the highly pleiomorphic nature of the bacterium and possibly LPS shedding. Ideally, we would have counted GBP recruitment events at single bacterium level. Yet, given the infection phenotype of *F. novicida* in U937 macrophages this method of quantification was impossible to do. Instead, we decided to count the numbers of infected cells with recruitment events. Interestingly, in the same cell not all bacteria are targeted by GBPs – this is true both for *F. novicida* and *S. flexneri*. For further discussion on the topic, see chapter **GBP ligands**.

Because of the phenotype of GBP recruitment to *F. novicida* in U937 cells, the quantification of GBP recruitment to *F. novicida* cannot be automatized like others have been able to do for *T. gondii* or *S.* Typhimurium [440]. Optimization of High-Content Screening (HCS) microscopy [441] remains highly challenging for *F. novicida*. Developing alternative assays such as proximity-based reporters (PLA, FRET) could provide an efficient system to analyse GBP recruitment.

Despite the limits of *F. novicida* as a model, it is still a very interesting bacterium to study. With regards to GBPs, the higher requirements for *F. novicida* targeting in comparison to *S. flexneri* have allowed us to pinpoint specificities in GBPs that would not have been possible to observe with other models. As seen with viruses and supported by their evolution patterns, GBPs have likely evolved pathogen or pathogen type-specific mechanisms. Thus, these studies are important in order to broaden the scope of knowledge on GBPs in the context of different pathogens. For example, as of today there have been no studies on GBPs and *Rickettsia* spp., Gram-negative cytosolic bacteria responsible for several severe vector-borne diseases (i.e., typhus, spotted fever).

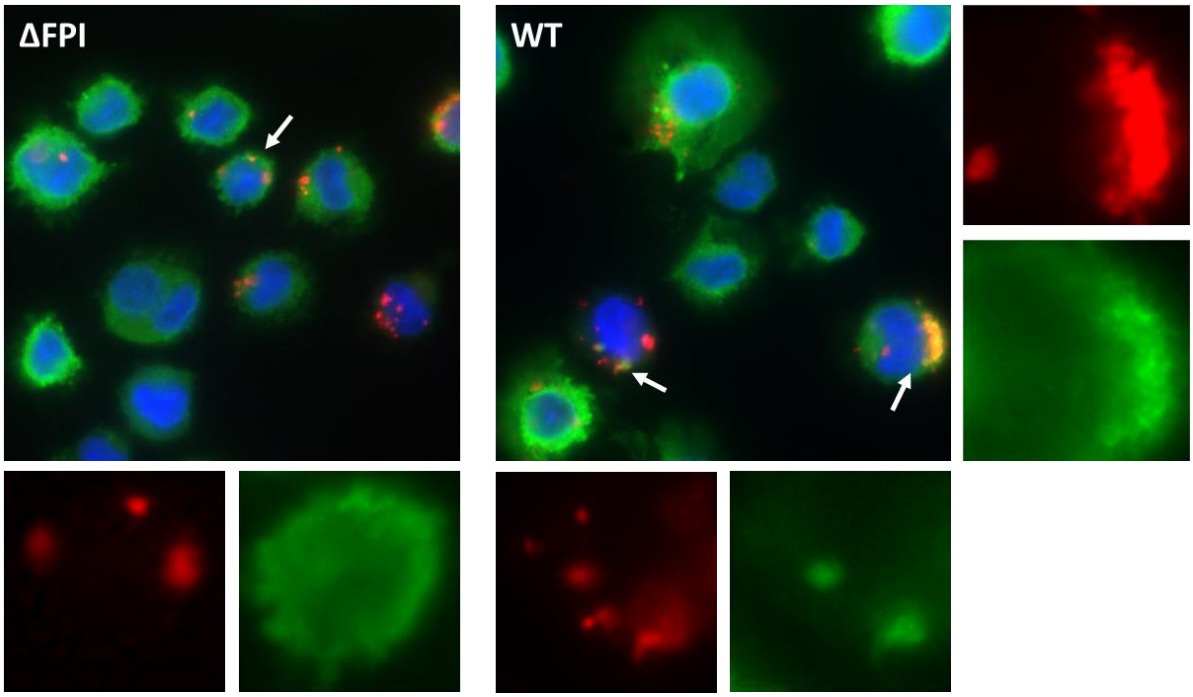

Figure 1. *A) Epifluorescence images of* F. novicida Δ*FPI or WT (red) in U937 macrophages expressing HA:GBP1 (green), infected at MOI 50 for 7h and pre-treated with IFNγ for 18h.*

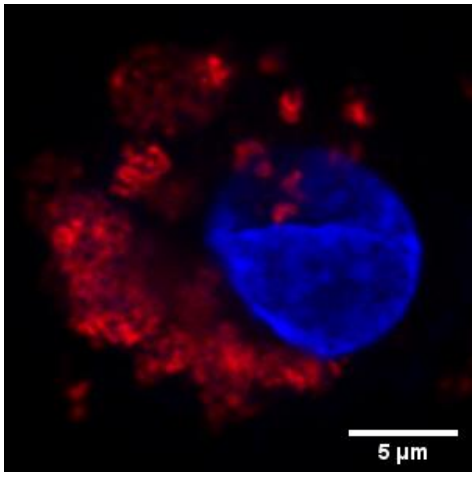

Figure 2. *Confocal image of a U937 macrophage infected with F. novicida U112 (red, anti-*Francisella *LPS antibody) at MOI 50 for 7h in the absence of IFNγ.*

Comparing *F. novicida* and *S. flexneri*

F. novicida and *S. flexneri* are two professional Gram-negative cytosol-dwelling pathogens but they have very different cell cycles. *S. flexneri* is primarily adapted to human epithelial cells where its replication is considerably more efficient than in macrophages [442]. Accordingly, studies on GBPs and *S. flexneri* have been predominantly done in HeLa cells [311,418,420]. In our observation, *F. novicida* infects close to 90% of U937 macrophages at MOI 50, while *S. flexneri* only infects around 30% to 50% of macrophages at MOI 50.

The kinetics of GBP recruitment are also very different between *F. novicida* and *S. flexneri*. As seen in Fig. 3, GBP1 and GBP2 recruitment doubles from 5h to 7h p.i. with *F. novicida* but stays relatively low

(between 20-25% of infected cells). Recruitment of GBP1 to *S. flexneri* reaches high numbers much earlier – between 50% to 80% in 3h.

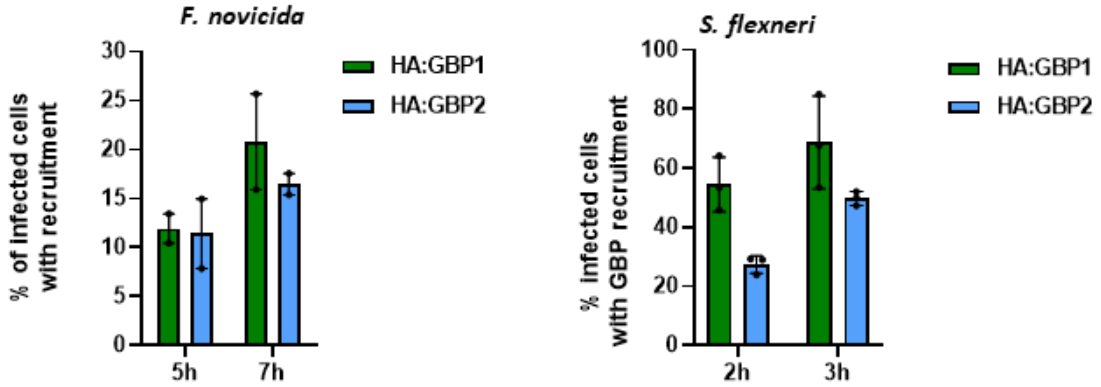

Figure 3. *Kinetics of HA:GBP1 and HA:GBP2 recruitment in U937 macrophages treated with IFNγ for 18h and infected at MOI 50 with F. novicida or* S. flexneri ΔIpaH9.8*.*

We cannot exclude that the late recruitment of GBP1 to *F. novicida* is influenced by the kinetics of bacterial escape to the cytosol. Due to a variety of methods and cell types used, there is no consensus on the timing of phagosomal rupture by *F. novicida* (Introduction chapter **Escape from the phagosome**). We have used the β-lactamase/CCF4 assay to determine that at least a portion of *F. novicida* has access to the cytosol at 3h p.i. (Fig. 4). Briefly, this method is based on the expression of β-lactamase in *Francisella* species [443]. Infected cells are incubated with the fluorescent probe CCF4, cleavable by the β-lactamase. A change in cytosolic fluorescence from 535 nm to 450 nm, measured by flow cytometry, indicates cytosolic β-lactamase. As every assay, it has its limitations – i.e., it measures cytosolic enzymatic activity instead of cytosolic bacteria. Although the two should be strongly correlated, the assay is likely influenced by the quantity of β-lactamase and possibly by the translocation of the β-lactamase from the periplasmic space to the bacterial surface/host cell cytosol. *S. flexneri* does not naturally express β-lactamase. In order to use the CCF4 assay for comparison with *F. novicida*, we would need to artificially introduce the β-lactamase gene in a Δ*ipaH9.8* background (to allow observation of GBP recruitment).

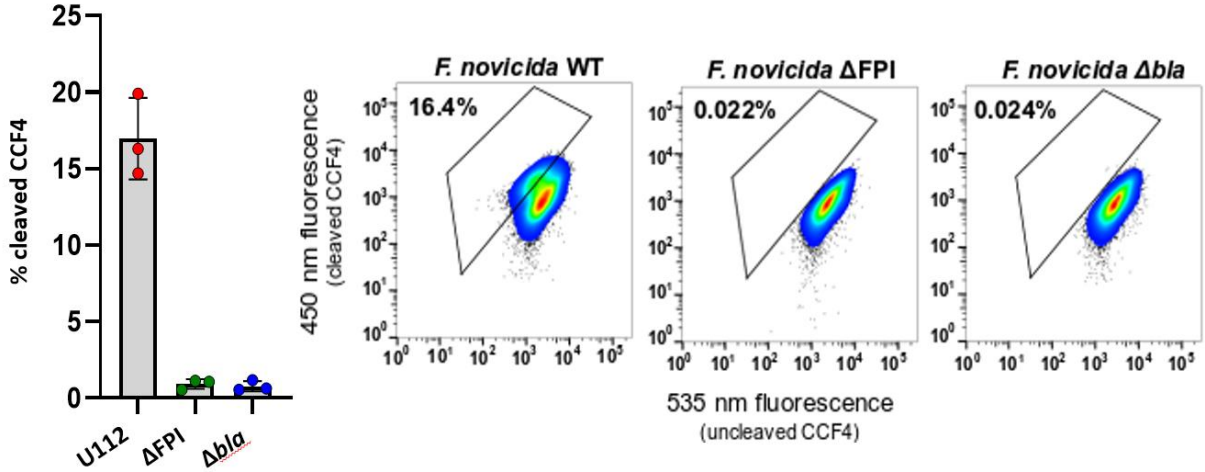

Figure 4. F. novicida *cytosolic escape as measured by β-lactamase activity 3h p.i. at MOI 50 in U937 macrophages (extract from Results Fig S6).*

A method for visualizing cytosolic bacteria was recently developed based on the use of a mutated version of lysenin, a toxin from the earthworm *Eisenia fetida*. Lysenin binds to the sphingomyelins exposed on the extracellular side of the cell membrane (also present on the inner side of vacuoles) and polymerizes to form pores [444]. The lysenin mutant W20A does not polymerize but can still bind to sphingomyelins [445]. When expressed in the host cytosol, GFP-lysenin W20A can beautifully mark the phagosomal permeabilization mediated by *Shigella* (Fig. 5A). Unfortunately, collocalization of lysenin with *F. novicida* is difficult to determine (Fig. 5B). Additionally, this method also does not directly mark cytosolic bacteria but rather ruptured phagosomes.

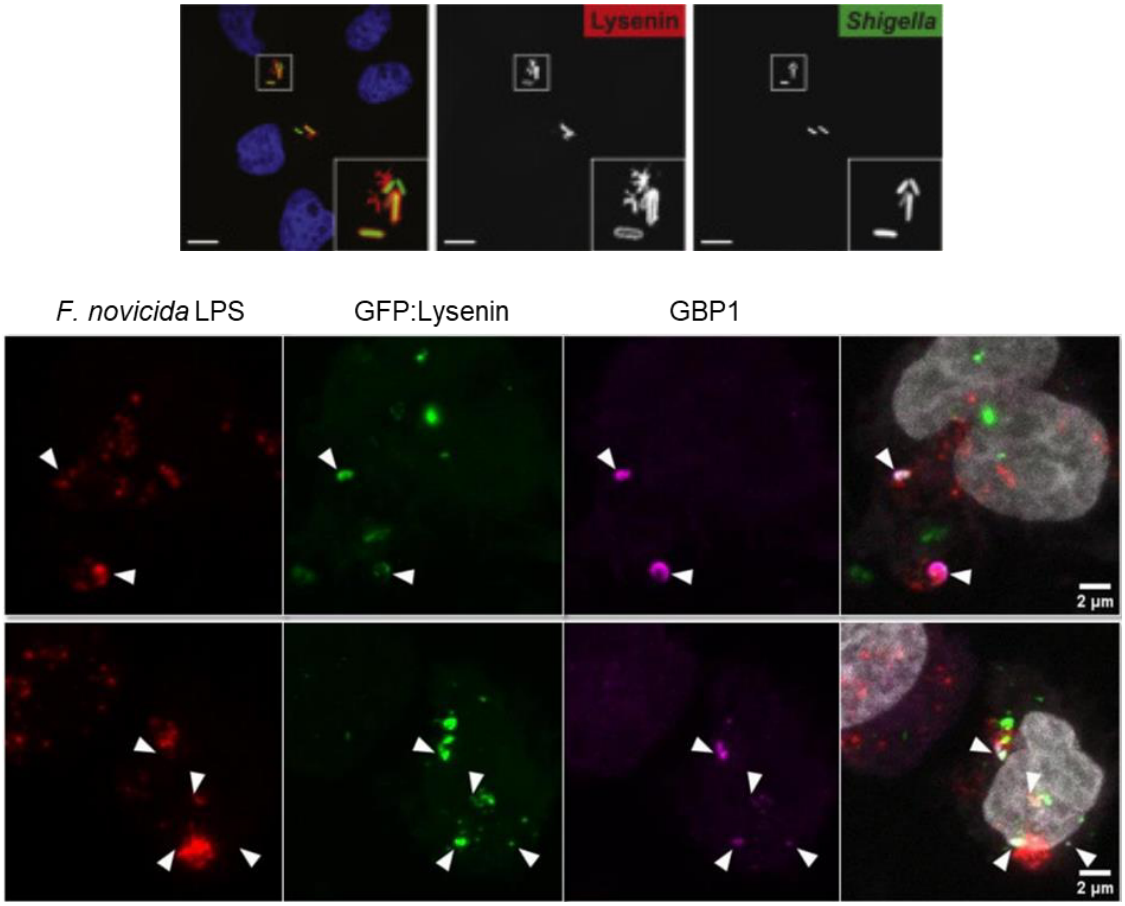

Figure 5. *Colocalization of W20A lysenin with cytosolic bacteria. A) HeLa expressing lysenin W20A were infected with* S. flexneri *at an unspecified MOI for 30 min.* [445] *B) U937 cells expressing GFP:Lysenin (green) infected with* F. novicida *(red) for 3h at MOI 50. GBP1 was stained with anti-GBP1 antibody (magenta).*

An alternative for staining cytosolic bacteria would be the selective permeabilization with digitonin, a detergent that binds cholesterol which is present on the plasma membrane. Intracellular membranes (e.g., phagosomes) have a different composition and will not be permeabilized [446], allowing to selectively stain cytosolic bacteria. If a quantification of cytosolic vs. phagosomal bacteria is to be done, either: 1. A subset of cells should be lysed by a classical method (triton or saponin) or 2. GFP-expressing bacteria should be used for quantification.

Recruitment of GBP1

GBP1 ligands

Despite GBP1 being at the focus of attention, there is no consensus yet on a GBP1 ligand for the targeting of pathogens.

GBPs mediate caspase-4/11 activation in response to cytosolic LPS [411,421]. Furthermore, shed LPS antagonizes GBP1 recruitment to *S. flexneri* [421] and purified GBP1 interacts with LPS *in vitro* whether farnesylated [421] or not [419]. GBP1 recruitment is decreased to *S. flexneri ΔrfaL* mutant missing the O-antigen [418], and it has been proposed that the C-terminal polybasic motif of GBP1 binds the negatively charged polysaccharide. Later it was demonstrated through cryo-electron microscopy that GBP1 can in fact bind *S. flexneri ΔrfaL* but does not coat the bacteria [421] suggesting that O-antigen promotes GBP1 polymerization around the bacterium but that the initial GBP1 docking proceeds independently of the O-antigen.

In parallel, GBP1 interaction with lipids is well documented. *In vitro*, GBP1 binds lipid vesicles in the presence of GTP thanks to the farnesyl moiety. The interaction is transient and is dissolved upon GTP hydrolysis [327,358]. Furthermore, murine Chr3-encoded Gbps mediate caspase-11 response to synthetic lipid A in the macrophage cytosol [417]. A preprint article describes that GBP1 coats *S.* Typhimurium outer membrane micelles lacking O-antigen (but still carrying the oligosaccharide core) [425].

It is possible that GBPs interact with lipids to dock onto bacterial surfaces but require carbohydrates like the O-antigen or the core to stabilize the polymer, for example by engaging the polybasic motif in an open conformation (Fig. 6). Though, this hypothesis is counterintuitive since lipid A is on the inner side of the LPS and the current model postulates that GBP1 binds the O-antigen to fragilize LPS and insure access for caspase-4 [421]. Considering the conflicting data, in my opinion this model does not completely explain GBP1 recruitment.

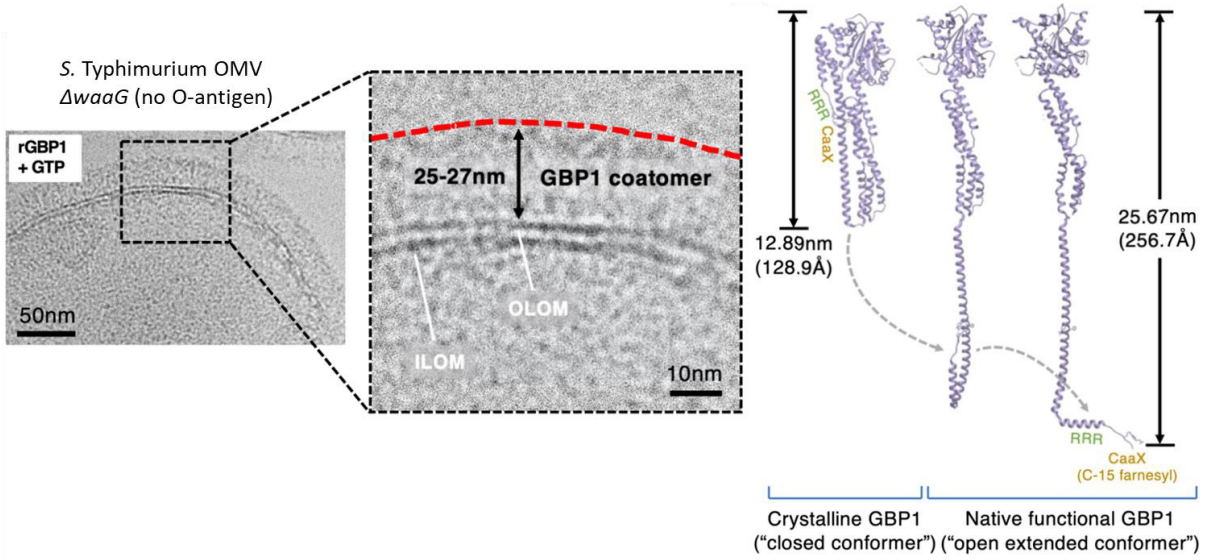

Figure 6. *Dynamic GBP1 modelling based on initial size 10 estimations from cryo-EM images of 25-27nm GBP1 coatomer length on StmDwaaG::pBAD-ftsZ OMVs. OLOM, outer leaflet of outer membrane. ILOM, inner leaflet of outer membrane. Pre-print from Zhu et al., 2021* [425].

Interestingly, GBP1 does not colocalize to all bacteria in a cell displaying GBP1 recruitment to bacteria (Results Fig. 1). The distinction between targeted or non-targeted bacteria could be based on bacterial factors (e.g., recruitment on dividing or weakened bacteria) or host factors (e.g., cellular trafficking or recruitment by an intermediary host protein). For instance, murine Gbps are associated with p62[14]-coated vesicles and localize to pathogen vacuoles marked by IRGs who recognize a missing-self phenotype [394].

Additionally, murine Gbps are recruited to pathogen-containing vacuoles perforated by bacterial secretion systems or to vesicles perforated by sterile stimuli (e.g., *Yersinia pestis* toxin YopD) [407,409], suggesting LPS-independent GBP recruitment is possible. In our experiments with GFP:lysenin W20A, GBP1 often colocalized with lysenin in aggregates devoid of *F. novicida* staining.

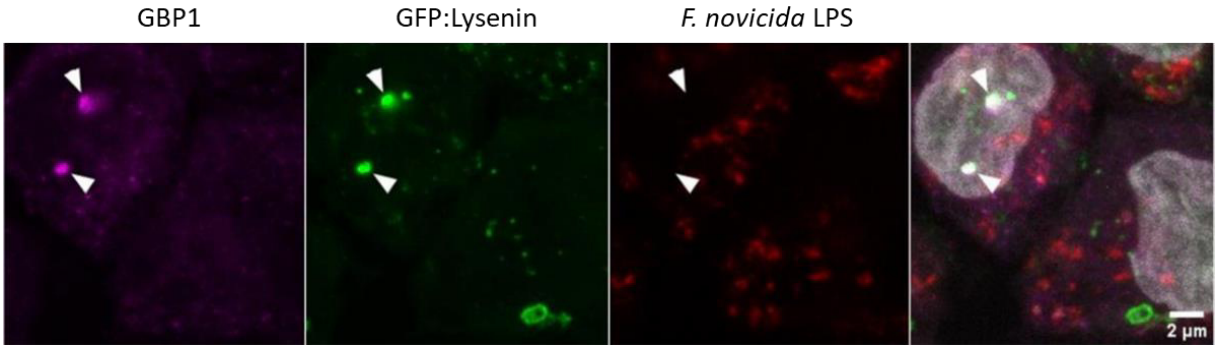

Figure 7. *U937 cells expressing GFP:Lysenin (green) infected with* F. novicida *(red) for 3h at MOI 50. GBP1 was stained with anti-GBP1 antibody (magenta).*

Murine Gbps bind *T. gondii*-containing vacuoles but a subset of Gbps can localize to the *T. gondii* membrane directly [391]. In a similar manner, GBPs may be shuttled to damaged vacuoles and from there, latch onto bacteria in the vicinity.

Affinity for *F. novicida* LPS

The requirements for GBP1 recruitment to bacteria, as established in the literature, are as follows: ability for GTP binding and hydrolysis, the presence of a farnesyl moiety, and a polybasic motif in the C-terminus [311,393,419]. GTP binding and hydrolysis is required for GBP1 polymerization, the farnesyl moiety for interaction with bacterial membranes, and the polybasic motif allows interaction with negatively charged LPS.

The above requirements are also true for GBP1 targeting of *F. novicida*, but they are not sufficient (Results Fig. 4).

First, an additional 61-63KKK patch in GBP1 contributes to *F. novicida* targeting. Curiously, *Francisella* LPS contains more than 60% free lipid A. This second polybasic motif could reinforce the interaction with the small quantity of *F. novicida* O-antigen.

Second, mutating GBP1 residues essential for GDP hydrolysis (G68A catalytic residue and the stabilizing guanine cap) completely abolished *F. novicida* targeting. Our results strongly suggest that GBP1 GDP

[14] p62 is part of the macroa)utophagy machinery.

hydrolysis is required to promote recruitment to *F. novicida*, while it is dispensable for *S. flexneri* targeting. Paradoxally, GMP formation dissolves the GBP1 polymer [327,363] which is strongest upon GTP binding. GBP1 recruitment to *F. novicida* may be highly dynamic and polymer turnover could be involved in a key process mediating GBP1-*F. novicida* interactions.

In the coinfection assays, we observed considerably less recruitment of GBP1 and GBP2 to *F. novicida* than to *S. flexneri* in coinfected cells (Results Fig 2, S2). We have additionally quantified the GBP recruitment to the bacteria in co-infected cells and our results show that *F. novicida* is significantly less targeted by GBP1 and GBP2 in co-infected cells in comparison to solo-infected cells from the same microscopic slides (Fig. 8).

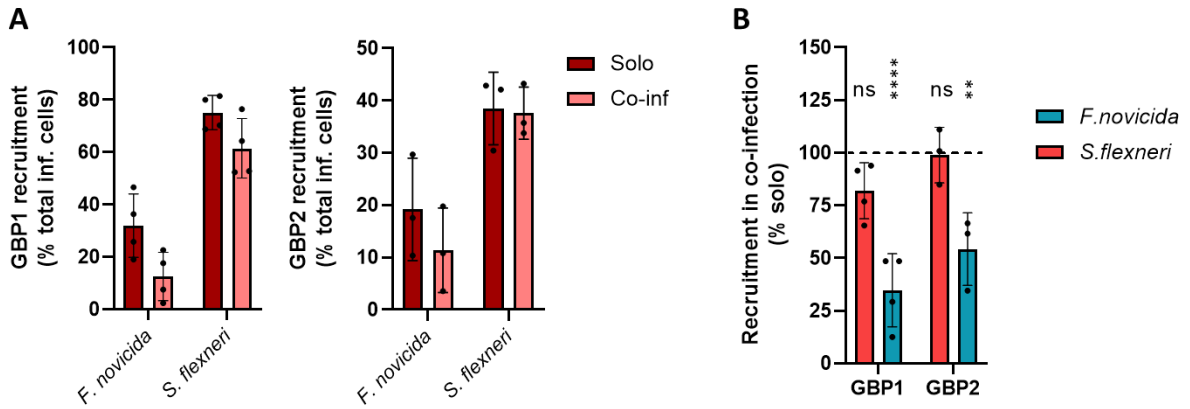

Figure 8. *Recruitment of GBP1 and GBP2 to* F. novicida *or* S. flexneri ΔIpaH9.8 *in co-infected or solo-infected cells. Coinfection assays were done as described in Results Fig. 2. A) GBP recruitment in solo- or co-infected cells was quantified from the same microscopic slide per bacteria. Each dot represents an independent experiment. B) Each dot represents a ratio of [GBP recruitment in co-infected cells] against [GBP recruitment in solo-infected cells]. Statistical analysis was done with ANOVA with Dunnett's correction; ****, p < 0.0001; **, p = 0.0024.*

The additional requirements, along with the overall lower and slower recruitment of GBP1 to *F. novicida* in comparison to *S. flexneri* hints at a lower affinity of GBP1 for *F. novicida*. Yet, this phenotype could also be a result of active suppression by *F. novicida* through an unknown mechanism (see chapter ***Francisella* adaptations that affect GBP recruitment**). The potential lower affinity of GBP1 for *Francisella* LPS should be confirmed by biochemical studies.

Recruitment of GBP2

As we have demonstrated in Results Fig. 3, and in accordance with the literature, GBP2 is recruited to *F. novicida* by GBP1. It is unknown whether the recruitment is direct or via an adaptor. Given the ability of GBP2 to interact with GBP1 [351] and the structural similarities between the two proteins [355], it is highly likely that GBP2 is recruited through dimerization and heteropolymerization with GBP1 onto the bacterial LPS. However, we cannot exclude the possibility that, similarly to the positive patches in GBP1, GBP2 would carry recognition motives to specifically interact with PAMPs.

We have shown that the CAAX box of GBP2 potentiates recruitment to *F. novicida* more efficiently than the CAAX box of GBP1 (Results Fig. 4). The longer (20C) geranylgeranyl moiety of GBP2 may allow a

better anchoring in the *Francisella* lipid A layer, which is composed of 16-18C acyl chains – longer than the usual 12C-14C encountered in *S. flexneri* or *E. coli*.

The type of GBP prenylation had a small, not statistically significant effect in modulating GBP targeting to *S. flexneri*. The experiments were performed at 2h p.i. instead of the 3h p.i. time point used in most other *S. flexneri* experiments. The earlier time point was chosen to give some leeway to observe an eventual increase in GBP1 recruitment in the GBP1-CNIL cell line. At this time, GBP1 recruitment is well established and GBP2 recruitment is increasing. The results suggest that prenylation type is of little importance to GBP recruitment to *S. flexneri.*

The GBP2 helical domain

The GBP2/5 chimera experiments identified parts of the helical domain and the GED of GBP2 (K340 in α9-R535 in α12) to control its GBP1-dependent recruitment to *F. novicida*. Specifically, replacing the central region of GBP5 with the K340-R535 of GBP2 allowed recruitment of the chimeric GBP5 to *F. novicida*.

The region α9-α12 of GBP2 has not been studied in the published literature. In GBP1, this region is involved in structural rearrangements allowing polymerization and insertion in lipid vesicles (Introduction chapter **GBP structure and biochemical properties**).

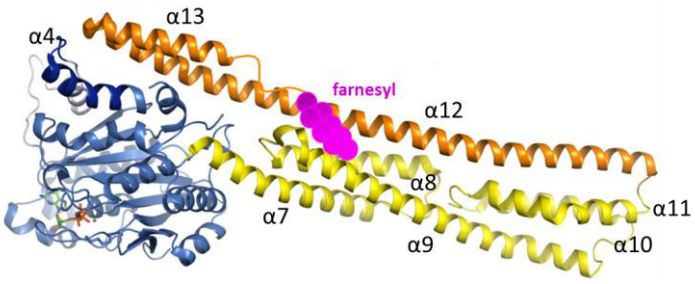

Figure 9. *Illustration of farnesylated GBP1.*
Blue, GTPase domain; yellow, helical stalk; orange, GED; pink, farnesyl group.

In GBP1, the globular domain interacts with the GED thanks to two arginine residues in α4 (globular domain) and several glutamine residues in α13 (GED) [361] (Fig. 9). These residues are present in GBP2 but absent in GBP5 (Introduction Fig. 26). Accordingly, GBP5 is thought to be an open monomer in contrast to GBP1 and probably GBP2 which are folded in a hairpin (closed) structure in steady-state [358]. Thus the geranylgeranyl tail of GBP5 is not hidden within a hydrophobic pocket between α9 and α12 as it is for GBP1 and possibly GBP2 [358].

Table 4. *Structural residues of the GBP1 central domain and implications for GBP2/5 recruitment.*

Residues of GBP1	Helix	Function	In GBP2?	In GBP5?	Chimera with GBP5 residues	Recruited to *F.n.*?
RK227-8	α4	Interaction with α4 for closed monomer.	Yes	QK	N5-340-C2	Yes
E563, E568, E575	α13	Interaction with α4 for closed monomer.	Yes	No	N2-535-C5	Yes
H378, Q381, K382, A385	α9	Hydrophobic pocket for farnesyl moiety.	Q-Q-K-A	Q-Q-R-G	N5-474-C2	0%
Y524, H527, L528, L531	α12	Hydrophobic pocket for farnesyl moiety.	Y-H-V-L	H-Q-V-M	N2-506-C5	50%
C589	α13	Hydrophobic pocket for farnesyl moiety.	Yes	Yes	N5-340-C2	Yes

As illustrated in Table 4, the GBP1 residues involved in α4-α9 interaction are present in GBP2 but not in GBP5, but they do not correlate with recruitment to *F. novicida* in the context of the GBP2/5 chimeras. The residues involved in formation of the hydrophobic pocket for GBP1 farnesyl moiety vary in GBP2 and GBP5 and coincide somewhat with the recruitment of chimeras but their variation cannot fully explain the divergence in *F. novicida* targeting. However, when it comes to structural motives, residue identity may not be as important as the availability of particular functional groups in the 3D space. Therefore, this region should be carefully examined in structural studies of geranylgeranylated GBP2 and GBP5.

The open conformation of GBP5 might play a role in its basal association with membranes, particularly the trans-Golgi apparatus. [350,351]. To the best of my knowledge, it is not clear whether GBP5 is located on the outer or inner side of the Golgi vesicles, and whether GBP5 is retained in the Golgi or localizes there by retrograde transport[15]. Generally speaking, GBP trafficking and maturation is poorly understood. CAAX proteins are prenylated in the endoplasmic reticulum. The AAX residues are cleaved by a Ras converting enzyme (RCE), then the prenylcysteine is methylated to protect the exposed carboxyl group [447]. GBP5 could localize specifically to the Golgi due to interaction with a Golgi-specific protein or thanks to a GBP5-intrinsic localization motif [448] but such a motif or interaction have not yet been identified. Based on data from the GBP2/GBP5 chimeras, gradual replacement of the GBP5 C-terminus with a GBP2 sequence reduces Golgi targeting. These results favour a structural mechanism or the involvement of hydrogen bonds/polarity, rather than a specific motif – if a motif was involved, loss of Golgi retention would be sudden rather than gradual.

The subcellular localization of the chimeras did not correlate with a particular phenotype of recruitment to *F. novicida*. This, plus the involvement of the GED in structural rearrangement and polymerization led us to hypothesize that the absence in GBP5 recruitment could be due to inability to oligomerize with GBP1.

The polymerization capacities of GBP2 or GBP5 have not been studied. We attempted cross-linking assays, combined with co-immunoprecipitation, to assess whether and to what degree GBP1 could oligomerize with GBP2 or GBP5. In Fig. 10, Flag-tagged GBP1 was transiently co-expressed with HA:GBP2 or HA:GBP5 in 293T cells. The cells were cross-linked, then the lysates were immunoprecipitated with HA agarose beads and assayed through Westen blotting. We observed robust interaction between GBP1 and GBP2, or GBP1 and GBP5. GBP1 and GBP2 co-immunoprecipitated in a dimer (140 kDa) or a >250 kDa oligomer, while GBP1 and GBP5 preferentially interacted in a dimer. We also noted a consistent increase in GBP2 protein level when co-expressed with GBP1 suggesting GBP2 is stabilized by GBP1. Unfortunately, while the results were promising, we could not robustly replicate them using HA:GBP1 co-expressed with Flag:GBP2 or Flag:GBP5. For further investigation on the subject a different biochemical approach could be envisioned, for example HPLC or calorimetry.

[15] GBP5 blocks HIV envelope maturation which happens inside the Golgi [379] but non-prenylated GBP1 and GBP2 can be recruited to the Golgi by GBP5 [351], suggesting GBP5 is located on the outer side.

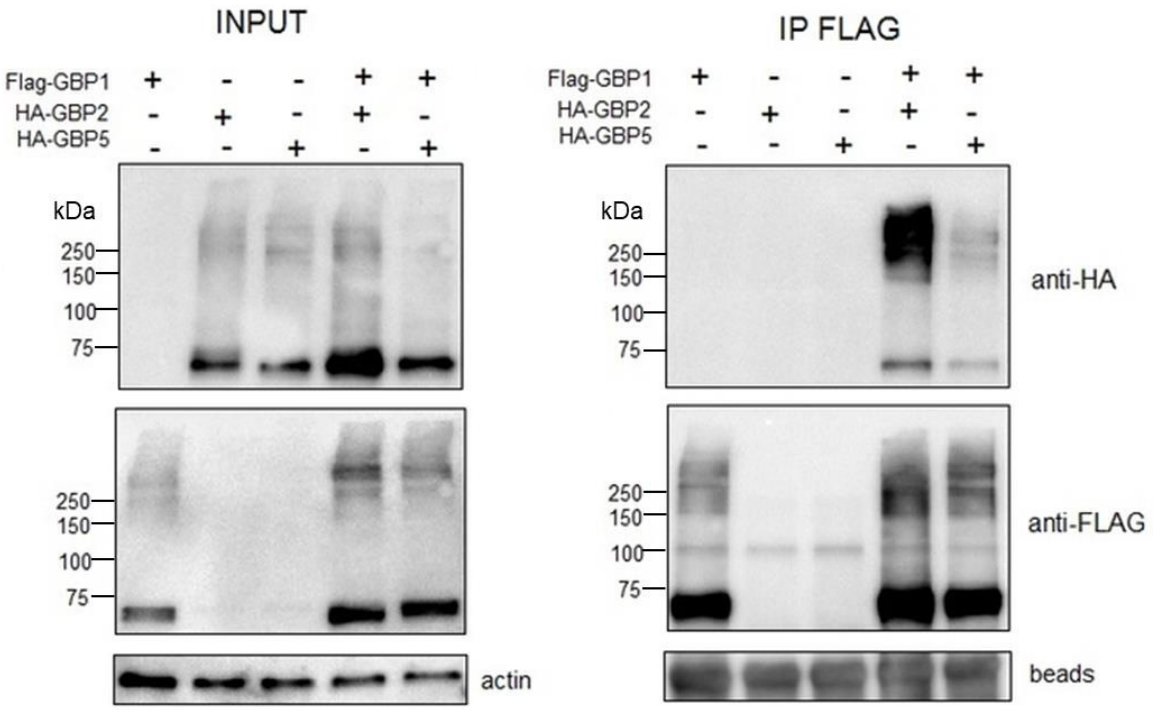

Figure 10. *Co-immunoprecipitation of Flag:GBP1 with HA:GBP2 or HA:GBP5. 293T cells were transfected with pMCV1.4-Flag:GBP1* [351] *and/or pAIP-HA:GBP2 or pAIP-HA:GBP5 for 24h using Lipofectamine 2000 (ThermoFischer), then crosslinked with 1mM DSS for 15 minutes at room temperature and quenched with Tris-Glycine pH7.4 for 5 min at RT. Co-immunoprecipitation was done with anti-Flag agarose beads (Sigma-Aldrich) with 800 mg protein from cell lysates. One experiment representative of three independent experiments is shown.*

Francisella adaptations that affect GBP recruitment

T6SS effectors

There are very few known *Francisella* secreted effectors and the ones with known functions are related to phagosomal escape (T6SS substrates PdpC and PdpD [118]) or resistance to oxidative stress (e.g. KatG secreted by a membrane fusion protein [182]). As of today, six T6SS effectors have been identified: OpiA, $OpiB_{1-3}$, PdpC, PdpD [156,158]. The role of OpiA and $OpiB_{1-3}$ in *Francisella* pathogenicity is not clear and the mechanism through which PdpC and PdpD mediate phagosomal escape remains unknown.

Coinfection of macrophages with *S. flexneri* and *F. novicida* did not inhibit GBP3 or GBP4 recruitment to *S. flexneri*, strongly suggesting that GBP3/4 escape by *F. novicida* is not mediated by a secreted effector. Nevertheless, mutants deleted for known T6SS effectors should be tested for GBP3/4 recruitment to fully exclude this hypothesis. Alternatively, GBP3/4 deposition could be inhibited by a membrane protein. It would be tempting to perform a large-scale screen for GBP3/4 recruitment to *F. mutants*, but the quantification of GBP-*Francisella* colocalization must be optimized and automatized before such a screen can be attempted.

The human pathogen *S. flexneri* actively and specifically antagonizes GBPs as a result of intensive host-pathogen co-evolution [339,344]. Humans are an accidental (dead-end) host for *Francisella* species.

Given the functional differences between human and other animal GBPs, specific GBP inhibition by *Francisella* is unlikely.

Francisella LPS modifications as an adaptive mechanism

The atypical *Francisella* LPS is synthesized, for the most part, as a classical LPS structure: the lipid A is initially phosphorylated and penta-acylated. In the later stages, lipid A is modified by phosphatases, deacetylases and transferases [179,222,223]. These modifications are adaptive mechanisms that allow survival in the host and escape from innate immunity.

LPS modification is common in pathogenic bacteria. The persistent coloniser *Helicobacteri pylori* has a lipid A very similar to the one of *F. novicida*: tetra-acylated LPS with longer (C16-C18) acyl chains and amino-modified disaccharide, connected to a single KDO unit [449]. These modifications mediate escape from TLR4 and resistance to cationic antibacterial peptides [449]. Many Gram-negative bacteria are prone to LPS deacylation in conditions resembling the host environment, such as *Yersinia pestis* which carries a tetra-acylated lipid A at 37°C [450].

On the other hand, the high percentage of free lipid A (>60%) is a unique property in *Francisella* species. Inversely, the lower percentage of O-antigen on the *F. novicida* surface might play a role in the overall lower rates of GBP-*F. novicida* colocalization. Unfortunately, it is still unclear which genetic mechanisms regulate the proportion of free lipid A in *Francisella* so this hypothesis cannot be tested through genetic manipulation.

LpxF and GBP3

We tested multiple *F. novicida* LPS biosynthesis gene mutants for recruitment of HA:GBP3 using confocal microscopy. We observed an enrichment of HA:GBP3 on a mutant deleted for the LpxF phosphatase. The HA:GBP3 enrichment was very clear on some images (Results Fig. 6C) but did not present a clear-cut phenotype like the HA:GBP3 recruitment to *S. flexneri* or HA:GBP1 recruitment to *F. novicida* (Results Fig. 1). To assess whether HA:GBP3 was significantly enriched on Δ*lpxF*, we decided to measure HA:GBP3 localization to single GBP1-positive bacteria as a ratio to the surrounding cytosolic HA:GBP3. Because of the distribution of bacteria and limited cytosol in U937 cells, the process could not be scripted but instead had to be manually evaluated for each cell using the steps described in Fig. S6 D.

The ΔlpxF mutant had a statistically significant enrichment of HA:GBP3, which was lost when the mutant was complemented either in cis or in trans (Fig. S6 B).

LpxF is a phosphatase that removes the 4' position phosphate in LPS-attached or free lipid A of *Francisella*. After the phosphate is removed, an unidentified deacetylase removes the acyl chain in 3' position. The consequences of *lpxF* deletion are a penta-acylated lipid A and a more negatively charged LPS due to the presence of the phosphate.

Underacylation of the LPS is a mechanism of immune evasion and host adaptation by different Gram-negative bacteria. For example, *Yersinia pestis* LPS is a mixture of tetra-, penta-, and hexaacylated forms at 26°C but is predominantly tetraacylated at 37°C [450]. *S. flexneri* is tetraacylated or triacylated while replicating in the host [451], although it is unclear if this occurs fast enough to impact the early and fast GBP recruitment onto *S. flexneri*. *Salmonella* LPS can be deacetylated by enzymes PagL or LpxR to decrease TLR4 activation [452,453].

LPS dephosphorylation or glycosylation is a strategy to increase resistance to cationic antimicrobial peptides [454,455]. The docking of GBP1 onto *Shigella* LPS is allowed by hydrogen bond interactions between positively charged triple arginine and negatively-charged LPS [421]. In *F. novicida*, the *ΔlpxF* mutation did not increase GBP1 recruitment but the *ΔlpxF* mutant also was deficient in cytosolic escape (Results Fig. S6).

GBP1 docking may be more stable onto *F. novicida ΔlpxF* compared to a WT strain, and this could increase GBP3 recruitment, for example through the formation of a stronger polymer or by allowing a more potent fragilization of the LPS layer and exposing possible ligands for GBP3. I do not believe that GBP3 interacts with the acyl chains directly. Indeed, GBP3 is not known to have a hydrophobic region. Still, GBP3 could interact with other bacterial components, such as the peptidoglycan (to my knowledge, GBP3 recruitment to Gram-positive bacteria has not been investigated).

Different bacterial LPS can be used to test whether tetraacylation directly impacts GBP recruitment (regardless of phosphorylation level). Homologs of the LpxL acetylase add the 3' acyl chain in Gram-negative bacteria [205]. For example, a *Burkholderia cenocepacia* strain carrying tetra-acylated LPS has been created by deleting LpxL [456] and such a mutagenesis could also be performed on the cytosol-dwelling *Burkholderia thailandensis*. On the other hand, to confirm or exclude the influence of the lipid A charge and phosphorylation level in GBP1/3 targeting, other *F. novicida* mutants can be tested: *lpxE*, *naxD*, *flmF1/F2*, *flmK.*

One caveat is that altering bacterial LPS also inevitably impacts bacterial fitness and survival in the host, which could also indirectly impact phagosomal escape or GBP recruitment by simple fragilization of the LPS. Alternatively, GBP1/3 polymerization can be attempted *in vitro* onto different bacterial LPS as in Kutsch *et al*., 2020 [421] with GBP1 and *Shigella* binding.

It would be interesting to investigate the structure of the GBP1/2/3/4 polymer on the bacterial surface, to see if the four GBPs interact on the same surface or if they form a multilevel polymer. Superresolution fluorescence microscopy is still limited in the number of fluorescent probes that can be imaged at the same time; but combinations of GBPs can be imaged in dual colour STED (stimlulated emission depletion) or SMLM (single-molecule localization microscopy). Alternatively, GBP-coated bacteria could be imaged by cryo-electron microscopy to see whether the absence or presence of particular GBPs alters the structure of the polymer or the LPS.

<u>Notes on GBP3 recruitment to bacteria</u>

Co-transfection of mCherry:GBP1 and eGFP:GBP3 in untreated HeLa cells is sufficient to allow recruitment of GBP3 to *S.* Typhimurium in the absence of IFNγ; the same is true for GBP4 [419]. These results indicate that GBP3 targeting to bacteria does not require other GBPs or IFNγ-inducible factors besides GBP1.

Since GBP1 and GBP2 are both prenylated, we wondered if prenylation was a requirement for any GBP targeting to *F. novicida*. We thus generated a plasmid encoding a prenylated GBP3 carrying the CAAX box of GBP2 (GBP3-CNIL). The HA:GBP3-CNIL chimeric protein was recruited to *S. flexneri* but did not target *F. novicida*. In the future, constructing GBP2/3 chimeras in a prenylated or non-prenylated background should help us understand the specificities and differences between GBP2 and GBP3.

Identifying the recruitment requirements of GBP3 could help in identifying a possible bacterial ligand (present in *Shigella* but absent in *Francisella*) or a potential host interactant of GBP3 (non-ISG).

Functional consequences of GBP escape

Roles of GBPs in inflammasome activation

F. novicida is not targeted by GBP3 and GBP4. Importantly, what are the functional consequences? In the current model, GBP3 and GBP4 control caspase-4 recruitment (GBP4) and activation (GBP3). In comparison to other bacteria (*E. coli*, *S. flexneri*), caspase-4 response to *F. novicida* is much weaker [234]. The lower level of caspase-4 activation could be a consequence by the lack of GBP3/4 recruitment but it is also explained by the tetraacylation of *F. novicida* LPS [234]. Nevertheless caspase-4 is activated in hMDM [234] and in U937 (Fig. 11 E).

In hMDM, LDH release (cell death) was decreased upon knock down of GBP1-4 but not GBP5, in accordance with the currently proposed model. However, IL-1β secretion (mediated by caspase-1 processing) was only affected by *GBP1-2* knock down (Fig. 11 A).

In U937, inflammasome activation is indeed dependent on GBP1/2 and surprisingly GBP5, despite its lack of recruitment and no discernible role in hMDMs (Fig. 11 B, C). GBP3 KO has no effect on cell death and cytokine release and the role of GBP4 is ambiguous. The data in U937 KO cells was confirmed by complementation experiments (not shown).

In U937 macrophages (Results Fig. S1), GBP3 is very weakly induced by IFNγ and *F. novicida* in comparison to other GBPs. This could explain the lack of effect of *GBP3* invalidation in U937, but GBP3 is also weakly induced in hMDM (Introduction Fig. 28, p.42 [234]) and still partially mediates cell death upon *F. novicida* infection.

Further functional studies are necessary to clarify the involvement of GBP3 and GBP4 in anti-*Francisella* immunity. The possibility of cell type-dependent effects should be strongly considered.

Uncoupling of GBP recruitment and inflammasome activation

If GBP3 and GBP4 mediate caspase-4 activation on the bacterial surface, how is caspase-4 activated by *F. novicida* in the absence of GBP3 and GBP4 recruitment?

In vitro, GBP1 by itself can bind and damage LPS [421]. Caspase-4 can directly bind LPS through its CARD domain [457]. Yet *in cellulo* GBP2-4 are required for caspase-4 recruitment and activation [419,420]. GBP-caspase-4 interactions have been demonstrated in the presence of LPS [420] but there is no evidence for direct interaction between GBPs and caspase-4. What are the actions of GBPs 2-4?

GBP2 is not recruited to *F. novicida* in *GBP1*^{KO} cells. Yet, GBP2 contributes to inflammasome activation in the absence of GBP1 (Fig. 11 D). Are GBP1 and GBP2 involved in independent, but complementary inflammatory pathways in *F. novicida*-infected macrophages?

What is the mechanism of GBP5-induced inflammasome activation, if recruitment to *F. novicida* is not involved?

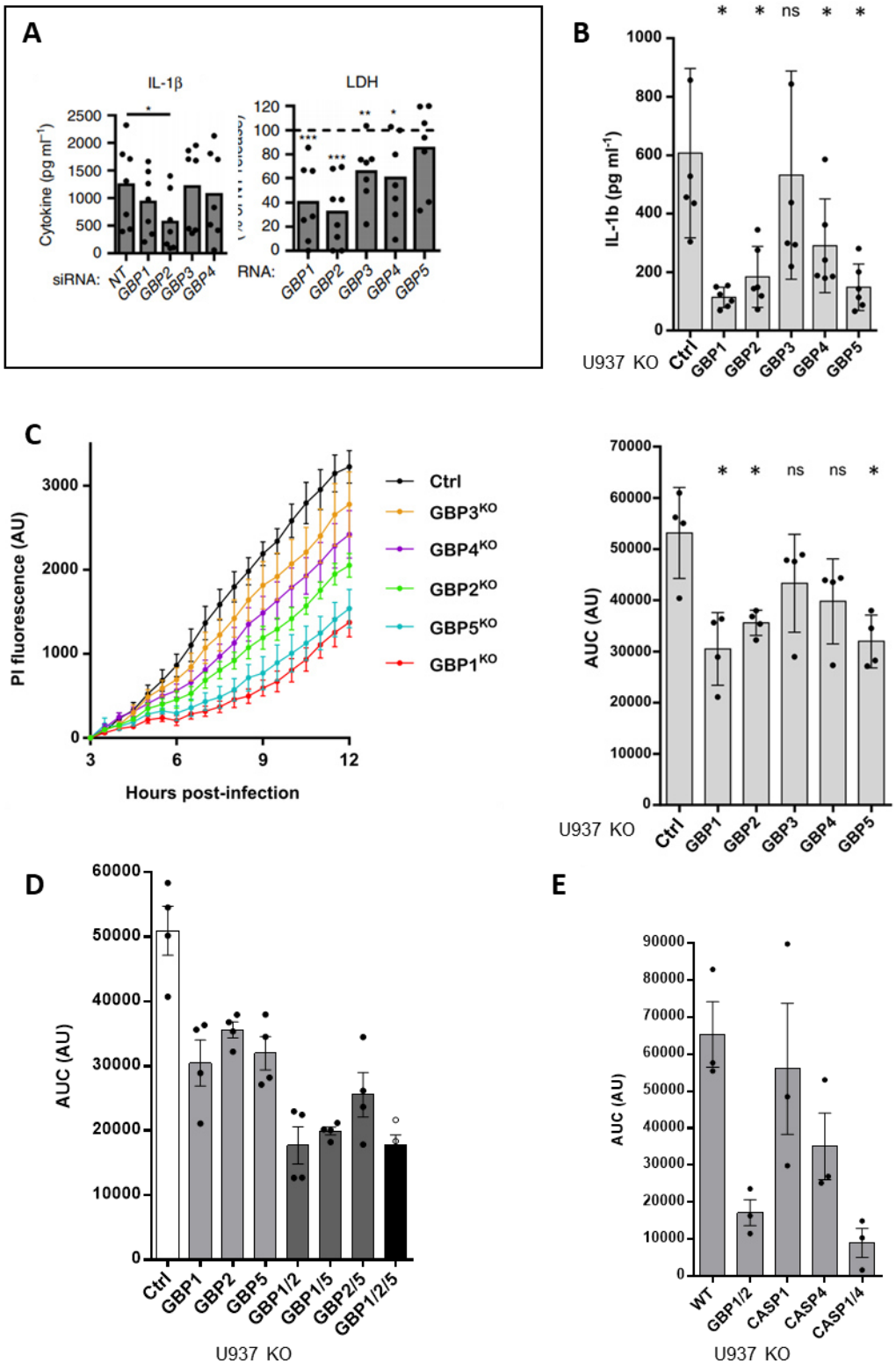

Figure 11. *Inflammasome activation by GBPs in human macrophages infected by* F. novicida*. A) IL-1ß and LDH release were measured in hMDM infected for 8h with* F. novicida *at MOI 10 [234]. B-E) IL-1ß and PI incorporation were measured in PMA-differentiated U937 KO macrophages, pre-treated with 100 U/ml IFNγ for 18h and infected with F. novicida at MOI 100 for 10h. AUC = area under the curve. ANOVA statistical analysis was done, p < 0.5. Unpiblished data by Brice Lagrange.*

In U937 cells, inflammatory response to *F. novicida* is partially caspase-4-independent (Fig. 11 E). Are there alternative inflammasome pathways that are activated by *F. novicida*? In hMDM, Aim2 or pyrin knock down does not influence inflammatory response to *F. novicida* [234]. But different inflammasomes could be involved in redundant secondary pathways that could partially complement a lack of *CASP4*.

GBPs mediate inflammasome activation in response to pathogens, but also to cytosolic OMVs or LPS directly. In fact, LPS shedding could be a GBP-evasive strategy for some bacteria [421,425,426]. It is possible that GBP1 breaks the cytosolic LPS micelles similarly to the detergent activity of GBP1 in contact with lipid vesicles [358], allowing access to lipid A for caspase-4. The contributions of GBPs 2/3/4 are still a mystery.

Our observations of GBP roles in *F. novicida*-infected human macrophages show a dissociation of recruitment and inflammasome activation in the roles of GBP2 and GBP5 in *F. novicida*. It is highly likely that GBP2 and GBP5 are involved in pathways, complementary but independent of GBP1-mediated recruitment to the bacteria.

The recruitment of GBP1 to *T. gondii* is well established [353,393]. But a recent study described roles of GBP2 and GBP5 in *T. gondii* killing, without localizing to the parasite in a detectable manner [398]. These recruitment-independent effects were dubbed 'distal control'. In addition, GBP1 and GBP2 are not recruited to *C. muridarum*, yet they control inflammasome activation in response to the pathogen [403].

Bacteria like *S. flexneri* and *S.* Typhimurium activate so quickly and robustly caspase-4 and pyroptosis, that alternative GBP recruitment-independent processes might not detectable. Alternative recruitment-independent pathways could be triggered based the membrane characteristics of the pathogen. In the cytosol, *T. gondii* and *Chlamydia* survive in modified phagosomes. Because *F. novicida* LPS is so unusual, it could activate parallel recruitment-dependent and independent GBP-controlled responses.

There is no mechanism proposed as to the distal control of pathogens exercised by GBPs but this phenomenon should absolutely be investigated. GBP1-independent effects of GBP2 and GBP5 should be explored in detail.

GBPs redundancy and specificity: The importance of broadening the scope

The literature shows, and we have demonstrated in this work, that subtle differences in GBP sequence and structure have important consequences on their function.

The current body of literature puts GBP1 in a central role. The model of GBP1, followed by GBP2/3/4 recruitment to activate caspase-4 may be compelling in its simplicity but does not draw the full picture of GBP roles in anti-bacterial immunity. The emergence of publications on the GBP distal control, and our unpublished data highlight the importance in exploring different models for GBP activity and alternative pathways of recruitment-independent inflammasome activation.

It is important to characterize all GBPs functionally and biochemically as rigorously as GBP1. GBPs encoded in the human genome have gone through extensive evolution and selection, pertaining to their key roles in cytosolic immunity. These roles are still unclear. For instance, GBP6 is recruited to

Gram-negative bacteria in overexpression systems [418,419]. Moreover, *GBP6* is basally expressed in the mucosal tissues, barriers to the outside environment. This implies an important role of GBP6 in innate immunity, which has been neglected.

GBPs are enzymes with no singular purpose (process substrate A to produce compound B) – they have a variety of roles to antagonize parasites, virus, bacteria through diverse mechanisms, in addition to their potential roles in cell proliferation, migration, differentiation. Hence, GBPs are integral part of the cell life and immunity. They function in an environment that is shaped by the pathogen (environment-dependent LPS remodelling, host-induced secretion of effectors, cell-type dependent adaptations) and by the repertoire of available host partners.

The subtle but important divergences between GBPs suggest they interact differently with pathogens or with host factors. GBPs might carry specific sequences to target different PAMPs or alternatively, sequences that promote different interactions with host factors and immunity pathways. GBP-controlled pathways might be redundant in the way that most of innate immunity is redundant: when one pathway is blocked, another can take its place to protect the host. To have a full understanding of GBP-mediated immunity, research should step beyond the established models and explore the facets of GBP functioning in diverse environments and conditions.

References

1. McCoy GW. Plague among Ground Squirrels in America. J Hyg (Lond). 1910;10: 589–601.
2. Public Health Bulletin. U.S. Government Printing Office; 1911.
3. McCoy GW, Chapin CW. Further Observations on a Plague-Like Disease of Rodents with a Preliminary Note on the Causative Agent, Bacterium tularense. The Journal of Infectious Diseases. 1912;10: 61–72.
4. Weekly Reports for JANUARY 22, 1937. Public Health Rep. 1937;52: 95–123.
5. Wherry WB, Lamb BH. Infection of Man with Bacterium Tularense. The Journal of Infectious Diseases. 1914;15: 331–340.
6. Weekly Reports for SEPTEMBER 12, 1919. Public Health Rep. 1919;34: 2061–2103.
7. Weekly Reports for JULY 29, 1921. Public Health Rep. 1921;36: 1731–1792.
8. Jellison WL. Tularemia: Dr. Edward Francis and his first 23 isolates of Francisella tularensis. Bull Hist Med. 1972;46: 477–485.
9. Francis E. A SUMMARY OF PRESENT KNOWLEDGE OF TULARAEMIA1. Medicine. 1928;7: 411–432.
10. Francis E. SYMPTOMS, DIAGNOSIS AND PATHOLOGY OF TULAREMIA. JAMA. 1928;91: 1155. doi:10.1001/jama.1928.02700160007002
11. Weekly Reports for JUNE 22, 1923. Public Health Rep. 1923;38: 1391–1447.
12. Weekly Reports for MAY 9, 1924. Public Health Rep. 1924;39: 1057–1112.
13. [Edward Francis innoculating a rabbit] - Digital Collections - National Library of Medicine. [cited 26 Jan 2022]. Available: https://collections.nlm.nih.gov/catalog/nlm:nlmuid-101679588-img
14. Scheel O, Sandvik T, Hoel T, Aasen S. [Tularemia in Norway. A clinical and epidemiological review]. Tidsskr Nor Laegeforen. 1992;112: 635–637.
15. Sjostedt A. Tularemia: History, Epidemiology, Pathogen Physiology, and Clinical Manifestations. Annals of the New York Academy of Sciences. 2007;1105: 1–29. doi:10.1196/annals.1409.009
16. Francis E. TULAREMIA. JAMA. 1925;84: 1243. doi:10.1001/jama.1925.02660430001001
17. Foshay L. SERUM TREATMENT OF TULAREMIA. JAMA. 1932;98: 552. doi:10.1001/jama.1932.27320330001009
18. Foshay L. STREPTOMYCIN TREATMENT OF TULAREMIA. JAMA. 1946;130: 393. doi:10.1001/jama.1946.02870070013004
19. Philip CB, Owen CR. Comments on the nomenclature of the causative agent of tularemia. International Bulletin of Bacteriological Nomenclature and Taxonomy. 1961;11: 67–72. doi:10.1099/0096266X-11-3-67
20. FRANCIS E, MOORE D. IDENTITY OF OHARA'S DISEASE AND TULAREMIA. Journal of the American Medical Association. 1926;86: 1329–1332. doi:10.1001/jama.1926.02670440003002
21. Weekly Reports for JULY 2, 1926. Public Health Rep. 1926;41: 1341–1402.
22. Weekly Reports for FEBRUARY 24, 1922. Public Health Rep. 1922;37: 387–456.
23. Overholt EL, Tigertt WD, Kadull PJ, Ward MK, David CN, Rene RM, et al. An analysis of forty-two cases of laboratory-acquired tularemia. The American Journal of Medicine. 1961;30: 785–806. doi:10.1016/0002-9343(61)90214-5
24. METRE JR TEV, J. KADULL P. LABORATORY-ACQUIRED TULAREMIA IN VACCINATED INDIVIDUALS: A REPORT OF 62 CASES* †. Annals of Internal Medicine. 1958 [cited 25 Jan 2022]. Available: https://www.acpjournals.org/doi/abs/10.7326/0003-4819-50-3-621
25. Harris S. Japanese Biological Warfare Research on Humans: A Case Study of Microbiology and Ethics. Annals of the New York Academy of Sciences. 1992;666: 21–52. doi:10.1111/j.1749-6632.1992.tb38021.x
26. Rider DR. Japan's Biological and Chemical Weapons Programs; War Crimes and Atrocities: Who's Who, What's What and Where's Where – 1928-1945. 2014; 761.
27. US Army Project CD 22 | Operation Human Guinea Pig. [cited 26 Jan 2022]. Available: https://usarmywhitecoat.com/

28. Saslaw S. Tularemia Vaccine Study: I. Intracutaneous Challenge. Arch Intern Med. 1961;107: 689. doi:10.1001/archinte.1961.03620050055006
29. Saslaw S. Tularemia Vaccine Study: II. Respiratory Challenge. Arch Intern Med. 1961;107: 702. doi:10.1001/archinte.1961.03620050068007
30. Sawyer WD, Dangerfield HG, Hogge AL, Crozier D. Antibiotic prophylaxis and therapy of airborne tularemia. Bacteriol Rev. 1966;30: 542–550.
31. Operation Whitecoat, The Movie. [cited 26 Jan 2022]. Available: http://operationwhitecoatmovie.com/index.html
32. Pittman PR, Norris SL, Coonan KM, McKee KT. An Assessment of Health Status among Medical Research Volunteers Who Served in the Project Whitecoat Program at Fort Detrick, Maryland. Military Medicine. 2005;170: 183–187. doi:10.7205/MILMED.170.3.183
33. Office of the Assistant Secretary of Defense (Health Affairs). Desert Test Center. 9 Mar 2009 [cited 26 Jan 2022]. Available: https://web.archive.org/web/20090309172516/http://fhp.osd.mil/CBexposures/pdfs/red_cloud.pdf
34. Engineering Bio-Terror Agents: Lessons from the Offensive U.S. and Russian Biological Weapons Programs. [cited 26 Jan 2022]. Available: https://irp.fas.org/congress/2005_hr/bioterror.html
35. Borzenkov VM, Pomerantsev AP, Pomerantseva OM, Ashmarin IP. [Study of nonpathogenic strains of francisella, brucella and yersinia as producers of recombinant beta-endorphin]. Biull Eksp Biol Med. 1994;117: 612–615.
36. Borzenkov VM, Pomerantsev AP, Ashmarin IP. [The additive synthesis of a regulatory peptide in vivo: the administration of a vaccinal Francisella tularensis strain that produces beta-endorphin]. Biull Eksp Biol Med. 1993;116: 151–153.
37. Arrêté du 30 avril 2012 fixant la liste des micro-organismes et toxines prévue à l'article L. 5139-1 du code de la santé publique.
38. Avery FW, Barnett TB. Pulmonary Tularemia. Am Rev Respir Dis. 1967;95: 584–591. doi:10.1164/arrd.1967.95.4.584
39. IuGItES WT. OROPHARYNGEAL TULAREMIA. THE JOURNAL OF PEDIATRICS. : 10.
40. Tärnvik A, editor. WHO guidelines on tularaemia: epidemic and pandemic alert and response. Geneva: World Health Organization; 2007.
41. Friend M. Tularemia. Reston, Va: U.S. Dept. of the Interior, U.S. Geological Survey; 2006.
42. Factsheet. In: European Centre for Disease Prevention and Control [Internet]. [cited 27 Jan 2022]. Available: https://www.ecdc.europa.eu/en/tularaemia/facts
43. CDC. Tularemia home | CDC. In: Centers for Disease Control and Prevention [Internet]. 13 Dec 2018 [cited 27 Jan 2022]. Available: https://www.cdc.gov/tularemia/index.html
44. Hestvik G, Warns-Petit E, Smith LA, Fox NJ, Uhlhorn H, Artois M, et al. The status of tularemia in Europe in a one-health context: a review. Epidemiology and Infection. 2015;143: 2137–2160. doi:10.1017/S0950268814002398
45. Tularemia — United States, 2001–2010. [cited 27 Jan 2022]. Available: https://www.cdc.gov/mmwr/preview/mmwrhtml/mm6247a5.htm?s_cid=mm6247a5_w
46. Tularemia --- United States, 1990--2000. [cited 27 Jan 2022]. Available: https://www.cdc.gov/mmwr/preview/mmwrhtml/mm5109a1.htm
47. Evans ME, Gregory DW, Schaffner W, McGee ZA. Tularemia: a 30-year experience with 88 cases. Medicine (Baltimore). 1985;64: 251–269.
48. Maurin M, Gyuranecz M. Tularaemia: clinical aspects in Europe. The Lancet Infectious Diseases. 2016;16: 113–124. doi:10.1016/S1473-3099(15)00355-2
49. Maurin M. Francisella tularensis, Tularemia and Serological Diagnosis. Front Cell Infect Microbiol. 2020;10: 512090. doi:10.3389/fcimb.2020.512090
50. Behan KA, Klein GC. Reduction of Brucella species and Francisella tularensis cross-reacting agglutinins by dithiothreitol. J Clin Microbiol. 1982;16: 756–757.
51. Pullen RL. TULAREMIA: ANALYSIS OF 225 CASES. JAMA. 1945;129: 495. doi:10.1001/jama.1945.02860410011003

52. Tularaemia - Annual Epidemiological Report for 2019. In: European Centre for Disease Prevention and Control [Internet]. 10 Feb 2021 [cited 31 Jan 2022]. Available: https://www.ecdc.europa.eu/en/publications-data/tularaemia-annual-epidemiological-report-2019
53. Peta V, Tantely LM, Potts R, Girod R, Pietri JE. A Francisella tularensis-Like Bacterium in Tropical Bed Bugs from Madagascar. Vector Borne Zoonotic Dis. 2022;22: 58–61. doi:10.1089/vbz.2021.0079
54. Colquhoun DJ, Duodu S. Francisella infections in farmed and wild aquatic organisms. Vet Res. 2011;42: 47. doi:10.1186/1297-9716-42-47
55. Aravena-Román M, Merritt A, Inglis TJJ. First case of Francisella bacteraemia in Western Australia. New Microbes New Infect. 2015;8: 75–77. doi:10.1016/j.nmni.2015.10.004
56. Chua HS, Soh YH, Loong SK, AbuBakar S. Francisella philomiragia bacteremia in an immunocompromised patient: a rare case report. Ann Clin Microbiol Antimicrob. 2021;20: 72. doi:10.1186/s12941-021-00475-2
57. Timofeev V, Titareva G, Bahtejeva I, Kombarova T, Kravchenko T, Mokrievich A, et al. The Comparative Virulence of Francisella tularensis Subsp. mediasiatica for Vaccinated Laboratory Animals. Microorganisms. 2020;8: 1403. doi:10.3390/microorganisms8091403
58. Huber B, Escudero R, Busse H-J, Seibold E, Scholz HC, Anda P, et al. Description of Francisella hispaniensis sp. nov., isolated from human blood, reclassification of Francisella novicida (Larson et al. 1955) Olsufiev et al. 1959 as Francisella tularensis subsp. novicida comb. nov. and emended description of the genus Francisella. International Journal of Systematic and Evolutionary Microbiology. 60: 1887–1896. doi:10.1099/ijs.0.015941-0
59. Johansson A, Celli J, Conlan W, Elkins KL, Forsman M, Keim PS, et al. Objections to the transfer of Francisella novicida to the subspecies rank of Francisella tularensis. Int J Syst Evol Microbiol. 2010;60: 1717–1718. doi:10.1099/ijs.0.022830-0
60. Busse H-J, Huber B, Anda P, Escudero R, Scholz HC, Seibold E, et al. Objections to the transfer of Francisella novicida to the subspecies rank of Francisella tularensis – response to Johansson et al. International Journal of Systematic and Evolutionary Microbiology. 60: 1718–1720. doi:10.1099/00207713-60-8-1718
61. Hollis DG, Weaver RE, Steigerwalt AG, Wenger JD, Moss CW, Brenner DJ. Francisella philomiragia comb. nov. (formerly Yersinia philomiragia) and Francisella tularensis biogroup novicida (formerly Francisella novicida) associated with human disease. J Clin Microbiol. 1989;27: 1601–1608. doi:10.1128/jcm.27.7.1601-1608.1989
62. Larsson P, Elfsmark D, Svensson K, Wikström P, Forsman M, Brettin T, et al. Molecular Evolutionary Consequences of Niche Restriction in Francisella tularensis, a Facultative Intracellular Pathogen. PLoS Pathog. 2009;5: e1000472. doi:10.1371/journal.ppat.1000472
63. Kingry LC, Petersen JM. Comparative review of Francisella tularensis and Francisella novicida. Front Cell Infect Microbiol. 2014;4: 35. doi:10.3389/fcimb.2014.00035
64. Jan H-E, Tsai C-S, Lee N-Y, Tsai P-F, Wang L-R, Chen P-L, et al. The first case of Francisella novicida infection in Taiwan: bacteraemic pneumonia in a haemodialysis adult. Emerg Microbes Infect. 11: 310–313. doi:10.1080/22221751.2022.2026199
65. Brett ME, Respicio-Kingry LB, Yendell S, Ratard R, Hand J, Balsamo G, et al. Outbreak of Francisella novicida Bacteremia Among Inmates at a Louisiana Correctional Facility. Clinical Infectious Diseases. 2014;59: 826–833. doi:10.1093/cid/ciu430
66. Leelaporn A, Yongyod S, Limsrivanichakorn S, Yungyuen T, Kiratisin P. Emergence of Francisella novicida Bacteremia, Thailand. Emerg Infect Dis. 2008;14: 1935–1937. doi:10.3201/eid1412.080435
67. Brett M, Doppalapudi A, Respicio-Kingry LB, Myers D, Husband B, Pollard K, et al. Francisella novicida Bacteremia after a Near-Drowning Accident. J Clin Microbiol. 2012;50: 2826–2829. doi:10.1128/JCM.00995-12
68. Telford SR, Goethert HK. Ecology of Francisella tularensis. Annu Rev Entomol. 2020;65: 351–372. doi:10.1146/annurev-ento-011019-025134

69. Luque-Larena JJ, Mougeot F, Arroyo B, Vidal MD, Rodríguez-Pastor R, Escudero R, et al. Irruptive mammal host populations shape tularemia epidemiology. PLoS Pathog. 2017;13. doi:10.1371/journal.ppat.1006622
70. Padeshki PI, Ivanov IN, Popov B, Kantardjiev TV. The role of birds in dissemination of Francisella tularensis: first direct molecular evidence for bird-to-human transmission. Epidemiol Infect. 2010;138: 376–379. doi:10.1017/S0950268809990513
71. Zhang F, Wang X, Yu G, Gao J, Niu H, Zhao J. Detection and Genotyping of Francisella tularensis in Animal Hosts and Vectors from Six Different Natural Landscape Areas, Gansu Province, China. Comput Math Methods Med. 2021;2021: 6820864. doi:10.1155/2021/6820864
72. Anda P, Segura del Pozo J, Díaz García JM, Escudero R, García Peña FJ, López Velasco MC, et al. Waterborne outbreak of tularemia associated with crayfish fishing. Emerg Infect Dis. 2001;7: 575–582.
73. Ahangari Cohan H, Jamshidian M, Rohani M, Moravedji M, Mostafavi E. Francisella tularensis survey among ranchers and livestock in western Iran. Comparative Immunology, Microbiology and Infectious Diseases. 2021;74: 101598. doi:10.1016/j.cimid.2020.101598
74. Kwit NA, Middaugh NA, VinHatton ES, Melman SD, Onischuk L, Aragon AS, et al. Francisella tularensis infection in dogs: 88 cases (2014–2016). Journal of the American Veterinary Medical Association. 2020;256: 220–225. doi:10.2460/javma.256.2.220
75. Kittl S, Francey T, Brodard I, Origgi FC, Borel S, Ryser-Degiorgis M-P, et al. First European report of Francisella tularensis subsp. holarctica isolation from a domestic cat. Vet Res. 2020;51: 109. doi:10.1186/s13567-020-00834-5
76. Abdellahoum Z, Maurin M, Bitam I. Tularemia as a Mosquito-Borne Disease. Microorganisms. 2020;9: 26. doi:10.3390/microorganisms9010026
77. Klock LE, Olsen PF, Fukushima T. Tularemia Epidemic Associated With the Deerfly. JAMA. 1973;226: 149–152. doi:10.1001/jama.1973.03230020019005
78. Hennebique A, Boisset S, Maurin M. Tularemia as a waterborne disease: a review. Emerg Microbes Infect. 2019;8: 1027–1042. doi:10.1080/22221751.2019.1638734
79. Hennebique A, Peyroux J, Brunet C, Martin A, Henry T, Knezevic M, et al. Amoebae can promote the survival of Francisella species in the aquatic environment. Emerg Microbes Infect. 2021;10: 277–290. doi:10.1080/22221751.2021.1885999
80. Hesselbrock W, Foshay L. The Morphology of Bacterium tularense. J Bacteriol. 1945;49: 209–231.
81. Eigelsbach HT, Braun W, Herring RD. STUDIES ON THE VARIATION OF BACTERIUM TULARENSE. J Bacteriol. 1951;61: 557–569. doi:10.1128/jb.61.5.557-569.1951
82. Larsson P, Oyston PCF, Chain P, Chu MC, Duffield M, Fuxelius H-H, et al. The complete genome sequence of Francisella tularensis, the causative agent of tularemia. Nat Genet. 2005;37: 153–159. doi:10.1038/ng1499
83. Croddy E, Krčálová S. Tularemia, Biological Warfare, and the Battle for Stalingrad (1942–1943). Military Medicine. 2001;166: 837–838. doi:10.1093/milmed/166.10.837
84. Eigelsbach HT, Downs CM. Prophylactic Effectiveness of Live and Killed Tularemia Vaccines: I. Production of Vaccine and Evaluation in the White Mouse and Guinea Pig. The Journal of Immunology. 1961;87: 415–425.
85. Larson CL, Wicht W, Jellison WL. A new organism resembling P. tularensis isolated from water. Public Health Rep. 1955;70: 253–258.
86. Hall JD, Woolard MD, Gunn BM, Craven RR, Taft-Benz S, Frelinger JA, et al. Infected-Host-Cell Repertoire and Cellular Response in the Lung following Inhalation of Francisella tularensis Schu S4, LVS, or U112. Infect Immun. 2008;76: 5843–5852. doi:10.1128/IAI.01176-08
87. Nano FE, Zhang N, Cowley SC, Klose KE, Cheung KKM, Roberts MJ, et al. A Francisella tularensis Pathogenicity Island Required for Intramacrophage Growth. J Bacteriol. 2004;186: 6430–6436. doi:10.1128/JB.186.19.6430-6436.2004
88. Ojeda SS, Wang ZJ, Mares CA, Chang TA, Li Q, Morris EG, et al. Rapid dissemination of Francisella tularensis and the effect of route of infection. BMC Microbiol. 2008;8: 215. doi:10.1186/1471-2180-8-215

89. Bosio CM, Bielefeldt-Ohmann H, Belisle JT. Active Suppression of the Pulmonary Immune Response by *Francisella tularensis* Schu4. J Immunol. 2007;178: 4538–4547. doi:10.4049/jimmunol.178.7.4538
90. Hall CA, Flick-Smith HC, Harding SV, Atkins HS, Titball RW. A Bioluminescent Francisella tularensis SCHU S4 Strain Enables Noninvasive Tracking of Bacterial Dissemination and the Evaluation of Antibiotics in an Inhalational Mouse Model of Tularemia. Antimicrob Agents Chemother. 2016;60: 7206–7215. doi:10.1128/AAC.01586-16
91. Fortier AH, Slayter MV, Ziemba R, Meltzer MS, Nacy CA. Live vaccine strain of Francisella tularensis: infection and immunity in mice. Infect Immun. 1991;59: 2922–2928.
92. Schricker RL, Eigelsbach HT, Mitten JQ, Hall WC. Pathogenesis of Tularemia in Monkeys Aerogenically Exposed to Francisella tularensis 425. Infect Immun. 1972;5: 734–744.
93. Glynn AR, Alves DA, Frick O, Erwin-Cohen R, Porter A, Norris S, et al. Comparison of Experimental Respiratory Tularemia in Three Nonhuman Primate Species. Comp Immunol Microbiol Infect Dis. 2015;39: 13–24. doi:10.1016/j.cimid.2015.01.003
94. White JD, Rooney JR, Prickett PA, Derrenbacher EB, Beard CW, Griffith WR. Pathogenesis of Experimental Respiratory Tularemia in Monkeys. Journal of Infectious Diseases. 1964;114: 277–283. doi:10.1093/infdis/114.3.277
95. Long GW, Oprandy JJ, Narayanan RB, Fortier AH, Porter KR, Nacy CA. Detection of Francisella tularensis in blood by polymerase chain reaction. J Clin Microbiol. 1993;31: 152–154.
96. Roberts LM, Tuladhar S, Steele SP, Riebe KJ, Chen C-J, Cumming RI, et al. Identification of early interactions between Francisella and the host. Infect Immun. 2014;82: 2504–2510. doi:10.1128/IAI.01654-13
97. Faron M, Fletcher JR, Rasmussen JA, Apicella MA, Jones BD. Interactions of Francisella tularensis with Alveolar Type II Epithelial Cells and the Murine Respiratory Epithelium. PLoS One. 2015;10: e0127458. doi:10.1371/journal.pone.0127458
98. Craven RR, Hall JD, Fuller JR, Taft-Benz S, Kawula TH. Francisella tularensis Invasion of Lung Epithelial Cells. Infect Immun. 2008;76: 2833–2842. doi:10.1128/IAI.00043-08
99. Law HT, Lin AE-J, Kim Y, Quach B, Nano FE, Guttman JA. Francisella tularensis Uses Cholesterol and Clathrin-Based Endocytic Mechanisms to Invade Hepatocytes. Sci Rep. 2011;1: 192. doi:10.1038/srep00192
100. Horzempa J, O'Dee DM, Stolz DB, Franks JM, Clay D, Nau GJ. Invasion of erythrocytes by Francisella tularensis. J Infect Dis. 2011;204: 51–59. doi:10.1093/infdis/jir221
101. Schmitt DM, Barnes R, Rogerson T, Haught A, Mazzella LK, Ford M, et al. The Role and Mechanism of Erythrocyte Invasion by Francisella tularensis. Front Cell Infect Microbiol. 2017;7: 173. doi:10.3389/fcimb.2017.00173
102. Plzakova L, Krocova Z, Kubelkova K, Macela A. Entry of Francisella tularensis into Murine B Cells: The Role of B Cell Receptors and Complement Receptors. PLoS One. 2015;10: e0132571. doi:10.1371/journal.pone.0132571
103. Marecic V, Shevchuk O, Ozanic M, Mihelcic M, Steinert M, Jurak Begonja A, et al. Isolation of F. novicida-Containing Phagosome from Infected Human Monocyte Derived Macrophages. Front Cell Infect Microbiol. 2017;7: 303. doi:10.3389/fcimb.2017.00303
104. Clemens DL, Lee B-Y, Horwitz MA. Francisella tularensis Enters Macrophages via a Novel Process Involving Pseudopod Loops. Infect Immun. 2005;73: 5892–5902. doi:10.1128/IAI.73.9.5892-5902.2005
105. Chong A, Celli J. The Francisella Intracellular Life Cycle: Toward Molecular Mechanisms of Intracellular Survival and Proliferation. Front Microbiol. 2010;1: 138. doi:10.3389/fmicb.2010.00138
106. Balagopal A, MacFarlane AS, Mohapatra N, Soni S, Gunn JS, Schlesinger LS. Characterization of the Receptor-Ligand Pathways Important for Entry and Survival of Francisella tularensis in Human Macrophages. Infect Immun. 2006;74: 5114–5125. doi:10.1128/IAI.00795-06
107. Geier H, Celli J. Phagocytic Receptors Dictate Phagosomal Escape and Intracellular Proliferation of Francisella tularensis ▿. Infect Immun. 2011;79: 2204–2214. doi:10.1128/IAI.01382-10

108. Mechaly A, Elia U, Alcalay R, Cohen H, Epstein E, Cohen O, et al. Inhibition of Francisella tularensis phagocytosis using a novel anti-LPS scFv antibody fragment. Sci Rep. 2019;9: 11418. doi:10.1038/s41598-019-47931-w
109. Brock SR, Parmely MJ. Francisella tularensis Confronts the Complement System. Front Cell Infect Microbiol. 2017;7: 523. doi:10.3389/fcimb.2017.00523
110. Hoang KV, Rajaram MVS, Curry HM, Gavrilin MA, Wewers MD, Schlesinger LS. Complement Receptor 3-Mediated Inhibition of Inflammasome Priming by Ras GTPase-Activating Protein During Francisella tularensis Phagocytosis by Human Mononuclear Phagocytes. Front Immunol. 2018;9: 561. doi:10.3389/fimmu.2018.00561
111. Clemens DL, Lee B-Y, Horwitz MA. The Francisella Type VI Secretion System. Front Cell Infect Microbiol. 2018;8: 121. doi:10.3389/fcimb.2018.00121
112. Clemens DL, Lee B-Y, Horwitz MA. Francisella tularensis Phagosomal Escape Does Not Require Acidification of the Phagosome. Infect Immun. 2009;77: 1757–1773. doi:10.1128/IAI.01485-08
113. Santic M, Asare R, Skrobonja I, Jones S, Abu Kwaik Y. Acquisition of the vacuolar ATPase proton pump and phagosome acidification are essential for escape of Francisella tularensis into the macrophage cytosol. Infect Immun. 2008;76: 2671–2677. doi:10.1128/IAI.00185-08
114. Chong A, Wehrly TD, Nair V, Fischer ER, Barker JR, Klose KE, et al. The early phagosomal stage of Francisella tularensis determines optimal phagosomal escape and Francisella pathogenicity island protein expression. Infect Immun. 2008;76: 5488–5499. doi:10.1128/IAI.00682-08
115. Matz LM, Petrosino JF. A study of innate immune kinetics reveals a role for a chloride transporter in a virulent Francisella tularensis type B strain. Microbiologyopen. 2021;10: e1170. doi:10.1002/mbo3.1170
116. Alam A, Golovliov I, Javed E, Sjöstedt A. ClpB mutants of Francisella tularensis subspecies holarctica and tularensis are defective for type VI secretion and intracellular replication. Sci Rep. 2018;8: 11324. doi:10.1038/s41598-018-29745-4
117. Clemens DL, Lee B-Y, Horwitz MA. Virulent and avirulent strains of Francisella tularensis prevent acidification and maturation of their phagosomes and escape into the cytoplasm in human macrophages. Infect Immun. 2004;72: 3204–3217. doi:10.1128/IAI.72.6.3204-3217.2004
118. Brodmann M, Dreier RF, Broz P, Basler M. Francisella requires dynamic type VI secretion system and ClpB to deliver effectors for phagosomal escape. Nat Commun. 2017;8: 15853. doi:10.1038/ncomms15853
119. Rigard M, Bröms JE, Mosnier A, Hologne M, Martin A, Lindgren L, et al. Francisella tularensis IglG Belongs to a Novel Family of PAAR-Like T6SS Proteins and Harbors a Unique N-terminal Extension Required for Virulence. Blanke SR, editor. PLoS Pathog. 2016;12: e1005821. doi:10.1371/journal.ppat.1005821
120. Santic M, Molmeret M, Klose KE, Abu Kwaik Y. Francisella tularensis travels a novel, twisted road within macrophages. Trends Microbiol. 2006;14: 37–44. doi:10.1016/j.tim.2005.11.008
121. Bradford MK, Elkins KL. Immune lymphocytes halt replication of Francisella tularensis LVS within the cytoplasm of infected macrophages. Sci Rep. 2020;10: 12023. doi:10.1038/s41598-020-68798-2
122. Brissac T, Ziveri J, Ramond E, Tros F, Kock S, Dupuis M, et al. Gluconeogenesis, an essential metabolic pathway for pathogenic Francisella. Molecular Microbiology. 2015;98: 518–534. doi:10.1111/mmi.13139
123. Meyer L, Bröms JE, Liu X, Rottenberg ME, Sjöstedt A. Microinjection of Francisella tularensis and Listeria monocytogenes Reveals the Importance of Bacterial and Host Factors for Successful Replication. Infect Immun. 2015;83: 3233–3242. doi:10.1128/IAI.00416-15
124. Chong A, Wehrly TD, Child R, Hansen B, Hwang S, Virgin HW, et al. Cytosolic clearance of replication-deficient mutants reveals Francisella tularensis interactions with the autophagic pathway. Autophagy. 2012;8: 1342–1356. doi:10.4161/auto.20808
125. Nakamura T, Shimizu T, Uda A, Watanabe K, Watarai M. Soluble lytic transglycosylase SLT of Francisella novicida is involved in intracellular growth and immune suppression. PLoS One. 2019;14: e0226778. doi:10.1371/journal.pone.0226778

126. Case EDR, Chong A, Wehrly TD, Hansen B, Child R, Hwang S, et al. The Francisella O-antigen mediates survival in the macrophage cytosol via autophagy avoidance. Cell Microbiol. 2014;16: 862–877. doi:10.1111/cmi.12246
127. Steele S, Brunton J, Ziehr B, Taft-Benz S, Moorman N, Kawula T. Francisella tularensis harvests nutrients derived via ATG5-independent autophagy to support intracellular growth. PLoS Pathog. 2013;9: e1003562. doi:10.1371/journal.ppat.1003562
128. Kelava I, Mihelčić M, Ožanič M, Marečić V, Knežević M, Ćurlin M, et al. Atg5-Deficient Mice Infected with Francisella tularensis LVS Demonstrate Increased Survival and Less Severe Pathology in Internal Organs. Microorganisms. 2020;8: E1531. doi:10.3390/microorganisms8101531
129. Celli J, Zahrt TC. Mechanisms of Francisella tularensis Intracellular Pathogenesis. Cold Spring Harb Perspect Med. 2013;3: a010314. doi:10.1101/cshperspect.a010314
130. Balzano PM, Cunningham AL, Grassel C, Barry EM. Deletion of the Major Facilitator Superfamily Transporter fptB Alters Host Cell Interactions and Attenuates Virulence of Type A Francisella tularensis. Infect Immun. 2018;86: e00832-17. doi:10.1128/IAI.00832-17
131. Steele SP, Chamberlain Z, Park J, Kawula TH. Francisella tularensis enters a double membraned compartment following cell-cell transfer. eLife. 8: e45252. doi:10.7554/eLife.45252
132. Steele S, Radlinski L, Taft-Benz S, Brunton J, Kawula TH. Trogocytosis-associated cell to cell spread of intracellular bacterial pathogens. eLife. 5: e10625. doi:10.7554/eLife.10625
133. Ramond E, Gesbert G, Guerrera IC, Chhuon C, Dupuis M, Rigard M, et al. Importance of Host Cell Arginine Uptake in Francisella Phagosomal Escape and Ribosomal Protein Amounts. Mol Cell Proteomics. 2015;14: 870–881. doi:10.1074/mcp.M114.044552
134. Gesbert G, Ramond E, Tros F, Dairou J, Frapy E, Barel M, et al. Importance of Branched-Chain Amino Acid Utilization in Francisella Intracellular Adaptation. Infect Immun. 2015;83: 173–183. doi:10.1128/IAI.02579-14
135. Alkhuder K, Meibom KL, Dubail I, Dupuis M, Charbit A. Glutathione provides a source of cysteine essential for intracellular multiplication of Francisella tularensis. PLoS Pathog. 2009;5: e1000284. doi:10.1371/journal.ppat.1000284
136. Ramsey KM, Ledvina HE, Tresko TM, Wandzilak JM, Tower CA, Tallo T, et al. Tn-Seq reveals hidden complexity in the utilization of host-derived glutathione in Francisella tularensis. PLoS Pathog. 2020;16: e1008566. doi:10.1371/journal.ppat.1008566
137. Ramond E, Gesbert G, Rigard M, Dairou J, Dupuis M, Dubail I, et al. Glutamate Utilization Couples Oxidative Stress Defense and the Tricarboxylic Acid Cycle in Francisella Phagosomal Escape. PLoS Pathog. 2014;10: e1003893. doi:10.1371/journal.ppat.1003893
138. Ramakrishnan G. Iron and Virulence in Francisella tularensis. Front Cell Infect Microbiol. 2017;7: 107. doi:10.3389/fcimb.2017.00107
139. Barel M, Harduin-Lepers A, Portier L, Slomianny M-C, Charbit A. Host glycosylation pathways and the unfolded protein response contribute to the infection by Francisella. Cellular Microbiology. 2016;18: 1763–1781. doi:10.1111/cmi.12614
140. Barel M, Charbit A. Role of Glycosylation/Deglycolysation Processes in Francisella tularensis Pathogenesis. Front Cell Infect Microbiol. 2017;7: 71. doi:10.3389/fcimb.2017.00071
141. Wyatt EV, Diaz K, Griffin AJ, Rassmussen JA, Crane DD, Jones BD, et al. Metabolic reprogramming of host cells by virulent Francisella tularensis for optimal replication and modulation of inflammation. J Immunol. 2016;196: 4227–4236. doi:10.4049/jimmunol.1502456
142. Radlinski LC, Brunton J, Steele S, Taft-Benz S, Kawula TH. Defining the Metabolic Pathways and Host-Derived Carbon Substrates Required for Francisella tularensis Intracellular Growth. mBio. 2018;9: e01471-18. doi:10.1128/mBio.01471-18
143. Pávková I, Brychta M, Strašková A, Schmidt M, Macela A, Stulík J. Comparative proteome profiling of host-pathogen interactions: insights into the adaptation mechanisms of Francisella tularensis in the host cell environment. Appl Microbiol Biotechnol. 2013;97: 10103–10115. doi:10.1007/s00253-013-5321-z

144. Rytter H, Jamet A, Ziveri J, Ramond E, Coureuil M, Lagouge-Roussey P, et al. The pentose phosphate pathway constitutes a major metabolic hub in pathogenic Francisella. PLoS Pathog. 2021;17: e1009326. doi:10.1371/journal.ppat.1009326
145. Böck D, Medeiros JM, Tsao H-F, Penz T, Weiss GL, Aistleitner K, et al. In situ architecture, function, and evolution of a contractile injection system. Science. 2017;357: 713–717. doi:10.1126/science.aan7904
146. Ho BT, Dong TG, Mekalanos JJ. A view to a kill: the bacterial type 6 secretion system. Cell Host Microbe. 2014;15: 9–21. doi:10.1016/j.chom.2013.11.008
147. Ramsey KM, Dove SL. A response regulator promotes Francisella tularensis intramacrophage growth by repressing an anti-virulence factor. Mol Microbiol. 2016;101: 688–700. doi:10.1111/mmi.13418
148. Cuthbert BJ, Ross W, Rohlfing AE, Dove SL, Gourse RL, Brennan RG, et al. Dissection of the molecular circuitry controlling virulence in Francisella tularensis. Genes Dev. 2017;31: 1549–1560. doi:10.1101/gad.303701.117
149. Clemens DL, Ge P, Lee B-Y, Horwitz MA, Zhou ZH. Atomic Structure and Mutagenesis of T6SS Reveals Interlaced Array Essential to Function. Cell. 2015;160: 940–951. doi:10.1016/j.cell.2015.02.005
150. Yang X, Clemens DL, Lee B-Y, Cui Y, Zhou ZH, Horwitz MA. Atomic Structure of Francisella T6SS Central Spike Reveals Unique α-Helical Lid and a Putative Cargo. Structure. 2019;27: 1811-1819.e6. doi:10.1016/j.str.2019.10.007
151. de Bruin OM, Duplantis BN, Ludu JS, Hare RF, Nix EB, Schmerk CL, et al. The biochemical properties of the Francisella pathogenicity island (FPI)-encoded proteins IglA, IglB, IglC, PdpB and DotU suggest roles in type VI secretion. Microbiology (Reading). 2011;157: 3483–3491. doi:10.1099/mic.0.052308-0
152. Ludu JS, de Bruin OM, Duplantis BN, Schmerk CL, Chou AY, Elkins KL, et al. The Francisella Pathogenicity Island Protein PdpD Is Required for Full Virulence and Associates with Homologues of the Type VI Secretion System. J Bacteriol. 2008;190: 4584–4595. doi:10.1128/JB.00198-08
153. Long ME, Lindemann SR, Rasmussen JA, Jones BD, Allen L-AH. Disruption of Francisella tularensis Schu S4 iglI, iglJ, and pdpC Genes Results in Attenuation for Growth in Human Macrophages and In Vivo Virulence in Mice and Reveals a Unique Phenotype for pdpC. Infect Immun. 2013;81: 850–861. doi:10.1128/IAI.00822-12
154. Cantlay S, Haggerty K, Horzempa J. OpiA, a Type Six Secretion System Substrate, Localizes to the Cell Pole and Plays a Role in Bacterial Growth and Viability in Francisella tularensis LVS. J Bacteriol. 2020;202: e00048-20. doi:10.1128/JB.00048-20
155. Ledvina HE, Kelly KA, Eshraghi A, Plemel RL, Peterson SB, Lee B, et al. A Phosphatidylinositol 3-Kinase Effector Alters Phagosomal Maturation to Promote Intracellular Growth of Francisella. Cell Host & Microbe. 2018;24: 285-295.e8. doi:10.1016/j.chom.2018.07.003
156. Eshraghi A, Kim J, Walls AC, Ledvina HE, Miller CN, Ramsey KM, et al. Secreted Effectors Encoded within and outside of the Francisella Pathogenicity Island Promote Intramacrophage Growth. Cell Host & Microbe. 2016;20: 573–583. doi:10.1016/j.chom.2016.10.008
157. Bröms JE, Sjöstedt A, Lavander M. The Role of the Francisella Tularensis Pathogenicity Island in Type VI Secretion, Intracellular Survival, and Modulation of Host Cell Signaling. Front Microbiol. 2010;1: 136. doi:10.3389/fmicb.2010.00136
158. Brodmann M, Schnider ST, Basler M. Type VI Secretion System and Its Effectors PdpC, PdpD, and OpiA Contribute to Francisella Virulence in Galleria mellonella Larvae. Infect Immun. 89: e00579-20. doi:10.1128/IAI.00579-20
159. Proksova M, Rehulkova H, Rehulka P, Lays C, Lenco J, Stulik J. Using proteomics to identify host cell interaction partners for VgrG and IglJ. Sci Rep. 2020;10: 14612. doi:10.1038/s41598-020-71641-3
160. Law HT, Sriram A, Fevang C, Nix EB, Nano FE, Guttman JA. IglC and PdpA Are Important for Promoting Francisella Invasion and Intracellular Growth in Epithelial Cells. PLoS One. 2014;9: e104881. doi:10.1371/journal.pone.0104881

161. Kopping EJ, Doyle CR, Sampath V, Thanassi DG. Contributions of TolC Orthologs to Francisella tularensis Schu S4 Multidrug Resistance, Modulation of Host Cell Responses, and Virulence. Infect Immun. 2019;87: e00823-18. doi:10.1128/IAI.00823-18
162. Doyle CR, Pan J-A, Mena P, Zong W-X, Thanassi DG. TolC-Dependent Modulation of Host Cell Death by the Francisella tularensis Live Vaccine Strain. Infect Immun. 2014;82: 2068–2078. doi:10.1128/IAI.00044-14
163. Alqahtani M, Ma Z, Ketkar H, Suresh RV, Malik M, Bakshi CS. Characterization of a Unique Outer Membrane Protein Required for Oxidative Stress Resistance and Virulence of Francisella tularensis. J Bacteriol. 2018;200: e00693-17. doi:10.1128/JB.00693-17
164. Forslund A-L, Salomonsson EN, Golovliov I, Kuoppa K, Michell S, Titball R, et al. The type IV pilin, PilA, is required for full virulence of Francisella tularensis subspecies tularensis. BMC Microbiol. 2010;10: 227. doi:10.1186/1471-2180-10-227
165. Ozanic M, Marecic V, Knezevic M, Kelava I, Stojková P, Lindgren L, et al. The type IV pili component PilO is a virulence determinant of Francisella novicida. PLoS One. 2022;17: e0261938. doi:10.1371/journal.pone.0261938
166. Forslund A-L, Kuoppa K, Svensson K, Salomonsson E, Johansson A, Byström M, et al. Direct repeat-mediated deletion of a type IV pilin gene results in major virulence attenuation of Francisella tularensis. Mol Microbiol. 2006;59: 1818–1830. doi:10.1111/j.1365-2958.2006.05061.x
167. Gil H, Benach JL, Thanassi DG. Presence of pili on the surface of Francisella tularensis. Infect Immun. 2004;72: 3042–3047. doi:10.1128/IAI.72.5.3042-3047.2004
168. Chakraborty S, Monfett M, Maier TM, Benach JL, Frank DW, Thanassi DG. Type IV Pili in Francisella tularensis: Roles of pilF and pilT in Fiber Assembly, Host Cell Adherence, and Virulence. Infect Immun. 2008;76: 2852–2861. doi:10.1128/IAI.01726-07
169. Bencurova E, Kovac A, Pulzova L, Gyuranecz M, Mlynarcik P, Mucha R, et al. Deciphering the protein interaction in adhesion of Francisella tularensis subsp. holarctica to the endothelial cells. Microb Pathog. 2015;81: 6–15. doi:10.1016/j.micpath.2015.03.007
170. Hager AJ, Bolton DL, Pelletier MR, Brittnacher MJ, Gallagher LA, Kaul R, et al. Type IV pili-mediated secretion modulates Francisella virulence. Molecular Microbiology. 2006;62: 227–237. doi:10.1111/j.1365-2958.2006.05365.x
171. Zogaj X, Chakraborty S, Liu J, Thanassi DG, Klose KE. Characterization of the Francisella tularensis subsp. novicida type IV pilus. Microbiology (Reading). 2008;154: 2139–2150. doi:10.1099/mic.0.2008/018077-0
172. McCaig WD, Koller A, Thanassi DG. Production of Outer Membrane Vesicles and Outer Membrane Tubes by Francisella novicida. J Bacteriol. 2013;195: 1120–1132. doi:10.1128/JB.02007-12
173. Sampath V, McCaig WD, Thanassi DG. Amino acid deprivation and central carbon metabolism regulate the production of outer membrane vesicles and tubes by Francisella. Molecular Microbiology. 2018;107: 523–541. doi:10.1111/mmi.13897
174. Zarrella TM, Singh A, Bitsaktsis C, Rahman T, Sahay B, Feustel PJ, et al. Host-Adaptation of Francisella tularensis Alters the Bacterium's Surface-Carbohydrates to Hinder Effectors of Innate and Adaptive Immunity. PLoS One. 2011;6: e22335. doi:10.1371/journal.pone.0022335
175. Hazlett KRO, Caldon SD, McArthur DG, Cirillo KA, Kirimanjeswara GS, Magguilli ML, et al. Adaptation of Francisella tularensis to the Mammalian Environment Is Governed by Cues Which Can Be Mimicked In Vitro. Infect Immun. 2008;76: 4479–4488. doi:10.1128/IAI.00610-08
176. Klimentova J, Pavkova I, Horcickova L, Bavlovic J, Kofronova O, Benada O, et al. Francisella tularensis subsp. holarctica Releases Differentially Loaded Outer Membrane Vesicles Under Various Stress Conditions. Front Microbiol. 2019;10: 2304. doi:10.3389/fmicb.2019.02304
177. Pavkova I, Klimentova J, Bavlovic J, Horcickova L, Kubelkova K, Vlcak E, et al. Francisella tularensis Outer Membrane Vesicles Participate in the Early Phase of Interaction With Macrophages. Front Microbiol. 2021;12: 748706. doi:10.3389/fmicb.2021.748706

178. Chen F, Cui G, Wang S, Nair MKM, He L, Qi X, et al. Outer membrane vesicle-associated lipase FtlA enhances cellular invasion and virulence in Francisella tularensis LVS. Emerg Microbes Infect. 2017;6: e66. doi:10.1038/emi.2017.53
179. Rowe HM, Huntley JF. From the Outside-In: The Francisella tularensis Envelope and Virulence. Front Cell Infect Microbiol. 2015;5: 94. doi:10.3389/fcimb.2015.00094
180. Wehrly TD, Chong A, Virtaneva K, Sturdevant DE, Child R, Edwards JA, et al. Intracellular biology and virulence determinants of Francisella tularensis revealed by transcriptional profiling inside macrophages. Cell Microbiol. 2009;11: 1128–1150. doi:10.1111/j.1462-5822.2009.01316.x
181. Huntley JF, Conley PG, Hagman KE, Norgard MV. Characterization of Francisella tularensis outer membrane proteins. J Bacteriol. 2007;189: 561–574. doi:10.1128/JB.01505-06
182. Ma Z, Banik S, Rane H, Mora VT, Rabadi SM, Doyle CR, et al. EmrA1 membrane fusion protein of Francisella tularensis LVS is required for resistance to oxidative stress, intramacrophage survival and virulence in mice. Mol Microbiol. 2014;91: 976–995. doi:10.1111/mmi.12509
183. Hoang KV, Chen CG, Koopman J, Moshiri J, Adcox HE, Gunn JS. Identification of Genes Required for Secretion of the Francisella Oxidative Burst-Inhibiting Acid Phosphatase AcpA. Front Microbiol. 2016;7: 605. doi:10.3389/fmicb.2016.00605
184. Melillo AA, Mahawar M, Sellati TJ, Malik M, Metzger DW, Melendez JA, et al. Identification of Francisella tularensis live vaccine strain CuZn superoxide dismutase as critical for resistance to extracellularly generated reactive oxygen species. J Bacteriol. 2009;191: 6447–6456. doi:10.1128/JB.00534-09
185. Su J, Yang J, Zhao D, Kawula TH, Banas JA, Zhang J-R. Genome-Wide Identification of Francisella tularensis Virulence Determinants. Infection and Immunity. 2007;75: 3089–3101. doi:10.1128/IAI.01865-06
186. Forestal CA, Gil H, Monfett M, Noah CE, Platz GJ, Thanassi DG, et al. A conserved and immunodominant lipoprotein of Francisella tularensis is proinflammatory but not essential for virulence. Microb Pathog. 2008;44: 512–523. doi:10.1016/j.micpath.2008.01.003
187. Kinkead LC, Whitmore LC, McCracken JM, Fletcher JR, Ketelsen BB, Kaufman JW, et al. Bacterial lipoproteins and other factors released by Francisella tularensis modulate human neutrophil lifespan: Effects of a TLR1 SNP on apoptosis inhibition. Cell Microbiol. 2018;20. doi:10.1111/cmi.12795
188. Clinton SR, Bina JE, Hatch TP, Whitt MA, Miller MA. Binding and activation of host plasminogen on the surface of Francisella tularensis. BMC Microbiol. 2010;10: 76. doi:10.1186/1471-2180-10-76
189. Chong A, Child R, Wehrly TD, Rockx-Brouwer D, Qin A, Mann BJ, et al. Structure-Function Analysis of DipA, a Francisella tularensis Virulence Factor Required for Intracellular Replication. PLoS One. 2013;8: e67965. doi:10.1371/journal.pone.0067965
190. Ren G, Champion MM, Huntley JF. Identification of disulfide bond isomerase substrates reveals bacterial virulence factors. Mol Microbiol. 2014;94: 926–944. doi:10.1111/mmi.12808
191. Mahawar M, Atianand MK, Dotson RJ, Mora V, Rabadi SM, Metzger DW, et al. Identification of a Novel Francisella tularensis Factor Required for Intramacrophage Survival and Subversion of Innate Immune Response. J Biol Chem. 2012;287: 25216–25229. doi:10.1074/jbc.M112.367672
192. Robertson GT, Case EDR, Dobbs N, Ingle C, Balaban M, Celli J, et al. FTT0831c/FTL_0325 contributes to Francisella tularensis cell division, maintenance of cell shape, and structural integrity. Infect Immun. 2014;82: 2935–2948. doi:10.1128/IAI.00102-14
193. Foshay L. A comparative study of the treatment of tularemia with immune serum, hyperimmune serum and streptomycin. The American Journal of Medicine. 1946;1: 180–188. doi:10.1016/0002-9343(46)90036-8
194. Kirimanjeswara GS, Olmos S, Bakshi CS, Metzger DW. Humoral and Cell-Mediated Immunity to the Intracellular Pathogen Francisella tularensis. Immunol Rev. 2008;225: 244–255. doi:10.1111/j.1600-065X.2008.00689.x
195. Ericsson M, Sandstrom G, Sjostedt A, Tarnvik A. Persistence of Cell-Mediated Immunity and Decline of Humoral Immunity to the Intracellular Bacterium Francisella tularensis 25 Years after

Natural Infection. Journal of Infectious Diseases. 1994;170: 110–114. doi:10.1093/infdis/170.1.110
196. Burke DS. Immunization against Tularemia: Analysis of the Effectiveness of Live Francisella tularensis Vaccine in Prevention of Laboratory-Acquired Tularemia. Journal of Infectious Diseases. 1977;135: 55–60. doi:10.1093/infdis/135.1.55
197. Elkins KL, Kurtz SL, De Pascalis R. Progress, challenges, and opportunities in Francisella vaccine development. Expert Review of Vaccines. 2016;15: 1183–1196. doi:10.1586/14760584.2016.1170601
198. Green TW. IMMUNITY IN TULAREMIA: Report of Two Cases of Proved Reinfection. Arch Intern Med (Chic). 1950;85: 777. doi:10.1001/archinte.1950.00230110052004
199. Nicol MJ, Williamson DR, Place DE, Kirimanjeswara GS. Differential Immune Response Following Intranasal and Intradermal Infection with Francisella tularensis: Implications for Vaccine Development. Microorganisms. 2021;9: 973. doi:10.3390/microorganisms9050973
200. Roberts LM, Wehrly TD, Leighton I, Hanley P, Lovaglio J, Smith BJ, et al. Circulating T Cells Are Not Sufficient for Protective Immunity against Virulent Francisella tularensis. J Immunol. 2022;208: 1180–1188. doi:10.4049/jimmunol.2100915
201. Roberts LM, Powell DA, Frelinger JA. Adaptive Immunity to Francisella tularensis and Considerations for Vaccine Development. Front Cell Infect Microbiol. 2018;8: 115. doi:10.3389/fcimb.2018.00115
202. Bahuaud O, Le Brun C, Lemaignen A. Host Immunity and Francisella tularensis: A Review of Tularemia in Immunocompromised Patients. Microorganisms. 2021;9: 2539. doi:10.3390/microorganisms9122539
203. Sunagar R, Kumar S, Franz BJ, Gosselin EJ. Tularemia vaccine development: paralysis or progress? Vaccine (Auckl). 2016;6: 9–23. doi:10.2147/VDT.S85545
204. Wayne Conlan J, Oyston PCF. Vaccines Against Francisella Tularensis. Annals of the New York Academy of Sciences. 2007;1105: 325–350. doi:10.1196/annals.1409.012
205. Kadrmas JL, Raetz CRH. Enzymatic Synthesis of Lipopolysaccharide in Escherichia coli: PURIFICATION AND PROPERTIES OF HEPTOSYLTRANSFERASE I *. Journal of Biological Chemistry. 1998;273: 2799–2807. doi:10.1074/jbc.273.5.2799
206. Muthuirulandi Sethuvel D p., Devanga Ragupathi N k., Anandan S, Veeraraghavan B. Update on: Shigella new serogroups/serotypes and their antimicrobial resistance. Letters in Applied Microbiology. 2017;64: 8–18. doi:10.1111/lam.12690
207. Vinogradov E, Perry MB, Conlan JW. Structural analysis of Francisella tularensis lipopolysaccharide. Eur J Biochem. 2002;269: 6112–6118. doi:10.1046/j.1432-1033.2002.03321.x
208. Yun J, Wang X, Zhang L, Li Y. Effects of lipid A acyltransferases on the pathogenesis of F. novicida. Microbial Pathogenesis. 2017;109: 313–318. doi:10.1016/j.micpath.2017.04.040
209. Li Y, Powell DA, Shaffer SA, Rasko DA, Pelletier MR, Leszyk JD, et al. LPS remodeling is an evolved survival strategy for bacteria. Proc Natl Acad Sci U S A. 2012;109: 8716–8721. doi:10.1073/pnas.1202908109
210. Wang X, Ribeiro AA, Guan Z, McGrath SC, Cotter RJ, Raetz CRH. Structure and biosynthesis of free lipid A molecules that replace lipopolysaccharide in Francisella tularensis subsp. novicida. Biochemistry. 2006;45: 14427–14440. doi:10.1021/bi061767s
211. Barker JH, Kaufman JW, Apicella MA, Weiss JP. Evidence Suggesting That Francisella tularensis O-Antigen Capsule Contains a Lipid A-Like Molecule That Is Structurally Distinct from the More Abundant Free Lipid A. PLoS One. 2016;11: e0157842. doi:10.1371/journal.pone.0157842
212. Okan N, Kasper D. The atypical lipopolysaccharide of Francisella. Carbohydrate research. 2013. doi:10.1016/j.carres.2013.06.015
213. Beasley AS, Cotter RJ, Vogel SN, Inzana TJ, Qureshi AA, Qureshi N. A variety of novel lipid A structures obtained from Francisella tularensis live vaccine strain. Innate Immun. 2012;18: 268–278. doi:10.1177/1753425911401054

214. Wang X, Karbarz MJ, McGrath SC, Cotter RJ, Raetz CRH. MsbA transporter-dependent lipid A 1-dephosphorylation on the periplasmic surface of the inner membrane: topography of francisella novicida LpxE expressed in Escherichia coli. J Biol Chem. 2004;279: 49470–49478. doi:10.1074/jbc.M409078200
215. Zhao J, An J, Hwang D, Wu Q, Wang S, Gillespie RA, et al. The Lipid A 1-Phosphatase, LpxE, Functionally Connects Multiple Layers of Bacterial Envelope Biogenesis. mBio. 2019;10: e00886-19. doi:10.1128/mBio.00886-19
216. Wang X, Ribeiro AA, Guan Z, Abraham SN, Raetz CRH. Attenuated virulence of a Francisella mutant lacking the lipid A 4'-phosphatase. Proc Natl Acad Sci U S A. 2007;104: 4136–4141. doi:10.1073/pnas.0611606104
217. Kanistanon D, Powell DA, Hajjar AM, Pelletier MR, Cohen IE, Way SS, et al. Role of Francisella Lipid A Phosphate Modification in Virulence and Long-Term Protective Immune Responses. Infect Immun. 2012;80: 943–951. doi:10.1128/IAI.06109-11
218. Robert CB, Thomson M, Vercellone A, Gardner F, Ernst RK, Larrouy-Maumus G, et al. Mass spectrometry analysis of intact Francisella bacteria identifies lipid A structure remodeling in response to acidic pH stress. Biochimie. 2017;141: 16–20. doi:10.1016/j.biochi.2017.08.008
219. Chin C-Y, Zhao J, Llewellyn AC, Golovliov I, Sjöstedt A, Zhou P, et al. Francisella FlmX broadly affects lipopolysaccharide modification and virulence. Cell Rep. 2021;35: 109247. doi:10.1016/j.celrep.2021.109247
220. Llewellyn AC, Zhao J, Song F, Parvathareddy J, Xu Q, Napier BA, et al. NaxD is a deacetylase required for lipid A modification and Francisella pathogenesis. Mol Microbiol. 2012;86: 10.1111/mmi.12004. doi:10.1111/mmi.12004
221. Wang X, Ribeiro AA, Guan Z, Raetz CRH. Identification of Undecaprenyl Phosphate-β-D-Galactosamine in Francisella novicida and Its Function in Lipid A Modification. Biochemistry. 2009;48: 1162–1172. doi:10.1021/bi802211k
222. Song F, Guan Z, Raetz CRH. Biosynthesis of undecaprenyl phosphate-galactosamine and undecaprenyl phosphate-glucose in Francisella novicida. Biochemistry. 2009;48: 1173–1182. doi:10.1021/bi802212t
223. Kanistanon D, Hajjar AM, Pelletier MR, Gallagher LA, Kalhorn T, Shaffer SA, et al. A Francisella mutant in lipid A carbohydrate modification elicits protective immunity. PLoS Pathog. 2008;4: e24. doi:10.1371/journal.ppat.0040024
224. Vinogradov E, Perry MB. Characterisation of the core part of the lipopolysaccharide O-antigen of Francisella novicida (U112). Carbohydrate Research. 2004;339: 1643–1648. doi:10.1016/j.carres.2004.04.013
225. Zhao J, Raetz CRH. A two-component Kdo hydrolase in the inner membrane of Francisella novicida. Mol Microbiol. 2010;78: 820–836. doi:10.1111/j.1365-2958.2010.07305.x
226. Okan NA, Chalabaev S, Kim T-H, Fink A, Ross RA, Kasper DL. Kdo Hydrolase Is Required for Francisella tularensis Virulence and Evasion of TLR2-Mediated Innate Immunity. mBio. 2013;4: e00638-12. doi:10.1128/mBio.00638-12
227. Wang Q, Shi X, Leymarie N, Madico G, Sharon J, Costello CE, et al. A typical preparation of Francisella tularensis O-antigen yields a mixture of three types of saccharides. Biochemistry. 2011;50: 10941–10950. doi:10.1021/bi201450v
228. Freudenberger Catanzaro KC, Champion AE, Mohapatra N, Cecere T, Inzana TJ. Glycosylation of a Capsule-Like Complex (CLC) by Francisella novicida Is Required for Virulence and Partial Protective Immunity in Mice. Frontiers in Microbiology. 2017;8. Available: https://www.frontiersin.org/article/10.3389/fmicb.2017.00935
229. Raetz CRH, Guan Z, Ingram BO, Six DA, Song F, Wang X, et al. Discovery of new biosynthetic pathways: the lipid A story. J Lipid Res. 2009;50 Suppl: S103-108. doi:10.1194/jlr.R800060-JLR200
230. Liu T, Zhang L, Joo D, Sun S-C. NF-κB signaling in inflammation. Sig Transduct Target Ther. 2017;2: 1–9. doi:10.1038/sigtrans.2017.23
231. Maeshima N, Fernandez RC. Recognition of lipid A variants by the TLR4-MD-2 receptor complex. Front Cell Infect Microbiol. 2013;3: 3. doi:10.3389/fcimb.2013.00003

232. Gutsmann T, Haberer N, Carroll SF, Seydel U, Wiese A. Interaction between lipopolysaccharide (LPS), LPS-binding protein (LBP), and planar membranes. Biol Chem. 2001;382: 425–434. doi:10.1515/BC.2001.052
233. Hajjar AM, Harvey MD, Shaffer SA, Goodlett DR, Sjöstedt A, Edebro H, et al. Lack of In Vitro and In Vivo Recognition of Francisella tularensis Subspecies Lipopolysaccharide by Toll-Like Receptors. Infection and Immunity. 2006;74: 6730–6738. doi:10.1128/IAI.00934-06
234. Lagrange B, Benaoudia S, Wallet P, Magnotti F, Provost A, Michal F, et al. Human caspase-4 detects tetra-acylated LPS and cytosolic Francisella and functions differently from murine caspase-11. Nat Commun. 2018;9: 242. doi:10.1038/s41467-017-02682-y
235. Guo Y, Mao R, Xie Q, Cheng X, Xu T, Wang X, et al. Francisella novicida Mutant XWK4 Triggers Robust Inflammasome Activation Favoring Infection. Front Cell Dev Biol. 2021;9: 743335. doi:10.3389/fcell.2021.743335
236. Wang B, Han Y, Li Y, Li Y, Wang X. Immuno-Stimulatory Activity of Escherichia coli Mutants Producing Kdo2-Monophosphoryl-Lipid A or Kdo2-Pentaacyl-Monophosphoryl-Lipid A. PLoS One. 2015;10: e0144714. doi:10.1371/journal.pone.0144714
237. Nakayasu ES, Tempel R, Cambronne XA, Petyuk VA, Jones MB, Gritsenko MA, et al. Comparative phosphoproteomics reveals components of host cell invasion and post-transcriptional regulation during Francisella infection. Mol Cell Proteomics. 2013;12: 3297–3309. doi:10.1074/mcp.M113.029850
238. Lai X-H, Shirley RL, Crosa L, Kanistanon D, Tempel R, Ernst RK, et al. Mutations of Francisella novicida that alter the mechanism of its phagocytosis by murine macrophages. PLoS One. 2010;5: e11857. doi:10.1371/journal.pone.0011857
239. Clay CD, Soni S, Gunn JS, Schlesinger LS. Evasion of Complement-Mediated Lysis and Complement C3 Deposition Are Regulated by Francisella tularensis Lipopolysaccharide O Antigen. J Immunol. 2008;181: 5568–5578.
240. Lindemann SR, Peng K, Long ME, Hunt JR, Apicella MA, Monack DM, et al. Francisella tularensis Schu S4 O-Antigen and Capsule Biosynthesis Gene Mutants Induce Early Cell Death in Human Macrophages. Infection and Immunity. 2011;79: 581–594. doi:10.1128/IAI.00863-10
241. Sorokin VM, Pavlovich NV, Prozorova LA. Francisella tularensis resistance to bactericidal action of normal human serum. FEMS Immunol Med Microbiol. 1996;13: 249–252. doi:10.1111/j.1574-695X.1996.tb00246.x
242. Brock SR, Parmely MJ. Complement C3 as a Prompt for Human Macrophage Death during Infection with Francisella tularensis Strain SCHU S4. Infect Immun. 2017;85: e00424-17. doi:10.1128/IAI.00424-17
243. Ben Nasr A, Klimpel GR. Subversion of complement activation at the bacterial surface promotes serum resistance and opsonophagocytosis of Francisella tularensis. J Leukoc Biol. 2008;84: 77–85. doi:10.1189/jlb.0807526
244. Dai S, Rajaram MVS, Curry HM, Leander R, Schlesinger LS. Fine Tuning Inflammation at the Front Door: Macrophage Complement Receptor 3-mediates Phagocytosis and Immune Suppression for Francisella tularensis. PLoS Pathog. 2013;9: e1003114. doi:10.1371/journal.ppat.1003114
245. Hoang KV, Rajaram MVS, Curry HM, Gavrilin MA, Wewers MD, Schlesinger LS. Complement Receptor 3-Mediated Inhibition of Inflammasome Priming by Ras GTPase-Activating Protein During Francisella tularensis Phagocytosis by Human Mononuclear Phagocytes. Front Immunol. 2018;9: 561. doi:10.3389/fimmu.2018.00561
246. Gunn JS, Ernst RK. The Structure and Function of Francisella Lipopolysaccharide. Ann N Y Acad Sci. 2007;1105: 202–218. doi:10.1196/annals.1409.006
247. Amemiya K, Dankmeyer JL, Bernhards RC, Fetterer DP, Waag DM, Worsham PL, et al. Activation of Toll-Like Receptors by Live Gram-Negative Bacterial Pathogens Reveals Mitigation of TLR4 Responses and Activation of TLR5 by Flagella. Front Cell Infect Microbiol. 2021;11: 745325. doi:10.3389/fcimb.2021.745325

248. Thakran S, Li H, Lavine CL, Miller MA, Bina JE, Bina XR, et al. Identification of Francisella tularensis Lipoproteins That Stimulate the Toll-like Receptor (TLR) 2/TLR1 Heterodimer*. Journal of Biological Chemistry. 2008;283: 3751–3760. doi:10.1074/jbc.M706854200
249. Crane DD, Ireland R, Alinger JB, Small P, Bosio CM. Lipids derived from virulent Francisella tularensis broadly inhibit pulmonary inflammation via toll-like receptor 2 and peroxisome proliferator-activated receptor α. Clin Vaccine Immunol. 2013;20: 1531–1540. doi:10.1128/CVI.00319-13
250. Sampson TR, Saroj SD, Llewellyn AC, Tzeng Y-L, Weiss DS. A CRISPR-CAS System Mediates Bacterial Innate Immune Evasion and Virulence. Nature. 2013;497: 254–257. doi:10.1038/nature12048
251. De Pascalis R, Rossi AP, Mittereder L, Takeda K, Akue A, Kurtz SL, et al. Production of IFN-γ by splenic dendritic cells during innate immune responses against Francisella tularensis LVS depends on MyD88, but not TLR2, TLR4, or TLR9. PLoS One. 2020;15: e0237034. doi:10.1371/journal.pone.0237034
252. Collazo CM, Sher A, Meierovics AI, Elkins KL. Myeloid differentiation factor-88 (MyD88) is essential for control of primary in vivo Francisella tularensis LVS infection, but not for control of intra-macrophage bacterial replication. Microbes Infect. 2006;8: 779–790. doi:10.1016/j.micinf.2005.09.014
253. Ghonime MG, Mitra S, Eldomany RA, Wewers MD, Gavrilin MA. Inflammasome priming is similar for francisella species that differentially induce inflammasome activation. PLoS One. 2015;10: e0127278. doi:10.1371/journal.pone.0127278
254. Katz J, Zhang P, Martin M, Vogel SN, Michalek SM. Toll-Like Receptor 2 Is Required for Inflammatory Responses to Francisella tularensis LVS. Infect Immun. 2006;74: 2809–2816. doi:10.1128/IAI.74.5.2809-2816.2006
255. Mazgaeen L, Gurung P. Recent Advances in Lipopolysaccharide Recognition Systems. International Journal of Molecular Sciences. 2020;21: 379. doi:10.3390/ijms21020379
256. O'Neill LAJ, Golenbock D, Bowie AG. The history of Toll-like receptors — redefining innate immunity. Nat Rev Immunol. 2013;13: 453–460. doi:10.1038/nri3446
257. Golovliov I, Sandström G, Ericsson M, Sjöstedt A, Tärnvik A. Cytokine expression in the liver during the early phase of murine tularemia. Infect Immun. 1995;63: 534–538.
258. Stenmark S, Sunnemark D, Bucht A, Sjöstedt A. Rapid Local Expression of Interleukin-12, Tumor Necrosis Factor Alpha, and Gamma Interferon after Cutaneous Francisella tularensis Infection in Tularemia-Immune Mice. Infect Immun. 1999;67: 1789–1797.
259. Leiby DA, Fortier AH, Crawford RM, Schreiber RD, Nacy CA. In vivo modulation of the murine immune response to Francisella tularensis LVS by administration of anticytokine antibodies. Infect Immun. 1992;60: 84–89.
260. Elkins KL, Rhinehart-Jones T, Nacy CA, Winegar RK, Fortier AH. T-cell-independent resistance to infection and generation of immunity to Francisella tularensis. Infect Immun. 1993;61: 823–829. doi:10.1128/iai.61.3.823-829.1993
261. Elkins KL, Rhinehart-Jones TR, Culkin SJ, Yee D, Winegar RK. Minimal requirements for murine resistance to infection with Francisella tularensis LVS. Infect Immun. 1996;64: 3288–3293.
262. Anthony LS, Ghadirian E, Nestel FP, Kongshavn PA. The requirement for gamma interferon in resistance of mice to experimental tularemia. Microb Pathog. 1989;7: 421–428. doi:10.1016/0882-4010(89)90022-3
263. Chaix J, Tessmer MS, Hoebe K, Fuséri N, Ryffel B, Dalod M, et al. Cutting edge: Priming of NK cells by IL-18. J Immunol. 2008;181: 1627–1631. doi:10.4049/jimmunol.181.3.1627
264. De Pascalis R, Taylor BC, Elkins KL. Diverse Myeloid and Lymphoid Cell Subpopulations Produce Gamma Interferon during Early Innate Immune Responses to Francisella tularensis Live Vaccine Strain. Infect Immun. 2008;76: 4311–4321. doi:10.1128/IAI.00514-08
265. Jessop F, Buntyn R, Schwarz B, Wehrly T, Scott D, Bosio CM. Interferon Gamma Reprograms Host Mitochondrial Metabolism through Inhibition of Complex II To Control Intracellular Bacterial Replication. Infect Immun. 2020;88: e00744-19. doi:10.1128/IAI.00744-19

266. Richard K, Vogel SN, Perkins DJ. Type I interferon Licenses Enhanced Innate Recognition and Transcriptional Responses to Franciscella tularensis LVS. Innate Immun. 2016;22: 363–372. doi:10.1177/1753425916650027
267. McNab F, Mayer-Barber K, Sher A, Wack A, O'Garra A. Type I interferons in infectious disease. Nat Rev Immunol. 2015;15: 87–103. doi:10.1038/nri3787
268. Henry T, Kirimanjeswara GS, Ruby T, Jones JW, Peng K, Perret M, et al. Type I Interferon signaling constrains IL-17A/F secretion by γδ T cells during bacterial infections. J Immunol. 2010;184: 3755–3767. doi:10.4049/jimmunol.0902065
269. Zhu Q, Man SM, Karki R, Malireddi RKS, Kanneganti T-D. Detrimental Type I Interferon Signaling Dominates Protective AIM2 Inflammasome Responses during Francisella novicida Infection. Cell Rep. 2018;22: 3168–3174. doi:10.1016/j.celrep.2018.02.096
270. Naschberger E, Werner T, Vicente AB, Guenzi E, Töpolt K, Leubert R, et al. Nuclear factor-kappaB motif and interferon-alpha-stimulated response element co-operate in the activation of guanylate-binding protein-1 expression by inflammatory cytokines in endothelial cells. Biochem J. 2004;379: 409–420. doi:10.1042/BJ20031873
271. McNab F, Mayer-Barber K, Sher A, Wack A, O'Garra A. Type I interferons in infectious disease. Nat Rev Immunol. 2015;15: 87–103. doi:10.1038/nri3787
272. Fox S, Leitch AE, Duffin R, Haslett C, Rossi AG. Neutrophil Apoptosis: Relevance to the Innate Immune Response and Inflammatory Disease. J Innate Immun. 2010;2: 216–227. doi:10.1159/000284367
273. Sollberger G. Approaching Neutrophil Pyroptosis. Journal of Molecular Biology. 2022;434: 167335. doi:10.1016/j.jmb.2021.167335
274. Moreland JG, Hook JS, Bailey G, Ulland T, Nauseef WM. Francisella tularensis directly interacts with the endothelium and recruits neutrophils with a blunted inflammatory phenotype. Am J Physiol Lung Cell Mol Physiol. 2009;296: L1076–L1084. doi:10.1152/ajplung.90332.2008
275. Kinkead LC, Allen L-AH. Multifaceted effects of Francisella tularensis on human neutrophil function and lifespan. Immunological Reviews. 2016;273: 266–281. doi:10.1111/imr.12445
276. Malik M, Bakshi CS, McCabe K, Catlett SV, Shah A, Singh R, et al. Matrix Metalloproteinase 9 Activity Enhances Host Susceptibility to Pulmonary Infection with Type A and B Strains of *Francisella tularensis*. J Immunol. 2007;178: 1013–1020. doi:10.4049/jimmunol.178.2.1013
277. Pulavendran S, Prasanthi M, Ramachandran A, Grant R, Snider TA, Chow VTK, et al. Production of Neutrophil Extracellular Traps Contributes to the Pathogenesis of Francisella tularemia. Front Immunol. 2020;11: 679. doi:10.3389/fimmu.2020.00679
278. Chen W, KuoLee R, Shen H, Wayne Conlan J. Susceptibility of immunodeficient mice to aerosol and systemic infection with virulent strains of Francisella tularensis. Microbial Pathogenesis. 2004;36: 311–318. doi:10.1016/j.micpath.2004.02.003
279. Sjöstedt A, Conlan JW, North RJ. Neutrophils are critical for host defense against primary infection with the facultative intracellular bacterium Francisella tularensis in mice and participate in defense against reinfection. Infect Immun. 1994;62: 2779–2783.
280. Steiner DJ, Furuya Y, Jordan MB, Metzger DW. Protective Role for Macrophages in Respiratory Francisella tularensis Infection. Infect Immun. 2017;85: e00064-17. doi:10.1128/IAI.00064-17
281. Sarria JC, Vidal AM, Kimbrough RC, Figueroa JE. Fatal infection caused by Francisella tularensisin a neutropenic bone marrow transplant recipient. Ann Hematol. 2003;82: 41–43. doi:10.1007/s00277-002-0570-4
282. McCaffrey RL, Allen L-AH. Pivotal Advance: Francisella tularensis LVS evades killing by human neutrophils via inhibition of the respiratory burst and phagosome escape. J Leukoc Biol. 2006;80: 1224–1230. doi:10.1189/jlb.0406287
283. McCaffrey RL, Schwartz JT, Lindemann SR, Moreland JG, Buchan BW, Jones BD, et al. Multiple mechanisms of NADPH oxidase inhibition by type A and type B Francisella tularensis. J Leukoc Biol. 2010;88: 791–805. doi:10.1189/jlb.1209811

284. Lindgren H, Shen H, Zingmark C, Golovliov I, Conlan W, Sjöstedt A. Resistance of Francisella tularensis strains against reactive nitrogen and oxygen species with special reference to the role of KatG. Infect Immun. 2007;75: 1303–1309. doi:10.1128/IAI.01717-06
285. Honn M, Lindgren H, Bharath GK, Sjöstedt A. Lack of OxyR and KatG Results in Extreme Susceptibility of Francisella tularensis LVS to Oxidative Stress and Marked Attenuation In vivo. Front Cell Infect Microbiol. 2017;7: 14. doi:10.3389/fcimb.2017.00014
286. Schwartz JT, Barker JH, Kaufman J, Fayram DC, McCracken JM, Allen L-AH. Francisella tularensis inhibits the intrinsic and extrinsic pathways to delay constitutive apoptosis and prolong human neutrophil lifespan. J Immunol. 2012;188: 3351–3363. doi:10.4049/jimmunol.1102863
287. Kinkead LC, Fayram DC, Allen L-AH. Francisella novicida inhibits spontaneous apoptosis and extends human neutrophil lifespan. J Leukoc Biol. 2017;102: 815–828. doi:10.1189/jlb.4MA0117-014R
288. Schwartz JT, Bandyopadhyay S, Kobayashi SD, McCracken J, Whitney AR, Deleo FR, et al. Francisella tularensis alters human neutrophil gene expression: insights into the molecular basis of delayed neutrophil apoptosis. J Innate Immun. 2013;5: 124–136. doi:10.1159/000342430
289. McCracken JM, Kinkead LC, McCaffrey RL, Allen L-AH. Francisella tularensis Modulates a Distinct Subset of Regulatory Factors and Sustains Mitochondrial Integrity to Impair Human Neutrophil Apoptosis. J Innate Immun. 2016;8: 299–313. doi:10.1159/000443882
290. Bosio CM, Elkins KL. Susceptibility to Secondary Francisella tularensis Live Vaccine Strain Infection in B-Cell-Deficient Mice Is Associated with Neutrophilia but Not with Defects in Specific T-Cell-Mediated Immunity. Infect Immun. 2001;69: 194–203. doi:10.1128/IAI.69.1.194-203.2001
291. Hagar JA, Powell DA, Aachoui Y, Ernst RK, Miao EA. Cytoplasmic LPS activates caspase-11: implications in TLR4-independent endotoxic shock. Science. 2013;341: 1250–1253. doi:10.1126/science.1240988
292. Zhao Y, Yang J, Shi J, Gong Y-N, Lu Q, Xu H, et al. The NLRC4 inflammasome receptors for bacterial flagellin and type III secretion apparatus. Nature. 2011;477: 596–600. doi:10.1038/nature10510
293. Rathinam VAK, Jiang Z, Waggoner SN, Sharma S, Cole LE, Waggoner L, et al. The AIM2 inflammasome is essential for host defense against cytosolic bacteria and DNA viruses. Nat Immunol. 2010;11: 395–402. doi:10.1038/ni.1864
294. Hansen K, Prabakaran T, Laustsen A, Jørgensen SE, Rahbæk SH, Jensen SB, et al. Listeria monocytogenes induces IFNβ expression through an IFI16-, cGAS- and STING-dependent pathway. EMBO J. 2014;33: 1654–1666. doi:10.15252/embj.201488029
295. Storek KM, Gertsvolf NA, Ohlson MB, Monack DM. cGAS and Ifi204 Cooperate To Produce Type I IFNs in Response to Francisella Infection. J Immunol. 2015;194: 3236–3245. doi:10.4049/jimmunol.1402764
296. Jones JW, Kayagaki N, Broz P, Henry T, Newton K, O'Rourke K, et al. Absent in melanoma 2 is required for innate immune recognition of Francisella tularensis. Proc Natl Acad Sci U S A. 2010;107: 9771–9776. doi:10.1073/pnas.1003738107
297. Henry T, Brotcke A, Weiss DS, Thompson LJ, Monack DM. Type I interferon signaling is required for activation of the inflammasome during Francisella infection. J Exp Med. 2007;204: 987–994. doi:10.1084/jem.20062665
298. Chen Q, Sun L, Chen ZJ. Regulation and function of the cGAS–STING pathway of cytosolic DNA sensing. Nat Immunol. 2016;17: 1142–1149. doi:10.1038/ni.3558
299. Fernandes-Alnemri T, Yu J-W, Juliana C, Solorzano L, Kang S, Wu J, et al. The AIM2 inflammasome is critical for innate immunity against Francisella tularensis. Nat Immunol. 2010;11: 385–393. doi:10.1038/ni.1859
300. Wang B, Bhattacharya M, Roy S, Tian Y, Yin Q. Immunobiology and structural biology of AIM2 inflammasome. Molecular Aspects of Medicine. 2020;76: 100869. doi:10.1016/j.mam.2020.100869
301. Lee S, Karki R, Wang Y, Nguyen LN, Kalathur RC, Kanneganti T-D. AIM2 forms a complex with pyrin and ZBP1 to drive PANoptosis and host defence. Nature. 2021;597: 415–419. doi:10.1038/s41586-021-03875-8

302. Liu X, Zhang Z, Ruan J, Pan Y, Magupalli VG, Wu H, et al. Inflammasome-activated gasdermin D causes pyroptosis by forming membrane pores. Nature. 2016;535: 153–158. doi:10.1038/nature18629
303. Bergsbaken T, Fink SL, Cookson BT. Pyroptosis: host cell death and inflammation. Nat Rev Microbiol. 2009;7: 99–109. doi:10.1038/nrmicro2070
304. Banerjee I, Behl B, Mendonca M, Shrivastava G, Russo AJ, Menoret A, et al. Gasdermin D restrains type I interferon response to cytosolic DNA by disrupting ionic homeostasis. Immunity. 2018;49: 413-426.e5. doi:10.1016/j.immuni.2018.07.006
305. Man SM, Karki R, Malireddi RKS, Neale G, Vogel P, Yamamoto M, et al. The transcription factor IRF1 and guanylate-binding proteins target AIM2 inflammasome activation by Francisella infection. Nat Immunol. 2015;16: 467–475. doi:10.1038/ni.3118
306. Man SM, Karki R, Sasai M, Place DE, Kesavardhana S, Temirov J, et al. IRGB10 liberates bacterial ligands for sensing by the AIM2 and caspase-11–NLRP3 inflammasomes. Cell. 2016;167: 382-396.e17. doi:10.1016/j.cell.2016.09.012
307. Meunier E, Wallet P, Dreier RF, Costanzo S, Anton L, Rühl S, et al. Guanylate-binding proteins promote AIM2 inflammasome activation during Francisella novicida infection by inducing cytosolic bacteriolysis and DNA release. Nat Immunol. 2015;16: 476–484. doi:10.1038/ni.3119
308. Wallet P, Benaoudia S, Mosnier A, Lagrange B, Martin A, Lindgren H, et al. IFN-γ extends the immune functions of Guanylate Binding Proteins to inflammasome-independent antibacterial activities during Francisella novicida infection. PLoS Pathog. 2017;13: e1006630. doi:10.1371/journal.ppat.1006630
309. Nandakumar R, Tschismarov R, Meissner F, Prabakaran T, Krissanaprasit A, Farahani E, et al. Intracellular bacteria engage a STING-TBK1-MVB12b pathway to enable paracrine cGAS-STING signaling. Nat Microbiol. 2019;4: 701–713. doi:10.1038/s41564-019-0367-z
310. Mitra S, Dolvin E, Krishnamurthy K, Wewers MD, Sarkar A. Francisella induced microparticulate caspase-1/gasdermin-D activation is regulated by NLRP3 independent of Pyrin. PLoS One. 2018;13: e0209931. doi:10.1371/journal.pone.0209931
311. Wandel MP, Pathe C, Werner EI, Ellison CJ, Boyle KB, von der Malsburg A, et al. GBPs Inhibit Motility of Shigella flexneri but Are Targeted for Degradation by the Bacterial Ubiquitin Ligase IpaH9.8. Cell Host Microbe. 2017;22: 507-518.e5. doi:10.1016/j.chom.2017.09.007
312. Olszewski MA, Gray J, Vestal DJ. In silico genomic analysis of the human and murine guanylate-binding protein (GBP) gene clusters. J Interferon Cytokine Res. 2006;26: 328–352. doi:10.1089/jir.2006.26.328
313. Downs KP, Nguyen H, Dorfleutner A, Stehlik C. An overview of the non-canonical inflammasome. Molecular Aspects of Medicine. 2020;76: 100924. doi:10.1016/j.mam.2020.100924
314. Van Den Eeckhout B, Tavernier J, Gerlo S. Interleukin-1 as Innate Mediator of T Cell Immunity. Frontiers in Immunology. 2021;11. Available: https://www.frontiersin.org/article/10.3389/fimmu.2020.621931
315. Mohammadi N, Lindgren H, Yamamoto M, Martin A, Henry T, Sjöstedt A. Macrophages Demonstrate Guanylate-Binding Protein-Dependent and Bacterial Strain-Dependent Responses to Francisella tularensis. Front Cell Infect Microbiol. 2021;11: 784101. doi:10.3389/fcimb.2021.784101
316. Crane DD, Bauler TJ, Wehrly TD, Bosio CM. Mitochondrial ROS potentiates indirect activation of the AIM2 inflammasome. Frontiers in Microbiology. 2014;5. Available: https://www.frontiersin.org/article/10.3389/fmicb.2014.00438
317. Dotson RJ, Rabadi SM, Westcott EL, Bradley S, Catlett SV, Banik S, et al. Repression of Inflammasome by Francisella tularensis during Early Stages of Infection. J Biol Chem. 2013;288: 23844–23857. doi:10.1074/jbc.M113.490086
318. Ramachandran R, Schmid SL. The dynamin superfamily. Current Biology. 2018;28: R411–R416. doi:10.1016/j.cub.2017.12.013
319. Jimah JR, Hinshaw JE. Structural Insights into the Mechanism of Dynamin Superfamily Proteins. Trends in Cell Biology. 2019;29: 257–273. doi:10.1016/j.tcb.2018.11.003

320. Katic A, Hüsler D, Letourneur F, Hilbi H. Dictyostelium Dynamin Superfamily GTPases Implicated in Vesicle Trafficking and Host-Pathogen Interactions. Front Cell Dev Biol. 2021;9: 731964. doi:10.3389/fcell.2021.731964
321. Shpetner HS, Vallee RB. Identification of dynamin, a novel mechanochemical enzyme that mediates interactions between microtubules. Cell. 1989;59: 421–432. doi:10.1016/0092-8674(89)90027-5
322. Cohen MM, Tareste D. Recent insights into the structure and function of Mitofusins in mitochondrial fusion. F1000Res. 2018;7: F1000 Faculty Rev-1983. doi:10.12688/f1000research.16629.1
323. Chen S, Novick P, Ferro-Novick S. ER structure and function. Current Opinion in Cell Biology. 2013;25: 428–433. doi:10.1016/j.ceb.2013.02.006
324. Membrane fission by dynamin: what we know and what we need to know. The EMBO Journal. 2016;35: 2270–2284. doi:10.15252/embj.201694613
325. Daumke O, Praefcke GJK. Invited review: Mechanisms of GTP hydrolysis and conformational transitions in the dynamin superfamily. Biopolymers. 2016;105: 580–593. doi:10.1002/bip.22855
326. Wehner M, Kunzelmann S, Herrmann C. The guanine cap of human guanylate-binding protein 1 is responsible for dimerization and self-activation of GTP hydrolysis. FEBS J. 2012;279: 203–210. doi:10.1111/j.1742-4658.2011.08415.x
327. Sistemich L, Kutsch M, Hämisch B, Zhang P, Shydlovskyi S, Britzen-Laurent N, et al. The Molecular Mechanism of Polymer Formation of Farnesylated Human Guanylate-binding Protein 1. J Mol Biol. 2020;432: 2164–2185. doi:10.1016/j.jmb.2020.02.009
328. Li G, Zhang J, Sun Y, Wang H, Wang Y. The evolutionarily dynamic IFN-inducible GTPase proteins play conserved immune functions in vertebrates and cephalochordates. Mol Biol Evol. 2009;26: 1619–1630. doi:10.1093/molbev/msp074
329. Pilla-Moffett D, Barber MF, Taylor GA, Coers J. Interferon-inducible GTPases in host resistance, inflammation and disease. J Mol Biol. 2016;428: 3495–3513. doi:10.1016/j.jmb.2016.04.032
330. Haller O, Staeheli P, Schwemmle M, Kochs G. Mx GTPases: dynamin-like antiviral machines of innate immunity. Trends Microbiol. 2015;23: 154–163. doi:10.1016/j.tim.2014.12.003
331. Dicks MDJ, Goujon C, Pollpeter D, Betancor G, Apolonia L, Bergeron JRC, et al. Oligomerization Requirements for MX2-Mediated Suppression of HIV-1 Infection. J Virol. 2016;90: 22–32. doi:10.1128/JVI.02247-15
332. Bekpen C, Hunn JP, Rohde C, Parvanova I, Guethlein L, Dunn DM, et al. The interferon-inducible p47 (IRG) GTPases in vertebrates: loss of the cell autonomous resistance mechanism in the human lineage. Genome Biology. 2005;6: R92. doi:10.1186/gb-2005-6-11-r92
333. Bekpen C, Xavier RJ, Eichler EE. Human IRGM gene “to be or not to be.” Semin Immunopathol. 2010;32: 437–444. doi:10.1007/s00281-010-0224-x
334. Rafeld HL, Kolanus W, van Driel IR, Hartland EL. Interferon-induced GTPases orchestrate host cell-autonomous defence against bacterial pathogens. Biochem Soc Trans. 2021;49: 1287–1297. doi:10.1042/BST20200900
335. Rai P, Janardhan KS, Meacham J, Madenspacher JH, Lin W-C, Karmaus PWF, et al. IRGM1 links mitochondrial quality control to autoimmunity. Nat Immunol. 2021;22: 312–321. doi:10.1038/s41590-020-00859-0
336. Klamp T, Boehm U, Schenk D, Pfeffer K, Howard JC. A giant GTPase, very large inducible GTPase-1, is inducible by IFNs. J Immunol. 2003;171: 1255–1265. doi:10.4049/jimmunol.171.3.1255
337. GVINP1 - Interferon-induced very large GTPase 1 - Homo sapiens (Human) - GVINP1 gene & protein. [cited 12 Apr 2022]. Available: https://www.uniprot.org/uniprot/Q7Z2Y8
338. Picard L, Ganivet Q, Allatif O, Cimarelli A, Guéguen L, Etienne L. DGINN, an automated and highly-flexible pipeline for the detection of genetic innovations on protein-coding genes. Nucleic Acids Res. 2020;48: e103. doi:10.1093/nar/gkaa680
339. Kohler KM, Kutsch M, Piro AS, Wallace GD, Coers J, Barber MF. A Rapidly Evolving Polybasic Motif Modulates Bacterial Detection by Guanylate Binding Proteins. mBio. 2020;11: e00340-20. doi:10.1128/mBio.00340-20

340. Côrte-Real JV, Baldauf H-M, Abrantes J, Esteves PJ. Evolution of the guanylate binding protein (GBP) genes: Emergence of GBP7 genes in primates and further acquisition of a unique GBP3 gene in simians. Mol Immunol. 2021;132: 79–81. doi:10.1016/j.molimm.2021.01.025
341. Côrte-Real JV, Baldauf H-M, Melo-Ferreira J, Abrantes J, Esteves PJ. Evolution of Guanylate Binding Protein (GBP) Genes in Muroid Rodents (Muridae and Cricetidae) Reveals an Outstanding Pattern of Gain and Loss. Front Immunol. 2022;13: 752186. doi:10.3389/fimmu.2022.752186
342. Tyrkalska SD, Candel S, Angosto D, Gómez-Abellán V, Martín-Sánchez F, García-Moreno D, et al. Neutrophils mediate Salmonella Typhimurium clearance through the GBP4 inflammasome-dependent production of prostaglandins. Nat Commun. 2016;7: 12077. doi:10.1038/ncomms12077
343. Krapp C, Hotter D, Gawanbacht A, McLaren PJ, Kluge SF, Stürzel CM, et al. Guanylate Binding Protein (GBP) 5 Is an Interferon-Inducible Inhibitor of HIV-1 Infectivity. Cell Host Microbe. 2016;19: 504–514. doi:10.1016/j.chom.2016.02.019
344. Ji C, Du S, Li P, Zhu Q, Yang X, Long C, et al. Structural mechanism for guanylate-binding proteins (GBPs) targeting by the Shigella E3 ligase IpaH9.8. PLoS Pathog. 2019;15: e1007876. doi:10.1371/journal.ppat.1007876
345. Lubeseder-Martellato C, Guenzi E, Jörg A, Töpolt K, Naschberger E, Kremmer E, et al. Guanylate-Binding Protein-1 Expression Is Selectively Induced by Inflammatory Cytokines and Is an Activation Marker of Endothelial Cells during Inflammatory Diseases. Am J Pathol. 2002;161: 1749–1759.
346. Wang Q, Wang X, Liang Q, Wang S, Xiwen L, Pan F, et al. Distinct prognostic value of mRNA expression of guanylate-binding protein genes in skin cutaneous melanoma. Oncol Lett. 2018;15: 7914–7922. doi:10.3892/ol.2018.8306
347. Honkala AT, Tailor D, Malhotra SV. Guanylate-Binding Protein 1: An Emerging Target in Inflammation and Cancer. Frontiers in Immunology. 2020;10. Available: https://www.frontiersin.org/article/10.3389/fimmu.2019.03139
348. GBP6 protein expression summary - The Human Protein Atlas. [cited 14 Apr 2022]. Available: https://www.proteinatlas.org/ENSG00000183347-GBP6
349. GBP7 protein expression summary - The Human Protein Atlas. [cited 14 Apr 2022]. Available: https://www.proteinatlas.org/ENSG00000213512-GBP7
350. Tripal P, Bauer M, Naschberger E, Mörtinger T, Hohenadl C, Cornali E, et al. Unique features of different members of the human guanylate-binding protein family. J Interferon Cytokine Res. 2007;27: 44–52. doi:10.1089/jir.2007.0086
351. Britzen-Laurent N, Bauer M, Berton V, Fischer N, Syguda A, Reipschläger S, et al. Intracellular trafficking of guanylate-binding proteins is regulated by heterodimerization in a hierarchical manner. PLoS One. 2010;5: e14246. doi:10.1371/journal.pone.0014246
352. Naschberger E, Geißdörfer W, Bogdan C, Tripal P, Kremmer E, Stürzl M, et al. Processing and secretion of guanylate binding protein-1 depend on inflammatory caspase activity. J Cell Mol Med. 2017;21: 1954–1966. doi:10.1111/jcmm.13116
353. Fisch D, Clough B, Domart M-C, Encheva V, Bando H, Snijders AP, et al. Human GBP1 Differentially Targets Salmonella and Toxoplasma to License Recognition of Microbial Ligands and Caspase-Mediated Death. Cell Rep. 2020;32: 108008. doi:10.1016/j.celrep.2020.108008
354. Schwemmle M, Staeheli P. The interferon-induced 67-kDa guanylate-binding protein (hGBP1) is a GTPase that converts GTP to GMP. J Biol Chem. 1994;269: 11299–11305.
355. Cui W, Braun E, Wang W, Tang J, Zheng Y, Slater B, et al. Structural basis for GTP-induced dimerization and antiviral function of guanylate-binding proteins. Proc Natl Acad Sci U S A. 2021;118: e2022269118. doi:10.1073/pnas.2022269118
356. Prakash B, Praefcke GJ, Renault L, Wittinghofer A, Herrmann C. Structure of human guanylate-binding protein 1 representing a unique class of GTP-binding proteins. Nature. 2000;403: 567–571. doi:10.1038/35000617

357. Sistemich L, Herrmann C. Purification of Farnesylated hGBP1 and Characterization of Its Polymerization and Membrane Binding. Methods Mol Biol. 2020;2159: 67–81. doi:10.1007/978-1-0716-0676-6_6
358. Shydlovskyi S, Zienert AY, Ince S, Dovengerds C, Hohendahl A, Dargazanli JM, et al. Nucleotide-dependent farnesyl switch orchestrates polymerization and membrane binding of human guanylate-binding protein 1. Proc Natl Acad Sci U S A. 2017;114: E5559–E5568. doi:10.1073/pnas.1620959114
359. Praefcke GJ, Geyer M, Schwemmle M, Robert Kalbitzer H, Herrmann C. Nucleotide-binding characteristics of human guanylate-binding protein 1 (hGBP1) and identification of the third GTP-binding motif. J Mol Biol. 1999;292: 321–332. doi:10.1006/jmbi.1999.3062
360. Praefcke GJK, Kloep S, Benscheid U, Lilie H, Prakash B, Herrmann C. Identification of residues in the human guanylate-binding protein 1 critical for nucleotide binding and cooperative GTP hydrolysis. J Mol Biol. 2004;344: 257–269. doi:10.1016/j.jmb.2004.09.026
361. Ghosh A, Praefcke GJK, Renault L, Wittinghofer A, Herrmann C. How guanylate-binding proteins achieve assembly-stimulated processive cleavage of GTP to GMP. Nature. 2006;440: 101–104. doi:10.1038/nature04510
362. Vöpel T, Hengstenberg CS, Peulen T-O, Ajaj Y, Seidel CAM, Herrmann C, et al. Triphosphate induced dimerization of human guanylate binding protein 1 involves association of the C-terminal helices: a joint double electron-electron resonance and FRET study. Biochemistry. 2014;53: 4590–4600. doi:10.1021/bi500524u
363. Kutsch M, Coers J. Human guanylate binding proteins: nanomachines orchestrating host defense. The FEBS Journal. 2021;288: 5826–5849. doi:10.1111/febs.15662
364. Lorenz C, Ince S, Zhang T, Cousin A, Batra-Safferling R, Nagel-Steger L, et al. Farnesylation of human guanylate-binding protein 1 as safety mechanism preventing structural rearrangements and uninduced dimerization. FEBS J. 2020;287: 496–514. doi:10.1111/febs.15015
365. Ince S, Kutsch M, Shydlovskyi S, Herrmann C. The human guanylate-binding proteins hGBP-1 and hGBP-5 cycle between monomers and dimers only. FEBS J. 2017;284: 2284–2301. doi:10.1111/febs.14126
366. Kutsch M, Ince S, Herrmann C. Homo and hetero dimerisation of the human guanylate-binding proteins hGBP-1 and hGBP-5 characterised by affinities and kinetics. FEBS J. 2018;285: 2019–2036. doi:10.1111/febs.14459
367. Ince S, Zhang P, Kutsch M, Krenczyk O, Shydlovskyi S, Herrmann C. Catalytic activity of human guanylate-binding protein 1 coupled to the release of structural restraints imposed by the C-terminal domain. The FEBS Journal. 2021;288: 582–599. doi:10.1111/febs.15348
368. Rajan S, Pandita E, Mittal M, Sau AK. Understanding the lower GMP formation in large GTPase hGBP-2 and role of its individual domains in regulation of GTP hydrolysis. FEBS J. 2019;286: 4103–4121. doi:10.1111/febs.14957
369. Sistemich L, Dimitrov Stanchev L, Kutsch M, Roux A, Günther Pomorski T, Herrmann C. Structural requirements for membrane binding of human guanylate-binding protein 1. FEBS J. 2021;288: 4098–4114. doi:10.1111/febs.15703
370. Haldar AK, Foltz C, Finethy R, Piro AS, Feeley EM, Pilla-Moffett DM, et al. Ubiquitin systems mark pathogen-containing vacuoles as targets for host defense by guanylate binding proteins. Proc Natl Acad Sci U S A. 2015;112: E5628-5637. doi:10.1073/pnas.1515966112
371. Anderson SL, Carton JM, Lou J, Xing L, Rubin BY. Interferon-induced guanylate binding protein-1 (GBP-1) mediates an antiviral effect against vesicular stomatitis virus and encephalomyocarditis virus. Virology. 1999;256: 8–14. doi:10.1006/viro.1999.9614
372. Carter CC, Gorbacheva VY, Vestal DJ. Inhibition of VSV and EMCV replication by the interferon-induced GTPase, mGBP-2: differential requirement for wild-type GTP binding domain. Arch Virol. 2005;150: 1213–1220. doi:10.1007/s00705-004-0489-2
373. Gol S, Estany J, Fraile LJ, Pena RN. Expression profiling of the GBP1 gene as a candidate gene for porcine reproductive and respiratory syndrome resistance. Anim Genet. 2015;46: 599–606. doi:10.1111/age.12347

374. Khatun A, Nazki S, Jeong C-G, Gu S, Mattoo S ul S, Lee S-I, et al. Effect of polymorphisms in porcine guanylate-binding proteins on host resistance to PRRSV infection in experimentally challenged pigs. Veterinary Research. 2020;51: 14. doi:10.1186/s13567-020-00745-5
375. Gu T, Yu D, Xu L, Yao Y-L, Zheng X, Yao Y-G. Tupaia guanylate-binding protein 1 interacts with vesicular stomatitis virus phosphoprotein and represses primary transcription of the viral genome. Cytokine. 2021;138: 155388. doi:10.1016/j.cyto.2020.155388
376. Yu P, Li Y, Li Y, Miao Z, Peppelenbosch MP, Pan Q. Guanylate-binding protein 2 orchestrates innate immune responses against murine norovirus and is antagonized by the viral protein NS7. J Biol Chem. 2020;295: 8036–8047. doi:10.1074/jbc.RA120.013544
377. Glitscher M, Himmelsbach K, Woytinek K, Schollmeier A, Johne R, Praefcke GJK, et al. Identification of the interferon-inducible GTPase GBP1 as major restriction factor for the Hepatitis E virus. J Virol. 2021; JVI.01564-20. doi:10.1128/JVI.01564-20
378. Zou Z, Meng Z, Ma C, Liang D, Sun R, Lan K. Guanylate-Binding Protein 1 Inhibits Nuclear Delivery of Kaposi's Sarcoma-Associated Herpesvirus Virions by Disrupting Formation of Actin Filament. J Virol. 2017;91. doi:10.1128/JVI.00632-17
379. Braun E, Hotter D, Koepke L, Zech F, Groß R, Sparrer KMJ, et al. Guanylate-Binding Proteins 2 and 5 Exert Broad Antiviral Activity by Inhibiting Furin-Mediated Processing of Viral Envelope Proteins. Cell Rep. 2019;27: 2092-2104.e10. doi:10.1016/j.celrep.2019.04.063
380. Krapp C, Hotter D, Gawanbacht A, McLaren PJ, Kluge SF, Stürzel CM, et al. Guanylate Binding Protein (GBP) 5 Is an Interferon-Inducible Inhibitor of HIV-1 Infectivity. Cell Host Microbe. 2016;19: 504–514. doi:10.1016/j.chom.2016.02.019
381. Tanabe Y, Sakamoto N, Enomoto N, Kurosaki M, Ueda E, Maekawa S, et al. Synergistic Inhibition of Intracellular Hepatitis C Virus Replication by Combination of Ribavirin and Interferon-α. J Infect Dis. 2004;189: 1129–1139. doi:10.1086/382595
382. Itsui Y, Sakamoto N, Kakinuma S, Nakagawa M, Sekine-Osajima Y, Tasaka-Fujita M, et al. Antiviral effects of the interferon-induced protein guanylate binding protein 1 and its interaction with the hepatitis C virus NS5B protein. Hepatology. 2009;50: 1727–1737. doi:10.1002/hep.23195
383. Raninga N, Nayeem SM, Gupta S, Mullick R, Pandita E, Das S, et al. Stimulation of GMP formation in hGBP1 is mediated by W79 and its effect on the antiviral activity. FEBS J. 2021;288: 2970–2988. doi:10.1111/febs.15611
384. Nordmann A, Wixler L, Boergeling Y, Wixler V, Ludwig S. A new splice variant of the human guanylate-binding protein 3 mediates anti-influenza activity through inhibition of viral transcription and replication. FASEB J. 2012;26: 1290–1300. doi:10.1096/fj.11-189886
385. Zhu Z, Shi Z, Yan W, Wei J, Shao D, Deng X, et al. Nonstructural protein 1 of influenza A virus interacts with human guanylate-binding protein 1 to antagonize antiviral activity. PLoS ONE. 2013;8: e55920. doi:10.1371/journal.pone.0055920
386. Pan W, Zuo X, Feng T, Shi X, Dai J. Guanylate-binding protein 1 participates in cellular antiviral response to dengue virus. Virol J. 2012;9: 292. doi:10.1186/1743-422X-9-292
387. Feng J, Cao Z, Wang L, Wan Y, Peng N, Wang Q, et al. Inducible GBP5 Mediates the Antiviral Response via Interferon-Related Pathways during Influenza A Virus Infection. J Innate Immun. 2017;9: 419–435. doi:10.1159/000460294
388. Hotter D, Sauter D, Kirchhoff F. Guanylate binding protein 5: Impairing virion infectivity by targeting retroviral envelope glycoproteins. Small GTPases. 2017;8: 31–37. doi:10.1080/21541248.2016.1189990
389. Li Z, Qu X, Liu X, Huan C, Wang H, Zhao Z, et al. GBP5 Is an Interferon-Induced Inhibitor of Respiratory Syncytial Virus. J Virol. 2020;94: e01407-20. doi:10.1128/JVI.01407-20
390. Biering SB, Choi J, Halstrom RA, Brown HM, Beatty WL, Lee S, et al. Viral Replication Complexes Are Targeted by LC3-Guided Interferon-Inducible GTPases. Cell Host Microbe. 2017;22: 74-85.e7. doi:10.1016/j.chom.2017.06.005
391. Kravets E, Degrandi D, Ma Q, Peulen T-O, Klümpers V, Felekyan S, et al. Guanylate binding proteins directly attack Toxoplasma gondii via supramolecular complexes. Elife. 2016;5: e11479. doi:10.7554/eLife.11479

392. Legewie L, Loschwitz J, Steffens N, Prescher M, Wang X, Smits SHJ, et al. Biochemical and structural characterization of murine GBP7, a guanylate binding protein with an elongated C-terminal tail. Biochem J. 2019;476: 3161–3182. doi:10.1042/BCJ20190364
393. Fisch D, Bando H, Clough B, Hornung V, Yamamoto M, Shenoy AR, et al. Human GBP1 is a microbe-specific gatekeeper of macrophage apoptosis and pyroptosis. EMBO J. 2019;38: e100926. doi:10.15252/embj.2018100926
394. Haldar AK, Piro AS, Pilla DM, Yamamoto M, Coers J. The E2-like conjugation enzyme Atg3 promotes binding of IRG and Gbp proteins to Chlamydia- and Toxoplasma-containing vacuoles and host resistance. PLoS One. 2014;9: e86684. doi:10.1371/journal.pone.0086684
395. Haldar AK, Saka HA, Piro AS, Dunn JD, Henry SC, Taylor GA, et al. IRG and GBP host resistance factors target aberrant, "non-self" vacuoles characterized by the missing of "self" IRGM proteins. PLoS Pathog. 2013;9: e1003414. doi:10.1371/journal.ppat.1003414
396. Johnston AC, Piro A, Clough B, Siew M, Virreira Winter S, Coers J, et al. Human GBP1 does not localize to pathogen vacuoles but restricts Toxoplasma gondii. Cell Microbiol. 2016;18: 1056–1064. doi:10.1111/cmi.12579
397. Qin A, Lai D-H, Liu Q, Huang W, Wu Y-P, Chen X, et al. Guanylate-binding protein 1 (GBP1) contributes to the immunity of human mesenchymal stromal cells against Toxoplasma gondii. Proc Natl Acad Sci U S A. 2017;114: 1365–1370. doi:10.1073/pnas.1619665114
398. Fisch D, Clough B, Khan R, Healy L, Frickel E-M. Toxoplasma-proximal and distal control by GBPs in human macrophages. Pathog Dis. 2022;79: ftab058. doi:10.1093/femspd/ftab058
399. Haldar AK, Nigam U, Yamamoto M, Coers J, Goyal N. Guanylate Binding Proteins Restrict Leishmania donovani Growth in Nonphagocytic Cells Independent of Parasitophorous Vacuolar Targeting. mBio. 2020;11: e01464-20. doi:10.1128/mBio.01464-20
400. Lindenberg V, Mölleken K, Kravets E, Stallmann S, Hegemann JH, Degrandi D, et al. Broad recruitment of mGBP family members to Chlamydia trachomatis inclusions. PLoS One. 2017;12: e0185273. doi:10.1371/journal.pone.0185273
401. Finethy R, Jorgensen I, Haldar AK, de Zoete MR, Strowig T, Flavell RA, et al. Guanylate binding proteins enable rapid activation of canonical and noncanonical inflammasomes in Chlamydia-infected macrophages. Infect Immun. 2015;83: 4740–4749. doi:10.1128/IAI.00856-15
402. Haldar AK, Piro AS, Finethy R, Espenschied ST, Brown HE, Giebel AM, et al. Chlamydia trachomatis Is Resistant to Inclusion Ubiquitination and Associated Host Defense in Gamma Interferon-Primed Human Epithelial Cells. mBio. 2016;7: e01417-16. doi:10.1128/mBio.01417-16
403. Tietzel I, El-Haibi C, Carabeo RA. Human guanylate binding proteins potentiate the anti-chlamydia effects of interferon-gamma. PLoS One. 2009;4: e6499. doi:10.1371/journal.pone.0006499
404. Al-Zeer MA, Al-Younes HM, Lauster D, Abu Lubad M, Meyer TF. Autophagy restricts Chlamydia trachomatis growth in human macrophages via IFNG-inducible guanylate binding proteins. Autophagy. 2013;9: 50–62. doi:10.4161/auto.22482
405. Xavier A, Al-Zeer MA, Meyer TF, Daumke O. hGBP1 Coordinates Chlamydia Restriction and Inflammasome Activation through Sequential GTP Hydrolysis. Cell Rep. 2020;31: 107667. doi:10.1016/j.celrep.2020.107667
406. Kim B-H, Shenoy AR, Kumar P, Das R, Tiwari S, MacMicking JD. A family of IFN-γ-inducible 65-kD GTPases protects against bacterial infection. Science. 2011;332: 717–721. doi:10.1126/science.1201711
407. Feeley EM, Pilla-Moffett DM, Zwack EE, Piro AS, Finethy R, Kolb JP, et al. Galectin-3 directs antimicrobial guanylate binding proteins to vacuoles furnished with bacterial secretion systems. Proc Natl Acad Sci U S A. 2017;114: E1698–E1706. doi:10.1073/pnas.1615771114
408. Betts-Hampikian HJ, Fields KA. The Chlamydial Type III Secretion Mechanism: Revealing Cracks in a Tough Nut. Front Microbiol. 2010;1: 114. doi:10.3389/fmicb.2010.00114
409. Zwack EE, Feeley EM, Burton AR, Hu B, Yamamoto M, Kanneganti T-D, et al. Guanylate Binding Proteins Regulate Inflammasome Activation in Response to Hyperinjected Yersinia Translocon Components. Infect Immun. 2017;85: e00778-16. doi:10.1128/IAI.00778-16

410. Liu BC, Sarhan J, Panda A, Muendlein HI, Ilyukha V, Coers J, et al. Constitutive Interferon Maintains GBP Expression Required for Release of Bacterial Components Upstream of Pyroptosis and Anti-DNA Responses. Cell Rep. 2018;24: 155-168.e5. doi:10.1016/j.celrep.2018.06.012
411. Pilla DM, Hagar JA, Haldar AK, Mason AK, Degrandi D, Pfeffer K, et al. Guanylate binding proteins promote caspase-11-dependent pyroptosis in response to cytoplasmic LPS. Proc Natl Acad Sci U S A. 2014;111: 6046–6051. doi:10.1073/pnas.1321700111
412. Costa Franco MM, Marim F, Guimarães ES, Assis NRG, Cerqueira DM, Alves-Silva J, et al. Brucella abortus Triggers a cGAS-Independent STING Pathway To Induce Host Protection That Involves Guanylate-Binding Proteins and Inflammasome Activation. J Immunol. 2018;200: 607–622. doi:10.4049/jimmunol.1700725
413. Meunier E, Dick MS, Dreier RF, Schürmann N, Broz DK, Warming S, et al. Caspase-11 activation requires lysis of pathogen-containing vacuoles by IFN-induced GTPases. Nature. 2014;509: 366–370. doi:10.1038/nature13157
414. Cerqueira DM, Gomes MTR, Silva ALN, Rungue M, Assis NRG, Guimarães ES, et al. Guanylate-binding protein 5 licenses caspase-11 for Gasdermin-D mediated host resistance to Brucella abortus infection. PLoS Pathog. 2018;14: e1007519. doi:10.1371/journal.ppat.1007519
415. Balakrishnan A, Karki R, Berwin B, Yamamoto M, Kanneganti T-D. Guanylate binding proteins facilitate caspase-11-dependent pyroptosis in response to type 3 secretion system-negative Pseudomonas aeruginosa. Cell Death Discov. 2018;4: 3. doi:10.1038/s41420-018-0068-z
416. Finethy R, Luoma S, Orench-Rivera N, Feeley EM, Haldar AK, Yamamoto M, et al. Inflammasome Activation by Bacterial Outer Membrane Vesicles Requires Guanylate Binding Proteins. mBio. 2017;8: e01188-17. doi:10.1128/mBio.01188-17
417. Santos JC, Dick MS, Lagrange B, Degrandi D, Pfeffer K, Yamamoto M, et al. LPS targets host guanylate-binding proteins to the bacterial outer membrane for non-canonical inflammasome activation. EMBO J. 2018;37: e98089. doi:10.15252/embj.201798089
418. Piro AS, Hernandez D, Luoma S, Feeley EM, Finethy R, Yirga A, et al. Detection of Cytosolic Shigella flexneri via a C-Terminal Triple-Arginine Motif of GBP1 Inhibits Actin-Based Motility. mBio. 2017;8: e01979-17. doi:10.1128/mBio.01979-17
419. Santos JC, Boucher D, Schneider LK, Demarco B, Dilucca M, Shkarina K, et al. Human GBP1 binds LPS to initiate assembly of a caspase-4 activating platform on cytosolic bacteria. Nat Commun. 2020;11: 3276. doi:10.1038/s41467-020-16889-z
420. Wandel MP, Kim B-H, Park E-S, Boyle KB, Nayak K, Lagrange B, et al. Guanylate-binding proteins convert cytosolic bacteria into caspase-4 signaling platforms. Nat Immunol. 2020;21: 880–891. doi:10.1038/s41590-020-0697-2
421. Kutsch M, Sistemich L, Lesser CF, Goldberg MB, Herrmann C, Coers J. Direct binding of polymeric GBP1 to LPS disrupts bacterial cell envelope functions. EMBO J. 2020;39: e104926. doi:10.15252/embj.2020104926
422. Knodler LA, Nair V, Steele-Mortimer O. Quantitative Assessment of Cytosolic Salmonella in Epithelial Cells. PLOS ONE. 2014;9: e84681. doi:10.1371/journal.pone.0084681
423. Kutsch M, González-Prieto C, Lesser CF, Coers J. The GBP1 microcapsule interferes with IcsA-dependent septin cage assembly around Shigella flexneri. Pathog Dis. 2021;79: ftab023. doi:10.1093/femspd/ftab023
424. Dilucca M, Ramos S, Shkarina K, Santos JC, Broz P. Guanylate-Binding Protein-Dependent Noncanonical Inflammasome Activation Prevents Burkholderia thailandensis-Induced Multinucleated Giant Cell Formation. mBio. 2021;12: e0205421. doi:10.1128/mBio.02054-21
425. Zhu S, Bradfield CJ, Mamińska A, Park E-S, Kim B-H, Kumar P, et al. Cryo-ET of a human GBP coatomer governing cell-autonomous innate immunity to infection. bioRxiv. 2021; 2021.08.26.457804. doi:10.1101/2021.08.26.457804
426. Li P, Jiang W, Yu Q, Liu W, Zhou P, Li J, et al. Ubiquitination and degradation of GBPs by a Shigella effector to suppress host defence. Nature. 2017;551: 378–383. doi:10.1038/nature24467
427. Feng S, Man SM. Captain GBP1: inflammasomes assemble, pyroptotic endgame. Nat Immunol. 2020;21: 829–830. doi:10.1038/s41590-020-0727-0

428. Place DE, Briard B, Samir P, Karki R, Bhattacharya A, Guy CS, et al. Interferon inducible GBPs restrict Burkholderia thailandensis motility induced cell-cell fusion. PLoS Pathog. 2020;16: e1008364. doi:10.1371/journal.ppat.1008364
429. Barz B, Loschwitz J, Strodel B. Large-scale, dynamin-like motions of the human guanylate binding protein 1 revealed by multi-resolution simulations. PLoS Comput Biol. 2019;15: e1007193. doi:10.1371/journal.pcbi.1007193
430. Mohammadi N, Lindgren H, Golovliov I, Eneslätt K, Yamamoto M, Martin A, et al. Guanylate-Binding Proteins Are Critical for Effective Control of Francisella tularensis Strains in a Mouse Co-Culture System of Adaptive Immunity. Front Cell Infect Microbiol. 2020;10: 594063. doi:10.3389/fcimb.2020.594063
431. Wallet P, Lagrange B, Henry T. Francisella Inflammasomes: Integrated Responses to a Cytosolic Stealth Bacterium. Curr Top Microbiol Immunol. 2016;397: 229–256. doi:10.1007/978-3-319-41171-2_12
432. Checroun C, Wehrly TD, Fischer ER, Hayes SF, Celli J. Autophagy-mediated reentry of Francisella tularensis into the endocytic compartment after cytoplasmic replication. Proc Natl Acad Sci U S A. 2006;103: 14578–83.
433. Ray K, Bobard A, Danckaert A, Paz-Haftel I, Clair C, Ehsani S, et al. Tracking the dynamic interplay between bacterial and host factors during pathogen-induced vacuole rupture in real time. Cell Microbiol. 2010;12: 545–56. doi:10.1111/j.1462-5822.2010.01428.x
434. Wehner M, Herrmann C. Biochemical properties of the human guanylate binding protein 5 and a tumor-specific truncated splice variant. The FEBS Journal. 2010;277: 1597–1605. doi:https://doi.org/10.1111/j.1742-4658.2010.07586.x
435. Chen W, KuoLee R, Shen H, Busa M, Conlan JW. Toll-like receptor 4 (TLR4) does not confer a resistance advantage on mice against low-dose aerosol infection with virulent type A Francisella tularensis. Microb Pathog. 2004;37. doi:10.1016/j.micpath.2004.06.010
436. Weiss DS, Brotcke A, Henry T, Margolis JJ, Chan K, Monack DM. In vivo negative selection screen identifies genes required for Francisella virulence. Proc Natl Acad Sci U S A. 2007;104: 6037–42.
437. Sidik S, Kottwitz H, Benjamin J, Ryu J, Jarrar A, Garduno R, et al. A Shigella flexneri Virulence Plasmid Encoded Factor Controls Production of Outer Membrane Vesicles. G3 Genes|Genomes|Genetics. 2014;4: 2493–2503. doi:10.1534/g3.114.014381
438. Abd H, Johansson T, Golovliov I, Sandstrom G, Forsman M. Survival and growth of Francisella tularensis in Acanthamoeba castellanii. Appl Environ Microbiol. 2003;69: 600–6.
439. Nothelfer K, Dias Rodrigues C, Bobard A, Phalipon A, Enninga J. Monitoring Shigella flexneri vacuolar escape by flow cytometry. Virulence. 2011;2: 54–7. doi:10.4161/viru.2.1.14666
440. Fisch D, Yakimovich A, Clough B, Wright J, Bunyan M, Howell M, et al. Defining host–pathogen interactions employing an artificial intelligence workflow. eLife. 8: e40560. doi:10.7554/eLife.40560
441. Martinez E, Cantet F, Fava L, Norville I, Bonazzi M. Identification of OmpA, a Coxiella burnetii protein involved in host cell invasion, by multi-phenotypic high-content screening. PLoS Pathog. 2014;10: e1004013. doi:10.1371/journal.ppat.1004013
442. Killackey SA, Sorbara MT, Girardin SE. Cellular Aspects of Shigella Pathogenesis: Focus on the Manipulation of Host Cell Processes. Front Cell Infect Microbiol. 2016;6: 38. doi:10.3389/fcimb.2016.00038
443. Kassinger SJ, van Hoek ML. Genetic Determinants of Antibiotic Resistance in Francisella. Frontiers in Microbiology. 2021;12. Available: https://www.frontiersin.org/article/10.3389/fmicb.2021.644855
444. Yamaji A, Sekizawa Y, Emoto K, Sakuraba H, Inoue K, Kobayashi H, et al. Lysenin, a novel sphingomyelin-specific binding protein. J Biol Chem. 1998;273: 5300–5306. doi:10.1074/jbc.273.9.5300
445. Ellison CJ, Kukulski W, Boyle KB, Munro S, Randow F. Transbilayer Movement of Sphingomyelin Precedes Catastrophic Breakage of Enterobacteria-Containing Vacuoles. Current Biology. 2020;30: 2974-2983.e6. doi:10.1016/j.cub.2020.05.083

446. Meunier E, Broz P. Quantification of Cytosolic vs. Vacuolar Salmonella in Primary Macrophages by Differential Permeabilization. J Vis Exp. 2015; 52960. doi:10.3791/52960
447. A SNARE geranylgeranyltransferase essential for the organization of the Golgi apparatus. The EMBO Journal. 2020;39: e104120. doi:10.15252/embj.2019104120
448. Banfield DK. Mechanisms of Protein Retention in the Golgi. Cold Spring Harb Perspect Biol. 2011;3: a005264. doi:10.1101/cshperspect.a005264
449. Cullen TW, Giles DK, Wolf LN, Ecobichon C, Boneca IG, Trent MS. Helicobacter pylori versus the host: remodeling of the bacterial outer membrane is required for survival in the gastric mucosa. PLoS Pathog. 2011;7: e1002454. doi:10.1371/journal.ppat.1002454
450. Knirel YA, Anisimov AP. Lipopolysaccharide of Yersinia pestis, the Cause of Plague: Structure, Genetics, Biological Properties. Acta Naturae. 2012;4: 46–58.
451. Intracellular Shigella remodels its LPS to dampen the innate immune recognition and evade inflammasome activation. In: PNAS [Internet]. [cited 11 May 2022]. Available: https://www.pnas.org/doi/abs/10.1073/pnas.1303641110
452. Manabe T, Kawasaki K. Extracellular loops of lipid A 3-O-deacylase PagL are involved in recognition of aminoarabinose-based membrane modifications in Salmonella enterica serovar typhimurium. J Bacteriol. 2008;190: 5597–5606. doi:10.1128/JB.00587-08
453. Kawasaki K, Teramoto M, Tatsui R, Amamoto S. Lipid A 3'-O-deacylation by Salmonella outer membrane enzyme LpxR modulates the ability of lipid A to stimulate Toll-like receptor 4. Biochem Biophys Res Commun. 2012;428: 343–347. doi:10.1016/j.bbrc.2012.10.054
454. Soni S, Ernst RK, Muszyński A, Mohapatra NP, Perry MB, Vinogradov E, et al. Francisella tularensis blue-gray phase variation involves structural modifications of lipopolysaccharide o-antigen, core and lipid a and affects intramacrophage survival and vaccine efficacy. Front Microbiol. 2010;1: 129. doi:10.3389/fmicb.2010.00129
455. Needham BD, Trent MS. Fortifying the barrier: the impact of lipid A remodelling on bacterial pathogenesis. Nat Rev Microbiol. 2013;11: 467–481. doi:10.1038/nrmicro3047
456. Fathy Mohamed Y, Hamad M, Ortega XP, Valvano MA. The LpxL acyltransferase is required for normal growth and penta-acylation of lipid A in Burkholderia cenocepacia. Mol Microbiol. 2017;104: 144–162. doi:10.1111/mmi.13618
457. An J, Kim SH, Hwang D, Lee KE, Kim MJ, Yang EG, et al. Caspase-4 disaggregates lipopolysaccharide micelles via LPS-CARD interaction. Sci Rep. 2019;9: 826. doi:10.1038/s41598-018-36811-4

ANNEX I. Roles of GBPs in cancer, cell proliferation, migration.

Table 1. Effects of GBPs on proliferation, differentiation and motility of different cell types.

GBP	Cell type	Effect	Notes	References
hGBP1	HeLa	Destabilizes actin stress fibers	Demonstrates *in vitro* interaction of hGBP1 with actin.	Ostler et al., 2014 [1]
hGBP1	Bone marrow-derived mesenchymal stromal cells	Inhibits osteogenic differentiation	hGBP1 promotes expression of IL-6, IL-8 and IDO[1]. Expression of hGBP1 decreases during osteogenesis but expression of hGBP2 increases.	Bai et al., 2018a [2]
hGBP1	Endothelial progenitor cells (T17b), *in vivo* migration assays	Inhibits cell migration and proliferation, induces differentiation; decreases apoptosis	hGBP1 is secreted by live endothelial progenitor cells. GBP1 increases secretion of VEGF[2] in differentiated endothelium. Decreased blood vessel surface area and branching.	Hammon et al., 2011 [3]; Bleiziffer et al., 2012 [4]
hGBP1	Endothelial cells (HUVEC), Kaposi's sacroma	Inhibits cell migration and tube formation	hGBP1 inhibits expression of MMP-1[3] trough GTPase activity; Induces expression of integrin chain α4 which interacts with fibronectin, resulting in negative effects on cell migration.	Guenzi et al., 2003 [5]; Weinlander et al., 2008 [6]
hGBP1	Endothelial cells (HUVEC, MVEC)	Inhibits proliferation	hGBP1 inhibits the effect of Angiogenic Growth Factor through the α9 helix of hGBP1.	Guenzi et al., 2001 [7]
hGBP1	Colorectal carcinoma cell lines, HeLa and patient tumor cells	Inhibits proliferation, migration and tumor invasion	The a9 helix of hGBP1 binds transcription factor TEAD, part of the pro-survival Hippo signaling pathway. This binding leads to downregulation of TEAD-controlled genes involved in proliferation.	Unterer et al., 2018 [8]; Britzen-Laurent et al., 2013 [9]
hGBP2	Colorectal carcinoma cell lines	Inhibits proliferation and increases sensitivity to paclitaxel[4]	hGBP2 overexpression decreases expression of Wnt pathway genes. The Wnt pathway is involved in embryogenesis, proliferation and differentiation.	Wang et al., 2020 [10]
hGBP1	Oral cavity and esophageal squamous cell carcinoma	Promotes proliferation, cell migration and tumor invasion	hGBP1 expression associated with poor prognosis. Overexpression of hGBP1 increases lymph node metastasis *in vivo*.	Yu et al., 2011 [11]; Li et al., 2015 [12]
hGBP1	Periodontal ligament stem cells (V54/2, DPSC)	Promotes cell migration and invasion	hGBP1 promotes upregulation of MMP-2 in the presence of IFNγ.	Bai et al., 2018b [13]

[1] IDO (indolenamine 2,3 dioxygenase) is a heme-containing enzyme involved in tryptophan catabolism with functions in immunity and tolerance.

[2] VEGF = Vascular Endothelial Growth Factor

[3] MMP-1, MMP-2, MMP9 (Matrix Metallopeptidases) degrade extracellular matrix proteins and promote cell migration. MMP-1 is a collagenase, MMP-2 and MMP-9 are gelatinases.

[4] Paclitaxel and docetaxel are microtubule stabilizing drugs.

hGBP1	Lung adenocarcinoma patient samples	Promotes cell migration and tumor invasiveness	hGBP1 expression is higher in mesenchymal-like than in epithelial-like lung adenocarcinoma cell lines.	Yamakita et al., 2019 [14]
hGBP1	Glioblastoma cells	No effect proliferation but promotes tumor invasion	GBP1 induces MMP-1 through mechanisms involving GBP1 helical domain but not GTPase domain. Expression of GBP1 is associated with poor diagnosis of glioblastoma patients.	Li et al., 2011 [15]; Lan et al., 2015 [16]; Ji et al., 2019 [17]
hGBP3	Adult brain tissue, glioma tissue and cell lines.	Promotes proliferation and tumor growth	Interaction with MAP4K4[5] demonstrated *in vitro* using adult brain cDNA library. Required for interaction are Nter 1-129 of hGBP3 and CNH domain of MAP4K4. hGBP3 activates cell cycle regulators ERK1/2 through increase in p62 expression. High hGBP3 expression in glioma patients is associated with bad survival prognosis.	Luan et al., 2002 [18]; Xu et al., 2018 [19,20]
hGBP1	Prostate cancer cells (DU145, PC3)	Promotes proliferation, cell migration, and tumor growth	hGBP1 expression is associated with higher tumor *in vitro* and *in vivo* (xenograph) aggressiveness and lower overall survival of patients.	Zhao et al., 2020 [21]
hGBP1	Ovarian cancer cell lines and tumor cells from patients	Decreases cell viability	Full-length hGBP1 is induced and secreted following cytokine treatment. The secretion pathway does not involve microvesicles. High hGBP1 expression correlates with better overall survival.	Carbotti et al., 2020 [22]
hGBP1	Ovarian cancer cells (OVCA 420, OVCAR8), tumor cells from patients	Confers resistance to paclitaxel and docetaxel	High expression of hGBP1 is associated with bad survival prognosis. hGBP1 interacts with βIII-tubulin and the 33kDa isoform of the pro-survival kinase PIM 1. GTP decreases the formation of hGBP1-PIM 1 complex.	Tipton et al., 2016 [23]; Wadi et al., 2016 [24]; Duan et al, 2006 [25]; De Donato et al., 2011 [26]; Persico et al., 2015 [27]
hGBP1	Non triple negative breast cancer cells (MCF-7, TMX-28)	Does not confer resistance to paclitaxel	High expression of hGBP1 is associated with good survival prognosis. Might interact with the 44 kDa isoform of PIM I, but not with βIII-tubulin.	Tipton et al., 2016 [23]
hGBP1	Triple negative breast cancer (TNBC) cell lines and patient tumor cells	Promotes cell proliferation and metastasis to the brain	hGBP1 has higher expression in TNBC than in non-TNBC. Downregulation of hGBP1 specifically affects TBNC cell growth. T cells promote expression of hGBP1 in TNBC cells.	Quintero et al., 2017 [28]; Mustafa et al., 2018 [29]
hGBP2	Triple negative and non-triple negative breast cancer cell lines and tumor cells from patients	Inhibits cancer cell migration and metastasis	hGBP2 interacts with Drp1[6] to inhibit mitochondrial fission through GTPase domain-related functions. Lower expression of hGBP2 and Drp1 in non-TNBC than in TNBC but similar effects *in vitro*. High expression of hGBP2 is correlated with better prognosis in patients with high expression of proliferation genes.	Godoy et al., 2014 [30]; Zhang et al., 2017 [31]

[5] MAP4K4 is a kinase also called HGK and NIK. It participates in cell proliferation, migration and adhestion. CNH (Citron homology) domain allows interaction with GTP-bound proteins.

[6] DrpI is a dynamin-related GTPase required for mitochondrial fission.

hGBP1	Murine mammary carcinoma	Suppresses tumor formation *in vivo*	Expression of hGBP1 in murine mammary carcinoma correlates with decreased VEGF-A in tumors cells.	Lipnik et al., 2010 [32]
hGBP1-5	Skin cutaneous melanoma	Improve patient survival prognosis	Higher overall survival increases with the number of highly-expressed GBPs. No effect of hGBP6.	Wang et al., 2018 [33]
hGBP1	Intestinal epithelial cells (T84, HT29, SKCO15)	Participates in integrity of the intestinal barrier; promotes cell survival	hGBP1 is constitutively expressed in intestinal cells. It localizes to the tight junctions with IFNγ treatment. Effect not observed in macrophages, HeLa, Caski and ARPE-19 cells.	Schoor et al., 2009 [34]
hGBP1	Intestinal epithelial cells (T84, SKCO15)	Inhibits cell proliferation	No expression of hGBP1 without IFNγ/TNFα treatment. Upon IFNγ/TNFα treatment, hGBP1 suppresses pro-mitogenic β-catenin/TCF (T-cell factor) signaling independently of proteasomal degradation (possibly through effects on transcription).	Capaldo et al., 2012 [35]
hGBP1	Primary salivary duct epithelial cells	Promotes epithelial barrier function and tight junction stability	Knockdown of hGBP1 decreases membrane translocation of tight junction proteins occludin and claudin-1. Higher hGBP1 quantities are observed in the presence of PKCα inhibitor.	Konno et al., 2018 [36]
hGBP1	T cells (Jurkat cells, human peripheral blood T lymphocytes)	Inhibits T cell activation and decreases IL-2 production	hGBP1 decreases TCR/CD3 and CD45 surface expression, probably trough interaction with cytoskeleton components such as plastin-2 and βII-spectrin[7].	Forster et al., 2014 [37]
mGBP2	Murine fibroblasts (NIH 3T3)	Inhibits cell migration and spread on fibronectin. Promotes proliferation, decreases contact inhibition, inhibits apoptosis and confers resistance to paclitaxel.	Inhibits PI3K/Akt and Rac pathways. Blocks transcription of NFκB-regulated genes (e.g., MMP-9) through inhibition of Rac kinase. Blocks binding of p65 on promoters but not translocation in the nucleus. Full length mGBP2 requires prenylation and GTPase function of mGBP2 to inhibit cell spread but the helical domain has the same effects on cell spread inhibition as the full length mGBP2. GTP binding capacity of mGBP2 is necessary to observe the effects on proliferation.	Gorbacheva et al., 2002 [38]; Balasubramanian et al., 2006 [39]; Messmer-Blust et al., 2010 [40]; Balasubramanian et al., 2011a [41]; Balasubramanian et al., 2011b [42]
mGBP1	Murine macrophages (Raw 264)	Promotes mitophagy, protects against mitochondrial dysfunction and senescence	Downregulation of mGBP1 promotes polarization towards a pro-inflammatory M1 phenotype. mGBP1 localizes in the cytoplasm and the mitochondria. mGBP1 knock-down stimulates the AMPK-p53 pro-senescence pathway.	Qiu et al., 2018 [43]
hGBP2	Glioma cell lines (U87, U251)	Stimulates proliferation and migration	Interacts with kinesin and stimulates epithelial growth factor receptor EGFR through kinesin signaling.	Ren et al., 2022 [44]
hGBP2	Breast cancer cells (4T1, 67NR)	Does not affect proliferation but inhibits	Impacts Rho GTPase signaling downstream and blocks invadosome formation.	Nyabuto et al., 2021 [45]

[7] Plastin-2 binds with actin and regulates surface expression of T cell receptors and βII-spectrin interacts with actin and underlines the cell membrane.

		cell migration and cancer metastasis		
hGBP2	Clear-cell Renal Cell Carcinoma (ccRCC) samples, human kidney cancer cells (Caki-1)	GBP2 correlates with malignancy	GBP2 is overexpressed in cancer cells an is a risk factor of ccRCC. GBP2 positively influences cancer cell proliferation, migration and invasion through interactions the Wnt/β-catenin pathway.	Liu et al., 2022[46]
hGBP2	Skin cutaneous melanoma tumor and cells	GBP2 inhibits cancer cell proliferation, migration, and invasion	GBP2 inhibits the Wnt/β-catenin pathway and promotes apoptosis, blocks epithelial-mesenchymal transition of cancer cells.	Ji et al., 2021[47]
hGBP1	Adenocarcinoma and adjacent lung samples from patients	High GBP1 expression correlates with advanced tumor features and negative prognosis	Epidemiological data correlates with immunohistochemistry detection of GBP1 expression.	Wan et al., 2021 [48]
hGBP1	Non-small lung cell cancer	GBP1 confers resistance to erlotinib used in cancer treatment.	GBP1 interacts with phosphoglycerate kinase 1 which controls epithelial-mesenchymal transition, increasing the resistance to erlotinib (EGFR-TKI[8] inhibitor).	Cheng et al.,2020 [49]
hGBP1	33 cancer types	GBP1 predicts improved outcomes	GBP1 expression correlates with enrichment of immune-related pathways and anti-tumor phenotypes	Zhao et al., 2022[50]
hGBPs	Head and neck squamous cell carcinoma	GBP1 linked to negative prognosis	High expression of GBP1 and low expression of GBP6/7 correlate with shorter overall survival. Might be related to B cell invasion.	Wu et al., 2020 [51]
hGBP2	Glioblastoma tumor and cell lines	GBP2 promotes cell migration and invasion	GBP2 induces fibronectin and promotes cancer cell migration through Stat3. GBP2 is associated with poor prognosis.	Yu et al., 2020 [52]
hGBP5	Oral squamous cell carcinoma	GBP5 is associated with poor prognosis	GBP5 is overexpressed in tumors. GBP5 promotes cell proliferation at the G1 mitosis phase; increases cell migration and cancer invasion.	Liu et al., 2021[53]
hGBP5	Triple-negative breast cancer biopsies	GBP5 is associated with poor prognosis	GBP5 expression is upregulated by IFNγ and NFκB signalling. GBP5 boosts IFNγ/STAT1 and TNFα/NFκB pathways and expression of PD-L1 (programmed cell-death ligand 1), involved in cancer metastasis.	Cheng et al., 2021 [54]
hGBP5	Triple-negative breast cancer	GBP5 is associated with favorable prognosis	GBP5 increases sensitivity to paclitaxel. GBP5 might activate Akt/mTOR pathway and reduce autophagy.	Cheng et al., 2021 [55]

[8] EFGR-TK1 is a tyrosine kinase targeted in some cancers because it promotes gain of mesenchymal markers in epithelial cells in cancer progression.

Table 2. GBP1 effects depending on the cell type, based on data from table 1.

Effects on proliferation		Effects on migration		Cancer survival prognosis	
Positive	Negative	Positive	Negative	Positive	Negative
Squamous cell carcinoma	Intestinal epithelium	Endothelium	Ovarian cancer	Ovarian cancer	Endothelium
Prostate cancer cells	Lung adenocarcinoma	HeLa cells	TN breast cancer	Non-TN breast cancer	HeLa cells
Intestinal epithelium	Prostate cancer cells	Intestinal epithelium	Skin melanoma	Squamous cell carcinoma	Intestinal epithelium
TN breast cancer cells	TN breast cancer cells	Non-TN breast cancer		Glioblastoma	Non-TN breast cancer
Ovarian cancer cells	Squamous cell carcinoma	Colorectal carcinoma		Lung adenocarcinoma	Ovarian cancer cells
	Periodontal ligament stem cells	Kaposi's sarcoma		Prostate cancer	Colorectal carcinoma

REFERENCES

1. Ostler N, Britzen-Laurent N, Liebl A, Naschberger E, Lochnit G, Ostler M, et al. Gamma Interferon-Induced Guanylate Binding Protein 1 Is a Novel Actin Cytoskeleton Remodeling Factor. Molecular and Cellular Biology. 2014;34: 196–209. doi:10.1128/MCB.00664-13
2. Bai S, Mu Z, Huang Y, Ji P. Guanylate Binding Protein 1 Inhibits Osteogenic Differentiation of Human Mesenchymal Stromal Cells Derived from Bone Marrow. Sci Rep. 2018;8: 1048. doi:10.1038/s41598-018-19401-2
3. Hammon M, Herrmann M, Bleiziffer O, Pryymachuk G, Andreoli L, Munoz LE, et al. Role of guanylate binding protein-1 in vascular defects associated with chronic inflammatory diseases. J Cell Mol Med. 2011;15: 1582–1592. doi:10.1111/j.1582-4934.2010.01146.x
4. Bleiziffer O, Hammon M, Arkudas A, Taeger CD, Beier JP, Amann K, et al. Guanylate-binding protein 1 expression from embryonal endothelial progenitor cells reduces blood vessel density and cellular apoptosis in an axially vascularised tissue-engineered construct. BMC Biotechnol. 2012;12: 94. doi:10.1186/1472-6750-12-94
5. Guenzi E, Töpolt K, Lubeseder-Martellato C, Jörg A, Naschberger E, Benelli R, et al. The guanylate binding protein-1 GTPase controls the invasive and angiogenic capability of endothelial cells through inhibition of MMP-1 expression. EMBO J. 2003;22: 3772–3782. doi:10.1093/emboj/cdg382
6. Weinländer K, Naschberger E, Lehmann MH, Tripal P, Paster W, Stockinger H, et al. Guanylate binding protein-1 inhibits spreading and migration of endothelial cells through induction of integrin alpha4 expression. FASEB J. 2008;22: 4168–4178. doi:10.1096/fj.08-107524
7. Guenzi E, Töpolt K, Cornali E, Lubeseder-Martellato C, Jörg A, Matzen K, et al. The helical domain of GBP-1 mediates the inhibition of endothelial cell proliferation by inflammatory cytokines. EMBO J. 2001;20: 5568–5577. doi:10.1093/emboj/20.20.5568
8. Unterer B, Wiesmann V, Gunasekaran M, Sticht H, Tenkerian C, Behrens J, et al. IFN-γ-response mediator GBP-1 represses human cell proliferation by inhibiting the Hippo signaling transcription factor TEAD. Biochem J. 2018;475: 2955–2967. doi:10.1042/BCJ20180123
9. Britzen-Laurent N, Lipnik K, Ocker M, Naschberger E, Schellerer VS, Croner RS, et al. GBP-1 acts as a tumor suppressor in colorectal cancer cells. Carcinogenesis. 2013;34: 153–162. doi:10.1093/carcin/bgs310

10. Wang J, Min H, Hu B, Xue X, Liu Y. Guanylate-binding protein-2 inhibits colorectal cancer cell growth and increases the sensitivity to paclitaxel of paclitaxel-resistant colorectal cancer cells by interfering Wnt signaling. J Cell Biochem. 2020;121: 1250–1259. doi:10.1002/jcb.29358

11. Yu C-J, Chang K-P, Chang Y-J, Hsu C-W, Liang Y, Yu J-S, et al. Identification of guanylate-binding protein 1 as a potential oral cancer marker involved in cell invasion using omics-based analysis. J Proteome Res. 2011;10: 3778–3788. doi:10.1021/pr2004133

12. Li L, Ma G, Jing C, Liu Z. Guanylate-binding Protein 1 (GBP1) Promotes Lymph Node Metastasis in Human Esophageal Squamous Cell Carcinoma. Discovery Medicine. 2015;20: 369–378.

13. Bai S, Chen T, Deng X. Guanylate-Binding Protein 1 Promotes Migration and Invasion of Human Periodontal Ligament Stem Cells. Stem Cells Int. 2018;2018: 6082956. doi:10.1155/2018/6082956

14. Yamakita I, Mimae T, Tsutani Y, Miyata Y, Ito A, Okada M. Guanylate binding protein 1 (GBP-1) promotes cell motility and invasiveness of lung adenocarcinoma. Biochem Biophys Res Commun. 2019;518: 266–272. doi:10.1016/j.bbrc.2019.08.045

15. Li M, Mukasa A, Inda M del-Mar, Zhang J, Chin L, Cavenee W, et al. Guanylate binding protein 1 is a novel effector of EGFR-driven invasion in glioblastoma. J Exp Med. 2011;208: 2657–2673. doi:10.1084/jem.20111102

16. Lan Q, Wang A, Cheng Y, Mukasa A, Ma J, Hong L, et al. Guanylate binding protein-1 mediates EGFRvIII and promotes glioblastoma growth in vivo but not in vitro. Oncotarget. 2016;7: 9680–9691. doi:10.18632/oncotarget.7109

17. Ji X, Zhu H, Dai X, Xi Y, Sheng Y, Gao C, et al. Overexpression of GBP1 predicts poor prognosis and promotes tumor growth in human glioblastoma multiforme. Cancer Biomark. 2019;25: 275–290. doi:10.3233/CBM-171177

18. Luan Z, Zhang Y, Liu A, Man Y, Cheng L, Hu G. A novel GTP-binding protein hGBP3 interacts with NIK/HGK. FEBS Lett. 2002;530: 233–238. doi:10.1016/s0014-5793(02)03467-1

19. Xu Y, Liu R, Liao C, Liu J, Zhao H, Li Z, et al. High expression of immunity-related GTPase family M protein in glioma promotes cell proliferation and autophagy protein expression. Pathology - Research and Practice. 2019;215: 90–96. doi:10.1016/j.prp.2018.10.004

20. Xu Y, Liao C, Liu R, Liu J, Chen Z, Zhao H, et al. IRGM promotes glioma M2 macrophage polarization through p62/TRAF6/NF-κB pathway mediated IL-8 production. Cell Biology International. 2019;43: 125–135. doi:10.1002/cbin.11061

21. Zhao J, Li X, Liu L, Cao J, Goscinski MA, Fan H, et al. Oncogenic Role of Guanylate Binding Protein 1 in Human Prostate Cancer. Front Oncol. 2020;9. doi:10.3389/fonc.2019.01494

22. Carbotti G, Petretto A, Naschberger E, Stürzl M, Martini S, Mingari MC, et al. Cytokine-Induced Guanylate Binding Protein 1 (GBP1) Release from Human Ovarian Cancer Cells. Cancers (Basel). 2020;12. doi:10.3390/cancers12020488

23. Tipton AR, Nyabuto GO, Trendel JA, Mazur TM, Wilson JP, Wadi S, et al. Guanylate-Binding Protein-1 protects ovarian cancer cell lines but not breast cancer cell lines from killing by paclitaxel. Biochem Biophys Res Commun. 2016;478: 1617–1623. doi:10.1016/j.bbrc.2016.08.169

24. Wadi S, Tipton AR, Trendel JA, Khuder SA, Vestal DJ. hGBP-1 Expression Predicts Shorter Progression-Free Survival in Ovarian Cancers, While Contributing to Paclitaxel Resistance. J Cancer Ther. 2016;7: 994–1007. doi:10.4236/jct.2016.713097

25. Duan Z, Foster R, Brakora KA, Yusuf RZ, Seiden MV. GBP1 overexpression is associated with a paclitaxel resistance phenotype. Cancer Chemother Pharmacol. 2006;57: 25–33. doi:10.1007/s00280-005-0026-3

26. De Donato M, Mariani M, Petrella L, Martinelli E, Zannoni GF, Vellone V, et al. Class III β-tubulin and the cytoskeletal gateway for drug resistance in ovarian cancer. J Cell Physiol. 2012;227: 1034–1041. doi:10.1002/jcp.22813

27. Persico M, Petrella L, Orteca N, Di Dato A, Mariani M, Andreoli M, et al. GTP is an allosteric modulator of the interaction between the guanylate-binding protein 1 and the prosurvival kinase PIM1. Eur J Med Chem. 2015;91: 132–144. doi:10.1016/j.ejmech.2014.07.093

28. Quintero M, Adamoski D, Reis LM dos, Ascenção CFR, Oliveira KRS de, Gonçalves K de A, et al. Guanylate-binding protein-1 is a potential new therapeutic target for triple-negative breast cancer. BMC Cancer. 2017;17. doi:10.1186/s12885-017-3726-2

29. Mustafa DAM, Pedrosa RMSM, Smid M, van der Weiden M, de Weerd V, Nigg AL, et al. T lymphocytes facilitate brain metastasis of breast cancer by inducing Guanylate-Binding Protein 1 expression. Acta Neuropathol. 2018;135: 581–599. doi:10.1007/s00401-018-1806-2

30. Godoy P, Cadenas C, Hellwig B, Marchan R, Stewart J, Reif R, et al. Interferon-inducible guanylate binding protein (GBP2) is associated with better prognosis in breast cancer and indicates an efficient T cell response. Breast Cancer. 2014;21: 491–499. doi:10.1007/s12282-012-0404-8

31. Zhang J, Zhang Y, Wu W, Wang F, Liu X, Shui G, et al. Guanylate-binding protein 2 regulates Drp1-mediated mitochondrial fission to suppress breast cancer cell invasion. Cell Death Dis. 2017;8: e3151. doi:10.1038/cddis.2017.559

32. Lipnik K, Naschberger E, Gonin-Laurent N, Kodajova P, Petznek H, Rungaldier S, et al. Interferon gamma-induced human guanylate binding protein 1 inhibits mammary tumor growth in mice. Mol Med. 2010;16: 177–187. doi:10.2119/molmed.2009.00172

33. Wang Q, Wang X, Liang Q, Wang S, Xiwen L, Pan F, et al. Distinct prognostic value of mRNA expression of guanylate-binding protein genes in skin cutaneous melanoma. Oncol Lett. 2018;15: 7914–7922. doi:10.3892/ol.2018.8306

34. Schnoor M, Betanzos A, Weber DA, Parkos CA. Guanylate-binding protein-1 is expressed at tight junctions of intestinal epithelial cells in response to interferon-gamma and regulates barrier function through effects on apoptosis. Mucosal Immunol. 2009;2: 33–42. doi:10.1038/mi.2008.62

35. Capaldo CT, Beeman N, Hilgarth RS, Nava P, Louis NA, Naschberger E, et al. IFN-γ and TNF-α induced GBP-1 inhibits epithelial cell proliferation through suppression of β-catenin/TCF signaling. Mucosal Immunol. 2012;5: 681–690. doi:10.1038/mi.2012.41

36. Konno T, Takano K, Kaneko Y, Kakuki T, Nomura K, Yajima R, et al. Guanylate binding protein-1-mediated epithelial barrier in human salivary gland duct epithelium. Experimental Cell Research. 2018;371: 31–41. doi:10.1016/j.yexcr.2018.07.033

37. Forster F, Paster W, Supper V, Schatzlmaier P, Sunzenauer S, Ostler N, et al. Guanylate binding protein 1-mediated interaction of T cell antigen receptor signaling with the cytoskeleton. J Immunol. 2014;192: 771–781. doi:10.4049/jimmunol.1300377

38. Gorbacheva VY, Lindner D, Sen GC, Vestal DJ. The interferon (IFN)-induced GTPase, mGBP-2. Role in IFN-gamma-induced murine fibroblast proliferation. J Biol Chem. 2002;277: 6080–6087. doi:10.1074/jbc.M110542200

39. Balasubramanian S, Nada S, Vestal D. The interferon-induced GTPase, mGBP-2, confers resistance to paclitaxel-induced cytotoxicity without inhibiting multinucleation. Cell Mol Biol (Noisy-le-grand). 2006;52: 43–49.

40. Messmer-Blust AF, Balasubramanian S, Gorbacheva VY, Jeyaratnam JA, Vestal DJ. The interferon-gamma-induced murine guanylate-binding protein-2 inhibits rac activation during cell spreading on fibronectin and after platelet-derived growth factor treatment: role for phosphatidylinositol 3-kinase. Mol Biol Cell. 2010;21: 2514–2528. doi:10.1091/mbc.e09-04-0344

41. Balasubramanian S, Fan M, Messmer-Blust AF, Yang CH, Trendel JA, Jeyaratnam JA, et al. The interferon-gamma-induced GTPase, mGBP-2, inhibits tumor necrosis factor alpha (TNF-alpha) induction of matrix metalloproteinase-9 (MMP-9) by inhibiting NF-kappaB and Rac protein. J Biol Chem. 2011;286: 20054–20064. doi:10.1074/jbc.M111.249326

42. Balasubramanian S, Messmer-Blust AF, Jeyaratnam JA, Vestal DJ. Role of GTP binding, isoprenylation, and the C-terminal α-helices in the inhibition of cell spreading by the interferon-induced GTPase, mouse guanylate-binding protein-2. J Interferon Cytokine Res. 2011;31: 291–298. doi:10.1089/jir.2010.0056

43. Qiu X, Guo H, Yang J, Ji Y, Wu C-S, Chen X. Down-regulation of guanylate binding protein 1 causes mitochondrial dysfunction and cellular senescence in macrophages. Sci Rep. 2018;8: 1679. doi:10.1038/s41598-018-19828-7

44. Ren Y, Yang B, Guo G, Zhang J, Sun Y, Liu D, et al. GBP2 facilitates the progression of glioma via regulation of KIF22/EGFR signaling. Cell Death Discov. 2022;8: 208. doi:10.1038/s41420-022-01018-0

45. Nyabuto GO, Wilson JP, Heilman SA, Kalb RC, Kopacz JP, Abnave AV, et al. The Large GTPase, GBP-2, Regulates Rho Family GTPases to Inhibit Migration and Invadosome Formation in Breast Cancer Cells. Cancers (Basel). 2021;13: 5632. doi:10.3390/cancers13225632

46. Liu Q, Hoffman RM, Song J, Miao S, Zhang J, Ding D, et al. Guanylate-binding Protein 2 Expression Is Associated With Poor Survival and Malignancy in Clear-cell Renal Cell Carcinoma. Anticancer Res. 2022;42: 2341–2354. doi:10.21873/anticanres.15713

47. Ji G, Luo B, Chen L, Shen G, Tian T. GBP2 Is a Favorable Prognostic Marker of Skin Cutaneous Melanoma and Affects Its Progression via the Wnt/β-catenin Pathway. Ann Clin Lab Sci. 2021;51: 772–782.

48. Wan Q, Qu J, Li L, Gao F. Guanylate-binding protein 1 correlates with advanced tumor features, and serves as a prognostic biomarker for worse survival in lung adenocarcinoma patients. J Clin Lab Anal. 2021;35: e23610. doi:10.1002/jcla.23610

49. Cheng L, Gou L, Wei T, Zhang J. GBP1 promotes erlotinib resistance via PGK1-activated EMT signaling in non-small cell lung cancer. Int J Oncol. 2020;57: 858–870. doi:10.3892/ijo.2020.5086

50. Zhao Y, Wu J, Li L, Zhang H, Zhang H, Li J, et al. Guanylate-Binding Protein 1 as a Potential Predictor of Immunotherapy: A Pan-Cancer Analysis. Front Genet. 2022;13: 820135. doi:10.3389/fgene.2022.820135

51. Wu Z-H, Cai F, Zhong Y. Comprehensive Analysis of the Expression and Prognosis for GBPs in Head and neck squamous cell carcinoma. Sci Rep. 2020;10: 6085. doi:10.1038/s41598-020-63246-7

52. Yu S, Yu X, Sun L, Zheng Y, Chen L, Xu H, et al. GBP2 enhances glioblastoma invasion through Stat3/fibronectin pathway. Oncogene. 2020;39: 5042–5055. doi:10.1038/s41388-020-1348-7

53. Liu P-F, Shu C-W, Lee C-H, Sie H-C, Liou H-H, Cheng J-T, et al. Clinical Significance and the Role of Guanylate-Binding Protein 5 in Oral Squamous Cell Carcinoma. Cancers (Basel). 2021;13: 4043. doi:10.3390/cancers13164043

54. Cheng S-W, Chen P-C, Lin M-H, Ger T-R, Chiu H-W, Lin Y-F. GBP5 Repression Suppresses the Metastatic Potential and PD-L1 Expression in Triple-Negative Breast Cancer. Biomedicines. 2021;9: 371. doi:10.3390/biomedicines9040371

55. Cheng S-W, Chen P-C, Ger T-R, Chiu H-W, Lin Y-F. GBP5 Serves as a Potential Marker to Predict a Favorable Response in Triple-Negative Breast Cancer Patients Receiving a Taxane-Based Chemotherapy. J Pers Med. 2021;11: 197. doi:10.3390/jpm11030197

Résumé substantiel[16]

Introduction

Francisella tularensis est une bactérie à Gram-négatif et l'agent de la tularémie – une zoonose transmise principalement par des rongeurs et des lagomorphes. L'Homme peut être infecté par plusieurs routes : inhalation d'aérosols, contact cutané, morsures de tiques, etc. La maladie est associée à des symptômes non-spécifiques qui varient en fonction du mode de transmission (fièvre, céphalées, ulcération du site d'infection...). La mortalité en absence de traitement (antibiotiques) est d'environ 2%. Cependant, la maladie a une longue période de convalescence et 15-20% des patients sont hospitalisés.

L'espèce *F. tularensis* contient quelques sous-espèces très proches qui ont une virulence variable. *F. tularensis* subsp. *tularensis* est la sous-espèce la plus virulente, la plus infectieuse et a été classée en tant qu'agent possible de bioterrorisme. *F. tularensis* subsp. *novicida* (ici appelée *F. novicida*) partage 97% d'identité génétique avec la sous-espèce *tularensis*. *F. novicida* ne provoque pas de maladie chez les personnes immunocompétentes mais elle est capable d'infecter des macrophages humains *in vitro* et provoque une maladie sévère chez la souris. Les faibles contraintes de biosécurité, la facilité de manipulation génétique et sa grande similitude avec les sous-espèces hautement virulentes de *F. tularensis*, font de *F. novicida* un bon modèle d'étude pour la tularémie.

F. novicida est un pathogène cytosolique professionnel. Elle est phagocytée par les cellules hôte (macrophages, neutrophiles) mais *F. novicida* s'échappe du phagosome grâce aux effecteurs sécrétés par un système de sécrétion de type VI atypique (T6SS) pour se répliquer abondamment dans le cytosol des cellules infectées.

En général, les bactéries à Gram-négatif sont détectées dans le cytosol par la caspase-11 chez la souris, ou par son homologue humain la caspase-4 qui sont activées la partie 'lipide A' du lipopolysaccharide (LPS) bactérien. L'activation de ces caspases induit une mort cellulaire pro-inflammatoire (la pyroptose) et l'activation de l'inflammasome non-canonique, qui permet le clivage et sécrétion de cytokines pro-inflammatoires. Le LPS de *Francisella* a une structure atypique grâce à plusieurs enzymes bactériennes. Par conséquent, *Francisella* n'est pas détectée par des senseurs innés du LPS comme le TLR4 ou la caspase-11, et active faiblement la caspase-4.

Dans le macrophage murin, *F. novicida* est détectée le senseur d'ADN cytosolique Aim2, ce qui permet de déclencher la cascade inflammatoire qui est essentielle à la réponse immunitaire contre *F. novicida*. L'activation de Aim2 requiert la libération de ligands bactériens qui est médiée par les protéines Guanylate-Binding Proteins (GBPs). Des souris déficientes pour les GBPs ne survivent pas à une infection avec des doses de *F. novicida* non-léthales pour les souris sauvages.

[16] Cette thèse étant écrite en anglais, un résumé substantiel/étendu est présenté.

Les GBPs sont des GTPases inductibles par les interférons. Elles jouent un rôle essentiel dans l'immunité cellulaire autonome et innée contre plusieurs pathogènes (virus, bactéries, protozoaires) à travers de mécanismes variés et souvent pathogène-spécifiques.

Le génome humain code pour 7 GBPs (GBP1-7) dont *GBP1-5* sont exprimés dans les cellules myéloides. En raison de forte pressions sélectives et d'une évolution rapide, les GBPs humaines ne sont pas homologues aux GBPs murines (mGbp1-11). Malgré la haute similarité de séquence et de structure entre les GBPs humaines, des faibles divergences résultent en des différences fonctionnelles importantes.

Parmi les GBPs humaines, GBP1 est la mieux caractérisée. Les GBPs sont composées d'un domaine N-terminal qui porte la fonctionnalité GTPase, suivi par une tige composée d'hélices α (le stalk) et par un domaine effecteur GED (GTPase effector domain). GBP1, GBP2 et GBP5 subissent l'ajout post-traductionnel d'un groupement lipidique (prénylation), dont la nature est dictée par un motif CAAX localisé dans le C-terminus. GBP1 est farnésylé (15 carbones), alors que GBP2 et GBP5 sont géranylgéranylées (20C). Les modifications sont déterminées par le dernier acide aminé du motif CAAX : CTIS pour GBP1 versus CNIL pour GBP2 ou CVLL pour GBP5.

Les GBPs sont des enzymes mécano-chimiques : l'interaction avec le GTP et l'hydrolyse se traduisent en changements conformationnels qui médient une dimérisation ou polymérisation des GBPs, et contrôlent leurs fonctions biologiques. Grâce au groupement lipidique, GBP1 peut se polymériser sur des vésicules lipidiques tels que les vacuoles contenant des pathogènes ou les membranes bactériennes (contenant du LPS).

Les bactéries à Gram-négatif *Shigella flexneri* et *Salmonella* Typhimurium sont très utilisées comme modèles pour l'étude des rôles antibactériens des GBPs humaines dans le cytosol des cellules HeLa. GBP1 lie le LPS de *S. flexneri* grâce à un motif polybasique près du C-terminus, ce qui permet sa polymérisation dans la membrane externe bactérienne riche en LPS. GBP1 recrute GBP2, GBP3 et GBP4 à la surface bactérienne ce qui induit le recrutement et l'activation de la caspase-4. Le mécanisme permettant dans l'activation de la caspase-4 par les GBPs reste encore inconnu.

Objectifs de ces travaux

Dans les macrophages primaires humains, *F. novicida* active la caspase-4 de façon GBP-dépendante. Cependant *F. novicida* porte un LPS atypique. Le recrutement des GBPs sur *F. novicida* et leurs rôles spécifiques dans le macrophage humain n'ont pas encore été caractérisées, et font l'objet de cette étude.

Résultats et discussion

Afin d'étudier le recrutement de GBPs sur *F. novicida*, nous avons créé des lignées stables de monocytes humains exprimant des GBPs wild-type ou mutées fusionnées avec le tag HA. Les HA:GBPs sont exprimées de façon constitutive mais l'expression des GBPs endogènes des U937 requiert un pré-traitement à l'IFNγ.

Dans les macrophages différenciés, traités à l'IFNγ, GBP1 et GBP2 sont recrutées à *F. novicida* dans environ 25% des cellules infectées à 7h post-infection. En revanche, GBP1, GBP2, GBP3 et GBP4 sont recrutées sur *S. flexneri* dans environ 50-70% des cellules infectées 3h p.i, en accord avec la littérature. Conformément à ce qui est observé avec d'autres bactéries, le recrutement de GBP2 sur *F. novicida* dépend de GBP1 alors que GBP1 est localisée sur *F. novicida* indépendamment des autres GBPs.

La farnésylation de GBP1 et la géranylgeranylation de GBP2 sont requises pour leur recrutement sur *F. novicida* et sur *S. flexneri*. De manière intéressante, en plus de la présence, le type de prénylation influence le ciblage des GBPs à *F. novicida*. Nous avons créé des lignées exprimant GBP1 ou GBP2 avec les CAAX interchangés : GBP1-CNIL et GBP2-CTIS. HA:GBP1-CNIL est localisée à *F. novicida* dans plus de cellules, et induit plus de mort cellulaire que HA:GBP1. D'autre part, le recrutement de GBP2-CTIS à *F. novicida* est plus faible que le recrutement de GBP2. Ces résultats suggèrent que le motif CAAX de GBP2 est plus efficace pour le ciblage de *F. novicida* que le CAAX de GBP1. Puisque le groupement géranylgéranyl (20C) est plus long que le farnésyl, le CAAX de GBP2 pourrait permettre un meilleur ancrage dans le LPS de *F. novicida*.

GBP5 est également prénylé mais n'est pas recruté sur *F. novicida*, ni sur *S. flexneri*. Afin de comprendre l'absence de recrutement de GBP5 sur les bactéries, nous avons créé des lignées U937 exprimant des chimères de GBP2 et de GBP5. Ainsi, nous avons identifié la région centrale de GBP2 (K340-R535) comme étant nécessaire et suffisante pour le ciblage de *F. novicida* dans un contexte de GBP prénylé. La fonction de cette région n'est pas décrite dans la littérature. Notre hypothèse est que les différences subtiles au niveau des régions centrales de GBP2 et de GBP5 influencent leurs capacités de changement conformationnel et permettent la polymérisation de GBP2 mais pas de GBP5 avec GBP1 à la surface de la bactérie.

Nous nous sommes également intéressés aux facteurs qui régulent le recrutement initial de GBP1 indépendamment des autres GBPs. Nous avons étudié le recrutement de chimères GBP1/GBP2 sur *F. novicida* en l'absence d'IFNγ après vérification de la fonctionnalité des chimères en présence d'IFNγ. Le motif polybasique dans le C-terminus de GBP1, quand il est ajouté à GBP2, est nécessaire et suffisant pour permettre le ciblage de GBP2 à *S. flexneri*. Au contraire, il est nécessaire, mais pas suffisant pour le recrutement sur *F. novicida*. D'autres facteurs ont été identifiés dans le N-terminus de GBP1 : un motif polybasique KKK31-36, ainsi que des résidus impliqués dans la formation de GMP, propriété unique à GBP1. Toutefois, ni l'hydrolyse de GDP, ni le motif KKK61-63, ne sont nécessaires pour le recrutement de GBP1 sur *S. flexneri*.

Les niveaux plus faibles de ciblage de *F. novicida* par les GBPs, l'absence de recrutement de GBP3 et de GBP4, en plus des facteurs supplémentaires requis pour le ciblage initial de GBP1 sur *F. novicida*, suggèrent que les GBPs ont moins d'affinité pour *F. novicida* que pour *S. flexneri*. Dans des cellules infectées simultanément avec *F. novicida* et *S. flexneri*, GBP1 est principalement localisée à *S. flexneri*. De plus, la co-infection par *F. novicida* n'inhibe pas le recrutement de GBP3 ou GBP4 sur *S. flexneri* ce qui suggère que les facteurs permettant l'échappement de *F. novicida* au ciblage par GBP3/4 seraient intrinsèques à la bactérie, et non secrétés. Nous avons identifié une souche mutée de *F. novicida* qui présentait un enrichissement en HA:GBP3 à sa surface. Cette souche est délétée pour une enzyme (LpxF) impliquée dans la modification du LPS. Le recrutement de GBP3 sur *ΔlpxF* n'a pas atteint les niveaux de recrutement de GBP1 et 2 sur *F. novicida*, suggérant que d'autres facteurs seraient impliqués dans l'échappement par *F. novicida* du ciblage par GBP3.

Conclusion

S. flexneri est un modèle très utilisé dans le champ grâce à sa facilité de manipulation. Cependant l'étude de *F. novicida* nous permet de décortiquer plus précisément les mécanismes d'action des GBPs. En effet, le recrutement sous-optimal des GBPs sur *F. novicida* permet de mieux situer la hiérarchie des GBPs et les facteurs cellulaires qui contribuent au recrutement. De plus, nos résultats sur *F. novicida* démontrent l'intérêt d'étudier les mécanismes de l'immunité avec des pathogènes particuliers et de dépasser les approches classiques sur les pathogènes modèles que sont *Shigella* et *Salmonella*.

Abstract

Francisella novicida is a professional cytosol dwelling pathogen, internalized by host cells (macrophages, neutrophils) through phagocytosis. *F. novicida* escapes from the phagosome using effectors secreted by an unconventional type 6 secretion system. *F. novicida* replicates abundantly in the cytosol of infected cells.

The *Francisella* lipopolysaccharide (LPS) has an atypical structure shaped by several LPS modifying enzymes, allowing the bacterium to avoid detection from LPS-binding immune receptors such as TLR4 or the murine pro-inflammatory caspase-11. Instead, *F. novicida* is detected by the DNA sensor Aim2. The human caspase-4 (caspase-11 ortholog) detects only weakly *F. novicida* LPS. Both caspase-4 in human cells and Aim2 activation in murine cells requires liberation of *F.novicida* ligands, mediated by Guanylate-Binding Proteins (GBPs).

GBPs are interferon-inducible GTPases that play a key role in cell autonomous responses against intracellular pathogens. Seven GBPs are present in humans. Despite sharing high sequence similarity, subtle differences among GBPs translate into functional divergences that are still largely not understood. A key step for the antimicrobial activity of GBPs towards cytosolic bacteria is the formation of supramolecular GBP complexes on the bacterial surface. Such complexes are formed when GBP1 binds lipopolysaccharide (LPS) from *Shigella* and *Salmonella* and further recruits GBP2, GBP3, and GBP4.

Because *F. novicida* has an atypical LPS and given the importance of GBPs in anti-*Francisella* immunity, our aim was to understand the molecular and cellular mechanisms controlling recruitment of GBPs to *F. novicida* in human macrophages.

F. novicida was coated by GBP1 and GBP2 in human macrophages but escaped targeting by GBP3 and GBP4. Coinfection experiments demonstrated that GBPs target preferentially *S. flexneri* compared to *F. novicida*. GBP1 and GBP2 features that drive recruitment to *F. novicida* were investigated revealing that the unique GBP1 GDPase activity is required to initiate GBP recruitment to *F. novicida* but facultative to target *S. flexneri*. Furthermore, analysis of chimeric GBP2/5 proteins identified a central region in GBP2 (K340-R535) necessary and sufficient to target prenylated GBPs to *F. novicida.* Finally, a *F. novicida* Δ*lpxF* mutant with a penta-acylated lipid A was targeted by GBP3 suggesting that LPS modification contributes to escape from GBP3. Altogether, our results indicate that GBPs have different affinity for different bacteria and that the repertoire of GBPs recruited onto cytosolic bacteria is dictated by GBP-intrinsic features and specific bacterial factors, including the structure of the lipid A.

Few bacteria have adapted to thrive in the hostile environment of the cell cytosol. As a professional cytosol-dwelling pathogen, *S. flexneri* secretes several effectors to block cytosolic immune actors, including GBPs. This study illustrates a different approach of adapting to the host cytosol: the stealth strategy developed by *F. novicida*. The lower affinity of GBPs for *F. novicida* allowed to decipher the different domains that govern GBP recruitment to the bacterial surface. This study illustrates the importance of investigating different bacterial models to broaden our understanding of the intricacies of host-pathogen interactions.

Keywords: *Francisella novicida*, *Francisella tularensis*, *Shigella flexneri*, Guanylate-Binding Proteins, cytosolic bacteria, cell autonomous immunity, innate immunity, inflammasome

Résumé

Francisella novicida est un pathogène cytosolique professionnel qui est internalisé par les cellules hôtes (macrophages, neutrophiles) par phagocytose. F. novicida échappe du phagosome grâce aux effecteurs sécrétés par un système de sécrétion de type 6 non-conventionnel. *F. novicida* se réplique abondamment dans le cytosol des cellules infectées. Le lipopolysaccharide (LPS) de *Francisella* porte une structure atypique formée par plusieurs enzymes modifiantes le LPS, ce qui permet à la bactérie d'éviter la détection par des récepteurs de l'immunité liant le LPS tels que le TLR4 ou la caspase murine pro-inflammatoire caspase-11. Dans le cytosol murin, *F. novicida* est détectée par le senseur d'ADN Aim2. L'orthologue humain de la caspase-11, la caspase-4, détecte faiblement le LPS de *F. novicida*. L'activation de la caspase-4 chez l'Homme et de Aim2 chez la souris nécessite la libération de ligand de F. novicida, processus médié par les Guanylate-Binding Proteins (GBPs).

Les GBPs sont des GTPases inductibles aux interférons qui jouent un rôle clé dans les réponses immunitaires contre les pathogènes intracellulaires (virus, bactéries, protozoaires). Sept GBPs sont présentes chez l'Homme. Malgré une haute homologie de séquence, des différences subtiles parmi les GBPs se traduisent dans des divergences fonctionnelles qui sont encore largement incomprises. Une étape clé pour l'activité antimicrobienne des GBPs vers les bactéries cytosolique est la formation de complexes supramoléculaires à la surface bactérienne. De tels complexes sont formés quand GBP1 lie le LPS de *Shigella* ou de *Salmonella* et recrute ensuite GBP2, GBP3 et GBP4.

Puisque *F. novicida* porte un LPS atypique, et au vu de l'importance des GBPs dans l'immunité anti-Francisella, notre objectif était de comprendre les mécanismes moléculaires et cellulaires contrôlant le recrutement des GBPs sur *F. novicida* dans les macorphages humains.

F. novicida a été recouverte de GBP1 et de GBP2 dans les macrophages humains mais a échappé le recrutement de GBP3 et de GBP4. Des expériences de co-infection suggèrent que les GBPs ciblent de préférence *S. flexneri* en comparaison avec *F. novicida*. Nous avons étudié les caractéristiques de GBP1 et GBP2 promouvant le recrutement à *F. novicida* et nous avons montré que l'activité GDPase unique de GBP1 et requise pour initier le ciblage de GBP1 à *F. novicida* mais est facultative pour le recrutement sur *S. flexneri*. De plus, des analyses de GBP2/5 chimériques ont permis d'identifier la région centrale de GBP2 (K340-R535) comme nécessaire et suffisante pour cibler des GBPs prénylées à *F. novicida*. Enfin, un mutant de *F. novicida* Δ*lpxF* portant un LPS penta-acylé a été enrichi en GBP3 suggérant que les modifications du LPS contribuent à l'échappement de GBP3. Somme toute, nos résultats suggèrent que les GBPs ont une affinité différente pour les espèces bactériennes différentes, et que le répertoire des GBPs recrutées sur une bactérie cytosolique est dicté par des facteurs GBP-intrinsèques et bactériens, tels que la structure du lipid A bactérien.

Peu d'espèces bactériennes sont adaptées à la vie dans le cytosol cellulaire. En tant que pathogène cytosolique, *S. flexneri* sécrète plusieurs effecteurs afin de bloquer des acteurs de l'immunité cytosolique, y compris les GBPs. Cette étude démontre une approche alternative : la stratégie furtive développée par *F. novicida*. La moindre affinité des GBPs pour F. novicida a permis de décortiquer les différents domaines qui permettent le recrutement des GBPs à la surface bactérienne. Cette étude illustre l'importance d'explorer différents modèles bactériens afin d'élargir notre compréhension des spécificités des interactions hôte-pathogène.

Mots-clés : *Francisella novicida*, *Francisella tularensis*, *Shigella flexneri*, Guanylate-Binding Proteins, bactéries cytosoliques, immunité cellulaire autonome, immunité inné, inflammasome